EFFECTS OF POST TANNING OPERATIONS AND *Aloe barbadensis* Miller-CARRAGEENAN MIXTURE ON PHYSICAL, STRUCTURAL AND CHEMICAL PROPERTIES AND ON HEXAVALENT CHROMIUM FORMATION IN LEATHER

KALLEN MULILO NALYANYA

A Thesis Submitted to the Graduate School in Partial Fulfillment for the Requirements of the Degree of Doctor of Philosophy in Physics of Egerton University

EGERTON UNIVERSITY

MAY, 2019

DECLARATION AND RECOMMENDATIONS

Declaration

This is my original work and has not been submitted in part or whole for an award in any institution.

Signature:……. Date:……..……..

KALLEN MULILO NALYANYA

SD13/14698/15

Recommendations

This Thesis has been submitted for examination with our approval as university supervisors.

Signature:……. Date……

DR. RONALD K. ROP

Department of Physics

Egerton University

Signature: ..... Date:…….

DR. ARTHUR S. ONYUKA

Leather Division

Kenya Industrial Research and Development Institute (KIRDI), Nairobi

Signature:……. Date……

DR. ZEPHANIA BIRECH

Department of Physics,

School of Biological and Physical Sciences

University of Nairobi

DEDICATION

This work is dedicated to my wife Ruth Mwenje Mulilo, my mother, Maxmillah Nasimiyu Murunga and my son, Joshua Murunga Mulilo.

ACKNOWLEDGEMENT

I am grateful to God for the good health and sound mind for the entire period of this work. I thank Egerton University, the Faculty of Science and Physics Department for the opportunity to do my PhD from there and for the tuition waiver during the third year of my studies.

I wish to extend my gratitude to my diligent supervisors Dr. Ronald K. Rop, Dr. Arthur Onyuka and Dr. Zephania Birech for their advice, guidance, continuous encouragement and financial support towards the successful completion of this work.

I can't appreciate enough the selflessness and technical help I got from Mr. Kamau of chemistry department Egerton University for the UV-VIS Spectrophotometry and Mr. Karubia of Egerton University Biotechnology Lab for assisting with thermal and photo ageing of the samples. I am greatly indebted to Alvin Sasia of KIRDI for the procurement, processing of bovine hide and Instron testing experiments. I thank the Department of Physics, University of Nairobi, specifically; special thanks to Justus Okonda, Moses Juma and Omucheni, for the technical assistance during the Raman spectroscopy and EDXRF spectroscopy experiments. I also acknowledge the assistance of Mr. Okonda in the analysis of EDXRF data using Origin.

I humbly thank my friends: Elsie Salano, Timothy Kabula, Moses Murunga, Douglas Sifuna, Moses Wambulwa and Timothy Murega, for their financial assistance towards sample procurement and experimental work.

I acknowledge the financial support through "The 1st PhD Research Grant" from the National Research Fund (NRF) which facilitated greatly this work to a successful end.

Finally, my sincere thanks to my wife Ruth Mwenje and my son Joshua Murunga, who have been patient and tolerant when I stayed long in the laboratory and sacrificed a lot for my research work.

ABSTRACT

Leather industry is a key player in most developing countries' economy. However, its tanning process has been associated with environmental and human health hazards due to formation of Cr (VI). To address these concerns, this study investigated effects of *Aloe barbadensis* Miller (ABM) mixed with carrageenan and of crusting operations on physical and structural properties, and elemental concentrations and on formation of Cr (VI) in leather crusts. Raw cow hide was conventionally processed to tanning, retanning, dyeing and fatliquoring and after each step, samples were cut for testing and others treated with ABM mixed with carrageenan. Results from the Instron tester showed that all the crusting operations significantly affect both physical and organoleptic properties of leather. Confocal Raman spectroscopic data showed that crusting operations and the incorporation of ABM and carrageenan causes structural alterations as indicated by shifts in peak positions and variations in intensities especially of amide bands. Predicted strength properties using empirical models and equations showed closer agreement with experimental data. The ideal quantity of ABM was calculated to be 3.78% and the incorporation stage done at fatliquoring process. Interaction of ABM/carrageenan is only majorly physical with minor interactions involving hydroxyl bonds and sulphur. Results from EDXRFs showed that the incorporation increases the levels of S, K, Ca, V, Fe and Zn. All the crusting processes affect the levels of Cr (VI) formed in both aged and non-aged leather crusts. The levels of Cr (VI) in leathers is detectably higher in retanned and fatliquored and minimum in dyed crusts. The levels of Cr (VI) in leather crusts processed with ABM Miller and carrageenan, aged and unaged, were below detection level. ABM and carrageenan have shown total inhibition of Cr (VI) formation. For purposes of crosslinking and improving the physical properties, the study recommends the incorporation process to be done during pretanning operations. However, for antioxidant purposes, the incorporation should be done after tanning process especially fatliquoring stage and at most 3.784 wt % of the ABM and carrageenan used. The study recommends more research to determine the ideal particle sizes of the ABM and carrageenan molecules to enhance the penetration and distribution within the matrix. The study suggests activation of the ABM and carrageenan by sulphiting for improved wetting and adhesion. More appropriate coupling agents need to be determined for adhesion and wetting back.

TABLE OF CONTENTS

LIST OF TABLES

LIST OF FIGURES

LIST OF PLATES

LIST OF ABBREVIATIONS AND ACRONYMS

AAS	Atomic Absorption Spectroscopy
ABM	*Aloe barbadensis* Miller
ABTS	Azino-bis (3-ethylbenzothiazoline-6-sulphonic acid
ASTM	American Society for Testing and Materials
BAT	Best Available Techniques
BOD	Biochemical Oxygen demand
CCD	Charge-Coupled Device
CG	Cartesian Geometry
COD	Chemical Oxygen Demand
Cr (III)	Trivalent Chromium
Cr (VI)	Hexavalent Chromium
DGSS	Dissymmetric Gemini Sulfosuccinate
DPC	Diphenylcarbazide
DPPH	Diphenyl-1-picrylhydrazyl.
EC	Ecolabel Criterion
EDXRFs	Energy Dispersive X-Ray Fluorescence spectroscopy
ESA	Ethiopian Standards Agency
FAAS	Flame Atomic Absorption Spectroscopy
FP	Fundamental Parameters
FRAP	Ferric Reduction Antioxidant Power
FTIR	Fourier Transform Infra-Red
FWHM	Full Width at Half Maximum
GC	Gas Chromatography
GDP	Gross Domestic Product
GFAAS	Graphite Furnace Atomic Absorption Spectroscopy
HRP	Horseradish Peroxide
ICP-OES	Inductively Coupled Plasma-Optical Emission Spectrometry
INAA	Instrumental Neutron Activation Analysis
ISO	International Standards Organization
KIRDI	Kenya Industrial Research and Development Institute

N-OITZ	N-Octyl-Isothiazolinone
NIR-FT	Near-infrared Fourier Transform
NIR	Near Infra-Red
OI	Orientation Index
ORAC	Oxygen Radical Absorbance Capacity
PCA	Principal Component Analysis
PPD	Phenylenediamine
PPM	Parts Per Million
REACh	Registration, Evaluation, Authorization and Restriction of Chemicals
RH	Relative Humidity
ROS	Reactive Oxygen Species
RPF-SQX	Rigaku Profile Fitting-Spectra Quant X
SATRA	Safety and Technical Rescue Association
SAX	Small Angle X-Ray
SPE	Solid Phase Extraction
TCMTB	Thiocyano-Methylthio Benzotiazole
TEAC	Transactions on Economics and Computation
TDS	Total Dissolved solids
THPS	Tetrakis Hydroxymethyl Phosphonium Sulphate
TKN	Total Kjeldahl Nitrogen
UNEP	United Nations Environemen Programme
USEPA	United States Environmental Protection Agency
UV	Ultraviolet Light
UV-VIS	Ultraviolet-Visible Light spectroscopy
WDXRF	Wavelength Dispersive X-Ray Flourescence
XRF	X-Ray Flourescence

LIST OF SYMBOLS

λ	Wavelength
D	Repeating unit of collagen molecule (e.g. 67 nm)
d	Lattice plane spacing
q	Scattering Vector
δ	Deformational vibrations
ν	stretching vibrations
ν_s	symmetric stretching vibrations
ν_{as}	asymmetric stretching vibrations

CHAPTER ONE
INTRODUCTION

This chapter introduces the conceptual framework of this study and the philosophical foundation upon which the study is founded. The chapter outlines the relevant background to the study, a clear statement of the problem, the objectives, hypotheses and the importance or justification or rationale of the study.

1.1 Background information

Leather tanning industry plays a critical role in the global economy especially in the developing countries. Among the benefits includes contribution towards the Gross Domestic Product (GDP), source of livelihoods, employment opportunities and support to other downstream industries (Ozgunay *et al.*, 2007; Habib *et al.*, 2015). This premier industry has been lauded for its innovativeness: the ability to utilize a highly putrescible meat by-product ie skins and hides, which would otherwise have been an environmental nuisance to produce useful commodities. The leather, its main product, forms an important intermediate industrial product in the down-stream sectors of the consumer products industry (Ozgunay *et al*., 2007; Beghetto *et al*., 2013; Mutlu *et al*., 2014). Among the conventional applications are footwear, clothing, upholstery, and furniture (Liu *et al*., 2006; Joseph and Nithya, 2009). Therefore, the potential of this industry is enormous owing to the increasing world population, which raises the demand for meat, leather and parchment products. However, the future of this vibrant industry is threatened by the stiff competition posed by the synthetics and the need to comply with the stringent environmental regulations (Habib *et al.*, 2015; Nalyanya *et al.*, 2015a). The challenges have been escalated by the growing awareness among consumers for products that meet the performance and durability criterion, according to Occupational and Safety Footwear EC mark (Dir.89/686/EEC). Furthermore, the growing awareness among the general public towards human and environmental health led by legislative policies such as UNEP and USEPA have compelled industries to comply with the stringent environmental regulations (Dixit *et al*., 2015). Therefore, the industry's strategy should be geared towards producing high quality leather within affordable and ecobenign manufacturing technologies (Krishnamoorthy *et al.*, 2013).

Conventionally, the leather making process is aimed at transforming hides' proteins called collagen into a physically and chemically stable material (Covington, 2009; Hui *et al*., 2010; Roig *et al*., 2012; Zengin *et al*., 2012; Nalyanya *et al*., 2015, Nalyanya *et al*., 2016). The process involves a sequence of chemical, manual and mechanical operations meant to produce a versatile product that meets customer's needs (Ozgunay *et al.*, 2007; Beghetto *et al.*, 2013). The operations make use of acids, bases, salts, enzymes and mechanical actions such as tanning, that render collagen with an entirely different bundle structure and chemical composition (Musa and Gasmelseed, 2013a; Habib *et al.*, 2015; Vornicu *et al.*, 2015). The structural alterations induced into the hierarchical organization of the collagen matrix by the actions range from molecular to macromolecular level (Masic *et al.*, 2011). The physical properties are also modified by the actions occasioned by the structural and chemical composition of the final leather (Landmann, 2003; Tillet *et al.*, 2011; Ali *et al.*, 2013; Krishnamoorthy *et al.*, 2013; Barcadit *et al*., 2014; Sizeland *et al.*, 2015; Vornicu *et al.*, 2015). It's estimated that more than 90% of global tanning is done by use of Cr (III) compounds due to the superior quality of the resultant leather and efficient processing (Saravanabhavan *et al*., 2005; Kanagaraj *et al*., 2008; Roig *et al*., 2012; Tegtmeyer and Kleban, 2013a; Musa and Gasmelseed, 2013a; Beghetto *et al*., 2013; Devikavathi *et al*., 2014). Although the Cr (III) salts are friendly to both environment and human health, cases of spontaneous and accelerated conversion of Cr (III) to Cr (VI) have been reported widely (Krishnamoorthy *et al.*, 2013; Barcadit *et al*., 2014; Devikavathi *et al*., 2014; Hedberg *et al*., 2015). There are several factors which facilitate accelerated oxidation such as low or high pH (during neutralization and dyeing), high temperatures, UV radiations, high or low humidity, contaminants, certain dyes, fatliquoring agents, and unfixed and leachable Cr (III) in leather (Hauber and Buljan, 2000; Rydin, 2002; Babu *et al*., 2005; Congzheng *et al.*, 2005; Candar *et al.*, 2008; Kolomaznik *et al.*, 2008; Fuck *et al*., 2011; Devikavathi *et al*., 2014; Dixit *et al.*, 2015; Kocurek *et al*., 2015). Cr (VI) is highly toxic and detrimental to both environmental and human health and its presence in leather products is highly restricted by the European Commission under the registration, evaluation, authorization and restriction of chemicals (REACh) (Roig *et al*., 2012; Hedberg *et al*., 2015). The presence of Cr (VI) in the final leather product has led to increased cases of leather rejection in the world market and lower market price (Kolomaznik *et al*., 2008; Bayramoglu *et al*., 2012). Thus, alternative and innovative methods of processing are needed to minimize or eliminate the formation of Cr (VI) along the chain of production (Fonseca *et al.*, 2011).

Several concerted efforts have advocated for cleaner tanning systems such as green chemistry protocol and ecobenign mitigation measures in order to safeguard the environmental and human health and also to enhance the quality of the leather by improving its organoleptic and physical properties and other functionalities (Saravanabhavan *et al*., 2004; Bayramoglu *et al*., 2008; Candar *et al*., 2008; Covington 2009; Hui *et al*., 2010; Bitlisli *et al*., 2010; Krishnamoorthy *et al*., 2013; Colak *et al*., 2014; Ozkan *et al*., 2017). In order to strike a balance between leather quality and environmental health, vegetable tanning agents, both condensed and hydrolysable have been combined with chromium compounds. This approach proved effective in minimizing the levels of formation of Cr (VI) and formaldehyde in leathers (Ozkan *et al*., 2017). Plants such as valonia, henna, hazel nuts, *Coridothymus capitatus, Olea europaea, Corylus avellana,* and *Juglans regia,* which have antioxidative characteristics have also been incorporated within chromium tanning technologies in order to minimize or curtail the formation of Cr (VI) (Bayramoglu *et al*., 2012; Ozgunay *et al*., 2012; Colak *et al*., 2014; Cannot *et al*., 2016; Ozkan *et al*., 2017). Most of these plants offer additional benefits such as antimicrobial, antifungal and antibacterial characteristics. Of all these plants, *Aloe barbadensis* Miller (ABM) has additional desirable benefits such as humectant characteristics and oily nature that makes the leather softer and offers a cooling effect (Litke and Widdemer, 2003; Bitlisli *et al*., 2010). Although ABM has lignin which aids its penetration into the leather fibrils, it has a strong tendency to agglomeration and poor dispersibility (Litke and Widemmer, 2003). Carrageenan molecules have negative charge which enables them to react with positive ions or protein in collagen (McHugh, 2003). Similarly, the molecules have the ability to suspend the ABM particles to maintain relatively better distribution within leather matrix (FMC Biopolymer, 2010). Therefore, carrageenan is capable of preventing the aggregation of the ABM thus reducing any possible incompatibility with leather matrices. Consequently, carrageenan may be a convenient carrier for incooperating ABM in the leather matrix. The mucopolysaccharides which binds moisture and causing the cooling effect of ABM retains more moisture from the atmosphere (Surjushe *et al.*, 2008). Softer leather implies that incorporated particles interface the collagens decreasing the adhesive forces between and within them, according to filler reinforcement and adhesion theory. The presence of ABM and carrageenan molecules may cause poor interfacial adhesion, non-uniform stress concentration (dispersion) and high filler loadings (volume fraction). Unnecessary stress concentration weakens the leather or act as barriers to crack growth hence leading to a reinforcing effect (Ervina *et al*., 2016). The phenols

in ABM contain OH while collagen contain NH_2 and carboxylic groups, which when reacted, form hydrogen bonds (Giurginca *et al*., 2007; Jithendra *et al*., 2013; Narsih *et al*., 2013). The hydrogen bonding together with other solvent molecules may alter the force constants in the leather, which determine the angle and direction of the vibration of the functional groups of the leather (Gonzalez and Wess, 2008). The bond formation alters structural and physical properties of leather. Additionally, moisture content in the leather affects the strength of hydrogen bonding in the collagen due to conjugation (Kavkler and Demsar, 2012). It's therefore necessary to investigate the effect of incorporation of these two natural plants on the physical, structural and chemical properties of leather.

Investigations into the effect of leather processing operations on the physical properties of leather are well documented (Zapletal *et al*., 1996; Valeika *et al*., 2010; Ali *et al*., 2013; Krishnamoorthy *et al*., 2013; Nalyanya *et al*., 2015, Salehi *et al*., 2013; Wells *et al*., 2013; Barcadit *et al*., 2014; Nalyanya *et al*., 2015; Negussie *et al*., 2015; Nalyanya *et al*., 2016a; Nalyanya *et al*., 2016b). Comprehensive literature on the effects of crusting operations on physical properties of leather is, however, scanty. Different methods have been applied to study Cr (VI) in leathers such as colorimetric method with 1, 5-diphenyl-carbazide (metal complexation), graphite furnace atomic absorption spectroscopy (GF AAS), flame Atomic Absorption Spectroscopy (FAAS) and Raman spectroscopy (Monteiro *et al.*, 2002; Kikuchi *et al*., 2005; Rezic and Zeiner, 2008; Kolomaznik *et al*., 2012). However, information on the effect of crusting operations on the conversion of Cr (III) to Cr (VI) is not published. Plant products with antioxidants and mixtures of phenols have been investigated with regard to their ability to prevent Cr (VI) formation in leathers and their scavenging activity on the photodegradation of collagen in solutions (Metreveli *et al*., 2006; Pereira *et al*., 2007; Bayramoglu *et al*., 2008; Contini, 2008; Owlad *et al*., 2009; Wang *et al*., 2009a; Metreveli *et al*., 2010; Bayramoglu *et al*., 2012). However, effects of ABM and carrageenan on the physical properties, chemical composition and molecular structure have not been reported. The effects of ABM and carrageenan on the conversion of Cr (III) to Cr (VI) has not been documented. A number of studies have been carried out to determine the chemical properties of leathers and tannery effluents such as Chemical Oxygen Demand (COD), Total Dissolved Solids (TDS), Nitrogen, Chromic Oxide content, total organic carbon, volatile fats and extractible fatty matter contents (Bitlisli *et al*., 2004; Abbas *et al*., 2012; Jankauskaite *et al*., 2012;

Roig *et al*., 2012; Zengin *et al*., 2012; Akinci *et al*., 2013; Naher *et al*., 2017; Naidansuren *et al*., 2017). Other studies have investigated the hazardous elements in parchments and finished leather using XRF, ICP-OES and Instrumental Neutron Activation Analysis (INAA) techniques (Aslan, 2009; Roig *et al*., 2012; Summerour, 2012; Okoh *et al*., 2013). Although extensive work has been done in this area of chemical properties of leather and the possible environmental pollution of tannery discharges, information on the effect of leather making processes on the elemental composition of the actual leather is scanty. Therefore, this study focused on investigating the effects of crusting operations and *Aloe barbadensis* Miller mixed with carrageenan on the physical, and structural properties of crusts and on the concentration of Cr (VI) in leather.

1.2 Statement of the problem

Chromium tanning technology is one of the landmark technologies that leather tanning industry has ever implemented due to superior quality of the resultant leather and the high tanning efficiency. However, this technology has faced a lot of criticism due to undesirable environmental and human health effects resulting from Cr (VI), which is hazardous to both the environment and human health. Cr (VI) is associated with health problems such as allergic contact dermatitis, acute toxicity, carcinogenicity and mutagenicity, skin rash or irritations, nasal septal perforation and ulcerations, weakened immune system, genetic material alteration, kidney and liver damage, eardrum perforation, lung carcinoma in humans, eye irritations and damages, pulmonary congestion and edema, diarrhea, upper abdominal pains, indigestion, vomiting and may even go as far as death of the individual. Chromium tanning puts the lives of the tannery workers and leather consumers at risk and this has contributed to the high rejection rates of leather products at international markets, especially Europe. Although several studies have advocated for alternative green and cleaner tanning technologies over chrome tanning, the resulting leathers have inferior quality that limits their penetration into the high-end market and hence giving an edge to the use of synthetic leather. Although studies have investigated the technologies that incorporate plants and their extracts into chromium technology in order to minimize the impact of Cr (VI), the levels of Cr (VI) are still much higher than the minimum permissible levels of 3 mg/kg. It's on this basis that this study sought to investigate the effect of crusting operations and *Aloe barbadensis* Miller

mixed with carrageenan on the physical, structural and chemical properties and on the formation of Cr (VI) in leather crusts.

1.3 Objectives

1.3.1 General Objective

To investigate the effects of crusting operations and *Aloe barbadensis* Miller on the physical, structural and chemical properties and on the formation of hexavalent chromium in post tanned leather crusts.

1.3.2 Specific Objectives

i. To determine, experimentally and theoretically, the effect of post tanning operations and of *Aloe barbadensis* Miller mixed with carrageenan on the physical properties of leather.
ii. To determine the effect of post tanning operations and *Aloe barbadensis* Miller mixed with carrageenan on the molecular structure of leather using Confocal Raman microscope.
iii. To determine the effect of post tanning operations and *Aloe barbadensis* Miller mixed with carrageenan on the elemental characterization of leather using EDXRF.
iv. To determine the effect of post tanning operations and *Aloe barbadensis* Miller mixed with carrageenan on the formation of Cr (VI) in leather using UV-VIS spectrophotometry.

1.4 Hypotheses (H_o)

i. Post tanning operations and *Aloe barbadensis* Miller and carrageenan have no signicant effect on the physical properties of leather.
ii. Post tanning operations and *Aloe barbadensis* Miller and carrageenan have no significant effect on the molecular structure of leather.
iii. Post tanning operations and *Aloe barbadensis* Miller and carrageenan have no significant effect on the elemental characterization of leather.
iv. Post tanning operations and *Aloe barbadensis* Miller and carrageenan have no significant effect on the formation of Cr (VI) in leather.

1.5 Justification

Leather tanning industry, *Aloe vera* harvesting in the Northern belt and sea weed harvesting in blue economy are the key sectors with untapped potential that have been earmarked by the Kenyan industrialization ministry and and developing countries at large. This venture is a viable venture due to the promising prospects of quality leather demand by the rising population especially among the developed countries. Therefore, any green chemistry technology which combines chrome tanning in order to minimize or inhibit the formation of Cr (VI) and maintain high quality leather is necessary. This study therefore investigated the effects of crusting operations and *Aloe barbadensis* Miller on the physical, structural and chemical properties and on the formation of Cr (VI) in leather. The findings of this study form the strong basis on which the industry can address the issues of environment and human health while utilizing cheap, readily available and renewable natural resources such as carrageenan and *Aloe vera*. Cost effective production of quality leather within ecobenign framework not only gurantee the market for the products but will also increase the profitability and sustainability of the industry. Other industries that process carrageenan and Aloe vera will benfit form the leather tanning industry.

CHAPTER TWO
LITERATURE REVIEW

This chapter presents a detailed overview of the current understanding of collagen with emphasis on the structure and leather-forming component and the leather processing operations and the physical properties of leather that form the main quality indicator. The chapter reviews the theoretical models and empirical models that can be used to predict physical properties of leather composites. A review on the use of natural plants to assess their potential on the quality of leather and environmental mitigations especially inhibition of the formation of Cr (VI) in leather are also outlined. The theoretical background, principles and applications of the Raman spectroscopy, UV-VIS spectrophotometry and EDXRFs are also explained as tools to determine the molecular structure, Cr (VI) and elemental concentration in leather. The chapter also highlights key components of the ISO 17075 procedures in determining the levels of Cr (VI).

2.1 Introduction to Leather

Mammalian skin or hide is an organ that fulfils many functions such as regulation of body temperatures, protection, elimination of wate products and sensory detection among others (Lawson, 2008). Once the mammal is slaughtered for food, the hides/skins are disposed of as wastes or converted into useful products as leather (Beghetto *et al.*, 2013). Production of leather involves tanning processes which are meant to enhance some natural properties, remove any unwanted matter, stabilize its structure and prevent the putrefaction process. The most important component of hide in the leather making process is collagen. The approximate composition of a mammal hide is 64% of water and 33% of structural and non-structural proteins. More specifically, structural proteins are collagen (29%), keratin (2%), and elastin (0.3%) while non-structural proteins are albumins, globulins (1%), mucins, mucoids (0.7%) (Gustauson, 1956). As minor components, fats (2%) and other substances (0.5% inorganic components, 0.5% pigments, etc.) are contained in the skin.

Leather is a strong and resilient viscoelastic biopolymer whose complex architecture is characterized by its unique hierarchical structure of collagen (Giurginca *et al*., 2007; Nalyanya *et al*., 2016a). It's manufactured from the dermal layer of animal skin or hide (Nalyanya *et al*.,

2016c). Dermis is a tough, resilient layer underneath the epidermis that forms the final leather (Gustauson, 1956). It's a matrix of connective tissues that are made up of collagen fibres and elastic fibres embedded in a ground substance (glycosaminoglycans). These collagen fibres are the foundation of the skin's ability to resist mechanical stress and their network imparts remarkably on the structural integrity and flexibility of the hide/skin. The fibres are both elastic and viscous and hence elasticity and viscosity of the leather (Nalyanya *et al*., 2016a; Nalyanya *et al*., 2016b). The dermis is made up of two parts: the papillary region making up about 20% of the dermis and the reticular region making up approximately 80%. The papillary region acts as the dermo-epidermal junction and the fibres in this region are thin. The bottom of the epidermis forms an uneven surface with fibres which project downwards into the connective tissue of the dermis. The fibres push into the connective tissue in order to increase the surface area between the dermis so that a strong junction is formed between these two layers (Lawson, 2008).

2.2 Collagen structure

Collagen is a hierarchical structural protein where specific sequences of amino acids form polypeptide chains and three polypeptide chains are twisted to form a collagen helix (Kennedy and Wess, 2003). The collagen helices are then arranged in a quarter stagger to form strands that bundle together to form a fibril. Collagen fibril bundles further to form fibres that form the main constituents of leather as shown in figure 2.1 (Maxwell *et al*., 2006).

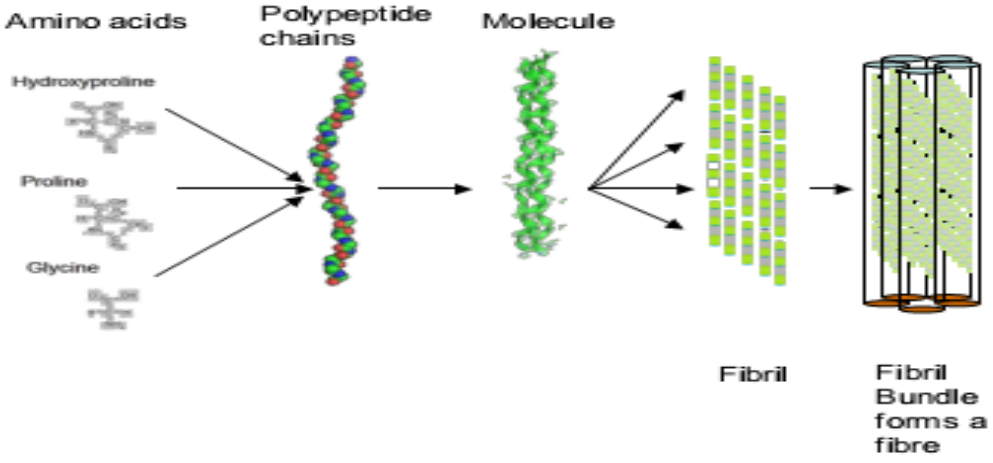

Figure 2.1: Schematic showing the hierarchical structure of collagen (Source: Maxwell *et al*., 2006)

There are at least 28 classified types of collagen with at least 46 distinct polypeptide chains, named in Roman numerals from I-XXVIII (Brinckman, 2005; Veit *et al*., 2006). Collagen have three main characteristics; contributes to the structural integrity of extracellular matrix, forms supramolecular aggregates such as network and fibrils and contain at least one triple-helical domain (Brickmann, 2005). Among the 28 types, types I, II, III and XI are the major fibril-forming collagen which form the structural basis of skins and hides (Rabotyagova *et al*., 2008). These collagen types, especially type I, are prevalent and are assembled with complex hierarchical structure (Gelse *et al*., 2003). Each polypeptide chain forms an alpha helix with a left-handed twist, then three of these left handed helices twist together in a right handed manner to form a triple helix, or tropocollagen. Collagen fibrils are assembled from multiples of five staggered tropocollagen which is responsible for banding structure of collagen. The alignment of the molecules in the fibres and the stabilization in these positions by the molecular cross-links endows collagen with a high degree of mechanical strength (Paul and Bailey, 2003). Fibrils combine to form fibres. Crosslinks provide strength and stability of collagen structure and prevents solubilization and denaturation (Paul and Bailey, 2003; Nalyanya *et al*., 2016a). Crosslinking occurs at four specific locations: two at telopeptide region and two in the helical region. The telopeptide region of one collagen molecule is covalently linked to the helical region of its neighbouring collagen molecule through lysine based crosslinks (Nagan and Kagan, 1994). The characteristic conformation of collagen provides the molecule with resilience with the inherent strength of the collagen triple helix translated through a number of hierarchical levels to endow that tissue with its specific strong mechanical properties (Metreveli *et al*., 2010).

The interactions of collagen with tanning agents occur with the ε-amino group of lysine residues, the carboxyl groups of glutamic and aspartic acids, or with hydroxyl groups (Paul and Bailey, 2003). These groups project radially from the rod-like molecules, which are held in parallel alignment in the collagen fibre, thereby ensuring intermolecular and interfibrillar cross-linking. These cross-links prevent the molecules from sliding past each other under load and therefore increase the mechanical strength of the fibre but also dramatically affect the thermal and biological properties of the fibre. The nature and stability of these different chemical bonds produces a significant difference in the particular properties of the cross-linked product. The chemical cross-linking can increase the shrinkage temperature to over 100 °C depending on the nature of the cross-

linking agent. The cross-links are formed between amino and carboxyside-chains of the triple helical regions of the molecule and might be expected to stabilise the molecules against thermal shrinkage but shrinkage occurs to the same extent.

2.2.1 The primary structure of collagen

The primary structure of collagen is the polypeptide chain, a linear array of α-amino acid sequence (Ramshaw *et al*., 1998). The unique collagen's amino acid pattern, triplet Gly-X-Y repeats, where X and Y are generally proline or hydroxyproline while Gly- is the glycine (Haine, 1999; Ramshaw *et al*., 1998; Gelse *et al*., 2003). In this structural arrangement, glycine always occupy every third position due to steric constraints from the close packing of the polypeptide chains. The amino acids are held together in the polypeptide by the covalent peptide bond between amine group (NH_2) of one amino acid and the carboxyl (COOH) group of another amino acid (Akkus *et al*., 2004). Three polypeptides form a triple helix in the higher levels of structural organization around an axis. The patterns form 10% of the collagen molecule (Ramshaw *et al*., 1998; Gelse *et al*., 2003; Bozec and Horton, 2005).

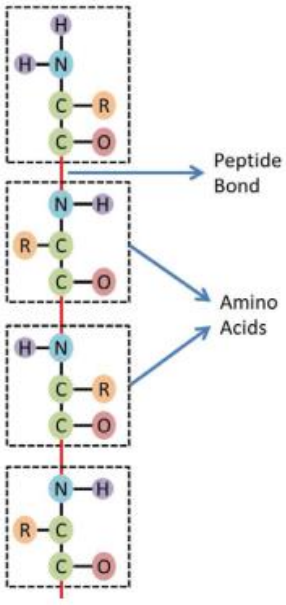

Figure 2.2: Primary structure of collagen showing the sequence of amino acid in the polypeptide (source: Karamanos et al, 2012).

The N-terminal and C-terminal sequences of the collagen molecule do not conform to the typical collagen triple amino acid repeat, and comprise about 2% of the molecule (Hulmes *et al*., 2002). Deviations from the standard Gly-X-Y repeating structure ensures that the collagen structure in these regions is significantly different, presumably due to the connectivity required between collagen molecules to give hierarchical strength to fibrils (Kadler *et al.,* 1996). Specific residues in these non-helical terminal regions are covalently bonded to the helical segment of an adjacent collagen molecule. As well as the major crosslinking between neighbouring collagen molecules, cross-linking also occurs between amino acid chains within a triple helix adding further stability to the assemblies (Malone and Veis, 2004). The amino (N-terminal) and carboxyl (C-terminal) telopeptides of type I collagen play crucial roles in the assembly of collagen fibrils, regulating the axial alignment of the molecules within a fibril, orientation of neighbouring molecules, and cross-link formation (Hulmes *et al*., 2002).

2.2.2 The Secondary structure of collagen

Amino acid sequence twists or folds to form secondary structure of collagen. The major two secondary structures are alpha helices and beta-pleated sheets. The main secondary structure for collagen is the alpha helix with a left handed twist (Gelse *et al*., 2003). Although the secondary structure of collagen remains stable when the water molecules are unavailable to support the hydrogen bonding network, the mechanical properties of the collagen are usually affected (Gautieri *et al*., 2012). The *in vivo* collagen structure consists of approximately 50% water with subsets of water populations which surround individual triple helices, fill the gap zone in the hydrated state and surround the fibrils and this water may be bound to the collagen molecule, or unbound with layers of "free" molecules (Mogilner *et al*., 2002). The triple helix of collagen is held together, in part, by the formation of water bridges which act as a stabilising factor in holding the three helical a-chains together (Bella *et al*., 1995). Oxygen atoms of water are linked to the peptide chain by water bridges (Bella *et al*., 1995; Mogilner *et al*., 2002). The water molecules bind to collagen through hydrogen bonds forming a cylindrical lattice-like structure around collagen (Bella *et al*., 1995). Three water shells surround the collagen triple helix. The first level hydration shell contains water molecules that are hydrogen bonded to amino acid groups of the triple helix. The second level hydration shell contains water molecules that are connected by hydrogen bonds to the water

molecules in the first shell. The third outer hydration shell includes water molecules that are bonded to the inner second shell (Bella *et al*., 1995). Many studies on the hydration of collagen have shown that the presence of water is essential in maintaining the overall native structure of collagen and the absence of water is known to cause many structural changes in the arrangement of collagen.

2.2.3 The tertiary structure of collagen (Triple helical structure)

Three collagen molecules (polypeptide) supercoil in a right hand manner into a triple helix (tropocollagen) around a common axis forming a tertiary structure (Rich and Crick, 1961). The three polypeptide chains forming triple helix are staggered by one residue in which the N- and C-residues are aligned (Akkus *et al*., 2004). Each of the collagen molecule is identified by its primary structures termed alpha chains and the chains with different primary structures are numbered with Arabic numerals e.g. α-1, α-2. For instance, collagen type I triple helices are composed of two α-1 chains and α-2 chain (Lee *et al*., 2001). A α-1 collagen molecule is composed of 1014 residues and a α-2 is composed of 1023 residues as shown in the figure 2.3 (Kucharz, 2011).

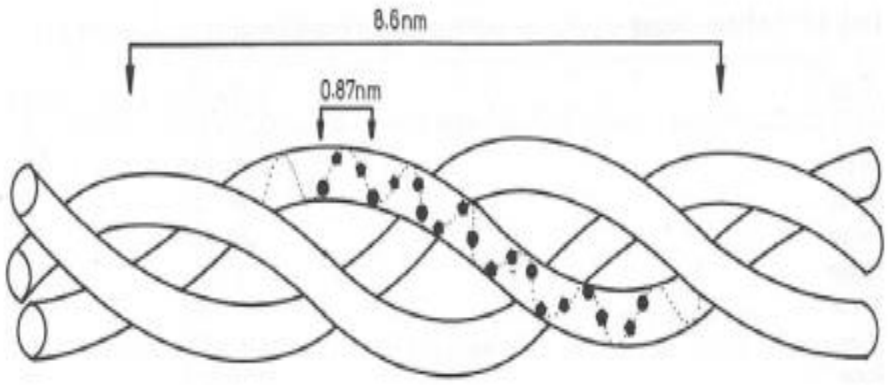

Figure 2.3: The collagen triple helix (tropocollagen) (Source: Kucharz, 2011).

The formation of triple helix is stabilized by the intramolecular crosslinks that link two alpha chains within the same molecule or intermolecular or covalent bonds between chains in different molecules. For instance, hydrogen bond crosslinks, formed between the N-H of the glycerine residues of one chain and C=O of the proline residues of another chain stabilize triple helices. Not

every peptide group participates in the hydrogen bonding, a reason why triple helix is not an alpha helix. A strong interchain hydrogen bond exists in every Gly-X-Y triplet between the NH of Gly in one chain and the C=O of the residue in the X position of the neighboring chain (Rich and Crick, 1961). Similarly, whenever a proline does not occupy the X position of the Gly-X-Y peptide triplets, a second interchain hydrogen bond usually forms between the NH group of the X position residue and the C=O of the glycine residue mediated by water molecule (Kramer *et al*., 1999; Kramer *et al*., 2000; Emsley *et al*., 2000). The hydration of the collagen provides these additional hydrogen bonds with hydroxyproline or its side chains. For every triplet, maximally six water molecules are involved in the hydrogen bonding network (Miles and Ghelashvili, 1999).

2.2.4 The Quaternary structure of collagen (Fibrillar structure of collagen)

Quaternary structure of collagen is the repetitive arrangement of five staggered tropocollagens relative to one another. This repetitive arrangement produces overlaps of adjacent triple helices and gaps between one triple helix with the preceding triple helix forming bands of collagen as shown in figure 2.4.

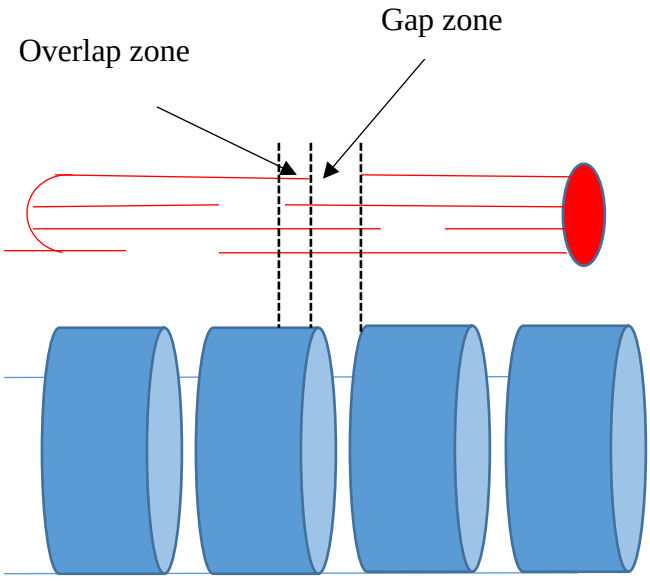

Figure 2.4: Longitudinal tropocollagen assemble into collagen fibrils with a 6.7 nm D-spacing that includes an overlap and a gap region.

Many experiments have determined that the axial periodicity or D-spacing is approximately 67 nm and each tropocollagen is approximately 4.4 D periods in length. The exact molecular periodicity of collagen fibrils contains 234.2 amino acids per D repeat (Sizeland *et al*., 2015). The stability of the quaternary structure and hence mechanical is dependent on the intermolecular crosslinks especially the hydrogen bond between the amino acid sidechains and the collagen mainchains and those bonds mediated by the water bridges (Bella *et al*., 1995). The content of hydroxyproline sequence, which has intrinsic water bridges, increases the mechanical stability of the triple helix collagen (Engel *et al*., 2013). Generally, five collagen triple helices (tropocollagen) aggregate in an organized fashion into fibril structure also known as five stranded Smith microfibril. An assembly of five triple helices in a filamentous structure with a 4 nm diameter, is an intermediate (microfibril). The aggregation of these triple helices occurs in a quarter staggered fashion (figure 2.5).

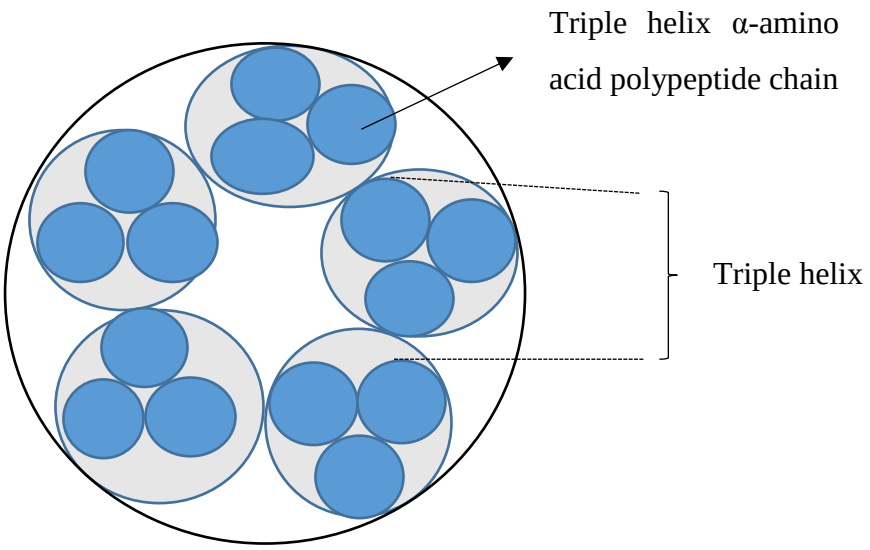

Figure 2.5: Organization of five triple helices in the cross-section of a Microfibril.

Tetragonal lattice of microfibril forms subfibril. Longitudinal and lateral aggregation of collagen subfibrils results in the formation of fibrils. These fibrils are cylindrical in shape with a diameter of 10-500 nm. The morphology of the fibril *in vivo* is defined by extracellular spaces at the surface of specific cells. Collagen fibrils possess a right-handed helical twist. Collagen fibrils form complex networks that can be linked to the physical properties of the material (Fratzl *et al*., 1998). The arrangement of collagen fibrils, particularly the extent of alignment or anisotropy, is an important contributor to the strength of the collagen material. The structure-function relationship

between collagen alignment and mechanical properties has been elucidated for a range of tissue types (Purslow *et al*., 1998; Liao *et al*., 2007). The orientation of collagen measured edge on (alignment in-plane) has been shown to be correlated with strength in a range of mammal skins processed to leather (Basil-Jones *et al*., 2013).

2.3 Leather processing

Hides and skins are highly putrescible materials and hence leather making process is a way of preserving hides from decomposition and subsequently improving its strength and flexibility. The process is a complex series of both chemical treatment and mechanical processes. Each of the treatments and mechanical processes alter the composition and structure of the final leather (Wess and Orgel, 2000; Maxwell *et al*., 2006). Among the best available techniques (BAT), leather processing is divided into three major operations: pretanning (beam house), tanning (tanyard) and post-tanning (crusting) (Musa and Gasmelseed, 2013b). However, a further operation exists and is called finishing operation or surface coating.

2.3.1 Pretanning (Beamhouse/preparatory/lime yard) operations

These processes are aimed at cleaning the hides/skins and preparing them for tanning (Covington, 2009; Musa and Gasmelseed, 2013b). They may include processes such as curing, soaking, and liming, deliming, dehairing and pickling.

Curing process

Usually, the hides/skins received in the tannery are of four categories: either fresh immediately after flaying, wet salted, dry salted or dried. The method of curing depends on the climate, country of origin and cost considerations. Salting is the most common type curing, that gives cattle hide temporary preservation. It's done with either solid salt or brine solution although solid salt is more preffered globally (Kesarwani *et al*., 2015).

Soaking process

This stage removes salts used during curing by rehydrating the hide from 45% to 55%. The unwanted materials such as dung, blood, soil, dirt, body fluids, mud, soils, salt, hyaluronic acid

and interfibrillary materials are also removed. The process is carried out in three steps: dirt soaking to remove the salts and dirt, main soaking to rehydrate the material and the final soaking where only water is used to remove all the salts associated with preservation. During main soaking, detergents, sodium poly sulphide, surfactants are added to accelerate the wetting of the fibre surface and increase soaking efficiency since they provide for appropriate pH of 9.0 – 10.0 (Kesarwani *et al*., 2015). Rehydration also helps opening up of the fibres preparing the collagen for subsequent liming process. Biocides are also added to curtail the putrefying bacterial activity. The duration of this process can range from few to several days depending on the size and the degree of drying of the raw stock (Sharphouse, 1983; Sarkar, 1991).

Liming and dehairing process

Liming facilitates removal of hair, flesh, fats (partially), and epidermis and interfibrillar proteins and opens up the fibrous structure for osmotic swelling. The process can be classified into two broad activities:

a. Dehairing by liming: This involves use of 8-10% sodium sulphide combined with suitable enzymes (bating) applied to the skin/hide. Lime dissolved in water and applied on the hide acts to break down and solubilize the hair keratin. These together break down and remove some of the non-fibrous proteins, glycosaminoglycans and other undesirable components. Lime or alkali disrupts hydrogen bonding between fibrils resulting in an opening up of the structure making available more acid and alkaline groups on the hide for subsequent chemical interactions (Sivakumar and Rao, 2001).
b. Reliming: Soda ash and caustic soda are applied to open up fibrous structure to enable better penetration of tanning chemicals in subsequent stages (Germann, 1997). In the process, the pH rises to 12-12.5.

Fleshing and scudding

Fleshing is the mechanical scrapping off of the excessive organic materials from the hide such as connective tissues and fats.

Deliming process

After liming process, the remaining lime and other alkali are no longer significant. Therefore, the pH needs to be lowered. Deliming involves gradual lowering of the pH by: washing in fresh water, adding weak acidic solutions, salts such as ammonium or calcium hydroxide or boric acid, increasing temperature, and removal of residual chemical and degraded skin components (Cassano *et al*., 2001). Lowering pH to 8.5-9.0 is ideal for the enzymatic digestion during bating. The ammonium salts and calcium hydroxide have appreciable buffering effect at the pH of interest and quickly penetrate into the cross-section of the pelts. This process also de-swells the pelt. The extent of deliming depends on the nature of the expected final leather such that thorough deliming results in a softer leather whereas partial deliming gives firmer leather (Cassano *et al*., 2001; Kesarwani *et al*., 2015).

Bating process

Dehairing process usually leaves some residual hair roots and pigments that are not desirable. Bating removes non-leather forming proteinous materials like albumins, globulins, scuds/short root hairs, epidermis, protein degradation products, and the scud on the surface of the skin and in the hair follicles and pores, pigments and mucoid from hides. Bating is an enzymatic action for removal of unwanted hide components. Bating allows splitting of collagen fibres and help penetration of tanning agents and other processing chemicals thereby giving the finished leather the desired feel, softness, pliability and other desired characteristics. This process takes from few hours to overnight depending on the type of the leather at preferred temperature of 37 °C and pH of 8.0-9.0 (Valeika *et al*., 2010). Contemporary bating involves use of enzymes (usually proteases) to catalyze hydrolysis of non-structured proteins. Bating usually de-swells swollen hide and prepares it for tanning process (Nalyanya *et al*., 2015). The process also increases degree of stretch, making the grain surface of the finished leather clean, smooth and fine.

2.3.2 Tanning operations

These are set of operations in the tanyard aimed at converting the skin/hide from the soluble pelt into an insoluble fibrous crust leather (Sharphouse, 1995). These operations stabilize the collagen fibres to prevent putrefaction of the raw material through crosslinking of the structure of the natural collagen (Sarkar, 2005). The operations introduce the properties that are required by the end user and prepare the material for other chemicals used during further treatments (Covington, 2009).

The operations involve pickling and tanning processes which form the main processes in leather manufacturing (Valeika et al, 2010).

Pickling process

This process is aimed at correctin the pH to the level suitable for tanning operation and to prevent swelling of the hide i.e. dehydration using salts and acid. Water (80%), salts (8-10%), formic acid (0.28-0.30%) and sulphuric acid (0.75-2%) based on the thickness are applied (Hui et al, 2010). Addition of formic and sulphuric acids helps to reduce the pH to typical value range of 2.8-3.5 prior to tanning. Pickling also sterilizes the hide, bringing to an end the bating process and improving subsequent penetration of tanning agents (Roig *et al*., 2012). Since the acids cause undesirable non-reversible swelling that disrupts hierarchical structure of collagen, salts, notably sodium chloride, are added to inhibit this action (Covington, 2009). Synthetic, organic crosslinking agents and surfactants are often added at this point assist in the subsequent stages (Pizzi *et al*., 2004; Zengin *et al*., 2012).

Tanning process

Tanning involves stabilization of the collagen matrix to retain separated fibre structure, increase hydrothermal stability, and stabilization of hide against enzymatic attack and thermo-mechanical stress (Hui *et al*., 2010; Roig *et al*., 2012; Zengin *et al*., 2012; Nalyanya *et al*., 2015a, Nalyanya *et al*., 2015b). The hide's collagen fibre is stabilized by the tanning agents to make the hide less susceptible to putrefaction or rotting (Pizzi *et al*., 2004; Covington, 2009). The stabilization is due to the crosslinking action of the tannages that enhance the hide's dimensional stability, mechanical strength, durability, resistance to heat and fastness (Chahine, 2000; Tegtmeyer and Kleban, 2013; Devikavathi *et al*., 2014). There are numerous tanning agents such as mineral tannages, vegetable tannins, syntans (synthetic organic tanning materials), aldehydes and oil tannages. Among the mineral tannages, Chromium tanning accounts for more than 90% of the tannage globally (Roig *et al*., 2012; Tegtmeyer and Kleban, 2013; Devikavathi *et al*., 2014). This is due to the versatility, unique and excellent physical properties and thermal resistance of shrinkage temperature as high as 104 ^{0}C that it confers (Roig *et al*., 2012; Musa and Gasmelseed, 2013a; Beghetto *et al*., 2013). The excellent power of chromium lies in its high capability, during olation process, to form

polymeric oxydrillic-bridged compounds that are allowed to coordinate and crosslink the collagen protein whose carboxyl groups that act as ligands into the chromium complex themselves (Covington, 2011). Although vegetable tanning has advantages such as comfort, compatibility with skin, high dimensional stability and ease of disposal, it lacks softness as it is very hard and firm and also lacks the affinity for anionic fat liquors. Vegetable tanned leathers also lack the customers' required degree of hydrothermal stability.

Application of Cr (III) salts interact by chemical bonding with the carboxylic groups of collagen in the hide, giving to the leather the strength and stability properties (Roig et al, 2012). Under some circumstances, these Cr (III) salts are partially oxidized to Cr (VI), a carcinogenic compound, which has considerable impact on the environment and human health (Roig *et al*., 2012). Exposure to Cr (VI) causes nausea, diarrhea, liver and kidney damage, dermatitis, internal hemorrhage and respiratory problems. Inhalation may cause acute toxicity, irritation and ulceration of the nasal septum and asthma or respiratory sensitization (Devikavathi *et al*., 2014).

Direct sources of Cr (VI) salts are contaminations in Cr (III) tanning agents, certain class of metal complex dyes and inorganic pigments based on lead chromate. Sometimes the tools, substances, auxiliaries, chemicals and process parameters contribute significantly to the conversion of Cr (III) into Cr (VI) (Devikavathi *et al*., 2014). The oxidizing agent present in the specialty chemicals used for leather making can lead to the formation of Cr (VI) under storage conditions well above the permissible limits. The fatliquors based on vegetable or animal oil such as fish oil and soya oil have the potential to trigger the formation of Cr (VI). The double bonds in fatliquor base are prone to be attacked by oxygen. Oxidation leads to formation of radicals and hydro peroxides. Peroxides formed are likely to react with the Cr (III) and convert it into Cr (VI) (Devikavathi *et al*., 2014). Studies show that subjecting leather to a heat treatment of 80 °C for 16 hours causes formation of Cr (VI) up to 46 mg/kg or ppm (Devikavathi *et al*., 2014).

2.3.3 Crusting or post tanning or wet finishing operations

These operations follow the tanning processes. They involve both mechanical and chemical processes, although, in this study, only the chemical processes were considered. The chemical operations include basification, neutralization, retanning, dyeing and fatliquoring processes (Ali *et al.,* 2013). These operations are an important part in the leather manufacturing process for they

impart bulk properties into the leather and greatly improve organoleptic properties (Fathima et al, 2010).

Basification and neutralization

After tanning, the pH needs to be raised to 3.8-4.0 (from 2.5) by mild alkali, usually Sodium Bicarbonate. The pH range is a suitable level for retanning, dyeing, and fatliquoring due to increased reactivity of the hide to the Chromium compound at a pH > 3.0. Hence basification and neutralization act to remove the acid liberated after tanning and aging, to remove neutral salts and unfixed/soluble/free chromium present in the leather and to increase the pH for the required product type thereby facilitating better penetration of syntans, dyes, and fatliquors (Covington, 2011).

Retanning process

After the pH is uniformly adjusted along the cross-section, a retanning process is frequently performed to correct the properties of the leather, thus defining its final character. Such a transformation is mainly to obtain the desired qualities in the final article, and different tanning chemistries can be used here on the main tannage. Although they do not strictly enter the tanning agent definition, hydrogen bondable polymers may be employed for this purpose, often to fill up the weaker/loose areas of the hides (flanks) and belly and produce more even leather, or a particular handle. A study by Ali *et al.* (2013) has shown that retanning improves wetting back property (susceptibility to rehydration) of hides especially during the dyeing process and increases resistance to alkali and perspiration. The rehydration helps to improve the penetration of anionic type of fat liquors, dyestuffs and finish adhesion. The results were echoed by Musa and Gasmelseed (2013a) who found out that retanning increases the cutting value or desirable area after filling even at belly/flank area. It was also observed that retanning reduces the shrinking of crust during drying.

Dyeing process

Dyeing is one of the stages in leather manufacturing during which base colour is applied on leather to avoid broken finishing coat (Kusumwati *et al*., 2016). The leather is desirably colored using dyestuffs such as anionic dyes, acid dyes, metal complex compounds and basic dyes. Dyestuffs,

which are mainly of azoic nature is to impart the color as desired by the customer or marketing and sales forecast. The introduction of one or more sulphonic functional groups is necessary to make the molecules water soluble and to allow an electrostatic bonding with the cationic amino groups of collagen. For a good penetration, the reactivity of the substrate is minimized by raising the pH value, while fixation is obtained by lowering it, typically with the formic acid. This plants the base color before finishing for grain based finished articles and gives an aesthetic look to final/finished leather (Candar *et al*., 2008).

The most commonly used dyes are permanent dyes, which are oxidative. Within these types of dyes, there are a complex mixture of a variety of different ingredients which will vary based on the type of dye. However, there are three types of ingredients found in nearly every dye. The first is a primary intermediate. These tend to be either p-diamines or p-aminophenols, such as para-phenylenediamine (PPD) or para-aminophenol. The second type includes hydrogen peroxide (H_2O_2) and an alkaline agent such as ammonia (NH_3) or ethanolamine (C_2H_7NO). The hydrogen peroxide both lightens the pigments naturally found in hair and acts as the oxidizing agent for the primary intermediates. The alkaline agent is used to raise the pH so that the hair cuticle expands, allowing for the dye molecules and the H_2O_2 to move into the cortex. The third type of component is a color coupler. Many of these molecules are aromatic alcohols, some with amino groups in different positions around the ring. These precursors help to give the dye their color.

Once the dye is applied, these precursor molecules react with the oxidized primary intermediate (when these intermediates do not couple to themselves) to produce other dye molecules. This occurs via an azo coupling reactions. The first step of this, is the oxidation of the primary intermediate (in this case para-phenylenediamine) to form a di-immine structure. Two equivalents of this oxidized form then reacts with one equivalent of one of the color couplers (in this case 3-aminophenol), resulting in the complex dye structure. As a result, at the time of application, there are many different components in the hair dye that interact with and move into the cortex of the hair (Redgrove *et al*., 1939).

Fatliquoring process

This process involves introducing fatty matters or/combination of fatliquoring agents such as sulphonated or sulphate oils that react with the fibrous structure of collagen to replace natural oils

lost in beam house and tanning processes. It's performed in a drum using an oil emulsion at temperatures of about 60 to 66 ^{0}C. It creates a sliding effect of the fibres and elasticity (Gutters and Santos, 2009; Zengin *et al.*, 2012). The sliding effect and elasticity makes leather soft, supple (flexible) and water resistant (Ali *et al.*, 2013). The oils used may be of animal or vegetable origin or may be synthetics based on mineral oils. This step lubricates the leather fibers so as to reduce internal friction while in use and to increase durability. Fatliquoring also forms physical or chemical crosslinks between the fibers, thereby to avoid collapsing or sticking even after drying. It also helps to achieve softness, pliability, stretch, compressibility and tensile strength. A study by Sizeland *et al*. (2015) has shown that fatliquoring process increases D-spacing of collagen.

2.3.4 Finishing operations

Finishing improves the leather wear properties in general and to protect it from wetting and soiling, to level out patches and garin faults, to apply an artificial grain layer and modify surface properties such as shade, luster and handle (Jankauskaite et al, 2006). Even after fatliqouring, without additional mechanical force, the fibres can still stick together making the leather rigid and hard (Liu *et al*., 2007). Therefore, the leather must be physically conditioned by staking and/or milling. Staking is a mechanical method that increases the pliability and softness of the Leather. The hide travels through the machine on a conveyor belt and is pounded by several thumb-sized rounded pins that stretch the fibers in every direction, thus separating the fibers and softening the leather. Finishing operations consist of surface operations to enhance the natural qualities of the skin and cover imperfections eventually present on the surface. Mechanical protection, evenness of color and touch properties are the main requirements for finishing. A number of acrylic, polyurethane and other film-forming synthetic polymers are common ingredients of finishing recipes; they are mixed with natural substances, both native and modified, like oils, waxes, caseins, albumins, cellulose esters and others. They include setting out, drying, conditioning, staking, dry milling, buffing, spray finishing, and plating. At this stage, the wet blue leather is referred to as crust. Setting removal of excess water and spreading the hide out prior to drying. Drying is aimed at drying the leather and optimizing the quality and the area yield. There are several methods of drying depending on the type of leather being produced. Upholstery leather is normally toggle dried (spreading the leather over expanding frames held by "toggles" or clips) hence the clip marks

around the entire hide. Drying techniques include sammying, hang drying, vacuum drying, toggle drying and paste drying. Sammying (squeezing between rollers) and setting are used to reduce the moisture content mechanically. Staking is a mechanical softening of the crust after drying, to make it more pliable. The hides may also be softened by milling which is dry tumbling with atomized moisture injected into the tumbler.

Milling is a physical softening process in which leather is tumbled in a dry drum Fitted with wood dowels with atomized moisture injected into the tumbler (Liu *et al*., 2007). Milling process softens leather for adequate compliance. This impacts on pliability and other properties of concern to the leather industry, such as mechanical strength and toughness. It's shown that milling leads to decrease in Young's modulus and tensile strength, consequently an improved hence increased compliance and softness (Liu *et al*., 2007). Liu *et al*. (2007) also showed that milling the structural change associated with this process results into removal of the residual stress introduced during other leather making processes.

2.4 Physical properties of leather

It has been found elsewhere that the physical properties of leather are formed on macro-level of collagen structure (Kozar et al., 2014). Leather products are rated on the basis of their performance requirements in terms of functional and aesthetic values that it possesses (Urbanija *et al*., 2004; Ork *et al*., 2014). These physical and organoleptic (hand or sensorial character) properties form essential index of assessing the utility of the final leather or quality indicators (Ali *et al*., 2013; Kozar *et al*., 2014). Physical properties determine the functionality of the end products and hence the routine quality and serviceability assessment of the material, leather's usability, the state of usage, and inform the entire process of manufacturing goods from leather (Valeika *et al*., 2010; Basil-jones *et al*., 2013; Nalyanya *et al*., 2015). These properties are deemed more important than chemical stability to a consumer (Valeika *et al*., 2010). Therefore, these properties remain vital indexes in assessing the utility of the leather for various applications (Ali *et al*., 2013; Ibrahim *et al*., 2013; Kozar *et al*., 2014). Therefore, determination of these properties is vital.

Leathers should possess appropriate physical properties depending on their fields of applications (Jankauskaite et al., 2006; Ork *et al*., 2014; Mutlu *et al*., 2014). For the applications of gloves and

clothing, the leather must be very soft, thin and extensible while for footwear it must be rigid and hard and stiff for soles (Jankauskaite et al., 2006). The physical properties include resistance to heat (shrinkage temperature), flexural resistance and endurance, grain crack resistance, tear and tensile strengths, viscoelasticity, elongation, and distension, crack endurance and strength (Ashebre, 2014; Negussie *et al*., 2015; Nalyanya *et al*., 2016). These properties are determined by the quantity of skin constituents (follicles, glands, and erector muscles), the amount of collagen fiber bundles, collagen fibril orientation, fibril diameter, orientation index and leather processing steps affect these properties (Jacinto *et al*., 2004; Nalyanya *et al*., 2015a). The features closely correlate with the thickness of the collagenous fibers bundles, their spacing and angle of weave (Zapletal *et al*., 1996; Valeika *et al*., 2010; Ashebre, 2014; Inanc and Gulumser, 2015).

2.4.1 Tensile strength

This is the longitudinal stress that the leather material can bear without tearing apart. It is the capacity of a material to withstand loads tending to elongate it without fracture (Liu *et al*., 2015a). It measures the ability of a material to withstand pulling/tensile force, specifying the point when a material goes from elastic to plastic deformation. Quantitatively, this is expressed as the force per unit cross-sectional area in linear direction. It determines the structural resistance of leather to tensile forces hence its state and usability (SATRA, 2011; ESA, 2012). In collagenous material, this strength is the combined ability of all the fibres taking part to resist the applied load. In fact, the tesnsile strength is high when majority of the fibres are aligned in the same direction as the applied load (Salehi *et al*., 2013; Nalyanya *et al*., 2015). The tensile strength of leather is determined by the fibrous structures that constitute the collagen network structure and the modification of this structure by the tanning agents (Covington, 2009). Similarly, the orienatation of the fibres affects this strength (Salehi *et al*., 2013). The strength has shown high correlation with the thickness of the collagenous fibre bundles, collagen fibril diameter and their spacing (Zapletal *et al*., 1996; Wells *et al*., 2013). Any chemical or mechanical process that occur in leather structure has the potential to affect tensile strength and elongation (Nalyanya *et al*., 2016a). The ISO 3376: 2002 test method accepts minimum requirement for the tensile strength as 15 N/mm^2 (Ashebre, 2014). The acceptable standard recommended by UNIDO for chrome-tanned shoe upper side leathers is 20 N/mm^2 (Inanc and Gulumser, 2015).

2.4.2 Percentage elongation

This is the ability of leather material to stretch under tensile forces without breaking (Nalyanya *et al*., 2015). It determines the elasticity of the material. It's expressed as the change in original gauge length divided by the original gauge length. Upper leather and footwear upper should possess high flexibility to prevent the appearance of cracks and tears in the ball area (SATRA, 2011; ESA, 2012). High elasticity allows the material to withstand the elongation stresses to which it is subjected to during footwear lasting, especially on the toe area (INESCOP, 2013). It's determined closely by fibrous quality of the leather (Valeika *et al*., 2010). The ISO 3376: 2002 test method and UNIDO recommend a minimum requirement for the percentage of elongation for chrome-tanned of greater to be 40% (Ashebre, 2014; Inanc and Gulumser, 2015). Elongation is an important property to be considered when choosing garment leathers because a low elongation value results in easy tear while a high elongation value causes leather goods to become deformed very quickly or even loose usability (Ork *et al.,* 2014). Leathers that have a lower tensile strength have a lower percentage elongation and vice versa. Good quality leathers should have a minimum percentage elongation of 40% (Roigi, 2012).

2.4.3 Baumann Tear Strength/ Slit Tear resistance

It is a measure of how well a material can withstand the effects of tearing forces or growth of any cuts when under tension, calculated by the maximum force or average of the peak forces in Newtons per unit thickness of the material in mm (Nalyanya *et al*., 2015). In the leather fracture behavior, deformation and crack growth, this strength measures the resistance to the formation of a tear (tear initiation) and its corresponding expansion or growth (tear propagation within the structure). The least recommended tear strength for chrome-tanned shoe upper side leathers is 40 N/mm (UNIDO, 1996; Roig *et al*., 2012; Liu *et al*., 2015a). In this test, the specimens were cut and tested in accordance to ISO 3377:2002. This property also depends on the viscoelastic and other dissipative processes occurring in the material since it is contributed by the elastin and collagen bundles in the hide (Salehi *et al*., 2013). Tear strength in bovine hide has been shown to correlate with collagen fibril diameters, collagen content, collagen fibril orientation and orientation index (OI) which vary significantly with the sampling position (Wells *et al*., 2013; Basil-Jones *et al*., 2013). Stronger leather has the fibrils arranged mostly parallel to the plane of the leather

surface (high OI), while weaker leather has more out-of-plane fibrils (low OI). High tear strength is due to interweaving and crosslinking of the fibre bundles (Basil-Jones *et al*., 2013; Wells *et al*., 2013). This is governed by the angle of weave, for instance, high tear strength is due to lower angle of weave. Additionally, fibre density aids tear strength as a result of the greater number of fibres available to bear the load. The ISO 3377-2: 2002 test method ascertains the minimum average tear load of leather upper of a typical footwear should be greater than 50 N/mm while UNIDO recommends a minimum for chrome-tanned shoe upper side leathers are 40 N/mm for minimum tear strength.

2.4.4 Grain crack and grain burst

This is a physical quality of leather that determines the grain resistance to cracking during lasting of the shoe uppers upon being folded. It indicates a level of elasticity derived from the specific processing step. he threshold recommended values for grain crack and grain burst for upper leathers is 6.5 mm and 7.0 mm, respectively (Roig *et al*., 2012). This method is applicable to all flexible leathers and it is particularly suitable to determine the lastability of leathers for footwear uppers as per ISO 3379:2015.

2.4.5 Flex resistance and endurance

Bally flex or pliability is an indication of the finishing resistance to crack and crease when repeatedly flexed, emulating the flexing of the actual use of the shoe. Flex is an inevitable encounter for majority of leather applications such as footwear at the vamp, toe and heel bends, hence a prerequisite property for any leather meant for footwear upper to endure a predetermined number of flexes to gain qualification. Flexing endurance of leather measures, the ability of leathers and leather-cloth to withstand repeated flexing without cracking. The ISO 5402: 2003 test method embarked that the performance requirement for the ball flex/linear flex to be no significant damage at 150K cycle at dry stage (Ashebre, 2014). The ISO 22288: 2003 test method illustrated that the performance requirement for the ball vamp flexes to be no damage for a minimum of 250 K cycles (Ashebre, 2014).

2.4.6 Distension, crack endurance and strength of the grains of the leather

Lastometer is a very important indicator of the ability of leather grain to withstand lasting operation during shoe making without cracks. These properties measure the `lasting' qualities and endurance of upper leathers (Negussie *et al*., 2015).

2.4.7 Shrinkage temperature (Ts)

This is a parameter used to characterize the thermal stability of leather. It's the temperature at which the leather starts to shrink in water or over a heating medium and it the temperature at which the energy input (heat) exceeds the energy bound in existing hydrogen bonding of the collagen structure resulting in the decomposition of the helical structure (Ali *et al.,* 2013). Shrinkage is simply the rupture of the hydrogen bonds (Paul and Bailey, 2003). It determines the degree of crosslinking in leather by the tanning agents, since the higher the degree of crosslinking, the higher the shrinkage temperature (Heidemann, 1993). The threshold of the shrinkage for a quality leather is 75 ^{0}C (Liu *et al*., 2015b). Due to this, the shrinkage temperature remains as important index, which reflects quantity of new bonds formed in collagen and quality of tanning and tanned leather. Usually, users of leather, as raw material for shoes, garment or other, require the shrinkage temperature of leather to be not less than 100 °C (Ali *et al*., 2013; Ibrahim *et al*., 2013). Such temperature is reached lightly when chrome compounds use in tanning process (Valeika *et al.*, 2010).

When collagen is wet, the matrix can be degraded by rising temperature, at the same time hydrogen bonds in the triple helix are broken, observed as shrinking, leading to gelatinization. Dimensional change under the action of heat on leather is an important characteristic feature (Nalyanya *et al*., 2016b). The hydrothermal stability of the wet white (tanned) leather is the measure of the leather to resist against hot water. This analysis is helpful in determining the suitability of the wet white leather for the production of crust as well as finished leathers. Hydrothermal stability is characterized by a shrinkage of the hide when heated in water at a defined temperature while denaturation characterizes transition taking place in the collagen crosslinks from triple-helix to randomly coiled form (Chahine, 2000; Ali *et al*., 2013; Ibrahim *et al*., 2013). The bonds which stabilize the super helix are hydrogen, hydrophobic, van der Waal's bonds and interactions between

oppositely charged residues on side chains (Chahine, 2000). The non-random distribution of ionizable and hydrophobic side chains along the repeating unit results in the occurrence of charged and hydrophobic patches that contribute to stabilization of the structures through electrostatic and hydrophobic interactions. On the other hand, hydrogen bonded water plays a big part in the stabilization of the molecule. All these non-covalent bonding break down on heating, starting at the weakest points of the helix, between the stabilizing clusters. A small region containing a few linkages of low energy will act as a favorable site to initiate denaturation. Covalent bonds increase the size of cooperating units through inter- and intramolecular cross-links and increase the temperature of denaturation (Td) (Nalyanya *et al*., 2016a). Alongside the type of the hide, the processing steps involved in leather manufacturing affect these temperatures due to scissions and crosslinking (Fathima *et al*., 2006). Therefore, these properties remain vital indexes in assessing the utility of the leather for various applications and the suitability of leather technology used (Ali *et al*., 2013; Ibrahim *et al*., 2013).

2.5 Theoretical models and empirical relations

Einstein (1956) developed an equation that theoretically relates the Young's modulus of matrix with that of the composites filled with spherical fillers as shown in equation (2.1)

$$M_c = M_m\left(1 + 1.25V_f\right), \tag{2.1}$$

where M_c and M_m are the Young's moduli of composite and matrix, respectively, and V_f is the particle volume fraction. This model assumes a perfect adhesion between the filler and matrix and no interaction between the particles (Islam *et al*., 2013). Hence, equation (2.1) is only valid for low volume fraction of the fillers and does not consider any inter-particle interactions (Fu *et al*., 2008). Guth (1945) considered a case where the particle interaction is inevitable at high volume fraction. He modified Einstein's equation to Equation (2.2)

$$M_c = M_m\left(1 + 2.5V_{f+}14.1V_f^2\right). \tag{2.2}$$

Further, Kalaprasad *et al*., (1997) showed that equations (2.1) and (2.2) are related to tensile strength,$\mathcal{E}_c$, of the composite as shown in Equation (2.3).

$$\mathcal{E}_c = \mathcal{E}_m\left(1 - V_f^{2/3}\right), \tag{2.3}$$

where, $£_m$ is the tensile strength of the matrix.

For poorly bonded fillers, where stress cannot be transferred from the matrix to the filler, the strength of the composite is purely from cross sectional area of the load-bearing matrix in the absence of the fillers. Danusso and Tieghi (1986) and Levita *et al*., (1989) considered this case and proposed a simple expression to predict composite strength as shown in Equation (2.4).

$$£_c = £_m(1 - V_f), \tag{2.4}$$

where $£_c$ and $£_m$ are, respectively, composite strength and matrix strength and V_f filler volume fraction. Equation (2.4) implies that the composite strength decreases linearly with filler concentration. For poorly bonded fillers, Nielsen (1966) proposed an equation that predicts the strength of the composite, given by Equation (2.5).

$$£_c = £_m\left(1 - V_f^{2/3}\right)Q, \tag{2.5}$$

where parameter *Q* accounts for weaknesses in the structure caused by discontinuities in stress transfer and generation of stress concentration at the interface. The greater the value of *Q*, the lesser the stress concentration. The theoretical maximum value of *Q* is unity. He also proposed a basic equation to determine composite elongation at break shown in Equation (2.6).

$$\epsilon_c = \epsilon_m\left(1 - V_f^{1/3}\right). \tag{2.6}$$

Piggot and Leidner (1974) developed a model in terms of the stress concentration that is used to determine the tensile strength of composite. They proposed a relation given by Equation (2.7).

$$£_c = £_m(1 - BV_f). \tag{2.7}$$

The parameter *B* in Equation (2.7) accounts for the weakness in the structure due to stress concentration. When *B* = 0, it implies that adhesion between matrix and filler is poor with voids. In this case, the filler occupies the voids without having any influence on the mechanical properties of the composites due to the absence of adhesion at the interfacial boundary. Guptha and Purwar (1984) used porosity theory; the specific change in tensile strength is directly proportional to porosity, *P* i.e. $-\frac{d£}{£} = aP$, where *a* is the proportionality constant, and the negative sign represents the decrease in tensile strength with an increase of porosity. Replacing the porosity with filler volume fraction and integrating leads to expression given in Equation (2.8)

$$£ = £_m \exp(-aV_f). \tag{2.8}$$

The proportionality constant *a* is related to the stress concentration; the higher the value of *a*, the greater the stress concentration effect and the poorer the adhesion. Nicolais and Narkis (1971) considered poor adhesion of particles and proposed a model given by Equation (2.9)

$$£_c = £_m\{1 - aV_f^b\} \tag{2.9}$$

The constants *a* and *b* depend on the shape and arrangement of the fillers. For the case when adhesion is ignored, *a* = 1.21 and *b* =2/3. When adhesion is factored, equation (2.9) becomes

$$£_c = £_m\left\{1 - KV_f^{2/3}\right\} \tag{2.10}$$

The parameter *K* in Equation (2.10) accounts for adhesion between filler particles and the matrix; the lower the value of *K*, the better the adhesion. For perfect adhesion, the strength of the composite is equal to the strength of the matrix. The theoretical value of *K* for extreme case of poor adhesion is *K*=1.21. Hence for a hypothetical case where there is no adhesion between the interface, Nicolais and Narkis (1971) modified Equation (2.10) to give Equation (2.11)

$$£_c = £_m\left(1 - 1.21V_f^{2/3}\right) \tag{2.11}$$

Leidner and Woodhams (1974) considered the contributions of particle/matrix friction and residual pressure to the composite strength and proposed a model as shown in Equation (2.12)

$$£_c = 0.83pfV_f + k£_m(1 - V_f) \tag{2.12}$$

where *p* is pressure, *f* is friction coefficient, and *k* is relative change in strength of matrix due to the presence of the filler. The first term on the right side of Equation (2.12) is the friction contribution.

When some adhesion exists between the filler and the matrix, the interface can transfer a part of the stress to the particles, making a contribution to the composite strength. Bigg (1987) modified Equation (2.11) for better prediction of composite strength as shown in Equation (2.13)

$$£_c = £_m\left(1 - 1.07V_f^{2/3}\right) \tag{2.13}$$

Another study by Purkanszky *et al*., (1988) and Turcsanyi *et al*., (1988) proposed a model for very strong filler-matrix interfacial bonding as shown in Equation (2.14)

$$£_c = £_m\left(\frac{1-V_f}{1+2.5V_f}\right)\exp(BV_f) \tag{2.14}$$

where *B* is an empirical constant, which depends on the surface area of particles, particle density and interfacial bonding energy. This parameter characterizes the degree of particle matrix reinforcement and hence adhesion (Svab *et al*., 2005). The value of *B* increases with specific surface area and the adhesion strength of the filler-matrix interface. Small particles enable both efficient dispersion and improved interfacial stress-transfer in the composite. For poor interfacial bonding, the particles do not carry any load, so $B = 0$ (Liang and Li, 1933). Higher interfacial bonding corresponds to higher work of adhesion at the interface of the composites in comparison with the others (Svab *et al*., 2005). Stronger interactions in composites with higher surface free energy filler increase thermodynamic work of adhesion at the interface and lead to improved tensile properties of composites. Goodier (1933) developed a model to determine the composite tensile strength based on the assumption that the polymer undergoes maximum plastic deformation. The model also assumes that the load carried by the components corresponds to their effective cross sections occupied by the specimen i.e. $(1-(1.21)V_f^{2/3}$ for the matrix and $(1.21)V_f^{2/3}$ for the fillers (Vollenberg and Heikens, 1989). The equation of Goodier model for the tensile strength of the composite is given by Equation (2.15)

$$£ =_c £_m\left\{1-(1.21)V_1^{2/3}\right\}+£^*\left\{(1.21)V_1^{2/3}\right\} \quad (2.15)$$

where $£^*$ is the average strength acting on the surface of the filler.

The load carried by the filler $£^*$ is always very smaller than the matrix tensile strength when the filler is with large particle size is used i.e. debonding. However, when the specific surface area of the filler is larger (smaller particles), $£^*$ can significantly exceed the tensile strength of the matrix.

2.6 Use of natural plants in leather tanning and their effect on the physical properties

Tannins are astringent, bitter plant polyphenols that either bind and precipitate or shrink proteins. Tannins can be classified into hydrolysable/pyrogallol, condensed tannins and complex tannins (Covigton, 1997). At the center of a hydrolyzable tannin molecule, there is a carbohydrate (usually D-glucose). The hydroxyl groups of the carbohydrate are partially or totally esterified with phenolic groups such as gallic acid (in gallotannins or tannic acid or from sumac) or ellagic acid (in ellagitannins such as from chestnut/oak). Hydrolyzable tannins are hydrolyzed by weak acids

or weak bases or enzymes to produce carbohydrate/sugar and related polyhydric alcohol and phenoli carboxylic acids. Examples of gallotannins are the gallic acid esters of glucose in tannic acid ($C_{76}H_{52}O_{46}$), found in the leaves and bark of many plant species. Presence of a trihydroxyphenyl moiety allows for the complexation of metal ions, resulting in a semi metal tan. Hydrolysable tannins break down by hydrolysis, then depositing esterifying acids with in the fiber structure – called a "bloom". Very reactive tannins due to the high number of hydroxy groups on the collagen.

Condensed/catechol tannins, also known as proanthocyanidins or proanthocyanidins, are polymers of 2 to 50 (or more) flavonoid units that are joined by carbon-carbon bonds, which are not susceptible to being cleaved by hydrolysis (Covigton, 1997). While hydrolyzable tannins and most condensed tannins are water soluble but few very large condensed types of tannin are insoluble**.**

Complex tannins are built up from a gallotannin unit or an ellagitannin unit and a catechin unit. One example of this group is acutissimin A, having a flavogallonyl (nonahydroxytriphenoyl) unit bound glucosidically to C-1, and linked via three further hydrolysable ester bridges to the D-glucose derived polyoll. Generally, the vegetable tannins recat with collagen molecule via hydroxyl bonding at the peptide links (Covington, 1997). Additionally, the polyphenols can fix to the amino and carboxylic acid groups on the amni acids side chains. Condensed tannins also can form covalent bonds between the collagen molecule and the aromatic carbon groups in the tannins via "quinoid" structures which are more stable than hydroxyl bonding and accounts for the increased shrinkage temperature for condensed tannins. In fact, quinone itself can tan collagen effectively.

2.6.1 Plants used during soaking process

Sirvaityte *et al*., (2012) investigated the possibility of using essential oils from *Thymus vulgaris* (thyme) as a natural alternative preservative in leather tanning technology. The essential oil of thyme was the more active component in the mixture of essential oil and synthetic biocide used for the preservation of leather. The shrinkage temperature of the leather treated with essential oils was 113 ºC. The tensile strength and elongation at break were 16.7 N/mm^2 and 66.5 %, respectively.

2.6.2 Plants used during tanning and retanning processes

Haroun *et al*., (2009) investigated the interactions of *Acacia nilotica* spp tomentosa pods (garad) as vegetable tanning agents and aluminum sulphate, with collagens at pretanning and retannage stages. In this tanning system, they evaluated two methodologies; the vegetable pretannage followed by Aluminium sulphate retannage and Aluminum pretannage followed by vegetable retannage. The results showed that vegetable pretannage followed by aluminum retannage perfomed better than the Aluminum pretannage followed by vegetable retannage. Optimal results were obtained when 10% vegetable tannins and 2% aluminum sulphate were used. At these concentrations, the percentage elongation of the final leather was 60.5%. The shrinkage temperature for 10% *Acacia nilotica* pretanning with different aluminum retanning was found to be 125 ºC. The high shrinkage temperature was attributed to increased cross-links, stability of the complexes and bond formation thus increasing hydrothermal stability of the resulting leather. Tensile strength and tear strength of vegetable pretannage followed by Aluminium retannage system showed higher values compared to Aluminium pretanning and vegetable retanning. This type of chrome free tannage system gives leathers with shrinkage temperature above 100 ºC, percentage elongation of 65.6 %, tensile strength of 38 N/mm^2, and tear strength of 98 N/mm. The study showed that a combination of vegetable tannage of garad followed by Aluminium sulphate retannage effectively crosslinks collagens resulting in good quality leather as evidenced by high strength properties and shrinkage temperatures.

Later in 2013a, Musa and Gasmelseed studied the possibility of using the garad as a vegetable tanning agent for upper leathers. In the same study, they compared the physical properties of the leathers tanned with garad with those tanned with chromium system. The difference between the tensile strength, tear strength, elongation at break, load at grain and distension at grain crack were not significant ($p<0.05$). The researchers extended the tanning system by combining garads and oxazolidine tannage for production of garment leathers (Musa and Gasmelseed, 2013b). Investigating different concentrations of garad powder and oxazolidine, a combination of 20% garad powder and 4% oxazolidine provided a shrinkage temperature of 102 ºC. The system also produced leathers with good organoleptic properties and physical properties comparable to chromium tanning system. Separately, Musa and Gasmelseed (2013a) developed a combination

tanning system based on garad and Aluminium. Results showed that a combination system of 2% of AlO_3 followed by 20% garad produces leathers of shrinkage temperature above 101 ºC. Similarly, the physical properties were above the UNIDO-recommended minimum. The study attributed the excellent hydrothermal stability and physical properties to Aluminium which enhances amount of garad fixation as indicated by the increased garad exhaustion.

Later in 2015, Ozkan and coworkers investigated the prowess of vegetable tannins of *Acacia nilotica L*. for tannage and determined a spectrum of the resulting physical characteristics. The lastometer tests were as follows: strength at grain crack-30.5 N, grain distension at crack-14.68 mm, strength at ball burst-35.5 N and ball burst grain distension-15.67 mm. Tensile strength-21.69 N/mm^2, percentage elongation-86.66 %, and tear load of 70.06 N. In the subsequent study, Ali *et al*., (2016) combined 80% of *Acacia nilotica* pods (garads) and 20% *Azadirachta indica* (neem) barks spray-dried powder mixture as full vegetable tanning system to produce shoe upper leathers. The parameters of the resulting leathers were as follows: tensile strength-20 N/cm^2, tear strength-4.4 N/cm, percentage elongation-40.5%, grain distension-8.9 mm and shrinkage temperature> 82 ºC. The results showed that the blend Garad-Neem enhances the quality of the final leather to almost double the magnitude of the leather tanned by conventional pure *Acacia nilotica* pods (garads). The blend also improved the fullness and fellness, quality parameters recommended for good leather. The complementing effect arises from the fact that *Acacia nilotica* contains hydrolysable tannin while *Azadirachta indica* bark contains condensed tannin. In 2016, Kuria and colleagues evaluated the physical properties of leathers tanned using *Acacia nilotica*, *Acacia xanthophloea* and *Hagenia abyssinica* plants and compared the results with those of leathers tanned with standard mimosa. Leathers tanned with *Acacia xanthophloea* recorded the highest shrinkage temperature of 85 ºC while the leathers tanned with commercial mimosa had 83 ºC, *Acacia nilotica*-82.5 ºC and *Hagenia abyssinica* 80 ºC. However, the leathers tanned with *Acacia xanthophloea* recorded the lowest tensile strength of 20 N/mm^2 while *Hagenia abyssinica*, commercial mimosa and *Acacia nilotica* had a tensile strength of 27.91 N/mm^2, 28.8 N/mm^2 and 29.22 N/mm^2, respectively. Later in 2017, Hussein extracted the tannins from *Acacia seyal* bark (Taleh) and used them for retanning of upper and garment materials. The tannins content of Taleh bark was found to be 28.9% and therefore a promising source of both tanning and retanning agents.

The physical properties of the leathers tanned with the extracts were quite satisfactory. The range of tensile strength was 21.5 - 31 N/mm^{2}and percentage elongation 42 - 3.5%.

Musa *et al*. (2008) investigated the possibility of using *Lawsonia inermis* (henna) leaves as retanning agents for wet blue leathers and the physical properties of the resulting leathers were compared with those of leathers retanned using wattle. Henna retanned leathers recorded good tightness and their dyeing characteristics were better compared with wattle retanned leathers. The shrinkage temperature of wet blue leathers was 109 ºC while that of henna-retanned leathers was 121 ºC and wattle-retanned was 123 ºC. The organoleptic properties of henna crust leathers such as fullness, grain tightness, roundness, grain smoothness, softness and general appearance were more superior to wattle-retanned crusted leathers. The tensile strength, elongation, tear strength, load at grain crack and distension at grain of the experimental leathers were 25.23 N/mm^2, 60.15 %, 39.93 N/mm, 24 kg and 10.64 mm, respectively while for control leathers were 25.09 N/mm^2, 64.58 %, 42.37 N/mm, 26 kg and 11.6 mm, respectively. In this case, the strength values of leather retanned with henna meet the standards stipulated by UNIDO (1996). The study also alludes to the possibility of using henna leaves as mordanting agents. In 2010 and 2013a, the same researchers extended their work by evaluating the combination tanning process based on *Lawsonia inermis* (henna**)** leaves extracts and tetrakis hydroxymethyl phosphonium Sulphate (THPS) for production of upper leather. Two methodologies were tested: henna extracts followed by THPS (Henna-THPS) and THPS followed by henna (THPS-Henna). The methodology of THPS-henna combination tanning, employing 20% henna and 1.5% THPS, provided a shrinkage temperature of 96 ºC and the characteristics of the leathers indicated that this methodology provides leathers with better organoleptic properties and comparable strength properties than control leathers (tanned with henna alone). The shrinkage temperature for control leather was 84 ºC. THPS–henna-tanned experimental crust leathers exhibited better softness, fullness, smoothness, general appearance and dye uniformity than control leathers. The physical strength properties of the experimental leathers were above the minimum required standards. The use of THPS increased henna fixation and exhaustion which lead to increased shrinkage temperature.

Nasr *et al*. (2013) investigated vegetable tanning systems that involved quebracho and mimosa plant extracts. They compared the physical properties of the resulting tanned leathers with those

of chrome-tanned leathers. From the results, chrome tanned leather had the highest tensile and tear strengths, elongation and water permeability followed by quebracho-tanned and then mimosa-tanned leathers. The superiority of quebracho over mimosa could be explained by higher tannin content (35%) against 18% tannin content in mimosa. Huantian *et al*, (2014) used 20% quebracho solution as vegetable tannins for tanning system. The shrinkage temperature of the resulting leathers was 79 ºC. When the quebracho tanning was followed by post-treatment with transglutaminases (enzymes), the shrinkage temperature slightly improved by 2 ºC. When quebracho was combined transglutaminase with laccase (another enzyme) in one step treatment, the shrinkage temperature increased to 84 ºC. Conclusively, enzymes assisted in collagen crosslinking and the phenol oxidizing hinders the uptake or penetration of the tannins in the leather. Later in 2016, Omur and Mutlu chemically modified the condensed tannins from mimosa and quebracho by applying sulphitation, sulpho methylation and novalac synthesis. This was to enhance the colour fastness of mimosa- and quebracho-tanned leathers that usually change colour and darken on exposure to light for prolonged period. Comparative light fastness test results showed that leathers tanned with sulpho-methylated mimosa and quebracho tannins had better colour fastness to light (Covigton, 2009). The modification was aimed at introducing UV stabilized groups to the flavonoid structure of mimosa and quebracho to avoid free radical oxidative bond rearrangements. Similarly, the physical properties of the leathers tanned with modified tannins were investigated to agree well with the leathers tanned with standard tannins and the values of the strength properties match with quality standard limits.

Aravindhan *et al*. (2015) evaluated the Tara-THPS combination tannage system. Pretannage with glutaraldehyde or THPS were employed in order to improve the tannin uptake/penetration. The resulting leathers recorded shrinkage temperature of 88 ºC. The system was found versatile in tannage of both upper and garment leathers. The physical and organoleptic properties of the resulting leathers were also found to be comparable to chrome tanned leathers. This combination is effective since it also has both scavenging effect of free formaldehyde and Cr (VI). The adjunct of THPS has additional importance. In the subsequent study by Plavan *et al*. (2017), tanning process based on Tara and mimosa tannins with Aluminium adjunct were used as tanning agents. Leathers tanned with Tara tannins have more stable properties than those without. The developed technology produced leathers of shrinkage temperature of 98 ºC, tensile strength of 18.2 N/mm^2,

and elongation at break of 42%. The treatment of pelt with THPS instead of chromium before Tara-Aluminium tanning allowed the shrinkage temperature to reach up to 106°C and the tannin used dropped to half the amount.

Tannic acid is a specific commercial form of tannin, a type of polyphenol, usually extracted from any of the plant parts of Tara pods (*Caesalpinnia spinose*), gallnuts from *Rhus semialata* or Quercus infectoria or Silician Sumac leaves (Rhus coriaria). It's a mixture of polygalloyl glucoses and polygalloylquinic acid esters, and highly soluble in water (1 gram per 0.35 mL of water). Tannic acid, as a precursor, has been used immensely in leather tanning process as a green material. This is partly due to its low molecular weight compared to other vegetable tannins, which makes it to effectively penetrate into collagen fibres. Fathima *et al*. (2004) studied the tanning system of tannic acid, aluminum and silica combination. Apart from improving hydrothermal stability, the presence of Aluminium in the precursor of tannic forms an Aluminium-tannic acid complex that forms a pastel colour to the leather. The presence of silica in the system gives leather softness and fluffy feel. The shrinkage temperature was found to increase with sodium metasilicate and Aluminium sulphate offers. It was shown that 5% of both sodium metasilicate and Aluminum Sulphate concentrations were optimum for better results. The physical strength and organoleptic properties of the leathers were at par or better than the conventional chrome tanned leathers. The optimum amount of tannic acid, Aluminium sulfate and sodium metasilicate was found to be 10, 5, and 5 wt %, respectively. The shrinkage temperature of the leathers obtained from this tanning system was 95 ºC. In a related study by Saravanabhavan *et al*. (2004), a combination tannage system based on tannic acid (10%), zinc (10%) and silica (5%) were used to tan garment leathers. The shrinkage temperature of the leathers obtained was 85 ºC. The physical strength and organoleptic properties of the leathers from the experimental system were generally comparable to those tanned using chromium salts. Later in 2006, Fathima *et al*. developed an organic tanning system using vegetable tannin precursor of tannic acid and THPS as an alternative to chrome tanning system. The shrinkage temperature of the experimental leathers reached 88 ºC while the physical and organoleptic properties were comparable to that of chrome tanned leathers. Apart from the use of tannic acid as an explicit tanning agent, Colak *et al*. (2014) investigated the antioxidant effects of tannic acid on the formation of formaldehyde and Cr (VI) in leathers. The wet blue sheep skins were treated with tannic acid of concentrations; 0.1, 0.5, 1, 2, and 3% at

retanning process. The results showed a significant improvement in the physical properties with increasing the concentration of tannic acid. The tensile strength, percentage elongation, tear load and shrinkage temperature at 3 wt % tannic acids were 17.8 N/mm^2, 49.5%, 35.9 N/cm, and 130.8 ºC, respectively. The system also showed effective inhibition rate of both formaldehyde and Cr (VI) formation in leathers. Similarly, tannic acid can also be used as an aftertreatment to improve wash fastness properties of acid dyed polyamide. Coupled with mordanting capacity in dyeing, tannic acid is a potential green agent in leather manufacturing processes.

Genipin is a naturally occurring biocompatible crosslinking agents isolated from the fruit of *Gardenia jasminoides* Ellis (Brown, 2013). In an acidic or neutral aqueus solution, genipin undergoes a ring opening reaction to form dialdehyde that polymerizes via aldol condensation. The extent of the polymerization varies, allowing for dimer, trimer, and larger crosslinking bridges between amino groups (Brown, 2013). The most probable genipin polymers could bridge peptide chains at distancesof 1.6–2.5 nm (Liang et al.,). Ding *et al*. (2008) used a combination of genipin and Aluminium for tanning system and evaluated the physical properties of the resulting leather against Aluminium-glutaraldehyde and mimosa-Aluminium leathers prepared as controls. In this system, bated pelts were pretanned with 6 % Aluminium and then tanned with 6 wt % genipin. The shrinkage temperature of the leathers produced from this technology was 89 ºC (using DSC) and 92 ºC using traditional measurement. The physical-mechanical properties of the experimental leathers were similar to controls. Ali *et al*., (2013) used extracts from *Faidherbia albida* (Haraz) combined with aluminum as alternative tanning system for the production of upper leathers. The methodologies involved tanning systems of Haraz followed by Aluminum (Haraz -Al) and Aluminum followed by Haraz (Al-Haraz) using 20 wt % Haraz and 2 wt % Al_2O_3. The shrinkage temperature of Haraz-Al was 100 ºC while 98 ºC for Al-Haraz methodology. Similarly, Haraz-Al combination system resulted in leathers with better organoleptic and strength properties that satisfy the standard quality leathers.

Bitlisli *et al*. (2010) treated split suede leather with *Aloe barbadensis* Miller *L.* (*Aloe vera*) and determined their physical properties. Leathers treated with 6 wt % *Aloe vera* had slightly higher tear load values when compared with control leathers (leather tanned with chromium only). Additionally, the moisture content and leather softness increased with *Aloe vera* concentrations. Eucalyptus bark contains simple phenolics such as gallic, ellargic, protocatechuic acid, and

derivatives, flavonoids. It also contains complex polyphenolic compounds such as ellagitannins (hydrolysable tannins) and proanthocyanidins (condensed tannins). Pinto *et al*. (2013) characterized the Eucalyptus globule bark as a source of tannin extracts and applied them for retanning process. The tensile strength, tear strength and elongation were all within the required standards.

2.6.3 Plants used during dyeing and fatliquoring processeses

Affiang *et al*. (2018) developed a fatliquoring system using extracted *Aradirachta indica* (neem) seed oil. They sulphated the extracts using sulphuric acid followed by addition of sodium hydroxide in order to maintain the pH at 5.0. The physical properties of goat skins processed by this fatliquoring system were compared with those processed using imported palm oil fatliquor. The tensile strength, elongation at break and tear resistance of experimental leathers were 14.15 N/mm^2, 49.0 % and 61.01 N, respectively while those for control were 19.03 N/mm^2, 56% and 67 N, respectively. The organoleptic properties for the experimental leathers were comparable to the control leathers and the difference was insignificant. Sivakumar *et al*. (2008) used castor oil as vegetable based fatliquors. The results indicated that strength properties of leathers fatliquored by these oils were comparable to leathers fatliquored using other imported fatliquors. The strength properties of the leathers were above the quality standards for tensile strength as per UNIDO, 1996. Quadery *et al*. (2015) extracted fatliquor oils from *Pongamia pinnata L*. (Karanja) seed oil by sulphation process followed by addition of sodium hydroxide to maintain the pH at 5.0 with concentrated sulphuric acid. The prepared fatliquor were applied for processing of goat skins. The physical properties of skins were compared with skins fatliquored by fatliquor form castor oil. The tensile strength, elongation and tear resistance of the leather fatliquored with experimental oils were comparable with those fatliquored using imported fatliquors.

Kusumawati *et al*. (2016) evaluated the effect of using different concentrations of *Indigofera tinctoria L* (indigo), as a natural dyeing, to the quality of tanned milk fish. The concentrations used were 20 %, 25 % and 30 %. The results showed that different concentrations have significant effect ($p < 0.05$) on the rub resistance on wet and dry coating, fastness to perspiration, tensile strength and elongation at break of the resulting leather. The 25% concentration gave the best quality in terms of the physical and dyeing characteristics. The highest score of tensile strength was obtained

when using 30 % indigofera solution showing the score of 1 8.94 N/mm^2. This value was higher as compared to the value of synthetic dyeing system; a fact attributed to the significant content in indigofera.

Therefore, natural plants have demonstrated to be effective in improving several physical and organoleptic properties of interest to the quality of leather, mainly the tensile strength, tear strength, elongation, distension at grain crack and grain burst. However, most of the studies were only conducted with physical and organoleptic properties in mind, while the overall concerns of the leather industry were not evaluated. Testing leather's quality limited to physical properties alone is insufficient, especially when additives of plant products are incorporated into leather matrix. As many researches delve into plant products that replace synthetic agents and producing leathers with greater variety of property profiles which can compete favorably with synthetic leather, the actual leather must adhere to both human and environmental health. The safety of these leathers in direct contact with foot application must be achieved. The overall and specific plant products must be tested thoroughly to demonstrate novelty in its use and meet the stringent requirements. The application of some plants may be limited due to their insufficient quality, safety and lifespan of its usage. More researches are needed to unravel suitable extraction methods, possible combination of plants for synergy and possible plants that can reduce the toxicity of chromium use.

2.7 Environmental implications of leather industry and leather tanning technology

2.7.1 Environmental impact of the leather production processes

From the critical review of the environmental impact of leather industry, every leather tanning process that employs conventional processing has a potential to impact negatively on the environment. Considerable impact comes from pretanning and tanning operations which causes increase in COD, BOD, TDS, chlorides and Sulphates. Pretanning and tanning operations have been estimated to contribute approximately 90% of the total tannery pollution (Aloy *et al*., 1976). This due to poor uptake of most chemicals, between 50-75%, such as the uptake efficacy of most chemicals chromium, syntans, oils, lime, sodium sulphide, resins, bactericides, biocides, fungicides, surfactants, acids, bases. The sulphides and amines used during liming and unharing

impact on the environment and generate by-products when they react with the skin material (Cassano *et al*., 1997). The COD this stage ranges between 20,000 and 40,000 mg/L of consumed oxygen (Cassano *et al*., 2001). The pickling stream contains high chlorides and sulphates amounts of up to 9g/L which when discharged into the environment, is hard to eliminate by conventional treatment. Chrome tanning creates a significant environmental impact since 25% of the chromium is present as Cr_2O_3 at 33 ºC of basicity which causes pollution at a high level (Cabeza *et al*., 1998; Malek *et al*., 2009). About 30% of the initial salt amount remains in the bath stream of the tanning process (Gauglhofer, 1986). Eventually, the tanning waste contains approximately 4.3% of chromium and 14% of nitrogen (Malek *et al*., 2009).

The presence of these chemicals in the waste waters from the tannery effluents contribute to COD, BOD, TDS, Sulphates, chlorides and TKN in the environment (Ramasami, 1999; Kanagaraj *et al*., 2006). Other chemicals such as ammonia, hydrogen sulphide and volatile hydrocarbons, amines and are emitted to the atmosphere. Formaldehydes are usually present in chemicals like synthetic tanning agents, resins, naphthalene based, oxazoline derivatives, phenol and sulphone compounds, dyeing auxiliaries, finishing chemicals and casein-based finishes (Wolf, 2002). The advent of synthetic dyes, which proved cheaper and more efficient, the use of natural dyes dropped drastically (Khan *et al*., 2014; Shahid and Muhammad, 2013). Synthetic dyes especially the azoic type, which forms 90% of all synthetic dyes, are nitrogen-based dyes made from petroleum and coal-tar sources (Sundari, 2015). The exhaustion rate of these synthetic dyes is between 65-90%, hence the rest of the unfixed dyes are discharged as effluents (Rai *et al*., 2005). These dyes produce carcinogenic and allergenic amines, therefore posing both environmental and human health hazard (EU Azo colourant Directive, 2002; Rai *et al*., 2005; Dixit *et al*., 2015).

2.7.2 Formation of Cr (VI) in leather

Although tanning and retanning processes are done using Cr (III) salts which are eco-friendly and no restriction on their use exists, cases of Cr (VI) formation due to oxidation have severally been reported (Roig *et al*., 2013; Devikavathi *et al*., 2014). Thermodynamically, spontaneous (natural) oxidation of Cr (III) to Cr (VI) do occurs. Although the probability of spontaneous oxidation is extremely low, however, accelerated oxidation has been documented as warranted by oxidation agents such as atmospheric oxygen, UV rays (photo ageing), free radicals (such as hydrogen

peroxide, Manganese Oxides), extreme high or low pH (such as during neutralization and dyeing), extreme high or low humidity, temperatures higher than 80 °C (thermo ageing), fatliquoring (especially those with double bond, vegetable oils, animal oils) and natural waxes and resins used during dry finishing (Fuck *et al*., 2011; Babu *et al*., 2005; Hauber and Buljan, 2000; Rydin, 2002; Congzheng *et al.*, 2005; Kolomaznik *et al.*, 2008; Devikavathi *et al.*, 2014; Dixit *et al.*, 2015; Kocurek *et al*., 2015; Candar *et al.*, 2008). Sometimes the tools, substances, auxiliaries, chemicals and process parameters contribute significantly to the conversion process (Devikavathi *et al.*, 2014). Oxidation mechanisms involves radical formation and hydro peroxides as summarized in equation (2.16).

$$Cr^{3+} \xrightarrow{\text{Oxidation by oxidants such as radicals}} Cr^{6+} + 3e^{-} \quad (2.16)$$

The Cr (VI) belongs to class of strictly monitored pollutants in the environment and human health. Their effect on human health include irritations of the skin, eye, respiratory system, carcinogenicity, mutagenicity, corrosiveness, sensitization, nausea, diarrhea, liver and kidney damage, dermatitis, internal hemorrhage, ulceration of the nasal septum and asthma or respiratory sensitization (Iyer and Mastorakis, 2006; Kocurek *et al.*, 2015; Devikavathi *et al.*, 2014). Cr (VI) has made the leather industry be classified as both environmentally and human health hazardous and contributed largely to the rejection rate of leather on the export market (Bayramoglu *et al.*, 2012). The formation of Cr (VI) has introduced a substantial barrier to using of chromium as a tanning agent and caused restrictions in the trade market for leather articles (Kolomaznik *et al.*, 2008).

2.7.3 Comparison of synthetic chemicals versus plant products used in tanning industry

Effluents containing synthetic products such as chromium are hard to treat since they are highly soluble in the environment and waste water (Padhi, 2012). Once in the environment, they are hazardous to human health, aquatic life, and general ecosystem (Thiyagarajan *et al.*, 2015). International directives have been imposed on the industry in terms of level of contents in the effluents, leather and due to the consequences of strict environmental standards. Natural products are non-carcinogenic, non-poisonous, biodegradable, and non-hazardous to human and environmental health (Saravanan *et al.*, 2014; Thiyagarajan *et al.*, 2015). Majority of natural plant products are renewable, sustainable, and outstanding performance in terms of the quality of the

leather they produce (Onal *et al.,* 2005; Pervaiz *et al.,* 2016). Since these plant products are agro-renewable products, they are inexpensive and economical (Jadhao and Rathod, 2013). Natural plant dyes have shown multiple benefits such as fragrance. Due to phenolic compounds in plant products, they are antimicrobial, antifungal, antibacterial and hence the leather is safe for skin contact. However, some plant products perform better when mixed with metals and synthetic products such as transition metals, mordants. Since exhaustion rate is not 100%, some metals remain in the unexhausted in the residual bath and hence the effluents disposed pose significant environmental hazard. Most plant products do not have standardized recipe and varied quality due to varied extraction methods, plant parts. For sufficient plant product yield, more plant need to be due to low yield rate.

2.7.4 Phytochemistry and leather tanning processing

Ethanoic extracts of *Mimosa pudica* Linn. (Mimosa) shows the presence of alkaloids, flavonoids, cardrac glycosides, phenols, saponins, coumarins, terpenoids, quinines and tannins (Jagetia and Lalhmangaihi, 2018; Gandhiraja *et al*., 2009). Free radical scavenging assays of the plant extracts demonstrated the potential of scavenging superoxide radicals, other free radicals and antioxidant activity due to the presence of phenols, alkaloids, flavonoids, cardiac glycosides, and saponins (Jagetia and Lalhmangaihi, 2018). The bioactive components such as alkaloids, terpenoids, phenols, saponins, coumarins, quinines and tannins possess antimicrobial activity that can be handy in leather processes (Gandhiraja *et al.,* 2009). The polyphenolic compounds such tannins are capable of precipitating proteins especially the collagen to form leather (Falcao and Araujo, 2018). As a matter of fact, most of the properties and the applications of these tannins are attributed to the ability of their proanthocyanidins to form complexes with collagens via hydrogen bonding. *Schinopsis lorentzii* and *S. balansae* (quebracho) contains condensed tannins, about 14-26 % weight of the heartwood and the tannins extracts contain oligomers based on catechins (Falcao and Araujo, 2018). *Quercus macrolepis* (valonia oak**)** has been used in the production of harder, firmer, heavier and quite impermeable leather. It contains ellagitannins, whose main constituents are castalagin, vescalagin and pentagalloylglucose (Falcao and Araujo, 2018). *Galla chinensis* and *Galla turcica* (gallnut) contains 50–70 % of tannin of the gallotannin type, mainly of penta-undeca-galloylglucoses. A review on the phytochemical and pharmacological profiles of *Castenea sativa*

Mill. (chestnut) have shown that it possesses both antibacterial, antifungal, antimicrobial, antiviral and antioxidant activities due to chemical compounds such as both condensed tannins (proanthocyanides) and hydrolysable tannins, flavonoids, lipids, gallic acid, proteins, fibres, ellagic acid, minerals, steroids, terpenoids, saponins, carbohydrates and free sugars (Sanz *et al.*, 2010). Colak (2006) extracted tannins from quebracho, mimosa, gallnut, chestnut and valonia and examined their antibacterial activities on leather at soaking process. Tannins from gallnut and chestnut showed more antimicrobial activity against bacteria in the soaking float during the first 8 hours while gallnut tannins were still effective at 24 hours of soaking. On the other hand, tannin extracts from valonia and quebracho supported bacterial growth. The stronger activity of tannins extracted from gallnut and chestnut were attributed to the higher content of tannins. The results of the study demonstrated that quebracho and chestnut are viable alternatives for soaking process while tannins from valonia and quebracho are not a viable alternative to soaking agents. Ozkan *et al.* (2017) studied the inhibitory activity on Cr VI formation in chrome tanned leathers of two condensed vegetable tannins: quebracho (72 % tannin) and mimosa (72% tannin) and four hydrolysable tannins; Tara (48 % tannin), chestnut (72.5 % tannin), valonia (68% tannin) and sumac powder (20.8 %) combined with copper mordant of 0.5 and 1 wt %. The study involved using tannins combined with copper mordants and using copper alone. The results showed that both using copper alone and combining copper with vegetable tannins inhibited Cr VI formation even after photo ageing, keeping Cr VI level below permissible limit. Averagely, 13.1 ppm of Cr VI were detected in leathers without either copper or vegetable tannins. Some high levels of Cr VI were also detected in leathers treated with 1 % of mimosa, quebracho and chestnut without copper mordant. On the other hand, both 0.5 % and 1% of copper mordant alone or combined with vegetable tannins were successful to keep Cr VI levels below detection limit in all the leathers.

Tannic acid is a polyphenol with hydrolysable gallotannin with numerous activities such as antimicrobial, radical scavenging, antioxidant and antibacterial (Saravanabhavan et al. 2004). The attribute of lower molecular weight enables efficient penetration and solubility as compared to other traditional vegetable tannins (Saravanabhavan *et al.,* 2004; Fathima *et al.,* 2006). Due to the numerous activities, Colak *et al.* (2010) investigated on tannic acid concentrations against some microorganisms at pickling process of leather making. Leather samples treated with 0.1, 0.5, 1, 2 and 3 % of tannic acid were assessed on yeast, bacteria and moulds. All concentrations of tannic

acid exhibited antimicrobial activity against all bacteria, yeast and moulds studied; and the activities were stronger as compared to that of commercial synthetic bactericides used at all concentrations. The antimicrobial activity increased with concentrations, the most effective concentration being at 3 %. Using tannic acid at pickling process reduced the COD and TKN values of the soaking effluents markedly. Zengin *et al.* (2014) investigated the effect of tannic acid on microorganisms on leather at soaking. The results showed that application of 0.5 and 1 wt % tannic acid concentrations was more effective than the commercial bactericides on the market probably due to their phenolic structure. Use of tannic acid for soaking process resulted in lower COD, and TKN values of the effluents. This system provides an alternative that's both environmental friendly due to low pollution and cheaper. Saravanabhavan et al (2004) carried out a study in which tannic acid was combined with zinc and silica as a white chrome-free tanning system to manufacture garment leathers. Optimum concentrations of zinc, tannic acid and silica, were for better performance system was found to be 10, 10, and 5 wt %, respectively. The BOD, COD and TDS loads of the effluents greatly reduced by 96, 94, and 74 %, respectively, as compared with the spent vegetable tan liquor while 44, 67, and 88%, respectively, as compared with chrome tan liquor. The tanning system increased the exhaustion of Zinc to 90 %. A study by Fathima *et al.* (2004) devised a tanning system by combining tannic acid with Aluminium sulphate and sodium metasilicate of concentrations 10, 5, and 5 wt %, respectively. The exhaustion rate of aluminum increased to more than 98 % and a significant reduction in the COD and TDS was reported compared to the conventional vegetable tanning system. Fathima et al (2006) combined tannic acid with THPS as an alternative cleaner tanning system. Alongside the versatile upper and garment leathers, the environmental assessment tests showed that COD of the spent liquor was higher compared to that of the conventional chrome tanning due to unfixed tannic acid and THPS while there was a decrease in TDS. Since tannic acid is easier to degrade, this system a viable alternative to chrome tanning. Furthermore, THPS has low toxicity to both human and environmental health, low recommended treatment level, rapid breakdown in environment, and no bioaccumulation (Fathima *et al.,* 2004). Colak et al (2014) applied tannic acid for retanning wet blue leathers and examined the activity of tannic acid to curtail the formation of Cr VI and formaldehyde compounds. From the results, 3 % offer of tannic reduced the level of Cr VI to values lower than 3 ppm, fulfilling the eco-label criteria for footwear. The reduction rate for Cr VI and formaldehyde was up to 98 % and 45.3 %, respectively, which was achieved after applying 3

% tannic acid. The formaldehyde concentrations were highest in control samples (44.9 mg/kg) but the levels progressively reduced as concentrations of tannic acid applied increased. All the concentrations of tannic acid (0.1, 0.5, 1, 2 and 3 %) maintained the formaldehyde concentrations under restricted limits. The study recommended the protective effect of tannic acid against formation of Cr VI and formaldehyde, attributed to its capacity to absorb UV light with a peak of maximum absorption spectrum below 250 nm.

The essential oil of *Thymus vulgaris* (Thyme) contains p-cymene, thymol, 1,8-cineole, linalool, geraniol, sabienene hydrate, borneol, carvacrol and γ-terpinene which have expressed strong fungicidal, antibacterial and anti-inflammatory activities (Klaric *et al.,* 2007). Sirvaityte *et al.* (2012) applied the thyme essential oils as an alternative preservative for chrome tanned leather at concentration rates from 0.05 to 5 % of the wet blue mass. Gram-positive bacteria were found to be more sensitive to the essential oils of thyme than gram-negative bacteria. The essential oils showed stronger protection against bacteria than that of the conventional (thiocyanomethylthio) benzothiazole after four weeks. Resistance to bacteria's action increased with concentrations of essential oils and the optimized concentrations of at least 3 %. A concentration of 5 % showed the highest resistance to *E. coli*. Although the study recommended the use of the essential oils mixed with reduced amounts of synthetic biocide, the resistance is sufficient without the synthetic bactericide. Bielak and Sygula-Cholewinska (2017) investigated the durability of antimicrobial effect on leather fatliquored using thyme and *Cinnamomum zeylanicum* (cinnamon) essential oils at percentage of 5 wt %. Results showed that the antimicrobial activity of the essential oils from the plants against *E. coli*, *S. aureus* and *C. albicans* strains lasts for more than 3 years after fatliquoring. This period of activity, optimum concentration of 5 % offered by the two bioactive substances and the mere cleanliness of the leather products is commendable in leather processing and they form a promising green alternative biocides for leather preservation during finishing process.

The phytochemical components of *Origanum vulgare L.* and *Oerganum minutiflorum* (oregano) essential oils are carvacrol, thymol, γ-terpinene, p-cymene, α-terpinene, caryophyllene, borneol, linalool, rosmarinic, acecetic acids and α-pinene (Ozkan *et al.,* 2010). These components offer high phenolic content, reducing/antioxidant and free scavenging, fungicidal and antimicrobial,

activities due to the phenolic metabolites such as rosmarinic and acecetic acids (Capecka et al. 2005). Accordingly, Bayramoglu *et al.* (2006) examined the applicability of *Origanum minutiflorum* (Oregano) essential oils as a fungicide on leather during leather pickling and tanning processes. The fungal activity of essential oils against common moulds species were compared with two other common commercial fungicides; the 2-Thiocyano-methylthiobenzotiazole (TCMTB) and N-octyl-isothiazolinone (N- OITZ). Leathers treated with the extracted essential oils were more resistant to moulds than those treated with the commercial fungicides. The antifungal activity of these essential oils increased with their concentrations. The essential oils from the three species of Oregano were applied on leather as alternative bactericides (Bayramoglu 2007). The three species recorded superior activity compared to all the concentrations of (7-25 %) commercial bactericides. Bielak and Sygula-Cholewinska (2017) assessed the durability of the antimicrobial effect of leather fatliquored using essential oils from oregano at percentage concentrations of 5 wt %. The antimicrobial activity of the essential oils from this plant against *E. coli, S. aureus* and *C. albicans* strains last more than 3 years after fatliquoring. The strength and period of the activity as bacterides and fungicides together with the commendable optimum concentration of 5% places this bioactive substance as a promising and viable phyto-preservative biocide for leather to replace the synthetic commercial biocides.

The phytochemical evaluation of the essential oils of *Eucalyptus globulus* shows presence of flavonoids, terpenoids, saponins, and reducing sugars which are have shown strong activities such as free radical scavenging and antimicrobial (Mishra *et al.,* 2010). Sirvaityte *et al.* (2011) applied the essential oils as alternative preservative for tanned leather. The resistance of the painted leathers to *Escherichia coli* bacteria greatly improved. The antibacterial effect decreases during one week of storage and the leather becomes nonresistant to *B. cereus*. The phytochemistry of *Lavandula officianalis* L. (lavender) have shown the organic compounds such as linalool oxide, α-pinene, α-terpinene, coumarins, tannins, borneol, camphene, menthol, eucarvone, terpinolene, β-caryophllene, viridiflorol, 1,8-cineole, sabinene, β-pinene, tannins, coumarins, flavaonoids, fitosterols, rosmarinic acid and related derivatives (Miri, 2018). Sirvaityte *et al.,* (2011) extracted essential oils from *Lavandulae officinalis* as alternative preservative for leathers tanned using mimosa and quebracho tannins and their mixtures. The essential oils of *Lavandulae officinalis* increase resistance of the leathers to *Ps. Aeruginosa*. Leathers tanned with mimosa tannin is more

resistant than tanned with quebracho or mixture of mimosa and quebracho tannins. The antibacterial effect decreases during one week of storage and chrome free leather becomes nonresistant to *B. cereus*. Compared with leathers painted with *E. globulus*, the antibacterial effect of lavender was stronger than that of E. *globulus*.

Phytochemicals of *Terminalla chebula Retzius* (myrobalan) include chebulin, ellargic acid, gallic acid, chebulinic acid, ethyl gallate, punicalagin, terchebin, terflavin, luledin, tannic acid, total phenolic, triterpenoids, alkaloids, flavonoids, anthraquinones, glycosides and tannins (Tariq and Reyaz, 2013; Upadhyay *et al.,* 2014). This plant has been reported to possess multiple activities such as antioxidant, antibacterial, antifungal, antiviral, antimicrobial, among others (Tariq and Reyaz, 2013; Upadhyay *et al.,* 2014). Sivakumar *et al.* (2016) investigated the antimicrobial activity of *Terminalia Chebula Retz*. (Myrobalan) nuts combined with common salts mixed in the same ratio as alternative preservation of leather. The synergistic action of the combination 10 % each (% w/w of raw skin) provided a short term preservation of raw skin/hide up to 45 days without any degradation/putrefaction. Conventionally, salt preservation employs 40-50 % of common salt. Hence this preservation system reduced the amount of common salt by 75 % and thereby reducing TDS content, COD and BOD. The antimicrobial activity suggests that synergistic composition of myrobalan powder and common salt in similar proportion have a better activity against wide range of micro-organism as compared to individual effect of either myrobalan powder or common salt.

The chemical constituents of *Lawsonia inermis Linn*. (henna) include lawsone (2-hydroxy-1, 4-naphthoquinone), mucilage, mannite, gallic acid, tannic acid, carbohydrates, cardiaglycosides, terpenoids, tannins, quinones, saponins, flavonoids, resins, alkanoids, phenolics, catechin, quertrin, β-sisterol glycoside, coumarins, xanthones and leucocyadin (Mahmoud *et al*., 1980; Musa and Gasmelseed, 2012). Lawsone (2-hydroxy-1, 4-naphthoquinone) in the henna leaves is the main coloring substance and these components confer the leaves with a variety of pleiotropic effects such as antioxidant, antibacterial, antifungal, and antimicrobial activities (Musa and Gasmelseed, 2012). Musa *et al.* (2010) investigated the possibility of using henna extracts combined with tetrakis hydroxymethyl phosphonium Sulphate (THPS) as a green tanning system for garment leathers. The optimum concentration and protocol of tanning system was 20 % henna and 1.5 % THPS applied in that order. The system resulted in a significant reduction in discharges

of TDS, CODs and BODs in the spent liquor and wastes. On the other hand, THPS improves the exhaustion of henna. Musa *et al.* (2008) applied extracts from air-dried henna leaves as a wet blue leather retanning agent against wattle retanning. From the trial, the dried leaf powder yielded tannin content range of 10.2-12 %, 5-10% gallic acid and 0.01-0.02% essential oils. The environmental impact tests on the spent liquor showed a significant decrease in COD and BOD as compared with the control spent liquor (wattle retannage). As expected however, the TDS content increased with henna treatment. Leathers treated with henna showed better dyeing quality implying the extracts can be used as a premordant as well. Ozgunay *et al.* (2014) determined the antioxidant activity of henna and valonia using FRAP and TEAC/ABTS methods against the formation of Cr VI and formaldehyde formation in wet blue leathers. The antioxidant powers were found to be 2.3 and 2.4 mmol/L, respectively, for henna while 48.1 mmol/L and 28.0 mmol/L, respectively, for valonia. The results from the study showed that the amounts of both Cr VI and free formaldehyde reduced considerably in both henna and valonia-treated leathers as compared to control (photoaged samples without any treatments). Due to lawsome (2-hydroxy 1,4 naphthoquinone), a natural coloring matter in henna, Musa *et al.* (2009) used leaves extracts to dye leather. The optimum extraction conditions were found to be maceration of ground henna leaves in water, at a temperature greater than 80 °C for 1 hour in water bath without agitation. The depth of the color increased with henna concentration while variation in color and light fastness was achieved by suitable mordants that improved the absorption and hence uptake. The dye uptake slightly decreased with henna offer and pH. From the exhaustion results, the appropriate pH for henna dyeing was 4 and high temperatures of 60 °C. The 20 and 25% concentration offer gave better shades and hence 20 % was observed to be sufficient. The dye was found to confer good rub and perspiration fastness characteristics while light fastness was moderate at these offers. The exhaustion rate at high temperature poses a challenge given that leather is sensitive to high temperatures. Hence leather dyeing using henna appears a viable option that can replace synthetic dyestuffs. Abba *et al. (*2013) compared the pure and sulphonated dyes extracted from henna and *Cola nitida* (kolanut) plants. They extracted the dyes using chloroform and acetone as solvents and the extracts were sulphonated using chlorosulphonic acid. The dyeing properties of henna were found to be superior to kolanut dyes. The exhaustion ranged from 52 to 85.04 %, fixation from 50.72 to 63.32 % and migration from 48.85 to 82.33 %. For both dyes, sulphonated dyes showed better results even for dyeing properties and fastness ratings compared to crude extracts. Similarly,

sulphonated dyes showed better exhaustion, fixation and migration. Although not yet explored, the tannin content in henna leaves is sufficient for leather tanning process while the non-tannin components can be beneficial to bring about filling action in the leather matrix. Hence, this is a promising ingredient in leather tanning technology for various processes, owing to its rich phytochemical components.

Hydrolysable gallotannins extracted from *Caesalpinia spinosa* (Tara) possess strong antibacterial and antioxidant potency (Aquilar-Gavez *et al.,* 2014). Aravindhan *et al.* (2015) investigated the inhibitory activity against formation of formaldehyde in leather of an alternative chrome tanning system involving a combination of Tara and THPS. The environmental impact assessment showed a significant reduction in TDS and a slight increase COD due to presence of unfixed Tara and THPS as compared to control chrome tanning. The optimized concentration of Tara was found to be 10% and the order of combination to be Tara followed by THPS. Both tara-THPS and THPS-tara tanned leathers showed almost 99% scavenging activity against formaldehyde due to the antioxidant activity of both Tara and THPS.

Phytochemical screening of *Acacia nilotica, Acacia Arabica, Acacia seyal* (Taleh) and *Acacia catechu* reveals presence of rich secondary metabolites such as tannins, sterols, glycosides, alkaloids, saponins, resins, phenolic acids, carbohydrates, proteins, amino acids, anthraquiones, and flavonoids, terpenes, and other therapeutic compounds that have shown marked fungicidal, antioxidant, antibacterial activities especially against both gram-positive and negative bacteria (Negi and Dave, 2010). Musa and Gasmelseed (2013a) determined tannin content extracted from *Acacia nilotica* pods (garads) and applied the tannins combined with Aluminium for leather tanning. The extracted tannin content was found to be 30%. The uptake of garad tannin in garad-Al tanning system with 20% followed by 2% of Al_2O_3 was found to be better than Al-Garad tanning system. The system also resulted into decreased discharge of COD by 13 %, BOD by 51% and TDS by 56% in the spent liquor and waste water as compared with control spent liquor (using garad tanning system alone). Consequently, Aluminium enhances the exhaustion of the garad tannins. Another tanning system was designed by Musa and Gasmelseed (2013b) using 20% garad tannin combined with 4% oxazolidine. Based upon the results, the exhaustion of garad improved by 10%. Consequently, the COD, BOD and TDS of the spent liquor processed using both Garad-

Oxazolidine and Oxazolidine-Garad tanning systems were lower than that for liquor from garad tanning (control). Conclusively, better results require that the order of combination to be garad followed by Oxazolidine. Hussein, 2017 determined the tannin content in *Acacia seyal* (taleh) bark and utilized the extracts as an alternative retanning system for garment leathers. The optimized conditions for extraction were; temperature of 50 °C, solvent ratio of 6:1 and leaching time of 1 hour. Tannin content determined was 28.9%. This tannin content gives an impressive and promising pretanning, tanning and retanning agent to replace the hazardous chrome tanning.

Uncaria gambier [Roxb.] (Gambier) contains tannins, catechins (complex flavonoids), alkaloids, sterol, resins, proteins, amino acids, carbohydrates and phenolic compounds; components which have shown excellent antibacterial, free radical scavenging and antioxidant activities (Amir et al. 2012). A study by Nurbalia (2016) on the characteristics identification of gambier as a possible leather tanning agent showed that the catechins in this plant are a natural ingredient for antioxidant effect. The tannin content was more than 50%, hence a promising pretanning, tanning or retanning agent in the leather tanning industry. The phytochemical analysis of *Camellia sinensis* (tea) have shown the presence of bioactive compounds such as alkaloids, flavonoids, steroids, terpenoids, carotenoids, benzoic acid, ascorbic acid, tocopherols, folic acid, and tannins consisting of catechin (flavonol) and gallic acids (Tariq and Reyaz, 2012). Majority of these metabolites are active components for antioxidant, antimicrobial, antifungal and antibacterial activities (Tariq and Reyaz, 2012). Bayramoglu *et al.* (2008) used 4 % green tea and *Vinca rosea* extracts to inhibit formation of formaldehyde in leather during retanning process. Both extracts were effective in eliminating formaldehyde but green tea showed far better effect. The effect can be improved by using different extraction techniques or increasing the amount of the extracts used in the process. Since the effect of formaldehyde elimination is based on antioxidant effect, the two vegetal extracts can also be used to eliminate Cr VI formation in leather.

Phytochemical screening and determination of phenolic content and antioxidant activity of *Cassia singueana* (Amharic hambo hambo) reveals the presence of alkaloids, sterols, coumarins, saponins, triterpenes, anthraquinones, quinoids, glycosides, carbohydrates and tannins which confer strong antioxidant, free radical scavenging and antimicrobial activities (Adzu *et al.*, 2003). Berhanu and Ratnapandian (2017) extracted and optimized natural dyes from *Cassia singueana*

bark and used them on dyeing tanned leather with natural mordants of *Aloe vera* juice and mango bark extracts. The optimized parameters for high strength dye were at temperature of 95 °C, concentration of 60 g/l and a duration of 1 hour. Good to excellent fastness were achieved and better colour fastness was obtained in the case of leather premordanted with *Aloe vera* juice. Similarly, the value of yellowness for premordanted leather with *Aloe Vera* juice was highest. The colour change was also achieved by varying the mordants used. Natural mordants of *Aloe vera* and mango bark gave the best shades, excellent rubbing and perspiration and very good light fastness with premordanting. Seabra et al (2017) investigated the influence of solvent additive on aqueous extraction of tannin from *Pinus pinaster* (maritime pine) bark in order to be used in leather tanning. Solvent additives used were sodium hydroxide (0.5, 1.0 and 1.5%), formic acid (0.5, 1.0 and 1.5%) and ethanol (5, 10 and 15%). Extractions were performed with and without the addition of sodium sulfite (1.0%). The optimized solvent additive for phenolic and condensed tannins was ethanol which achieved 34.8% of gallic acid equivalents and 62.8% of catechin monohydrate equivalents and favorable pH value of 3.5. The extracts had relatively low viscosity which is ideal for leather tanning system since the low pH is already an appropriate for tanning without use of acids and bases. This is a value-added scheme that is meant to improve the extraction of tannins form the plants. This is a potential alternative protocol for tanning and retanning agents.

Dyeing is a crucial process in leather tanning that confers a desirable permanent color to the leather. Based on coloring ability of some plant phytochemicals, several plant extracts have shown excellent potential in leather dyeing process. Numerous plant extracts with dyeing potential such as *Arbutus unedo* L. (strawberry) leaves, *Arucaria angustifolia* (araucaria) leaves, *Callistemon citrinus* L. (bottle brush) flowers and leaves, *Ficus benghalensis* Linn. (Banyan) roots, *Iresine paniculata* L. (blood leaf) leaves, *Mangifera indica* L. (mango) bark, *Moringa oleifera* Lam. (drum stick), *Morus alba* Linn. (Mulberry) leaves, *Musa cuminate* L. (banana) bark, *Nerium oleander* L. (oleander) flower, *Polyalthea longifolia* Sonn. (False ashoka), *Punica granatum* L. (pomegranate) fruit peel, *Syzygium cumini* L. (black pum) bark, *Rosa damascenes* Miller petals and *Tagetes erecta* L. (marigold) flowers have been studied (Pervaiz *et al.,* 2016a, b; Pervaiz *et al.,* 2017). These plants produced different yields of dyes and shades. Bottle bush flowers produced the highest yield while aerial roots the least yield. Leaves, flowers and aerial roots yielded light and soft shades such as yellow, grey and light green while barks yielded dark and light shades. Soft pleasing shades

were obtained with the *T. erecta* dye. It has been demonstrated that it's possible to vary the colour of leather by using dyes from different plants and different plant parts. Further variations can be achieved by using appropriate premordants and mordants. Dyes showed fair to good evenness on both corium and grain sides of the leather and good to excellent results on colour fastness. In all these studies, the dyed leather showed appropriate colour value, strength and fastness properties. Sundari (2015) used extracts from *Mucuna pruriens* as a dyeing agent of chrome tanned leather. The optimized conditions that yielded 47% were at a temperature of 60 °C, for 1 hour and a feed to solvent ratio of 1:5 and 0.75mm particle size. As inferred from the reflectance and visual assessment, the dyed leather showed better colour value, fastness and strength properties. Based on significant quantity of tannins, alkaloids, flavonoids, carbohydrates, glycosides, terpenoids, phenols and a blue colour substance, Kusumawati *et al.* (2016) established the possibility of using *Indigofera tinctoria* L. (indofera) to dye milkfish leather. The substance has tannin which also improves the quality of the tanned leather. Although the three indigo concentrations in this study (20, 25, and 30 %) showed significant effect to rub resistance, fastness to perspiration, 25 % concentration yielded the best results based on rub resistance. Out of the three indofera extract concentrations; 20, 25, and 30 %, concentration of 25 % showed the best quality in terms of physical performance. *Beta vulgaris* (Beetroot) contains betalains (red cyanins), betanins and xanthins (yellow) which have shown to possess antimicrobial and antioxidant activities (Nayak *et al.,* 2006; Sivakumar *et al.,* 2009). The red cyanins represents more than 75 % of the total color present in beetroot. Sivakumar *et al.* (2009) extracted natural dyes from beet root and applied them for dyeing leather. Use of ultrasound was found to significantly improve the efficiency of extraction. The ethanol to water of 1:1 with 80 W ultrasonic power for 3-hours contact were optimum for better yield. The coloring ability of extracted beet dye has been tested on substrates such as leather and paper and found to be suitable for dyeing. Ultrasound is also found to be beneficial in natural dyeing of leather with improved rate of exhaustion. Both the dyed substrates have better color values for ultrasonic beet extract as inferred from reflectance measurement.

Bixa orellana (urucum) seed contains tannins and a mixture of eight colorants of carotenoid type such as bixin and nor-bixin (Das *et al.,* 2007). Bordingnon *et al.* (2012) determined the effect of temperature during fixation and addition of tocopherol on dye's diffusion and fixation of urucum extracts. The dye showed commendable surface coating of the leather, good penetration, good bath

exhaustion and equalization in the dyeing. Selvi *et al.* (2013) then used extracts from urucum seeds to dye and finish leather. The dyed and finished leather exhibited better coloring properties with dye exhaustion of 81 %. The intense shade on both grain and corium was uniform due to smaller particle size of dye molecules (225 nm). Results demonstrated a viable option of dyeing and finishing leather using urucum instead of synthetic dyestuffs.

Ma *et al.* (2017) synthesized natural surfactants from vegetable oil, dissymmetric gemini sulfosuccinate surfactant (DGSS) and compared its performance on leather with oils synthesized from petrochemicals. The natural surfactants exhibited outstanding environmental friendliness and superior surface activity than oils from petrochemicals. The results also showed that DGSS significantly reduces the surface tension and shows good emulsification ability, good wetting ability and poor foaming performance. The leather treated with 8 wt % of DGSS as fatliquor was comparable to leather treated with 14% of commercial fatliquoring agent hence use of oils from DGSS reduces TDS. DGSS showed better fatliquoring effect (softness) better than the oils from petrochemicals. *Ricinus communis* (castor plant) contains important triglyceride components such as ricinoleate, linoleate and oleate. Tawfik *et al.* (2017) extracted oil from the castor plant using Sohlet extraction method and hexane solvent. The extracted oil was converted to fatliquors by sulphation process using sulphuric acid. It is a triglyceride in which approximately 90% of fatty acid chains are ricinoleate. The values of free fatty acid, specific gravity, refractive, acid, saponification and iodine values of both the crude and refined castor oil produced were determined and found to meet the standards leather fatliquors.

Azadirarachta indica (neem) contains a variety of phytochemicals such as alkanoids, flavonoids, saponins, resins, glycosides, terpenoids, triglycerides, tannins and steroids with high antioxidant and antibacterial effects (Affiang *et al.*, 2017). Affiang *et al.* (2018) extracted oil from neem seeds using Sohlet extraction method and applied it on goat leather as alternative ecofriendly fatliquors. The oil was sulphated using sulphuric acid and sodium hydroxide to keep the pH at 5.0. The leather processed using the neem oil fatliquors was comparable to leather processed using imported palm oil in terms of performance. Oils extracted from *Citrullus colocynthis* contains secondary metabolites such as oleic, linoleic, stearic and palmitic acids that possess antimicrobial, antifungal, and antibiotic properties. Based on fungicidal property, Sahu *et al. (*2017) extracted oils from *Citrullus colocynthis* and sulphonated them with sulphuric acid at varied temperatures. It was

found out that *Citrullus colocynthis* is a rich source of fatliquor due to high percentage of unsaturation oil.

2.7.5 The potential of using plants in environmental mitigation in leather tanning industry

The review establishes that indeed significant researches have been done to identify appropriate plants that are potential alternatives to conventional leather making agents that xenobiotics. Analysis of the reviewed papers shows that enormous capacity of plants to replace synthetic inorganic agents in leather processing viably exist. Other plants have shown the capacity to be combined with the conventional protocol in order to minimize their negative impact on the environment and human health. Plant products have a greater applicability in the industry over conventional tanning ingredients:

a) Plants have multiple beneficial actions such as antimicrobial characteristics.
b) Some plants can be used at all tanning processes. For dyeing process, diferent colours can be achieved by varying mordants and different parts of the plant.
c) Majority of the plants have resulted into final leather that is more superior to the conventionally produced leather. Natural dyes have exhibited excellent to good qualities in terms of colour fastness to light, washing, shade, rubbing, perspiration.
d) The green technology of using plants is a cleaner technology that results to lower waste that decrease the effluent pollution load, and better still produces solid wastewater that can be treated easily since they are degradable.
e) Most of the plants are renewable and readily available, hence the process can be relatively less costly and inexpensive.

Although the potential of the green technology is eminent, some glaring gaps have been identified. More researches are required to identify best methods of extraction, optimized conditions, replacement of metallic mordants and avoid the less toxic minerals in tanning to make this green technology a success. Optimization of the extraction methods can be determined for each plant tannin to maximize their quality in the application of leather tanning processes such as particle size, temperature, methanol content and time on the extraction of tannin from plants. Another gap is the challenge that most plant extracts perform better with metal mordants which are not eco-

benign. The gaps allude to the possibility of some plant products that have the potential in the industry but yet to be utilized. For diversification, many plants need to be tested for their applications, their processability, their impact on the performance of final leather and the shelf life of the products. The overall and specific plant products of all the possible products must be investigated thoroughly under different conditions to demonstrate that the products meet legal requirements. The green chemistry technologies and systems involving plants highlighted in this review have shown the capacity to reduce the environmental wastes and pollution especially the Cr VI. However, the levels are still higher than the recommended minimum levels. Therefore, more research is required in order to minimize the Cr (VI) levels to lower than 3 mg/kg.

2.8 *Aloe barbadensis* Miller and carrageenan

Aloe barbadensis Miller, commonly known as *Aloe vera*, is a perennial succulent spiky, cactus-like xerophyte plant with green, dagger- shaped leaves that are fleshy, tapering, spiny, marinated and filled with a clear viscous gel (Joseph and Raj, 2010). This plant belongs to the lily (Liliaceae) or Aloeaceae family (Nejatzadeh-Barandozi *et al.*, 2013; Ray *et al.*, 2013). The genus *Aloe* contains over 400 different species, among which *Aloe barbadensis* Miller, *Aloe aborescens*, and *Aloe chinensis* are the most popular. *Aloe barbadensis* Miller, is the most famous species of the genus *Aloe* and probably one of the most commercially valuable, being cultivated globally (Dagne *et al.*, 2000). This herb grows in temperate and subtropical parts of the world (Joseph and Raj, 2010).

Phytochemically, *Aloe barbadensis* Miller contains five major components; Phenolics and non-phenolics (anthraquinones, flavonoids, indoles), vitamins (A, B1, B2, C, E, and α-tocopherol), saccharides, enzymes and low molecular weight substances (Ray *et al.*, 2013; Anitha, 2012). The anthraquinones are mainly composed of *Aloe* emodin, aloin, aloetic acid, anthranol, isobarbaloin emodin and ester of cinnamic acid (Hamman, 2008). The phenolics especially aloin and *Aloe* emodin have shown antioxidant activity (reducing power) and the potential to scavenge free radicals (Tian and Hua, 2005; Nejatzadeh-Barandozi, 2013; Pizzi *et al.*, 2014). Separately it has been shown that *Aloe barbadensis* Miller has glutathione peroxidase, superoxide dismutase enzymes and phenolic antioxidants which enhance the antioxidant activity (Khilfi *et al.*, 2006; Hamman, 2008; Singh *et al.*, 2011). The antioxidant activity of ABM has been determined by

DPPH assay (%) to be 88.31 % and 65.65% of α-tocopherol (Anilakumar *et al*., 2010; Narsih *et al*., 2013). The higher content of the antioxidant activity is attributed to the high content of phenolic content, ascorbic acid, tocopherol and pigment (Patras *et al*., 2009; Pengseng *et al*., 2010). The polysaccharides contained in ABM are emollient polysaccharides, glucomannan (moisturizer), arabinan, arabinorhamnogalactan, glactan, galactogalacturan, glucogalactomannan and glucoronic acid (Sanghi, 2015).

Antioxidants interfere with the oxidative processes by scavenging the free radicals, chelating free catalytic metals and by acting as electron donors (Gulcin *et al.,* 2005). Phenolic compounds have an inhibitory effect on the oxidation of oleic acid that influences the oxidation of Cr (III) to Cr (VI) (Yu *et al*., 2010). From Oxygen radical absorbance capacity (ORAC) and ferric reduction antioxidant power (FRAP) analyses, it has shown antioxidant activity acting as UV-protection due to the antioxidant polyphenols, indoles, and alkaloids present in *Aloe Barbadensis* leaf gel (Nejatzadeh-Barandozi, 2013). Both ORAC and FRAP are attributed to the synergistic action of the compounds contained in the leaf rather than a single fraction (Dagne *et al.*, 2000). Minimizing oxidation helps to increase the scavenging activity (Tegtmeyer and Kleban, 2013). Hence *Aloe barbadensis* Miller can be impregnated in the leather matrix to minimize the oxidation of Cr (III) to Cr (VI) in leather. Although Litke and Widdemer, (2003) have used *Aloe Barbadensis* Miller gel to retan leather, they only tested the comfortability of the gloves, garment and shoes from resulting leather to the wearer. Bitlisli *et al*., (2010) also used *Aloe barbadensis* Miller during fatliquoring to treat split suede leather. However, they only investigated the antimicrobial characteristics of the resulting leather. It has been investigated that *Aloe vera* juice can be used a natural mordant for optimizing natural dye from the Hambo Hambo (Cassia singueana) (Berhanu and Ratnapandian, 2017). However, no study has examined the effect of *Aloe Barbadensis* Miller gel on the formation of Cr (VI) and its effect on the molecular structure, physical properties, elemental composition and formation of Cr (VI) in leather.

Carrageenan is an assortment of sulphated polyelectrolyte hetero-polysaccharides extracted from Rhodophyceae (red seaweeds) (Pereira *et al*., 2003; Pereira *et al*., 2013; Krol *et al*., 2016). The chemical structure of carrageenan are chains of alternating β-D-galactose and α-D-galactose

connected by together by β-(1,4) and α-(1,3). These polysaccharides have excellent rheological properties that makes them gelling and thickening agents.

2.9 Effects of Solar and UV radiations on collagenous polymers

Polymeric materials, primarily those of an organic nature such as collagen, are susceptible to degradation from high energy radiation (Metreveli *et al.*, 2006). UV radiations initiate polymeric photo-oxidation (Nalyanya *et al.*, 2016b). Collagen in leather is composed of UV-absorbing endogenous chromophores such as epidermis, aromatic amino acids, nucleic acids, and melanin which makes it more susceptible to photo-oxidative degradation (Park *et al.*, 2015; Nalyanya *et al.*, 2015b; Metreveli *et al.*, 2010). Among the amino acid chromophores are tyrosine, phenylalanine, tryptophan and histidine which absorb in the range of (250 − 300) nm with a maximum at 275 nm (Metreveli *et al.*, 2010). When exposed to UV radiations, the absorbed energy induces photochemical reactions in the collagen by free radical mechanisms. UV irradiations of wet collagen fibres causes the formation of hydroxyl radical (OH-) from water. The OH radicals attack the peptide backbone to produce peptide radicals (-NH-C*-CO-) (Paul and Bailey, 2003). The covalent bonds split to create two unstable moieties. The free radicals (reactive oxygen species) formed react with oxygen developing very reactive derivatives such as superoxide ions (O^{2-}.) and hydroxyl radicals (OH^{-}) as well as non-free radical species such as hydrogen peroxide (H_2O_2) (Tsuboi *et al.*, 2001; Yildrim *et al.*, 2001). Peroxide radicals further react with the organic constituents of leather, and dyes, tanning agents and fat liquors, breaking some of the bonds between the said products and collagen (de Volder *et al.*, 2007). The breaking of the bonds leads to loss of physical, chemical and mechanical properties of the hide (Larsen, 2000; Thomson, 2002; Metreveli *et al.*, 2006; Sionkowska *et al.*, 2006). These radicals are strong oxidants that react with the Cr (III) in leather and consequently converting it into Cr (VI) (Devikavathi *et al.*, 2014).

Practical approaches to preventing or retarding photo-oxidative degradation are the reduction in absorption of UV light, reduction in the energy absorbed by certain molecular groups (“quenching”) and finally antioxidant action (*et al.*, 1994). Antioxidant action terminates the chain reactions (oxidation reactions) taking place hence decreasing the kinetic chain length and stabilizing the polymer against the light and heat.

2.10 Raman Spectroscopy

2.10.1 Raman scattering theory

When electromagnetic field interacts with a molecule, light can either be absorbed, scattered or does not interact at all. The absorption may occur when the energy of the incident photons corresponds or is really close to the energy gap between electronic levels and when the photon is absorbed, the molecule reaches a new excited level (Smith and Dent, 2013; Mullertz *et al*., 2016). Scattering is produced when a photon rises to a virtual state and immediately dissipate the energy by emitting a photon. There are two forms of scattered radiation; Rayleigh and Raman shift. When a molecule is excited by a photon from the ground state to a virtual energy state, the molecule can relax or return to the ground state by emission of a photon whose energy is the same as that of the exciting radiation resulting into elastic Rayleigh scattering. This scattering is the most intense among the two scattering. Raman scattering has a frequency which is shifted higher or lower than that of the incident beam. A small proportion of the scattered light can have frequencies that are smaller than those of the elastically scattered part because a part of the energy of the incoming photons was employed to excite to excite molecules to a higher vibrational state. As a result, the emitted photons will be shifted to lower energy i.e. light with a lower frequency. This shift is designated the Stokes shift. The difference in energy between the original state and the final state corresponds to a vibrational mode far from the excitation wavelength. If the process starts from a vibrationally excited state and relaxes to the ground state, then the emitted photons will be shifted to higher frequency which is designated the Anti-Stokes shift (Engel *et al*., 2013; Robinson *et al*., 2014; Granger and Hank, 2016).

As explained by Maxwell-Boltzmann distribution law, more molecules exist in the ground state than in the excited state and hence Stokes lines are more intense compared to anti-stokes lines at ambient temperatures. Therefore, the Stokes side of the spectrum is used for analysis. These processes are illustrated in a simple energy level diagram in figure 2.6.

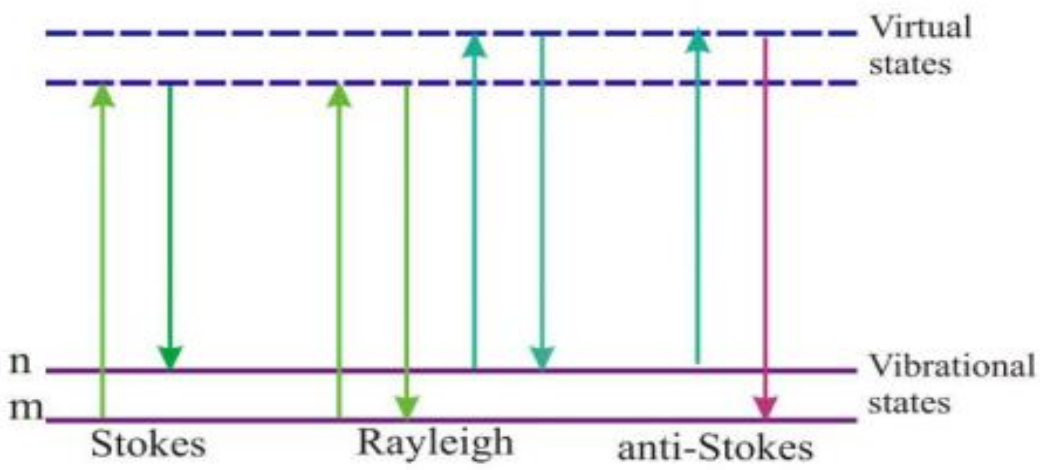

Figure 2.6: Energy level diagram of Raman scattering effect

Raman scattering is a less frequent event and weak inelastic scattering Effect since it involves only one in 10^6- 10^8 of the scattered photons (Raman and Krishna, 1928; Smith and Dent, 2013). The process involves two events: the incident that is absorbed and then the second is created due to the relaxation of the excited level. The process involves electronic transitions between vibrational energy levels of the same electronic state of a molecule. When a light wave passes near a molecule, it interacts and distorts the cloud of electrons surrounding the nuclei, causing the polarization of the electrons and go to a higher state. At that instant, the energy present in the light wave is transferred to the molecule, resulting in a higher state of the molecule, called 'virtual state', which is not stable and the energy is released as scattered radiation. This event occurs when the light and the electrons interact and the molecule nuclei start to move at the same time. The nuclei are heavier than the electrons, causing a change in the energy of the molecule either to a lower or a higher state, depending on the starting conditions of the molecule, if it was in ground state (*Stokes* scattering) or in a vibrational excited state (*anti-Stokes* scattering) (Engel *et al*., 2013; Robinson *et al*., 2014; Granger and Hank, 2016).

In the molecule, the nuclei are spaced and rotation is fixed about their equilibrium positions, but they are free to vibrate in harmonic motion along a given coordinate. The vibrations in a molecule are defined as oscillation of the atoms in the neighborhood of their equilibrium positions, and can be considered as a harmonic oscillator. The frequency of the vibrations is related with the mass of

the collective vibrating atoms. The intensities of the Raman spectrum depend of the nature of the vibration under study and instrumentation factors. Since different functional groups present different vibrational types, every molecule present a unique Raman spectrum. The Raman spectrum contains bands which are specific to individual compounds due to their modes of molecular vibration. These bands are analysed to identify an unknown compound or material (Janko *et al.*, 2010; Masic *et al.*, 2011). This molecular polarizability changes as the molecular are perturbed and change its equilibrium position (Schafer and Schmidt, 2012).

The electric field effect of the electromagnetic excitation (laser beam) which is considered as oscillating wave makes the electrons in the molecule to follow their behavior and experience an induced dipole moment (mu), causing the scattered light at the oscillation frequency. This is Rayleigh radiation. The molecule suffers a distortion in its electron cloud when interacts with light, and the ease of the electrons to follow the light field, will determine the intensity of the distortion. The elasticity of the electron cloud is called polarizability α, when the sample is irradiated with a laser light. In Raman scattering, the molecule vibrates as a consequence of a change in polarizability of the electron cloud.

The change in frequency experimented by the photons in the Raman scattering is called 'Raman shift', expressed in cm^{-1}, correspond to the wavenumber of the vibrational mode that is involved in the scattering process. Molecular vibrations can be seen either by IR or Raman spectroscopy. Nevertheless, they offer different information, while in IR, there must exist a change in the dipole moment, in Raman must exist a change in the polarizability of the molecule. In Raman spectroscopy, the inelastic scattering contains information about the vibrational states of the sample, evidenced by a shift on the frequency of the incident light. This is, the vibrations modulate the polarizability and induce the radiation of the dipole moment at different frequencies from the incident electromagnetic radiation, this response is the one that is measured and stored by the detector.

Thus, most of the peaks seen in Raman spectra are caused by the Stokes scattering of molecule being studied. These particular peaks from the Stokes scattering results in a characteristic Raman spectrum that acts as a "fingerprint" for the molecule and can allow for the identification of unknown samples (Robinson *et al*., 2014). Generally speaking, there are two main types of

vibrations: stretching and bending. In stretching, it is the bond length that is changing and this change can either be symmetric and asymmetric. It is the bond angle that changes in bending which can produce either a wagging, twisting, rocking, or scissoring motion. Of these options, symmetric stretching is the most common in Raman spectroscopy. This is due to the fact that it contributes the most to a change in polarizability which is what makes the molecule Raman active. Asymmetric stretching is not very common because this motion tends to cancel the changes in polarizability occurring, leading to no net change in polarizability of the molecule as a whole. All four of the bending vibrations are also not very common in Raman spectroscopy. Consequently, the majority of the scattering events in Raman spectroscopy occur due to a symmetric stretch of a couple of the bonds within the molecule being studied (Granger and Hank, 2016).

As with other spectroscopic methods, a light source is necessary for these vibrations and scattering events to occur. With Raman spectroscopy, though, the shifts seen in the spectra should not change based on the wavelength of the light source. Thus, there are a variety of different light sources available for use. The main requirement is that the light source must be monochromatic. Because of this, lasers are very common and desirable sources as they are an intense, monochromatic and coherent light source. Many labs use blue or green lasers since they generally give high intensities of Raman scattering. However, this wavelength of laser has been cited to cause decomposition of the sample or fluorescence of the molecule. This is because these shorter wavelengths are closer to the ultraviolet and visible region of the electromagnetic spectrum where more electronic transitions occur. In these situations, lasers with a longer wavelength, such as a red or infrared laser, are preferred. In general, instruments where multiple lasers can be used are favored so that multiple spectra can be taken.

Raman microscopy involves illuminating laser monochromatic light source focused on a sample by a microscope objective, resulting in Raman scattering. The Raman backscattered light is then directed through a pinhole into a spectrograph containing a holographic grating, which diverts different wavelengths at different angles. The decomposed wavelengths are then collected by a deep cooled charge coupled capacitor (CCD) camera, of which the data is then recorded by a computer (Bicchieri *et al.*, 2011). The technique allows Raman spectra to be collected from structures on a micrometer scale. Raman microscopy can be used for mapping samples to allow

distribution of the constituents and molecular bonding within a sample to be observed (Kocurek *et al.*, 2015). Mapping in this case allows spectra to be taken at several points in a grid formation and then spectra are analyzed with respect to the constituents present at each point. Mapping makes Raman microscopy suitable to study leather especially owing to its gradual anisotropic nature.

2.10.2 Advantages of Raman spectroscopy for collagenous materials analysis

a) The vibrations involving the covalent and ionic bonds that are prevalent in leather are stronger in Raman than other vibrational techniques such as FTIR. The vibrations include stretching vibrations (C≡C, C=C, P=P, C-S and S-S. Bending vibrations are generally weaker than stretching in Raman spectroscopy (Granger and Hank, 2016).
b) Due to the smaller diameter of laser beam (1-2 mm), only a small amount of the sample is required for analysis.
c) Acts as a molecular fingerprint containing highly unique and detailed features allowing highly selective determinations (Kikuchi *et al.*, 2005; Kolomaznik *et al.*, 2012).
d) Can be applied to any sample which can be accessible by laser and the resulting emitted photons can be detected whether organic, inorganic or biological.
e) Can measure solids, liquids, gas, transparent and non-transparent samples.
f) Since Raman scattering arises from the change of polarizability or orientation of the electron distribution in the molecule as it vibrates, Raman peaks are usually composed of a series of isolated bands and therefore the water and CO_2 have weak Raman scattering properties and produce few interference (Baeten *et al*., 1998). Therefore, aqueous samples present no problem unlike other vibrational techniques.
g) The scanning is completely non-invasive and reproducible and hence non-destructive (Schutz *et al.*, 2013).
h) Raman bands for non-polar groups such as C=C that form the skeletal backbone of collagen are stronger in Raman spectroscopy than other techniques (Baeten *et al*., 1998).
i) The other advantages are that this technique is convenient, rapid, contactless, and doesn't require sample preparation which in many cases distort the sample (Schutz *et al.*, 2013).

2.10.3 Disadvantages of Raman spectroscopy

a) Some compounds fluorescence when irradiated by the laser beam. This a broad spectral emission which can inundate the Raman signal. This is so especially when the energy of the incident light corresponds to the electronic transition energy of the material, higher intensity fluorescence than the Raman which makes the Raman signals undetectable. This drawback has been minimized by excitation with laser monochromatic light of bigger wavelength such as NIR (λ=1064 nm) which rarely excites fluorescence (Keller *et al*., 1993).
b) The Raman Effect. The weak Raman signals mean that noise, which can come from a variety of sources, can make the acquisition of good quality data difficult.
c) It's difficult to acquire rotational and rotation-vibration spectra with high resolution in Raman since Raman spectra are observed in the UV-VIS region where high resolving power is difficult.

The intensity of the bands in Raman spectroscopy is determined by the change in polarizability, of the molecule as it vibrates. The factors that affect the polarizability of the molecules include:

a) Polarity of groups in the material. Non-polar or slightly polar groups often give rise to stretching vibration of high Raman scattering intensity.
b) Type of the vibration mode. Raman scattering bands from stretching vibrations are more intense than those from deformation vibration since stretching vibrations are generally stronger scatterers than bending vibrations.
c) The nature of the bonds. Raman scattering bands from symmetrical vibrations which do not distort the molecule, have higher intensities than those from antisymmetric vibrations.
d) The stretching vibrations of multiple bonds such as C=C often cause intense Raman scattering bands (Baranska *et al.,* 1987; Grasseli and Bulkin, 1991).

Although Raman spectroscopy has a unique spectrum for each material, the band positions or vibration frequencies are modified by the factors such as the interatomic distances, the spatial arrangement groups, the Fermi resonance, the physical state of the sample, the polarity of the environment, the formation of hydrogen bond, and the inductive, mesomeric, and field effects of neighboring groups (Baranska *et al*., 1987; Masic *et al.*, 2011). This therefore requires that before deciding to use Raman spectroscopy, the molecules being examined must Raman active. The

requirement dictates that the molecules must have a change in polarizability. Essentially, the electron cloud around the vibrating atoms need to be distorted in some manner. This distortion changes as the bond length changes. Resultantly, the polarizability is able to be changed as the atoms vibrate.

2.10.4 Applications of Raman microscopy in collagenous materials' analysis

The technique has been used to identify molecular bonds and structural changes in materials (Kocurek *et al.,* 2015). The use of Raman spectroscopy to study the molecular structures of collagenous materials is documented (Jastrzebska *et al.,* 2003; Dolgin *et al.,* 2007; Metreveli *et al.,* 2010; Plavan *et al.,* 2010; Janko *et al.,* 2010; Bicchieri *et al.,* 2011; Mozir *et al.,* 2012). Characterization and deterioration estimation of parchment using Raman technique has been published (Mannucci *et al.,* 2000; Edwards *et al.,* 2001; Garp *et al*., 2002). Chemical bonds are appropriately assigned to the wave numbers. For instance, amide I vibration accounts for the dominant peak in a spectrum at 1600-1700 cm^{-1} and represents a set of stretching vibrations of the C=O (vC=O) and C-N fractions. Amide II peak which occurs at 1510-1580 cm^{-1} contains a series of bands and depends predominantly on the N-H bending vibrations (δNH and CN stretching). The peaks at 1500-1600 cm^{-1} are for v(CCH) aromatic ring stretch modes of the amino acids proline/hydroxyproline and tyrosine/phenylalanine. The peaks at 1245-1270 cm^{-1} are for amide III (Peptide bonds within the proteins of collagen pointing to the helical conformation of the collagen molecules). The peaks at 1470-1510 cm^{-1} are for vOH (from water absorbed into collagen structure and allows identification and strength of the hydrogen bond from peptide chain). The peaks at 1900-1920 cm-1 are for bands given by valence and deformation vibrations (vOH+ δOH) for hydrogen groups from peptide chain while 1480-1500 cm^{-1} band partially correlates with shrinkage temperature pointing to the changes in the hydrogen bond structure (associated with intra/intermolecular hydrogen bonds).

In this technique, vibrational characteristics, represented by the Raman peak position, intensity and spectral range, area under the curve and full wdith at half maximum can be assigned to their specific bonds and analyzed (Liu *et al*., 2015b). Structural modification can then be determined by monitoring the shifting of the positions of the bonds and intensity change of the very peaks.

Position and intensity of the maide amide I and II bands shift whenever any processes that alter the structure (collagen conformation) occurs such as degradation (Janko *et al.*, 2010; Mozir *et al.*, 2012). Intensity drop signifies aging or deterioration of the material (Dolgin *et al.*, 2007). For instance, increase of OH stretching leads to increase in intensity of the amide I while carboxyl compounds cause an increase in the peak area or shoulders at amide I (Derrick, 1991). Plavan *et al.*, (2010) and Mozir *et al.*, (2012) defined hydrolysis degree as the ratio of the amide I intensity to amide II intensity. Using Raman spectroscopy, Kolomaznik *et al.* (2012) distinguished between the Cr (III) and Cr (VI) spectra in leathers (Kikuchi *et al.*, 2005). It was found that compounds of Cr (VI) have their most absolute characteristic peak at 907 cm^{-1} while that of Cr (III) is at 554 cm^{-1}. It was pointed out that intensities at these wavenumbers depend on the concentrations of Cr (VI) and Cr (III), respectively. Metreveli *et al.* (2010) studied UV-irradiated collagen in the presence of ascorbic acid. The results showed that intensity of the amide bands decreases with an increase of the UV-radiation dose. Liu *et al*. (2015b), Dehring *et al*. (2006) and Riaz *et al*. (2018) used the intensity ratio of amide III to the peak at 1454 cm^{-1} to indicate the level of orderliness of the triple helical structure. The ratios closer to a unity implies intact triple helix of collagen. Lower ratio is an indication of lower collagen content or higher randomness in the triple helix. From the brief review, it can be deduced that the potential of Raman spectroscopy in studying collagenous materials is unlimited. This therefore qualifies Raman spectroscopic methods to study molecular structure of post tanned leather to determine the effect of crusting operations and Aloe barbadensis Miller and carrageenan.

2.11 X-ray fluorescence (XRF) spectroscopy

2.11.1 X-ray flourescence

X-rays are a short wavelength (from 0.01 to 10 10 nm) form of electromagnetic radiations in the region between gamma rays and Ultraviolet radiation. When x-rays (ionizing radiations) propagated through matter, it can either be scattered or absorbed by the material's constituent atoms. In the case of absorption, if the incident x-ray has sufficient energy, it can cause an electron to be emitted from the atom. The emitted electron is of lower energy than the primary incident x-ray and is termed as fluorescence. Hence attenuation of the incident x-ray beam occurs which leads to emission of secondary radiation by the matter. This process is known as photoelectric effect.

The interaction involves two processes that may either cause fluorescent emission of x-rays characteristic of the elements present in the matter or emission of photoelectron and Auger electrons. The ejected electrons can be from the inner shells in the atom which creates vacancies and the resulting atom is in excited state. To return to the stable state, an electron from a higher energy shell drops down to fill the vacancy. The energy difference in this scenario between the two shells is emitted as a characteristic x-ray. Each element has a unique set of energy levels. Therefore, the energy of the emitted characteristic x-ray is unique and fixed to the element that produced it.

Through detection of and measurement of an x-ray's energy, it's possible to identify the element that produced it. The x-ray intensity increases with the concentration of a particular element within a sample. For this reason, x-rays have been used to detect and quantify elements in a given sample in a large dynamic range (ng/g to 5) with a high precision (approximately 0.1 %) and minimal sample preparation required (Wobrauschek and Christina, 2010; Shackley, 2011). This technique suffers the following drawbacks;

a) Sample destructivity
b) Weak excitation of low atomic number elements and the strict sample geometry requirement (Bechoff, 2006).
c) Interference of element characteristic lines due to poor resolution of the normally used solid state detectors.
d) Matrix effects which makes a direct conversion of fluorescence peak intensities into elemental concentrations difficult. The secondary X-Rays from the sample to the detector are attenuated by absorption and X-ray fluorescence enhancement resulting into characteristic peak intensity that is a function of element's concentration and that of other elements in the sample (Potts and Webb, 1992).

XRF can be subdivided into different classes of techniques: wavelength dispersive XRF (WDXRF) and energy dispersive XRF (EDXRF) with latter being the most preferred in the elemental determination (Kaniu *et al.,* 2011).

2.11.2 Energy Dispersive X-Ray Fluorescence Spectroscopy (EDXRFs)

The EDXRF technique is a simultaneous multi-element technique which analyzes the surface layer and determines major, minor, and trace elements (elements with atomic number Z=11) in different matrices where the samples require minimal or no preparation. The technique is nondestructive, relatively easy, fast and capable of detecting elements down to the limit of mg/L (He and Espen, 1991; Wegrzynek *et al*., 2004). The technique is also relatively cheaper (Mandal *et al*., 2003).

There are two different configurations of exciting the sample: 1) Direct excitation where the X ray beam is pointed directly at the sample, 2) secondary excitation where the source points at a secondary target, the target element is excited and fluoresced, and then the target fluorescence is used to excite the sample (Wobrauschek *et al*., 2010). The measurement of fluorescence spectral peak positions aids in determining which elements are in the sample and by a conversion of measured intensities of radiation to the concentration of elements it is possible to make a quantitative determination of them (Yi *et al*., 2015). This is because there is a relationship between the concentration of analyte, the measured X-rays, and the intensity of the excitation source along with the overall composition of the sample and its absorption properties (Markowics, 2011).

2.11.3 EDXRF instrumentation and Analysis

An EDXRF system comprises an X-ray source (radioactive sources or X-ray tube), an X-ray detection device, and a data acquisition system. The basic principle involves the impact of the primary X-rays in the sample; later, the emerging fluorescent X-rays produced are detected by an energy dispersive detector; and, subsequently, the characteristic X-rays of different elements are identified (Mandal et al, 2002). This spectrometer provides a versatile analytical technique for qualitative and quantitative determination of both major and minor atomic elements in samples ranging from gaseous to solids.

The versatility of this equipment lies in the uniqueness and performance of its components such as the close-coupled Cartesian Geometry (CG) optical kernel that dramatically increases signal-to-noise. Monochromatic or polarized excitation technique from secondary targets, instead of conventional “noisy” white radiation (Bremsstrahlung) direct excitation improves significantly the detection limits (lower limits) for elements in highly scattering matrices like water, hydrocarbons,

and biological materials by reducing background noise, and simultaneously increasing element peaks. This allows the spectrometer the ability to analyze routine trace element even in difficult sample types. Up to five standard polarization and secondary targets (RX9, Cu, Si, Al and Mo) cover the complete elemental range, from Na to U, with optimized sensitivity. The fifth excitation target provides enhanced excitation of Na and Mg. This is achieved by the 3D optics whereby the polychromatic X-rays from the tube irradiates a secondary target placed along the first axis. After scattering 90^{o}, monochromatic X-rays travel along the second axis to the sample. The spectra from the sample is then recorded by a detector on the third axis.

The indirect radiation in the secondary target optics offers low x-ray radiation dose to the sample and hence minimal or no damage to the collagen samples used in this study which are sensitive to heat (Moriyama, 2013). Excitation is provided by a close-coupled 50 W 50 kV-2mA Pd-anode end-window X-ray tube. For maximum flux stability, the tube is fitted with a shutter so that the tube may remain on at all times for maximum stability and durability and an available uninterruptible power supply (UPS) which compensates for power line fluctuations and extends tube life. This superior counting statistics and designed-in high stability translate into extraordinary analytical performance. The quantification of samples' concentration was done using fundamental parameters method and inbuilt software. The NEX CG has advanced FP (fundamental Parameter) software-RPF-SQX (Rigaku Profile Fitting-Spectra Quant X) technology that allows semi-quantitative analysis of almost all sample types without standards – and rigorous quantitative analysis with standards (Kataoka, 1989). Additionally, RPF-SQX features a scattering X-ray FP method that automatically estimates the concentration of the non-measurable components (low atomic number elements) from the Compton and Thomson scattering X-ray intensities of the Mo-K_{α} line from the Mo secondary target (Kataoka *et al*., 2005). This an accurate profile fitting algorithm that suits all samples including those with complex matrices (Moriyama, 2013).

The fundamental parameter evaluation procedure was calibrated and set up to analyze 32 pure elements from sodium to lead. The high-performance SDD detector and high throughput thermo-electrical Peltier cooling which delivers superior peak shape, large active detection area and optimal balanced spectral resolution and high throughput for superior counting statistics. For circular samples in pellet assays placed on sample plates with spinner with a number of position auto sampler provides superior results with inhomogeneous samples. The system provides various

environments such as vacuum that comes with high capacity pump and vacuum sensor, delivering superior light element sensitivity for non-volatile samples and short pump-down times. The analysis is controlled by a PC data acquisition system. Figure 2.7 shows a typical schematic EDXRF (RIGAKU NEX CG) spectrometer operated at applied power and voltage of 50 W and 50 kV, respectively, in the X-ray tube and current of 2 mA.

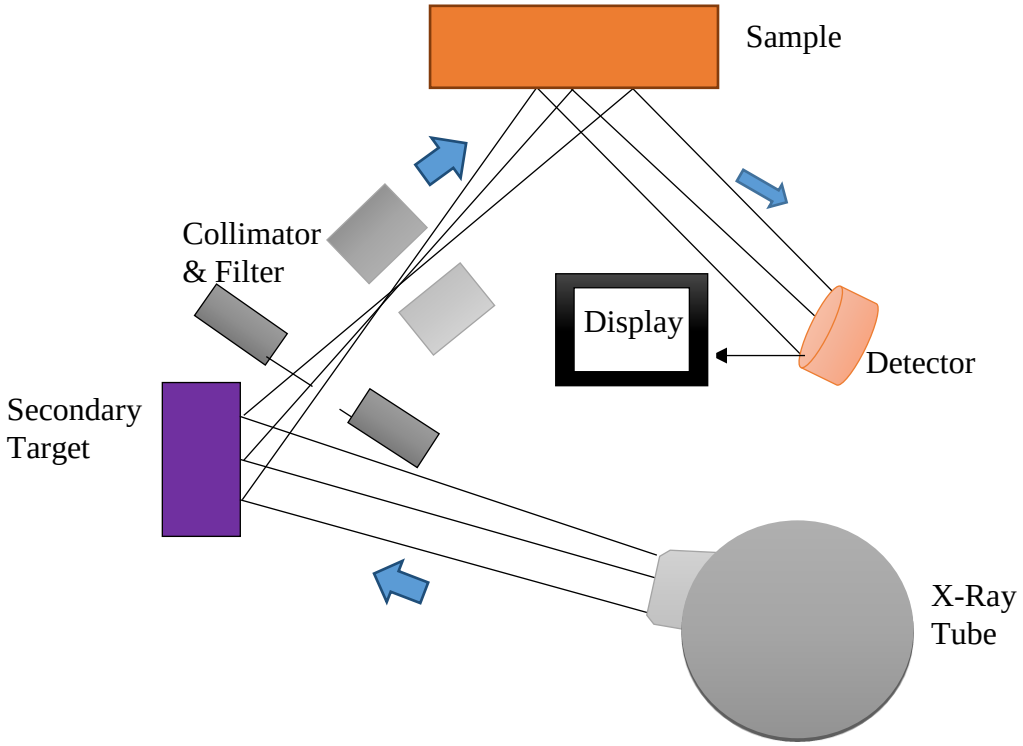

Figure 2.7: Schematic illustration of EDXRF Rigaku NEX CG secondary excitation.

2.12 UV-VIS Spectrophotometry

2.12.1 Determination of Cr (VI) in leather samples

Different methods have been applied to determine the presence and concentrations of Cr (VI) in leather such as colorimetric method with 1, 5-diphenyl-carbazide (metal complexation), graphic furnace atomic absorption spectroscopy (GF-AAS), Flame Atomic Absorption Spectroscopy (FAAS) and Raman spectroscopy (Monteiro *et al.*, 2002; Kikuchi *et al.*, 2005; Kolomaznik *et al.*, 2012). Colorimetric methods are more preferred since they reduce any possible interference from

Cr (III) organic complexes are 1, 5-diphenyl-carbazide spectrophotometry since many organic ligands (proteins, amino acids, and organic acids) react with the investigated Cr (III) (Walsh and Halloran, 1996). The spectrophotometric method suffers minor interferences attributable to a nonspecific turbidity effect unlike methyl isobutyl ketone extraction, and co-precipitation methods suffer many severe interferences with Cr (III) protein complexes. Further comparison with ICP-OES, FAAS, and UV–VIS (1, 5-diphenyl-carbazide method) by Balasubramanian and Pugalenthi (1999) showed that UV–VIS is the most suitable method: other methods suffered from severe matrix effects arising from high concentrations of mineral acids and electrolytes.

2.12.2 ISO 17075:2007 Procedure

This International Standard specifies a method for determining Cr (VI) in solutions leached from leather under defined conditions. The method described is suitable to quantify the Cr (VI) content in leathers down to 3 mg/kg. The principle behind this procedure is that soluble Cr (VI) oxidizes 1,5-diphenylcarbazide to 1,5-diphenylcarbazone that is red/violet compound that absorbs maximally at 540 nm in a mineral acid environment. Using the absorbance at 540 nm and known concentrations of stock solutions, the concentration of Cr (VI) can be quantified photometrically at 540 nm using Beer-Lambert's law. This procedure specifies the reagents and their preparations. The soluble Cr (VI) is leached from the sample in phosphate buffer at pH 7.5 to 8.0 and substances which influence the detection are removed by solid phase extraction if necessary. The extraction of Cr (VI) from waste samples is carried up under alkali conditions in order to eliminate the to Cr (III).

2.13 Principal Components Analysis (PCA)

PCA is a data reduction technique aimed at reducing the dimensionality of any given data set, and finding important spectral features which hold a significant influence on the spectral variance and to identify subtle relationship within data which contains a large number of variables (Varmuza and Filzmoser, 2009). The technique performs dimension reduction, data modeling, detection of outliers, and selection of main variables, classification, validation and prediction of samples (Brereton, 2003). For this, the PCA rotates the original variables within the dataset and transformed into new variables which lie in new planes of maximum variance, such that the first few axes

reflect most of the variations within the data. The new variables are referred to as principal components (PCs). PCs are orthogonal to each other to ensure that each of the new variables are not related. The PCs are computed in order of maximum variance, which means that PC 1 represents the largest amount of variance followed by PC 2 and PC 3. The PCs are sorted out in decreasing order of importance as dictated by their associated eigenvalues.

This technique often used for exploratory analysis of data (ie to find underlying similarities or differences in the data set) and hence also referred to as unsupervised method. A common method for determining the optimum number of PCs is by plotting the PCA eigenvalues, which correspond to the PC variances, versus the PC number to obtain a scree plot (Cattell, 1966; Varmuza and Filzmoser, 2009). The eigenvalues represent the amount of total variance of a principal component (Bryant and Yarnold, 2010; Varmuza and Filzmoser, 2009). According to Cattell (1966), breaks or drops in the scree plot indicate components that should be used in subsequent analyses, as they indicate components representing a significant amount of variance in the data. The flat region in the graph represents components with a small amount of variance, which is not optimum for subsequent analyses, and thus should not be retained (Varmuza and Filzmoser, 2009). According to the eigenvalue criterion, only the PCs with eigenvalues greater than one are considered important (Pellerano *et al*., 2012).

The relationship between the old and new variables is demonstrated by the loadings plot. This plot essentially illustrates the contribution of the old variables, such as the Raman intensities at differing Raman shifts in spectra, to the principal component. This allows the regions of the spectra which account for the greatest amount of variance (largest contribution) to be distinguished from noise, the spectroscopic structures which are not relevant to the structure of the PC. Each analyzed sample is assigned a score with respect to a particular PC. By plotting two PCs against each other, samples will be separated based on their scores for each PC. This plot is referred to as the scores plot and is the method by which the subtle differences in spectra due to differing constituent concentrations can be used to distinguish the sample. Loadings reflect both the contribution of variable to PC and how well the PC takes into account the variation of the same variable over the whole points in the data. In geometrical terms, loading is simply the cosine of the angle lying between the variable and the current PC. Therefore, smaller angle has a larger loading. Hence loading can only vary from -1 to +1.

CHAPTER THREE
MATERIALS AND METHODS

3.1 Materials

3.1.1 Leather processing and sampling

Freshly flayed raw bovine hide of mass 33 kg was procured from Abattoir. The hide was cured temporarily by salting. The hide was weighed and soaked in 200% water and 1% detergents by weight for 30 minutes to remove dirt. The hide was processed to tanning chrome tanning stage as summarized in tables 3.1 to 3.2.

Table 3.1: Beam house operations recipe

Process/step	**%, chemicals**	**Temp ±1** ^{0}C	**Duration**	**Remarks**
Dirt Soaking	200%, water 1%, Detergents		30 min	
Main soaking	200%, water 1%, bactericide		Overnight	Run slowly in drum
Dehairing	300%, Water 3%, Sodium Sulphide		30 mins	pH=12
Liming	3%, lime 300%, water		Overnight	Drain and wash
Reliming	3%, lime, 300%, water		16 hours	
Fleshing and scudding	Add: 1%, Lime Soak	25	Overnight	Drain and wash
Deliming	2%, Ammonium Sulphate 1%, Sodium Metabisulphite	25	1 hour	Check X-section p.H=8.3
Bating	100%, Water 1%, microbates-1600 LVU	35-37	Run for 1hr	Drum speed=3 rpm Drain and wash
Draining/washing	200%, water	20-25	20 mins	Drain

Table 3.2: Tanning operations recipe

Process/Step	**(%) Chemicals**	**Temp (±1°C)**	**Time**	**Remarks**
Pickling	100% water float, 10% industrial salt 1% H_2SO_4(98%),(1:10) 1% Sodium Formate,	20-22	10 min Overnight	Check pH=8 Lower pH=2.5 by adding H_2SO_4
Tanning	6% CrSO4, (33% basic) Add 0.5% Fungicide	25-27	Overnight	Drum speed= 3 rpm
	Then add Second 6% CrSO4, Add 0.5% Fungicide	25-27	Overnight	Drum speed= 3 rpm Penetration complete through x-section pH = 2.16-3.0 Drain
Drain & washing	200%, water	25	25	Drain
Basification	1%, Sodium bicarb		1 hr	Check pH=3.8
washing	200%, water		20 mins	Drain Horse up overnight
Sammying & Shaving				Sample piece for Ts=106 ^{0}C
Neutralization	150%, water 1%, Antimould 2%, Ammonium Bicarb 1.5%, Sodium formate	45 ^{0}C	45 mins	Check pH=6.5
Splitting				Split 1.0 mm

Tanning was done using chromium sulphate in a drum. Afterwards, the wet blue leather was wetted in water, basified using sodium bicarbonate and then neutralized using ammonium bicarbonate. The 1% of antimould and 2% of the sodium formate were also added during neutralization stage to prevent bacterial growth and adjust the pH to 6.5, respectively. After neutralization, the butt area of the crust was cut out. The butt area was divided into 8 parts, with sample codes T, TA, R, RA, D, DA, F, and FA, as shown in figure 3.1.

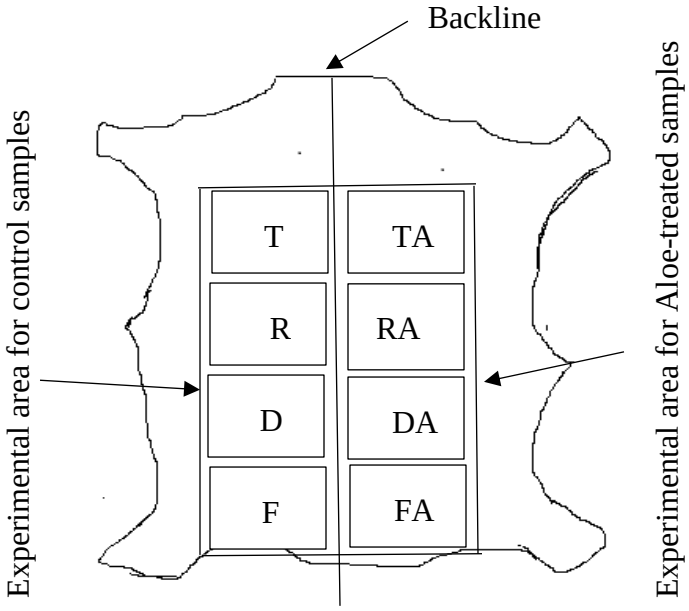

Figure 3.1: Representation of sample preparation for control and samples treated with additives

The parts labelled T and TA were cut out while the rest proceeded tanning process as summarized in table 3.3.

Table 3.3: Retanning process recipe

Process	**%, chemicals**	**Temp(±1°C)**	**Duration**	**Remarks**
Retannage	150%, warm water			
	6%, Retannage agent	45 ^{0}C	45 mins	Check retan penetration
Fixing	1.5%, formic acid mixed with water 1:10		30 mins	
Drain, wash & toggle	200%, water		Overnight	

Retannage was carried out using 150% water at 45^{o}C and 6% retannage agents (chromium sulphate) in a drum running moderately slowly for 45 minutes. After penetration check of retanning agents, 1.5% formic was added to fix the crust. The crust was then drained, washed and toggled overnight prior to dyeing process as shown in plate 3.1.

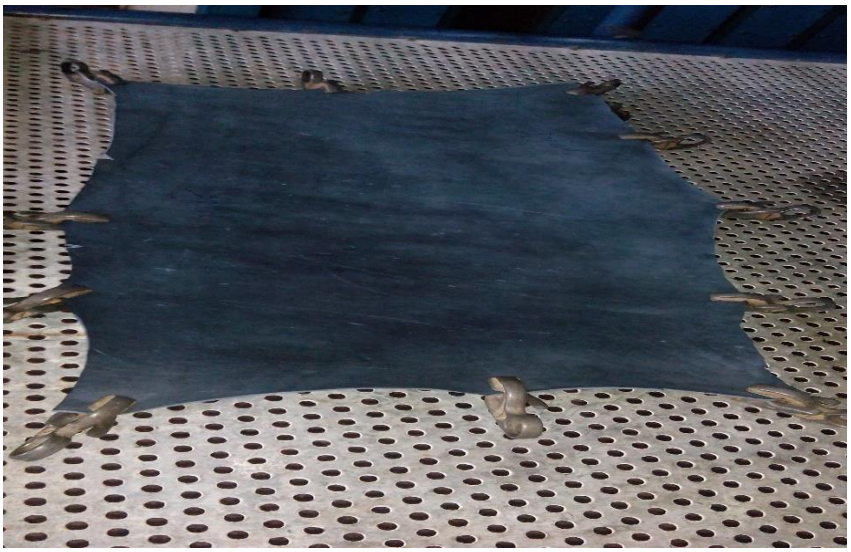

Plate 3.1: Toggled crust

The parts labelled R and RA were cut out. The rest of the crust proceeded to dyeing process as shown summarized in table 3.4.

Table 3.4: Dyeing process recipe

Process	**%, chemicals**	**Temp (±1°C)**	**Duration**	**Remarks**
Basification	Ammonium bicarb			Check pH until 6.5
Dyeing	100%, warm water	50 ^{0}C	45 mins	
	2%, novolene black dye			Through the axle as drum runs
Fixing	1%, formic acid mixed with water 1:4		45 mins	
Drain, wash & toggle	200%, water		Overnight	

To prepare the crust for dyeing, the remaining piece was basified using ammonium bicarbonate to adjust the pH to 6.5. Dyeing involved 100% water at 50^0C and 2% of black dye added through the axle as the drum runs. The crust was then fixed using formic acid before it was drained, washed and toggled overnight. After dyeing process, the parts labelled D and DA were cut out and the remaining crust proceeded to Fatliquoring process as summarized in table 3.5.

Table 3.5: Fatliquoring process recipe

Process	**%, chemicals**	**Temp (±1°C)**	**Duration**	**Remarks**
Fatliquoring	100%, warm water 2%, fat liquor	50 ^{0}C	45 mins	
Fixing	1.5%, formic acid mixed with water 1:4		45 mins	Check pH=3.5
Drain, wash & toggle	200%, water		Overnight	

Fatliquoring involved 100% of water at 50^0C and 2% fatliquor was run in a drum for 45 minutes. The fatliquored crust was then fixed in 1.5% of formic acid to lower the pH to 3.5. The crust was then drained and washed in 200% water, and toggled overnight.

3.1.2 *Aloe barbadensis* Miller and carrageenan preparation and sample incorporation

By weight of the crust, 6% of both *Aloe barbadensis* Miller powder and carrageenan powder, were reconstituted with 100 parts of water at 37 ^{0}C as shown in plate….

Plate 3.2: Reconstituted mixture of *Aloe barbadensis* Miller and carrageenan

The pH of the gel formed was measured to be 5.5. The parts labelled TA, RA, DA and FA, one a time, were then run in a drum with water 100 % at 37 ^{0}C. The prepared gels of *Aloe barbadensis* Miller and carrageenan was introduced into the drum via the axle. One at a time, the drum was run at 20 rpm for one hour. After one hour, the penetration of the gel was checked against the control samples. Well penetrated crusts assumed yellow-brown color.

3.1.3 Sampling, Sample location and sample conditioning

The specimens for mechanical tests were kept in a standard atmosphere of temperature 25 ±2 ^{o}C and Relative Humidity of 65% ± 2% for at least 48 hours according to ISO 2419: 2012. Sampling was done in accordance with the standard ISO 2418 (2005). In this procedure, the samples were cut within the "official sampling position (OSP)" within which, the variation in strength properties and anisotropy are gradual and minimal (Mutlu et al, 2014). For tensile strength, tear strength, percentage elongation and flexing endurance, eight (8) samples were cut; 4 sampled parallel while 4 sampled perpendicularly to the backline as shown in figure 3.2.

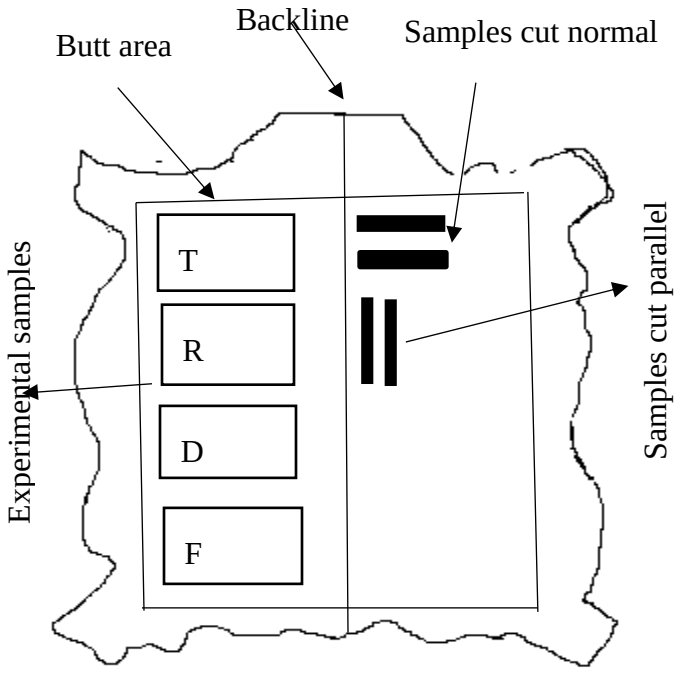

Figure 3.2: Representation of sample cutting and official sample location.

3.1.4 Thermal and photo aging of samples in the heat and UV chamber

Suitably cut samples were aged in a heat-adjustable cabinet at 80ºC for 24 hours and UV cabinet (UV light of wavelength 254 nm-UV-C) for 132 hours. The samples were then conditioned in a standard atmosphere (Temperature = 23 ± 2 °C and humidity = 50 ± 5% R.H.) for 48 hours before testing (ISO 2419: 2002).

3.1.5 Leather grinding and extraction of Cr (VI)

The samples were milled using Thomas-Wiley laboratory mill in quadruplets of 2.00 ± 0.01 g and placed into a 250-ml flask, and 100 ml of K_2HPO_4 solution added. The reagent solution was prepared by dissolving 22.8 g of the salt in 1,000 ml of distilled water and adjusting the pH value to 8.0±0.1. The flask was tightly sealed and the solution mixed on an automatic shaker for 3 hours at room temperature. After mixing, the pH value of the solution obtained was checked again to maintain it at 8.0. Afterward the samples were filtered, and the filtrates analyzed for their Cr (VI) contents. Blank solutions were prepared in the same way but without leather samples.

3.2 Methods

3.2.1 Physical properties

Tensile Strength and Percentage Elongation at break

For tensile strength and elongation, eight dumbbell-shaped or dog-bone shaped test samples (four from each principal direction) (figure 3.3) were cut from the crusts using special steel knife (figure 3.4) in template according to ISO 3376:2012 as described in Kowaiska and Zbikowska (2014).

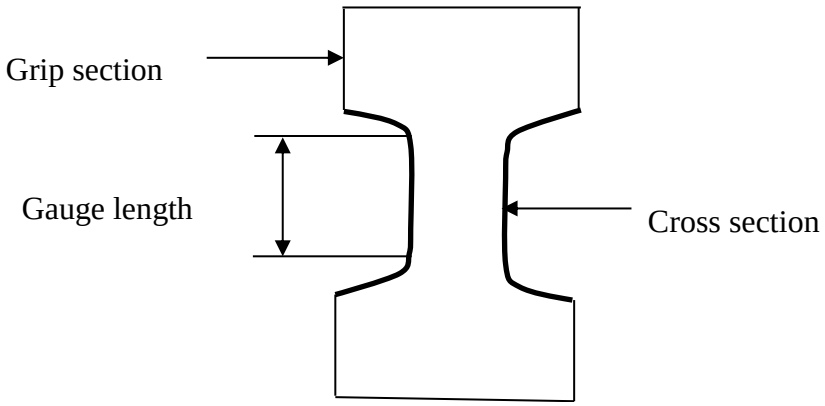

Figure 3.3: Schematic illustration of a standard tensile test sample

The press knife cut outs the specimen such that the angle formed at the cutting edge between the internal and external surfaces of the press knife was about 20° and the depth of the wedge of the cutting knife, *d* was greater than the thickness of the cut leather, as shown in figure 3.4.

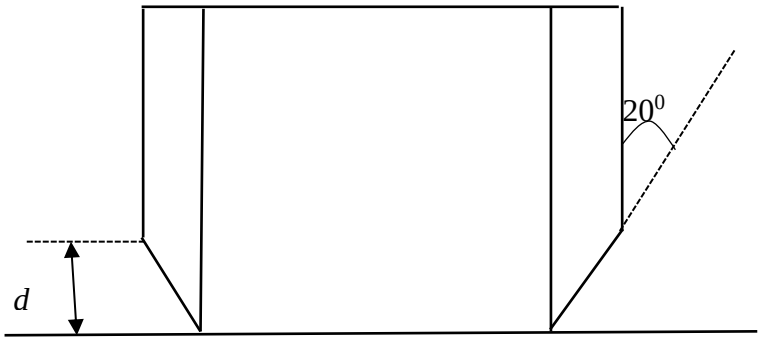

Figure 3.4: Schematic illustration of the shape of a press knife

The thickness of each specimen and mean thickness was measured in accordance to ISO 2589. These tests were carried out using tensile tester (Instron machine 1011) according to ISO 3376:2012 at a cross-head speed of 100 mm/min at room temperature. The jaw of the machine was set 50 mm apart, and then the sample was clamped in the jaws so that the edges of the jaws lie along the midline. The machine was allowed to run until the specimen breaks, and the highest load reached was registered as the breaking load in Newtons and the elongation was also recorded in mm. Tensile strength load is in Newton. The tensile strength and percentage elongation were calculated using equations (3.1) and (3.2), respectively.

$$Tensile\ strength = \frac{Maximum\ breaking\ force\ (N)}{Cross\text{-}section\ area\ (mm^2)} \quad (3.1)$$

Then the cross sectional area of the specimen was calculated by multiplying its width by its thickness in mm.

$$Percentage\ Elongation\ at\ break\ (\%) = \frac{Elongation\ (mm)}{Original\ free\ length\ (mm)} \times 100\% \quad (3.2)$$

The actual specimen used in this study are shown in plate 3.3.

Plate 3.3: The actual standard test sample

Determination of Baumann Tear strength/Slit tear resistance

The tearing strength was measured using the same machine (Instron-1101) according to the official method (ISO 3376: 2002) with pneumatic grips replaced in the jaws of the Instron testing machine. The samples were cut as a rectangle 50 mm long and 25 mm wide by use of a press knife which cuts out the specimen and slot in one operation (Template machine) parallel and perpendicular at each position as shown in figure 3.5.

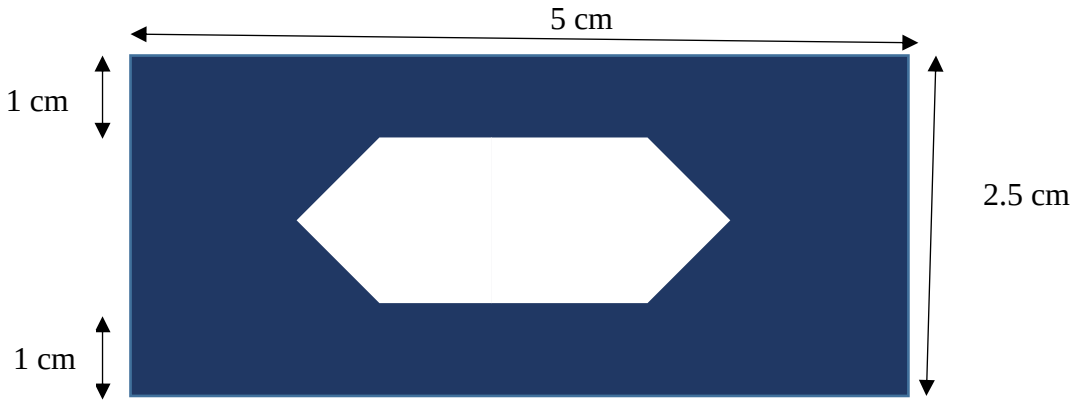

Figure 3.5: Schematic of a standard sample for tear strength

A steady speed of separation of the jaws of 100 mm per minute was used, and the readings of load fall in that part of the scale which has been shown by calibration to be correct within 1%. The machine was run until the specimen was torn apart and the highest load reached during tearing was recorded as the breaking load in Newtons. Thickness (t) and width (W) of each sample were measured according to ISO 2589:2002 to the nearest 0.1 mm at areas between the grain side and the flesh side. Image of the actual test sample for tear strength is shown in plate 3.4.

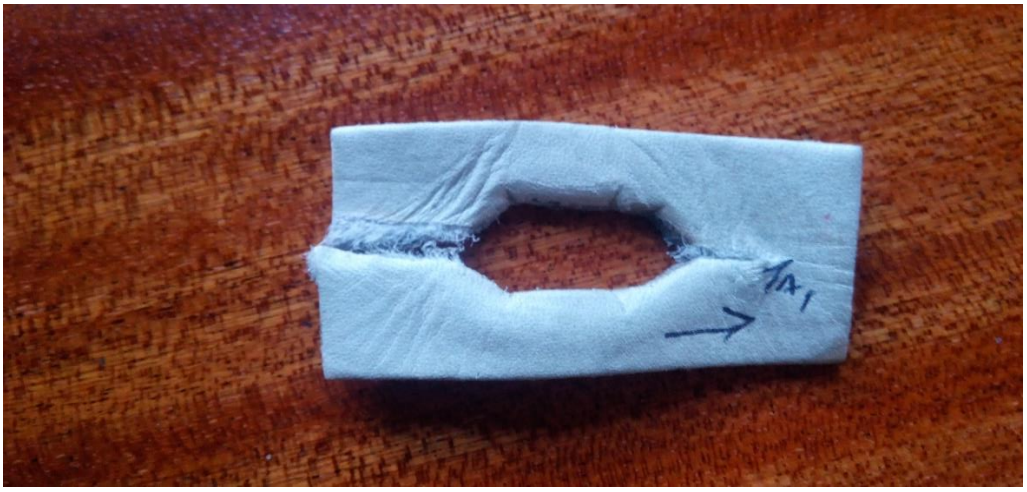

Plate 3.4: The actual standard sample for tear strength testing

Measurement of Distension of grain by the Ball burst test

The distension of grain was measured by the Ball burst test, using a lastometer STD 104 according to the official method ISO 3379: 2005. A disc-shaped specimen of the leather was firmly held with the grain side up between the clamping rings, with the spherical tip of the steel rod just touching the flesh surface as shown in plate 3.5.

Plate 3.5: The actual standard sample for grain distension testing

The specimen was moved downward against the rod, distending the grain of the leather immediately above the rod, simulataneously observing for incipient cracking and bursting. The point at which the grain side of the leather cracked and bursted was noted and the corresponding distension values were recorded.

Flexual resistance and endurance

The flexual endurance was measured using SATRA STM 701 Bally flexometer 2184 according to ISO 5402:2002. The leather specimen of dimension 70 × 45 mm was folded and fixed to the jaws of the instrument in such a manner that the grain side remained outside with fold on the specimen. Plate 3.6 shows a sample folded and fixed to the jaws of a flexometer.

Plate 3.6: The actual sample folded and fixed in a flexometer

The motor was switched on having one clamp fixed and the other moved backward and forward causing folds in the specimen to run along it. The leather samples were subjected to pre-determined 100, 500, 1,000, 5,000, 10,000, 20,000, 50,000, 100,000, 200,000 and 250,000 flexes/cycles and it was observed periodically for any signs of crack on the grain surface of the leather using a hand magnifying lens.

Shrinkage temperature (Ts)

The shrinkage temperature of the tanned skins was measured using SATRA STD 114 test apparatus according to ISO 3380:2002. Strips of leather 50 mm × 2mm were cut from the leather. The specimens were cut along and across the backbone. Holes were punched at the ends of the leather to allow the specimen to be held vertically in the test chamber filled with water and a small weight was attached to the lower end. The position of the lower end was indicated by an adjustable marker outside the tube to help judge when the shrinkage occurs. The apparatus was then closed and water heated at the rate of 2 °C/min by applying the external heat source to the boiler components as shown in plate 3.7.

Plate 3.7: The arrangement of shrinkage temperature apparatus

The temperature at which the leather starts to shrink was taken as the shrinkage temperature.

3.2.2 Confocal Raman Microscopy

The Raman spectra of post tanned crust samples were collected by placing suitable prepared samples onto an Aluminium substrate and using a Confocal Laser Raman microscope system (STR, SEKI Technotron Corp) equipped with a 785-nm laser excitation and spectrometer (Princeton Instruments). The laser beam was focused onto a spot size of diameter approximately 1.5 μm and the Stokes Raman scattered radiation were collected using high magnification optics with x50 objective lens. Various scans were conducted in 20 different random points of the sample by moving the sample on an x-y translation stage. The beam centering (baseline) and Raman spectra calibration was performed prior to each acquisition using the first order phonon of silicon chip with characteristic peak at 520.5 cm^{-1}. The laser excitation power of irradiation was 11.74 mW. The exposure time was 15 seconds, with 10 accumulations and the spectra were collected in the 15.38-1788.82 cm^{-1} range with 2.0 cm^{-1} resolution and centre wave number 1100 cm^{-1}. The grating was 600 lines per millimeter grating in order to cover a wider spectra range. The confocal Raman Microscope with spectrometer and Raman optical filters are shown in plates 3.8 and 3.9, respectively.

Plate 3.8: Confocal Raman Microscope with spectrometer

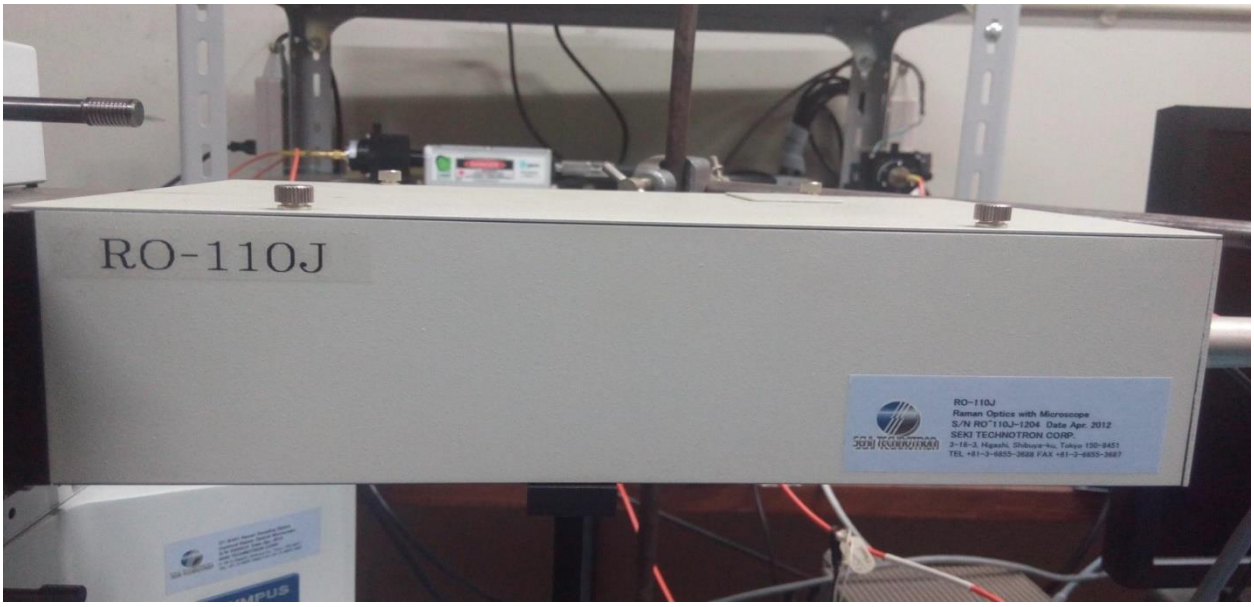

Plate 3.9: Raman Optical Filters

3.2.3 EDXRF Spectroscopy

Elemental concentration in leather samples was done using RIGAKU NEX CG Energy Dispersive X-ray Fluorescence (EDXRF) spectrometer. Circular leather samples were prepared in form of pellet assays with the diameter equal to 32 mm and placed sample cups with the spinner with 9-position auto-sampler that accepts standard 32 mm diameter sample cups and pellets for automated sample handling. The spectral data were recorded within 0-42 keV energy range at an interval of 0.02 keV and data acquisition dead time of less than 1 %. The measurements were carried out in vacuum. The samples were irradiated for 50 s and 100 s with same operating conditions. The analysis was controlled by a PC data acquisition system. The results of analysis were expressed in parts per million (ppm) which is equivalent to mg/kg. Image of the Rigaku NEX CG EDXRF spectrometer and the 15-autosampler are shown in plate 3.10 and 3.11, respectively.

Plate 3.10: The Rigaku NEX CG spectrometer and PC system

Plate 3.11: The 15-autosampler

3.2.4 UV-VIS Spectrophotometry

The Cr (VI) content in the extract was determined by spectrophotometry, utilizing the pink colour of the complex between Cr (VI) and Diphenyl carbazide (DPC), with an absorption maximum at 540 nm in accordance with ISO 17075 standard as shown in plate 3.12.

Plate 3.12: Volumeteric flasks of Cr (VI) extracts mixed with diphenylcarbazide

All the chemical reagents used in this study were of analytical grade purity. The samples (tanned, retanned, dyed and fatliquored) were sampled according to ISO 2418 and ground in accordance with ISO 4044 using Thomas-Wiley Laboratory Mill model 4, shortly before the extraction process. 2.0+0.01g of ground leather was added into 100 ml of degassed dipotassiumhydrogen phosphate solution in a 250-ml conical flask and tightly sealed. Dipotassium hydrogen phosphate solution was prepared by dissolving 22.8 g dipotassium hydrogen phosphate in 1000 ml distilled water to pH 8.0 with phosphoric acid and degassed using nitrogen gas for 5 mins. The leather powder suspension was gently shaken for 3 hours on a mechanical shaker. The contents of the conical flask were then filtered through a membrane filter into a glass bottle and pH checked to maintain it at 7.5-8.0. The Cr (VI) content of the filtrate was then analyzed.

The chromium (VI) analysis of leather samples was conducted at 540 nm using a JENWAY UV-VIS spectrophotometer mode according to ISO 17075 standard method. Ground samples in

triplicates of 2.00 ± 0.01 g were placed into a 250-ml flask, and 100 ml of K_2HPO_4 solution added. The reagent solution was prepared by dissolving 22.8 g of the salt in 1,000 ml of distilled water and adjusting the pH value to 8.0±0.1. The flask was tightly sealed and the solution mixed on an automatic shaker for 3 h at room temperature. After mixing, the pH value of the solution obtained was checked again to maintain 8.0. Afterward the samples were filtered, and the filtrates analyzed for their Cr (VI) contents. Blank solutions were prepared in the same way but without leather samples. Ten microliters of the filtered solution were placed in a 25-ml flask, and 0.5 ml of the 1, 5-diphenyl-carbazide solution was added. The reagent solution was prepared by dissolving 1.0 g of reagent in 100 ml of acetone and acidifying with glacial acetic acid; 0.5 ml of phosphoric acid solution in distilled water (7:10 parts per volume) was added. After filling up to volume, the solution was left for 15 min to form a stable colored metal complex. The absorption was then measured by UV–VIS spectrophotometry at 540 nm.

Cr (VI) determination

Ten (10) ml of the filtered solution from ground leather was transferred to 25-ml volumetric flask through the cartridge on an SPE system with vacuum device. The volume was made up by degassed dipotassium hydrogen phosphate solution. 10 ml of the resulting solution was pipetted into 25-ml volumetric flask. 0.5 ml of the 1, 5-diphenyl-carbazide solution and 0.5 ml of phosphoric acid were added and the flask made up by extraction solution. The solution was allowed to stand for 15 minutes and thereafter, the absorbance was measured at 540 nm in a 4 cm cell against the blank solution. The reagent solution was prepared by dissolving 1.0 g of reagent in 100 ml of acetone and acidifying with glacial acetic acid; 0.5 ml of phosphoric acid solution in distilled water (7:10 parts per volume) was added. After filling up to volume, the solution was left for 15 min in order to form a stable colored metal complex. The absorbance was then measured by UV–VIS spectrophotometry at 540 nm using a JENWAY 7315 UV-VIS spectrophotometer.

Standard calibration

The calibration was performed using a stock standard Cr (VI) solution prepared by dissolving 2.829 g of $K_2Cr_2O_7$ (dried for 16.5 h at 102°C) in 1.000 ml of distilled water. One microliter of this stock solution was diluted up to 1,000 ml, and the resulting solution was used for preparing

the calibration standards in a concentration range from 50 micrograms/l to 1 mg/l. 1ml of this stock solution contains 1mg of chromium. 1 ml of the stock solution was pipetted into 1000 ml volumetric flask and made up to the mark with degassed dipotassium hydrogen phosphate solution. 1 ml of this solution contains 1 microgram of chromium. Calibrating solutions were made using six standards: 1ml, 3ml, 6ml, 9 ml, 12 ml and 15 ml of standard solution. The solutions were pipetted into 25 ml volumetric flasks, 0.5 ml of phosphoric acid and 0.5 diphenylcarbazide solution were added into each volumetric flask. The volumes in each were made to 25 ml using degassed dipotassium hydrogen phosphate solution, mixed well and left for 15 minutes. The absorbance of the solutions was measured in the same photometric cell as the samples at 540 nm against the distilled water as blank solution. Calibration curve of the absorbance of the six standard solutions against chromium (VI) concentrations in micrograms per ml was plotted.

Calculation of Cr (VI) content

The chromium (VI) content was calculated using equation (3.3)

$$w_{Cr(VI)} = \frac{(A_1 - A_2) \times V_0 \times V_2 \times V_4}{V_1 \times V_3 \times m \times F} \quad (3.3)$$

Where $w_{Cr(VI)}$ is the mass fraction, expressed in mg/kg of soluble Cr (VI) in leather crust; A_1 is the absorbance of sample solution with DPC; A_2 is the absorbance of sample solution without DPC; F is the gradient of calibration curve (y/x), in ml/µg; m is the mass of the leather sample taken, expressed in grams; V_0 is the extract volume of the initial sample; V_1 is the aliquot taken from the extract volume of the initial sample; V_2 is the total eluate (S_1) volume, after passage through the SPE column, to which the aliquot V_1 was made up; V_3 is the aliquot taken from solution S_1 while V_4 is the final make-up volume of the aliquot from S_1. All the volumes are expressed in milliliters.

Determination of the recovery rate

This was done to determine the influence of the matrix on the results obtained. 10 ml aliquot of the analytical solution (filtrate) was spiked with chromium (VI) solution to double approximately the content of the Chromium (VI) concentration of the extract. Their absorbance was determined

with and without DPC and recorded A_{1s} and A_{2s}, respectively. Recovery rate (η), expressed as a percent, was calculated using equation (3.4):

$$\eta = \frac{[(A_{1s}-A_{2s})-(A_1-A_2)]}{\rho \times F} \times 100\% \quad (3.4)$$

where ρ is the mass concentration of chromium (VI) spiked in µg/ml; A_{1s} and A_{2s} are the absorbance of solution after adding chromium (VI) with DPC and without DPC, respectively.

Presentation of data

The data are presented as mean values of triplicate samples. Limit of quantification and limit of detection were calculated using equations (3.5) and (3.6), respectively.

$$Quantification\ Limit\ (QL) = \frac{10\sigma}{slope\ of\ the\ calibration\ curve} \quad (3.5)$$

$$Limit\ of\ Detection\ (LOD) = \frac{3.3\sigma}{slope\ of\ the\ calibration\ curve} \quad (3.6)$$

where σ is the standard deviation of the y-intercepts of regression lines.

3.3 Data analysis

3.3.1 Student's t-test

To identify the statistical significance of observed differences of physical properties among crusted and samples modified with ABM and carrageenan, a student's t-test in Origin 2018 of unpaired data with unequal variance was used. Statistical significance of observed difference between Cr (VI) formed in samples modified with *Aloe barbadensis* Miller and non-modified samples was used. Differences were counted and denoted as "significant" when $p<0.05$, with higher significance for smaller p values.

3.3.2 Raman data preprocessing

Savitsky-Golay nine-point smoothing function of second order in Origin 2018 was applied over the range 400-1800 cm^{-1} of each spectrum to filter out noise affecting the Raman spectral quality. The auto fluorescence background elimination performed using a Vancouver Raman Algorithm based on fifth-order polynomial fitting method. The data analysis was performed using Origin

2018 to determine the peak heights, full width at half maximum (FWHM) values of the peaks. The analysis was confined to the Raman scattering region 400-1800 cm^{-1}. The average of measurements at 20 locations was taken to determine the mean.

3.3.3 Multivariate statistical analysis

Due to large number of spectra for each crusts sample, PCA was employed to evaluate useful information in these spectra that cannot be manifest by univariate analysis. Therefore, multivariate statistical analysis using PCA in Origin 2018 was to differentiate among Raman spectral data profiles from post tanned crusts from the treated post tanned crusts. The PCA was used to reduce the original dimensions of the spectral data and represent the original data using new principal component (PC) scores that capture the maximum variance in the data. In such case, the transportation matrix was applied to the spectra of the crusts. The main components that describe majority of the variations were extracted from the data as PCA loadings. These loadings were plotted as a function of wavenumber in order to reveal the most important diagnostic wavenumbers related with the differences found in the Raman spectra. Peaks with large amplitudes or intensive in the loadings were identified as the most influential in the differentiation. Differences in the loadings of the principal component analysis were used to infer the effect of the crusting operations and *Aloe barbadensis* Miller and carrageenan on the physical, molecular and elemental concentrations.

CHAPTER FOUR
RESULTS AND DISCUSSION

This chapter presents the results of the investigations of the effect of crusting operations on the physical properties, molecular structure and on the elemental concentrations of leather crusts. Effects of *Aloe barbadensis* Miller mixed with carrageenan on the physical properties, molecular structure and elemental concentrations of post tanned leather crusts. Also detailed discussions of the effects of the crusting operations and *Aloe barbadensis* Miller mixed with carrageenan on the physical properties, molecular structure and elemental concentrations. The results and the scientific discussions have ultimately provided a basis for better leather tanning technology that employs chromium salts with minimal environmental and human health impact.

4.1 Effect of post tanning operations on the physical properties of leather

The mean values of tensile strength, tear strength, percentage elongation and distension at crack and burst are reported in table 4.1.

Table 4.1: Physical properties of tanned, retanned, dyed and fatliquored leather crusts (±SD)

Physical Properties	**Direction**	**Tanned**	**Retanned**	**Dyed**	**Fatliquored**
Tensile Strength (N/mm^2)	Normal	20.05±0.21	22.34±2.01	19.7±1.79	18.16 +1.80
	Parallel	21.28±1.03	24.15±2.08	22.28 ±2.40	19.04 + 1.67
Tear Strength (N/mm)	Normal	88.20±5.73	106.14±7.31	75.04±19.49	86.87±9.69
	Parallel	74.60±3.08	98.18±5.39	70.10±13.88	84.51±13.87
Elongation (%)	Normal	60.38±4.06	50.67±3.43	56.92±6.95	69.25±6.83
	Parallel	52.75±6.53	45.50±2.88	47.17±3.62	67.58±2.23
Ball Burst Distension (mm)	Crack	8.26±0.42	13.09±0.22	13.77±0.96	17.66±0.06
	Burst	9.19±0.67	16.40±0.23	16.38±0.48	17.77±0.03
Flexing Endurance (flexes)	Normal	No damage @ 50,000	No damage @ 50,000	No damage @ 50,000	No damage @ 50,000
	Parallel	No damage @ 50,000	No damage @ 50,000	No damage @ 50,000	No damage @ 50,000
Shrinkage Temperature (℃)		108	115	118	115
Uniformity coefficient (K_{unif})		1.1446	1.1136	1.206699	1.024

4.1.1 Anisotropic effect on the physical properties of leather

Tensile strength values for samples cut in parallel to the backline were higher than for perpendicular samples. Structurally, for the samples cut along the backline, majority of their fibres are already aligned in the same direction as the applied strain, hence they have little room to orient towards the strain axis (Nalyanya *et al*., 2015). This therefore means that the fibres themselves are directly strained at low levels of nominal strain and the process of fibre orientation is limited. For samples cut perpendicularly, many fibres are aligned normal to the direction of the applied strain, therefore, the fibres orient towards the strain axis. This orientation minimizes levels of nominal strain and deformation occurs by straining themselves. Further deformation is associated with

straining of the fibres themselves. Since tensile strength is proportional to the number of fibres aligned in that direction, its value is higher in the parallel orientation because the strain is being applied to a more orientated network of fibres than the case for perpendicular sampling. Fibre orientation will cause frictional damage to the fibres, and therefore increases the tensile strength. In perpendicular sampling, more fibre orientation thereby increases the possibility of fibre damage and reducing tensile strength.

Tear strength and percentage elongation values for specimens sampled along the backline were less than the value for specimen sampled perpendicular to the backline. When specimens are oriented parallel to the backbone, the general fibre direction is assumed to be in the same direction as the strain axis. Under these conditions, the specific work of fracture is higher because the tear does not propagate through fibre diameters. Instead, the fibres bridge the advancing tear and are subject to more of a straightforward rupturing process. In addition, when specimens are oriented in a direction perpendicular to the backline, the general fibre direction is assumed to be nearer 90^0 to the strain axis. Therefore, the specific work of fracture is lower because the tear is able to propagate directly through the felt work of fibres and tear strength is higher. In addition to the above explanation, when the samples for tear analysis are taken in parallel, the direction of tearing is in perpendicular and vice versa (Nalyanya *et al*., 2015). This explains the higher tear strength and elongation for samples cut in perpendicular, a negative trend, compared to tensile strength.

4.1.2 Effect of retanning process on the physical properties of leather

Retanned samples were observed to be structurally more compact and full and their grain surfaces were mechanically tighter compared to other crusts. Retanning process slightly increased tensile strength, tear strength, distension at crack and burst and shrinkage temperature. On the other hand, percentage elongation decreased after retanning process. For all the tanned and retanned specimens tested for flexual endurance, there was no observable damage at 50,000 flexes. Results from this study show that leather crusts at both tanned and retanned stages of processing are appropriate for most of the conventional leather applications. The margins of the results and patterns reported in this study are comparable to other related publications (Looney et al., 2002; Ashebre, 2014; Jian *et al*., 2012; Hassan *et al*., 2014; Seggiani *et al*., 2014; Inanc and Gulumser, 2015). Looney et al., 2002 observed an increase in tear strength, almost double, after retanning process. An increase in

flexural endurance after retanning process has also been observed by Gumel and Dambatta (2013). Nashy *et al*., (2011) and Zengin *et al*., (2012) reported an increase in tensile strength and shrinkage temperature after retanning process. Retanning using chromium salts impart extra crosslinks into the crust. These alkali salts form hydrogen bonds with hydroxyl components from the carboxyl units present in the aspartic and glutamic acids from the collagen of the crust (Liao *et al*., 2005a). Kinetic theory predicts increase in strength as the degree of crosslinking increases (Flory, 1953; Treloar, 1956; Tyagi, 2017). This explains the increase in tensile strength, tear strength, shrinkage temperature, and distension properties. Extra crosslinks reduce fibrillar (molecular) mobility and increased rigidity of the leather matrix between fibrils and within fibre bundles which impose mechanical restraints. These additional crosslinks act as rigid particulate fillers to a leather polymer matrix which decreases the elongation at break. Similarly, retanning induces bonding between the basic fibres. Mechanically, the bonds formed inhibit the realignment and straightening process of the fibres which slightly weakens the extensibility of the retanned leather.

4.1.3 Effect of dyeing process on the physical properties of leather

The chemical nature and intrinsic poly-functionality of dyes allows the formation of chemical bonds, van der Waals interactions and additional hydrogen bonds. Although these functionalities were expected to improve the physical properties, dyeing process was observed to decrease both tensile and tear strengths while it increased elongation, shrinkage temperature and distensions at grain crack and burst. Looney et al., (2002) made similar observations that dyes and pigments decreases tear strength up to 9%. This therefore, means that the bonds or links formed are weaker (Nedkova *et al*., 2005). Decrease in shrinkage temperature after dyeing has been reported by Jian et al (2012) who attributed the decrease in tensile strength and tear strength to poor adhesion between the dye and leather matrix. In our present study, the claims can be refuted because the dye bath was slightly acidic, hence facilitating the swelling of the leather substrate especially in the presence of water. Similarly, the temperatures of the dyeing process were slightly higher than room temperature hence there is an increased mobility of the molecule segments in the biopolymer (Nedkova *et al*., 2005). The two factors work together to improve the dispersion and distribution of dye molecules in the leather substrate and suitable adhesion between the substrate and molecules. On the other hand, the very penetration of the dye particles into leather matrix decreases

the energy of the intermolecular interaction and therefore destroys a significant portion of the already stable intermolecular bonds. Additionally, increased segmental mobility due to the said temperatures favours the disorientation of the collagen fibres. Modeling dyed crust as the heterogeneous composite, the mechanism of micromechanical deformations and macroscopic properties depend on local stress distribution around the fillers/inclusions. Poor adherence of the filler to the crust implies that the fillers are unable to carry any load, making it a weak body. This is because stress concentrations will be created around the particles, reducing the composite strength. We also hypothesized the mechanism whereby the oily nature of dyes in collagen imparts water retention ability. The polar or amphoteric nature of dyes has also been associated with level of hydration which also increases collagen's D-spacing (Sizeland *et al*., 2017). The increased D-spacing leaves more free volume for water attachment. The water retention alters the collagen's structure at fibrillar scale. The water attached disrupts hydrogen bonds which provide structural integrity to the molecular backbone of collagen and therefore decreases the strength properties of leather.

4.1.4 Effect of Fatliquoring process on the organoleptic and physical properties of leather

Fatliquored samples were softer, loose in structure and more pliable compared to other crust samples. Our observations agree with results reported by Sizeland *et al*., (2017) and Loony et al., (2002). Looney et Al., (2002) observed that sulfated glycerides and sulfited fatliquors decrease tear strength while Dutta (2008) observed that penetration of fatliquors into leather increases its looseness. It was also observed in this study that fatliquoring process modified mode of break; it induced both fibre rupture and pull-out (fine break). Fatliquored samples tore instead of snapping abruptly. This is fine break, which is normally dominant where collagen distribution is uniform and there are many fine wrinkles per unit length, an indication good quality leather (Diebschlag, 1975). Although it has been argued by Roig *et al*. (2012) that any tannery processes that prevents the fibrils from sticking together tightly on the grain surface definitely produces fine break, the tanned, retanned and dyed samples (fatliquor-free crusts) were almost brittle and snapped at break. This type of break is a result of the snapping of individual fibres themselves. This deformation behavior can be explained by using fibre recruitment model by Kronick and Beuchler (1986). In this model, it si hypothesized that fatliquoring process effectively lubricates the crust weave which

opens up its structure allowing its collagen fibres to align along the direction of the applied stress at low strains before the fibres themselves get elongated at high strains. Since there are different degrees of tautness of the collagen fibres in the weave, only few fibres get taut at the beginning of the strain but as the strain increases, more fibres get taut and the strength increases (Attenburrow, 1993). During break, some of the fibres pull apart while some get taut before others and break. However, in the unfatliquored (tanned, retanned and dyed) crusts, where the higher degree of fibre adhesion makes the material to have closed, compact and solid structure. In such a weave, the constituent fibres do not slide but extend on their own during elongation. This means that no fibre gets taut at low strains due to fibre adhesion. At break, some fibres get taut before others and rupture making the weave to snap. For this reason, fatliquoring process can be recommended since this type of break is desirable for quality and enthuses majority of consumers.

Fatliquored samples recorded lower tensile strength and shrinkage temperature as compared to dyed samples. The same pattern was observed by Bajza and Vrcek (2001), Gutters and Santos (2009) and Hassan *et al*., (2014). Bajza and Vrcek (2001) observed that shrinkage temperature decreases as the percentage of fatliquoring increases. The range of results for fatliquored samples is comparable to other studies (Sivakumar *et al*., 2008; Quadery *et al*., 2015; Valeika *et al*., 2012). The tear strength, percentage extension and distensions at crack and burst of fatliquored crust were significantly greater than those for dyed crusts ($p=0.01267$). This indicates that fatliquoring increases tear strength, elongation at break and distension of leather. This trend resonates with results reported by Gutters and Santos (2009) and Hassan *et al*., (2014). The results for elongation of fatliquored leather agree with those published by previous work (Liu *et al*., 2002; Quadery *et al*., 2015; Zengin *et al*., 2014). The increase in elongation was attributed to the sliding effect of the fatliquors in the fibres (Gutters and Santos, 2009). The trend for tensile strength and shrinkage temperature contradicted our hypothesis. It's expected that fatliquored crust permits the easy sliding of fibres against each other and aid in the stress distribution during the extension, a fact that ought to raise tensile strength and shrinkage temperature (Covington and Alexander, 1993). The decrease decrease of tensile strength and shrinkage temperature and increase in tear strength, elasticity and distension can be explained in three ways. The fatliquors in the collagen network can be modeled as primary plasticizers, secondary plasticizers and humectants (Sizeland *et al*., 2017; Jun *et al*., 1998; Zhengjun *et al*., 2015). As primary plasticizers, the synthetic sulphated oils

used in this study are anionic colloids with large molecules carrying a negative charge. Usually, after chrome tanning, the wet blue crust is neutralized, making them slightly acidic and hence cationic in nature. This ensures that the anionic oil molecules penetrate into the gaps of collagen fibres, their polar groups being attracted to the crust fibres through the cross section; forming a lubricant film around the collagen fibres. This ionic interaction of the two polar groups neutralizes the attractive forces between crust matrixes, weakening the Van der Waals forces between adjacent polymer chains. Hence in aqueous environment, it's accurate to model fatliquors as primary plasticizers. As secondary plasticizers, the inert molecules of fatliquors disperse within the leather matrices like fillers, providing mechanical spacers that separate adjacent collagen chains hence reducing Van der Waals forces. This reduces the number of fibre adhesion in the weave (Hu et al, 2003). Low or poor adhesion between the crust matrix and fatliquors can explain the decrease in tensile strength and shrinkage temperature while supporting the explanation for increase in extensibility and tear strength (Hu *et al*., 2003; Ervina *et al*., 2016). As humectants, findings from synchrotron scattering experiments have shown that fatliquors enhance water-retention capacity in the collagen (Sizeland *et al*., 2017). The high hydration level which is the reason for increased d-spacing of collagen also affects the physical properties. Therefore, the decrease in elasticity and increase in tensile strength are consequence of the increased d-spacing. In all the three explanations above, the leather structure weakens as a result of decreasing Van der Waals forces. The decrease consequently reduces the resistance of the crust to deformation (Liu *et al*., 2002). Kronick (1996) termed the weakening as destabilizing the crust and reversing the crosslinking action of the chrome tanning. Reversing crosslinking action definitely reduces the tensile strength and shrinkage temperature (Nalyanya *et al*., 2016a; Nalyanya *et al*., 2015; Nalyanya *et al*., 2016b). This also explains why the fibre bundle allows the constituent fibres to straighten up and align themselves in the direction of the deforming force before the fibres actually get to be stretched and hence elongation at break, softness and pliability.

4.1.5 Effect of post tanning processes on leather's anisotropy and uniformity

It was anticipated in this study that some features of the collagen structure can purposefully change and transform its fibrous structure during the crust processing, and this influences the deformation properties of the resulting leather. The degree of anisotropy in the leather was estimated according

to relaxation and deformation properties. The uniformity coefficient K_{unif} of the physical properties of leather was determined as the ratio of the average values of the elongations in transverse directions to the average values in the longitudinal direction. The changes in the coefficient were employed to infer dermal microstructural changes due to the underlying crust process. The coefficients of the crusted leathers were calculated using equation (4.1).

$$K_{unif} = \frac{\epsilon_{normal}}{\epsilon_{parallel}} \quad (4.1)$$

It was found out that retanning process decreases the coefficient by 2.7 %. This implies that retanning process disrupts the hierarchy of collagen hence disrupting the uniformity. Dyeing increased the coefficient by 8.36 % which means that dyeing stabilizes the structure of collagen. Fatliquoring decreased the coefficient by 15.14 %. This is the greatest decrease among the three processes considered. This implies that Fatliquoring is the most destructive crusting process to the leather uniformity. This observation corroborates the results by Sizeland *et al*., (2017) and Dutta (2008); penetration of fatliquors into leather increases looseness, softness and pliability.

The results in this section have been published in the Leather and Footwear journal (Appendix 1).

4.2 Effect of *Aloe barbadensis* Miller and carrageenan on the physical properties of leather

The physical properties of control crusts (crusts not treated with *Aloe barbadensis* Miller and carrageenan) were compared with those of the crusts treated with *Aloe barbadensis* Miller mixed with carrageenan. The effect of the *Aloe barbadensis* Miller mixed with carrageenan on the physical properties was inferred from the comparisons of the control and those treated samples at tanning, retanning, dyeing, and Fatliquoring stage as shown table 4.2. Each value of the tear strength, tensile strength, percentage elongation at break and distension is the average mean of eight samples; four specimens sampled parallel to the backline and four normal to the backline. The value for shrinkage temperature and flexing endurance for the 4 samples.

Table 4.2: Averages (±SD) of physical properties of post tanned crusts and their corresponding treated samples

	T[a]	**TA[b]**	**R[c]**	**RA[d]**	**D[e]**	**DA[f]**	**F[g]**	**FA[h]**
Tensile strength (N/mm^2)	20.66 ± 0.54	19.05 ± 0.52	23.24 ± 1.41	20.10 ± 0.37	20.99 ± 1.47	16.82 ± 0.60	18.60 ± 1.15	18.28 ± 1.1
Tear strength (N/mm)	89.81 ± 4.22	94.88 ± 6.55	104.64 ± 6.42	79.88 ± 6.89	82.49 ±17.99	67.77 ± 4.48	86.94 ±11.29	78.99 ± 2.49
Percentage elongation	56.57 ± 5.07	45.58 ± 1.38	48.09 ± 3.11	41.44 ± 0.76	52.05 ± 5.26	43.16 ± 0.86	68.42 ± 4.45	57.72 ± 1.65
Distension at grain crack (mm)	8.26 ± 0.42	10.49 ± 2.57	13.09 ± 0.22	9.37 ± 1.43	13.77 ± 0.96	11.85 ± 0.31	17.66 ± 0.06	12.39 ± 2.35
Distension at grain burst (mm)	9.19 ± 0.67	12.75 ± 2.92	16.40 + 0.23	10.44 ± 1.82	16.38 ± 0.48	16.19 ± 1.04	17.77 ± 0.03	13.81 ± 2.32
Shrinkage temp ℃)	108	108	117	116	118	114	115	114
Flexual endurance (flexes)	Over 50,000	Over 50,000	Over 50,000	Over 50,000	Over 50,000	Over 50,000	Over 100k	Over 100k

Footnote:

a-tanned, b-tanned treated with ABM, c-retanned, d-retanned treated with ABM, e-dyed, f-dyed treated with ABM, g-fatliquored, h-fatliquored treated with ABM.

The tensile strength, tear strength, elongation and distensions for control samples at all stages of post tanning processing were not significantly different from those of *Aloe barbadensis* Miller-treated samples at significance levels of p= 0.0972, 0.1324, 0.1565 and 0.040741, respectively. The shrinkage temperature and flexual endurance for both samples were more or less the same at almost all stages of crusting operations. This implies that the particles of both *Aloe barbadensis* Miller and carrageenan enter the interstices between the collagen fibres without affecting the physical strength. Although there was no significant difference, the values for control samples were slightly higher compared to the values of the treated samples. From the literature, both decrease and increase in the physical properties were expected as a result of both *Aloe barbadensis* miller and carrageenan. The *Aloe barbadensis* Miller has functions such as hydroxyl (-OH), amine groups ($-NH_3$), carboxylate (-COOH), ester and ethers which are anticipated to form hydrogen

bonds to cause crosslinking. A study by Surjushe *et al*. (2008) found out that *Aloe barbadensis* Miller increases collagen crosslinking which in this case was expected to least increase the physical properties. Similarly, when starch is oxidized and reduced, the available hydroxyl groups could participate in the formation of hydrogen bonds which act as crosslinking agents (Liu *et al*., 2009). A study by Lu *et al*. (2005) confirmed an improvement in tear strength, tensile strength and elongation at break after using starch with acrylic acid, acrylonitrile and acrylamide as a leather retanning agent. Ohan *et al.* (2002) added glucose into collagens and it had no effect on the mechanical properties. After irradiating the collagens with UV radiations, the mechanical properties synergistically improved due to crosslinking action. When thiourea, a potent antioxidant, was added into the collagens and glucose, the mechanical properties showed no effect. Another study by Liu *et al*. (2009) confirmed the same trend when they used starch-polyacrylamide graft copolymer by means of horseradish peroxidase (HRP) in retanning leather. Lv *et al*. (2011) confirmed an increase in shrinkage temperature when they used graft copolymer of phenols and starch with HRP in tanning. However, in the above two cases, it's not clear if the increase is due to starch or the other copolymers.

Conversely, other studies have reported starch to be poor in both dimensional stability and mechanical properties, a reason why native starches are usually hydrolyzed before applied in various end products (Liu *et al*., 2009; Ozkan *et al*., 2016). Naviglio *et al*. (2009) used potato during retanning of lambskins and the results affirmed the poor hydrothermal stabilization (Ts=76 °C). Later on, Xiaosheng *et al*. (2012) used oligosaccharides in leather and the resulting leather exhibited low moisture content and good separation characteristics of fibre bundles. Mechanically, separation of fibre bundles creates regions of weakness, where the propagation/distribution of stress within the structure is hindered. This leads to congestion of stress in one region hence breaking/failure at lower applied forces of deformation. In this study, the slight decrease in physical properties as a result of *Aloe barbadensis* Miller and carrageenan were explained as follows. Based on the phytochemistry of *Aloe barbadensis* Miller and carrageenan, they contain water loving (hydrophilic) functions such as hydroxyl (-OH), amine groups ($-NH_3$) from amino acids, carboxylate (-COOH), esters and ethers. Hence there is a tendency to absorb moisture (humectant) from the surrounding and retaining them in the leather crust matrix, causing leather to be hydrated (Hamman, 2008; Millikan, 2001; Agarry *et al*., 2005). This effect of leather

hydration due to humectant effect has been observed by Bitlisli *et al.* (2010). The moisture interacts with collagen to alter the structure at the fibrillar scale and hence physical properties of leather (Komanowsky, 1990; Budrugeac *et al*., 2003). This hydration by humectant effect has been associated with increase in the D-spacing (d-periodicity) of collagen (Rich and Krick, 1961; Huang and Meek, 1999). Increase in d-spacing reflects the expansion of fibrillar and disruption of the hydrogen bonds that provide the structural integrity and strength to the molecular backbone. This can explain the decrease of the physical properties of leather treated with *Aloe barbadensis* Miller and carrageenan-treated leather. The slight decrease was also discussed using theory of reinforcement and adhesion theory. The decrease may be attributed to the size of the particles, interaction (adhesion) and concentration of *Aloe barbadensis* Miller and carrageenan. The first two factors affect the distribution of stress within the matrix and adhesion of the *Aloe barbadensis* Miller and carrageenan. Large particles have inefficient dispersion and poor interfacial stress transfer. The poor interfacial stress transfer limits the alignment of topographical regions in thickness and reduces the tensile strength and stress of the finished leather (Heidemann, 1993; Zhang *et al*., 2005). The size of the particles affects their distribution within the leather matrix. Uniform distribution allows even areas of stress concentration. Large particles lead to uneven distribution of stress concentration. Regions of high internal stress concentration create defects within the matrix and the break/ failure takes place at lower force (Wells *et al*., 2017; Basil-Jones *et al*., 2012). Large particles weaken adhesion (interface) between the leather matrix and the *Aloe barbadensis* Miller-carrageenan (Fu *et al*., 2008).

From filler reinforcement theory, interface is mandated to transfer stress between the mixtures and leather matrix via frictional shear forces resulting from the mixture slippage through the matrix (Hu *et al*., 2003). Poor adhesion is analogous to cracks and voids which make deformation to propagate easily and lowers stress transfer capacity which consequently reduces the strength (Ervina *et al*., 2016; Song and Youn, 2005). Large particles effectively reduce the stress transfer capacity of the interface since the effective cross section area is greatly reduced and this increases stress concentration at the points of the mixture (Hoshino *et al*., 2004). Large particle size reduces the interaction from the attractive intermolecular forces which diminishes the stress distribution ability and particular carrying load. Ultimately, this creates a region of weakness where plastic deformation/breaking takes place at minimal stress. Tearing occurs along the weakest part of the

structure. The smaller the particle size, the more the specific area hence the greater the tensile strength and other physical properties (Hoshino *et al*., 2004). The agglomeration and poor dispersibility of *Aloe barbadensis* Miller limits the load transfer from the matrix to the particles, initiating cracks and propagate easily (Ervina et al, 2016). This reduces the stress and strength of the resulting material. A proposition for the decrease of elongation at break for treated leather may also be attributed to the *Aloe barbadensis* Miller and carrageenan loadings. Concerning the volume fraction or concentration of *Aloe barbadensis* Miller in the leather matrix, results show that *Aloe barbadensis* Miller lubricates the leather matrix, reducing friction (Litke and Widdemer, 2003). From Litke and Widdemer (2003), we expected a crack blunting mechanism, where the lubricated fibre structure enables the network to distribute applied load, hence stronger leather. Against our expectation, crack blunting mechanism didn't work. This implies that overlubrication took place as result of higher volume fraction. Overlubrication of fibres results to a structure that disentangles easily to a low coefficient of sliding friction between the fibres. The resultant leather has low energy of rupture and hence low strength properties as observed from the results.

The samples treated with *Aloe barbadensis* Miller and carrageenan samples were softer, tight and full than their corresponding control samples. These results agree with previous studies using *Aloe barbadensis* Miller on leather by Litke and Widdemmer (2003) and Bitlisli *et al*. (2010). Bitlisli *et al* (2010) observed that *Aloe barbadensis* Miller-treated leathers had decreased compression and decompression energy which implied increase in pliability and softness. Similarly, studies on starch and leather showed an improvement in softness, fullness, selective filling property, uniformity, tightness, thickness and shrinkage temperature (Liu *et al*., 2009; Lu *et al*., 2005; Lv *et al*., 2011; Xiaosheng *et al*., 2012). The softness may have been induced by the moisturizing effect of the *Aloe barbadensis* Miller (Litke and Widdemer, 2003). The oily nature may have also played a role in softening the leather.

4.3 Investigating physical properties of leather treated with *Aloe barbadensis* Miller and carrageenan using existing theoretical models and empirical equations

Leather composites analyzed in this study were the leather crusts that have been mixed with *Aloe barbadensis* Miller and carrageenan at tanning (TA), retanning (RA), dyeing (DA) and at

Fatliquoring (FA) stages. The corresponding leather crusts at tanning (T), retanning (R), dyeing (D) and Fatliquoring (F) were the leather matrices. The results of the averages of tensile strength and percentage elongation, measured by Intron machine, are shown in table 4.3.

Table 4.3: Results for means of tensile strength and elongation at break of crust and crust composite

Strength property	**T**	**TA**	**R**	**RA**	**D**	**DA**	**F**	**FA**
Tensile strength (MPa)	20.66 ± 0.54	19.05 ± 0.52	23.24 ± 1.41	20.10 ± 0.37	20.99 ± 1.47	16.82 ± 0.60	18.60 ± 1.15	18.28 ± 1.1
Elongation Break (%)	56.57 ± 5.07	45.58 ± 1.38	48.09 ± 3.11	41.44 ± 0.76	52.05 ± 5.26	43.16 ± 0.86	68.42 ± 4.45	57.72 ± 1.65

Tensile strength and elongation at break showed a decrease with incorporation of *Aloe barbadensis* Miller mixed with carrageenan. The experimental results were compared with theoretical predictions.

4.3.1 Comparison of experimental and theoretical elongation by Nielsen model

Theoretical values of elongation of crust composite were calculated using Nielsen (1966) model and compared with the experimental results (table 4.4). The results were not significantly different (P=0.47546). Therefore, this model would be appropriate to predict the elongation of crust composites at all stages of crusting operations.

Table 4.4: Experimental versus theoretical elongation values of crust composite using Nielsen model

Parameter	**Tanned**	**Retanned**	**Dyed**	**Fatliquored**
Experimental Elongation value (%)	49.59	41.44	43.16	57.73
Theoretical elongation value (%)	45.52	38.69	41.88	50.06

4.3.2 Comparison of experimental and theoretical tensile strength using various models

The experimental and theoretical tensile strength values using various modes are shown in table 4.5.

Table 4.5: Experimental strength and predicted values using other models

	Tanned	**Retanned**	**Dyed**	**Fatliquored**
Experimental tensile strength (MPa)	19.05	20.10	16.815	18.28
Tensile strength predicted using Danusso and Tieghi (1986); Levita *et al*., (1989) models	20.51	23.07	20.94	18.46
Tensile strength predicted using Kalaprasad et al (1997) model	19.87	22.35	20.19	17.89
Tensile strength predicted using Bigg (1987) model	19.82	22.29	20.13	17.84
Tensile strength predicted using Nicolais and Narkis (1971) model	19.71	22.17	20.02	17.74

The dissimilarities between the predicted values using models and the experimental were not significantly different. Kalaprasad et al. (1997) equation showed p=0.30924, Danusso and Tieghi (1986) and Levita *et al*., (1989) model had p=0.328948 while Bigg (1987) model showed p=0.329745. From the table 4.5 and calculated p values, Kalaprasad et al. (1997) model gives a more accurate prediction.

4.3.3 Prediction of volume fraction of the filler

The empirical equations were used to predict the volume fraction of *Aloe barbadensis* Miller at different stages of leather making processes (table 4.6).

Table 4.6: Volume Fractions ($\times 10^{-3}$) using various theoretical empirical equations and models

	Tanned	**Retanned**	**Dyed**	**Fatliquored**
Experimental volume fraction	7.444	7.444	7.444	7.444
Nielsen (1966) model of elongation	7.332	2.64	4.98	3.825
Kalaprasad et al. (1997) equation	21.75	49.67	88.55	2.257
Bigg (1987) model	19.65	44.87	80.0	2.256
Nicolais and Narkis (1971) model	16.34	37.31	66.6	1.695

The values of volume fraction predicted by Nielsen (1966) model of elongation agreed closely with the experimental values (table 4.6). Similarly, the values predicted by Kalaprasad *et al*., (1997) equation, Bigg (1987) and Nicolais and Narkis (1971) models showed close agreement with the experimental values at fatliquoring stage. At fatliquoring stage, the values of the predicted volume fraction by all models and equations were on the same order as the experimental values. From table 4.6, it can be seen that all the values predicted by the models were lower than the experimental value used in the present study. Using the predicted values from the four models, the average predicted value for volume fraction of *Aloe barbadensis* Miller and carrageenan at Fatliquoring is 2.508×10^{-3}. In this case, Nielsen (1966) was seen to agree well with experimental volume fraction. Therefore, this model was used to calculate the ideal volume fraction from the average volume fraction at tanning, retanning, dyeing and fatliquoring processes. The value was calculated to be 4.964×10^{-3}. Using this value, the predicted percentage of the *Aloe barbadensis* Miller and carrageenan is 3.78 %.

4.3.4 Determination of stress concentration and stress transfer discontinuity and adhesion

Stress concentration and adhesion characteristics of the post tanned crust leathers were calculated using the models. The elongation at break and tensile strength value of the untreated fatliquored and tanned crusts were almost same as those of the corresponding treated crusts which show better adhesion for tanned and fatliquored crusts. The Nielsen (1966), Guptha and Purwar (1984) and Piggot and Leidner (1974) models were used to predict the *Q*, *a*, and *B* values, respectively (table 4.7). The *Q* values of all the leather crusts were on the higher side of the range (Q>0.5), the stress concentration is lower hence the weaknesses in the structure caused by discontinuities is stress transfer and generation of stress concentration at the interface is low. Stress concentration is lowest in fatliquored composites. The latter observation is further corroborated by the "*a*" and *B* values from the Guptha and Purwar (1984) and Piggott and Leidner (1974) models, respectively. From the Guptha and Purwar (1984) porosity theory, the value of B, which accounts for weaknesses in the structure due to stress concentration, is lowest in fatliquored crust. Similarly, fatliquored crust had the lowest "*a*" mean value, supporting the prior observations. This observation indicates that stress concentration is lowest in fatliquored crust composite. Adhesion of the *Aloe barbadensis*

Miller and carrageenan was inferred from the Purkanszky *et al*., (1988) model (B value) and Nicolais-Narkis (1971) model (*K* values) in table 4.7.

Table 4.7: Adhesion of Leather Crust Composites

	Tanned	**Retanned**	**Dyed**	**Fatliquored**
Nielsen (1966) model (*Q*)	0.9586	0.8992	0.8328	1.0217
Guptha and Purwar (1984) model *(a*)	10.9	19.5	29.79	2.33
Piggot and Leidner (1974) model (*B*)	10.47	18.15	26.72	2.33
Purkanszky et al. (1988) (*B*)	-7.418	-16.01	-26.27	1.1495
Nicolais and Narkis (1971) model *(K*)	2.044	3.544	5.217	0.451
Goodier (1933) model (Filler load £*)	-14.24	-44.83	-6.941	1.828
Friction and residue pressure contribution (0.83 P_fV_f)	17.45	16.98	12.68	17.96

The "*B*" value, the filler-matrix reinforcement (a measure of adhesion strength), was highest in fatliquored crusts. For the other leather crusts, the *B* values were negative. The fatliquored crust recorded the lowest value of *K*, slightly lower than the range 0.5-0.6, the theoretical value for poor adhesion (1971). The tanned, retanned and dyed crust recorded values greater than 0.6, implying poor adhesion. The load carried by the fillers (*Aloe barbadensis* Miller and carrageenan) as predicted by the Goodier (1933) model highest in fatliquored crust followed by tanned, retanned and then dyed crusts. For tanned, retanned and dyed crusts, the load carried by the filler was negative except the fatliquored crust which had positive filler load (1.828 MPa). The strength reduction and contributions of filler-matrix friction and residue pressure values in crust leather composites were predicted using Leidner and Woodhams (1974) model, respectively. Since the applied load on the treated leather crust is transferred from the leather matrix fibres through frictional forces in the interface from fibre slippage, the predicted contributions from the friction and residue pressure factors determine the stress transfer capacity due to adhesion. Fatliquored crusts had the highest contribution from the friction and pressure factor (0.83 P_fV_f) followed by tanned, retanned and finally dyed crusts. The general order of adhesion follows a trend; fatliquored > tanned > retanned > dyed crusts. This confirms that fatliquored crusts had the highest stress transfer capacity. Since the particle size of the fillers used in this study was similar, the difference

in the load carrier cannot be attributed to the debounding. Rather to the higher adhesion which improves the stress transfer between the leather crust and the fillers and adhesion strength. Fatliquors or agents used during fatliquoring plays a significant role in enhancing adhesion (Moloney *et al*., 1987). These chemicals increase the wetting effect and the work of adhesion (strong interfacial interactions) and hence dispersion or distribution (Sumita *et al*., 1983; Pukanszky, 1990; Svab *et al*., 2005; Buggy *et al*., 2005).

The results in this section have been published in the journal of Polymer Bulletin (Appendix 2).

4.4 Effect of post tanning operations on the molecular structure of leather

4.4.1 Effect of retanning process on the molecular structure of leather

The mean Raman spectra of the tanned and retanned crusts is shown in figure 4.1.

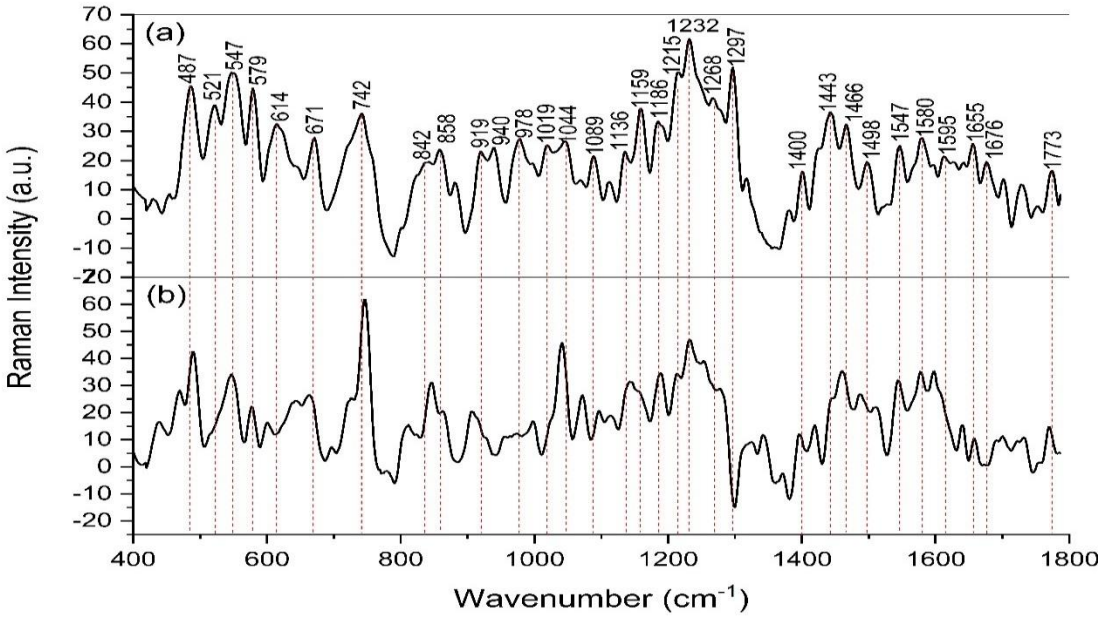

Figure 4.1: Mean Raman spectra of (a) Tanned crusts (b) Retanned crusts

The strong bands below 1700 cm^{-1} indicate that the post tanned crusts are either amides or carboxylate (carboxylic acids) compounds or both. The positions of amide bands were monitored to determine the effect of crusting operations since their positions are highly sensitive to the secondary structure of proteins. The amide bands positioning is governed by the variability in both

the strength and bonding and proteins transition dipole coupling (Metreveli *et al*., 2010). The intensity of amide I region is essential in analyzing conformational changes that occur within the crust's collagens (Payne and Veis, 1988). Generally, intensity of any peak is dependent upon spectral contributions from the transition dipole of several vibrating bands within the system at that frequency/wavenumber (Gonzalez and Wess, 2008).

The strong bands at 1642, 1655 and 1676 cm^{-1} in the spectrum of tanned crust correspond to amide I which is mostly due to the C=O stretching vibrations, C-N stretching and C_{α}-C-N bending along with the N-H in-plane bending of the peptide groups (Rabotyagova *et al*., 2006; Plavan *et al*., 2010; Gasior-Glogowska *et al*., 2010; Kurouski *et al*., 2013). Intact alpha helices have their amide I band below 1655 cm^{-1} while disrupted helices or random chains have peaks above 1656 cm^{-1} (Rabotyagova *et al*., 2006). The first two bands therefore can be assigned to the alpha helix structure content while the 1676 cm^{-1} peak attributed to the random chain structure content. From the spectrum in figure 4.1, it's clear that tanned crust has both intact triple helical contents and disrupted random coil chains. The most intensive peak of the three bands, 1655 cm^{-1}, indicates that tanned crust exhibits more content of alpha-helix structure as compared to the random coil structures (Riaz *et al*., 2018). This is true owing to the tanning and pretanning operations performed on the crust that are capable of disrupting and transforming some ordered triple-helical structures in the native collagen into disorderly random coil structure of collagen (Frushour and Koenig, 1975; Paschalis *et al*., 2001; Freeman *et al*., 2002).

After retanning process, only the 1640 cm^{-1} peak was sufficiently intensive to be detected. It is being implied that retanned crust contains orderly triple helical structures only. Given that the intensity of this peak was far less than the 1642 cm^{-1} peak in the tanned crust spectrum, it means that during retanning process, all the random coils chains and some triple helical structures took part in the crosslinking action. Since retanning process in this present study was simply a second tanning process, there was increased degree of Cr complexation between the carboxyl groups of peptide bonds and the chromium complexes (Jastrzebska *et al*., 2003). This bond involves the carbons and nitrogen in the collagen hence reducing the number of groups participating in C-N-H bending deformation which reduce the intensity (Yao *et al*., 2008). As observed in section 4.1, retanned crusts are more full and tighter compared to other crusts. Further formation of crosslinks

of Cr and collagen due to chrome-retanning expel water from the matrix. Since water or hydration of the C=O bond alters the in-plane bending frequency as well as vibrational coupling to the C-C stretching internal coordinate resulting in intensity increase, then retanning definitely decreases the intensity by dehydrating the crust (Frushour and Koenig, 1975). The extinction of the peak related to the random coil implies that in retanned crust there are less random coil of the collagen. Retanning process aligns the helices or the molecules. It's accurately hypothesized that removal of water reverses the effects of hydrolytic reactions that usually results into disintegration of the collagen triple helices or change in the content of the triple helical structure (Mori *et al*., 2013). It's true to say that pretanning operations are responsible for disrupting the collagen triple helical structure. During tanning process, the structure is transformed to triple helical structure but not complete and therefore retanning progresses the process of ordering the helices. The results by Wu *et al*. (2009) has shown that increased concentration of Cr^{3+} in the collagen fibril does not destroy the triple helices but decreases the structural order. They also observed that order of intermolecular lateral packing and crystallite structure within helical chains decreases and the distortion of N and C telopeptide regions occurs because of the complexation between the Cr^{3+} and amino acid residues of collagen molecules.

Amide II band of the tanned crust appeared at 1547 and 1580 cm^{-1} due to the peptide carboxyl vibrations comprising of N-H in-plane bending (60%) and C-N stretching vibrations (40%) of the peptides (Rabotyasgova *et al*., 2006; Mobili *et al*., 2010; Plavan *et al*., 2010; Badar *et al*., 2017). These peaks are generally contributed by the carboxyl groups from glutamic and aspartic acids in collagen, a characteristic of amino acids (Ibrahim et al, 2015. After retanning process, these bands slightly shifted to 1543, 1577 and 1598 cm^{-1}, respectively. The decrease in frequencies of vibrations explains the slight change in structural order of the collagen (Rabotyagova *et al*., 2008). The decrease of these carbonyl frequencies may be attributed to crosslinkages and conjugation with double bond in the crust such as unsaturated groups which shifts the peaks to lower frequencies as a result of retanning process (Mayo *et al*., 2003; Jastrzebska *et al*., 2003; Li *et al*., 2009; Riaz *et al*., 2018). The complex chromium crosslinking involving the chemical reactions of olation and oxolation appears as the alkaline milleu of the tanning solution increases which results in dehydration (Martinnetti, 1995). The downshift may also be due to loss of water in the collagen

as a result of retanning process since hydration plays key role in the vibrational bond and hence frequency (Gonzales and Wess, 2008).

Amide III band arise from the vibrations of C-N stretching and N-H in-plane bending modes of the peptide bond (Olsztynska-Janus *et al*., 2012). This band reflects both the ordered protein secondary structure such as alpha-helix or beta-sheet and disordered structure such as random coil (Dehring *et al*., 2006). Hence the peaks in this region are related to the biphasic nature of tropocollagen molecules i.e. high-proline or non-polar regions and low-proline or polar Regions distributed along the chain (Frushour and Koenig, 1975; Olsztynska-Janus *et al*., 2012). In Raman spectrum, the lower wave number or frequency of amide III reflects the random coil content in the protein secondary structure while the upper wavenumber is indicative of the alpha-helix content in the protein secondary structure (Dehring *et al*., 2006). In tanned crust spectrum, the strong bands at 1232, 1268 and 1297 cm^{-1} are assigned to amide III band. Therefore, in tanned crust, there are intermediate states of the collagen as observed using amide I band. After retanning process, the peaks of amide III occurred at 1232, 1252, 1277, and 1299 cm^{-1}. Again the slight shifts in frequencies shows that retanning process causes structural and conformational alterations involving collagen reorientation or fibre ordering and rearrangement into stretching (Janko *et al*., 2010). The rearrangement of the helical structure tends to reverse the disruption caused by the previous pretanning processes due to increased crosslinking within or between triple helices (Janko *et al*., 2010; Badar *et al*., 2017; Jastrzebska *et al*., 2003). Similarly, amide III band intensity in retanned crust was weaker than in tanned crust. Crosslinking action influences the structure by weakening the bonds due to the bonds generated in the collagen and hence the intensity of amide III decreases after retanning process (Jastrzebska *et al*., 2003; Tylingo *et al*., 2016). The Cr (III) clusters are usually deposited among the collagen fibrils while smaller Cr (III) complexes diffuse into microfibrils (Wu *et al*., 2009). These gives rise to both intermolecular and intramolecular crosslinking that induce stress inside the crust. When the induced forces are high, as also observed in tighter structure of retanned crusts in section 4.1, the amide intensity decreases to almost negligible due to crustal stress.

Using principal component analysis, the first two PCs explained the variance within tanned and retanned dataset. The two PCs explained 48.8% of the variations in data and the rest of the variance

is evenly distributed among a large number of further PCs, each of which will only explain little of the remaining variance as shown in figure 4.2.

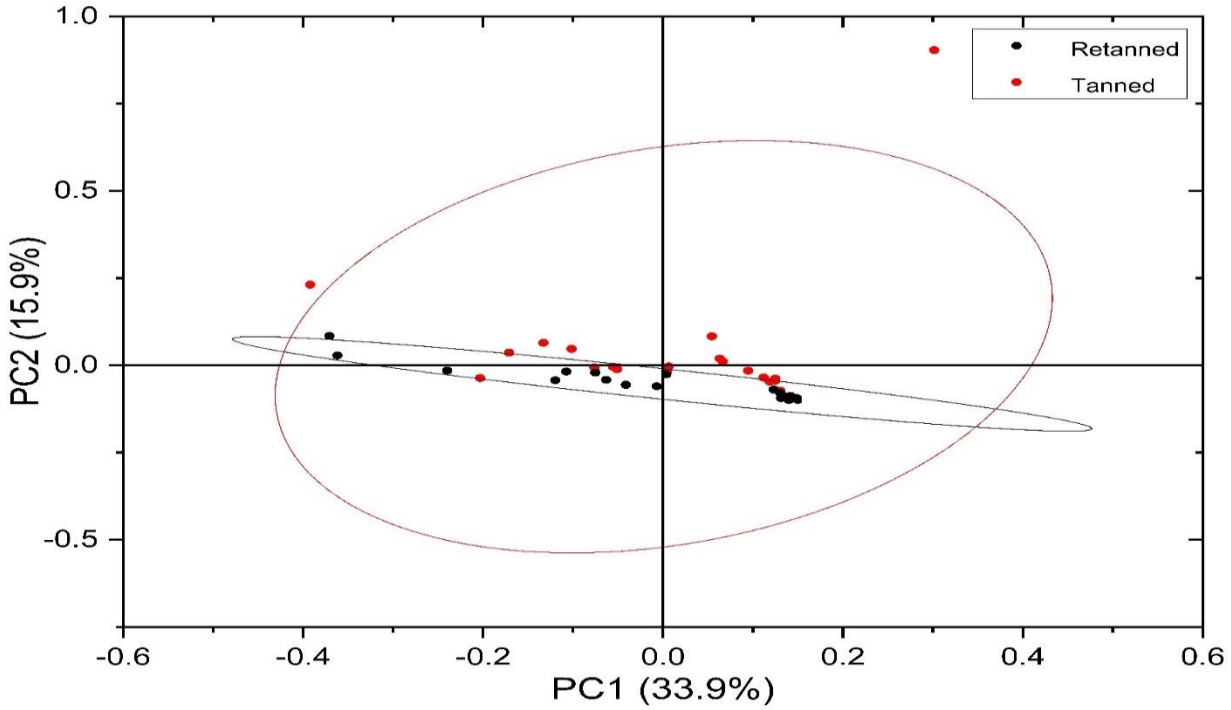

Figure 4.2: Score plot of the PC 1 Versus PC 2 for tanned and retanned crusts spectra

Majority of sample set repetitions showed similar trends, indicating that only two PCs are sufficient to explain the variance. The overlaps in the scores showed that there were minimal outliers within the dataset. However, majority of the retanned spectra showed negative scores along PC 2 compared to majority of positive scores for tanned spectra along the PC 2. Therefore, PC 2 can be used to distinguish the structural changes that occurred during retanning process. The peaks underlying most of the variations were extracted and plotted as loadings versus wavenumbers as shown in figure 4.3.

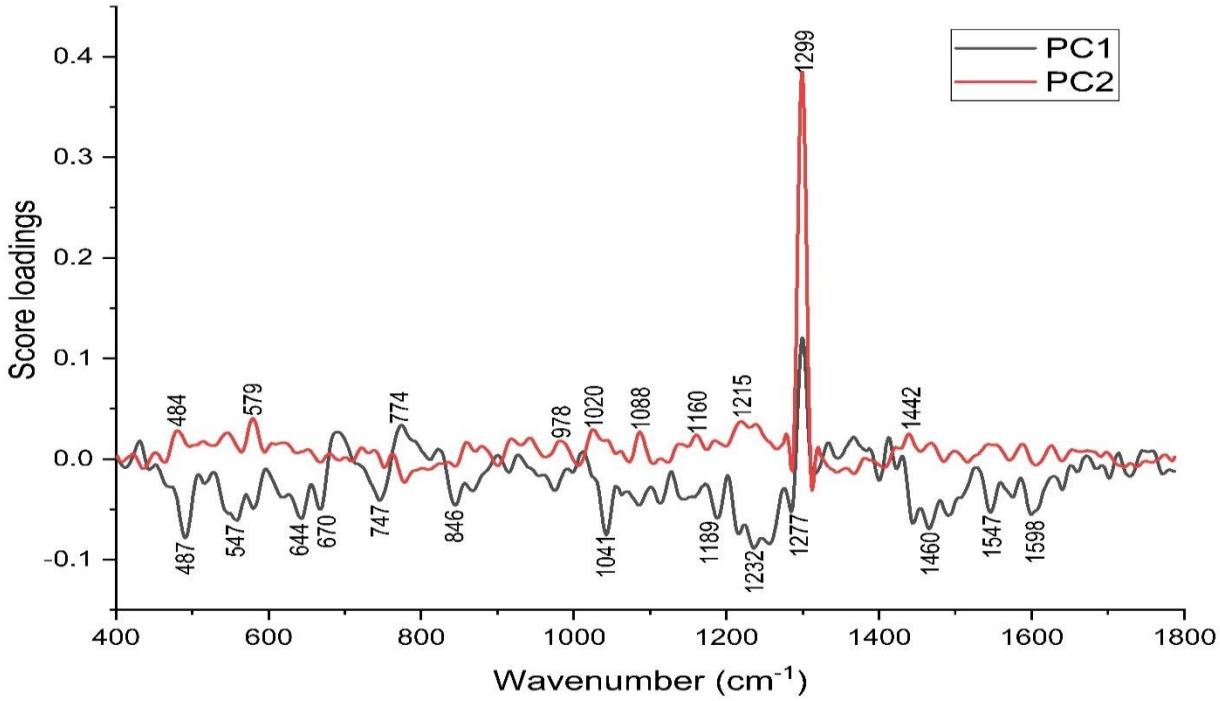

Figure 4.3: PC loadings of the Raman spectra differences in tanned and retanned crusts

The differences are spread across the entire range of the wavenumbers including those frequencies assigned to the amide bands. Therefore, the results indicate that discrimination of tanned crusts from retanned crusts is influenced by protein structure. The peak with the highest amplitude and hence highest influence on the variability is observed at 1299 cm^{-1}.

The peaks at 547 cm^{-1} in tanned crust spectrum were assigned to the vibration stretching of S-S (Edwards *et al*., 2001; OlszTynska *et al*., 2012; Rygula *et al*., 2013). These bonds in the matrix are attributed to the tertiary intermolecular structure of sulphur-containing residues such as keratin or from the processing system such as sulphuric acids and chromium sulphate. Those bonds emanating from the processing system are the sulphate ions in crust matrix either the bidentately coordinated to the Cr (III) species or the residual sulphuric acids used during liming process (Rygula *et al*., 2013; Hedberg *et al*., 2014). After retanning process, the bonds showed peaks at 547 cm^{-1}. Since the S-S bond at 547 cm^{-1} remained unchanged even after retanning process, this therefore means that the source of this bond is the inherent sulphur in collagen. The other S-S bonds may be attributed to other sources of sulphur in the leather such as sulphuric acid during

pickling process and chromium sulphate during tanning/retanning. The disappearance of peak at 521 cm^{-1} in retanned crusts may imply that the source of this bond is the residual sulphuric acids at liming process (Rygula *et al*., 2013; Hedberg *et al*., 2014). This implies that the supramolecular units formed at the previous processes become stronger by a secondary tanning i.e. retanning process, which causes some molecules such as sulphate from the coordination of other species (Aslan, 2009). The intensities of the two peaks increased after retanning process implying the number of the bonds increased after retanning process (Yao *et al*., 2003). The strong loading at 1044 cm^{-1} was identified as symmetric stretching vibration of SO_3 group that is related to the sulphate from the second retanning process (Gorshkova *et al*., 2016). The loading is due to increased intensity after retanning process. The asymmetric stretching mode of SO_3 group was observed at 1189 cm^{-1} to support the assignment of this loading to Sulphur (Gorshkova *et al*., 2016). Loading peak at 644 cm^{-1} assigned to stretching modes of C-S is associated with higher sulphur content that is only present in retanned crust spectra (Edwards *et al*., 2001). Other peaks corresponding to sulphur bonds appeared at 670 and 747 cm^{-1} attributed to cysteine C-S stretching with H at the S atoms and with C at the trans position of the S atoms, respectively (Rygula *et al*., 2013). Higher content of sulphur in the retanned crust may be attributed to the sulphur in the chromium used in the retanning process.

The strong loading at 846 cm^{-1} is due to frequency shift after retanning process corresponding to the skeletal vibrations of C-C stretch of the peptide backbone such as tyrosine amino acid chain modes (Rabotyagova *et al*, 2006; Wu *et al*, 2009; Olsztynska-Janus *et al*, 2012; Rygula *et al*., 2013). These bonds are typical of the alpha-helix conformation, characteristic of collagen: hydroxyproline and proline which are indicative of the triple helical structure (Kavkler and Demsar, 2012; Jastrzebska *et al*, 2003; Gasior-Glogowska *et al*, 2010; Pappas *et al*, 2000; Wang *et al*, 2000). The shift in the frequency is a characteristic feature of structural and conformational modification (Frushour and Koenig, 1975). The loadings at 1441 and 1460 cm^{-1} assigned to wagging vibration of CH_2 and deformation vibration of CH_3. These loadings are attributed to shifts in frequency as a consequence of changed vibrations in the carbon atom region. This is accompanied by a decrease in frequency of vibration (Wu *et al*, 2009). The other form of C-C bond in tanned crust spectrum occurred at 1400 cm^{-1} attributed to the calcium carbonate introduced into the tanning system during liming process (Safandowska and Pietrucha, 2013;

Manfredi *et al*, 2015). This peak was conspicuously missing in the retanned crust spectrum. This implies that retanning agents expel or displace calcium carbonate from the crust.

4.4.2 Effect of dyeing process on the molecular structure of leather

The average Raman spectra of retanned and dyed crusts are as shown in figure 4.4.

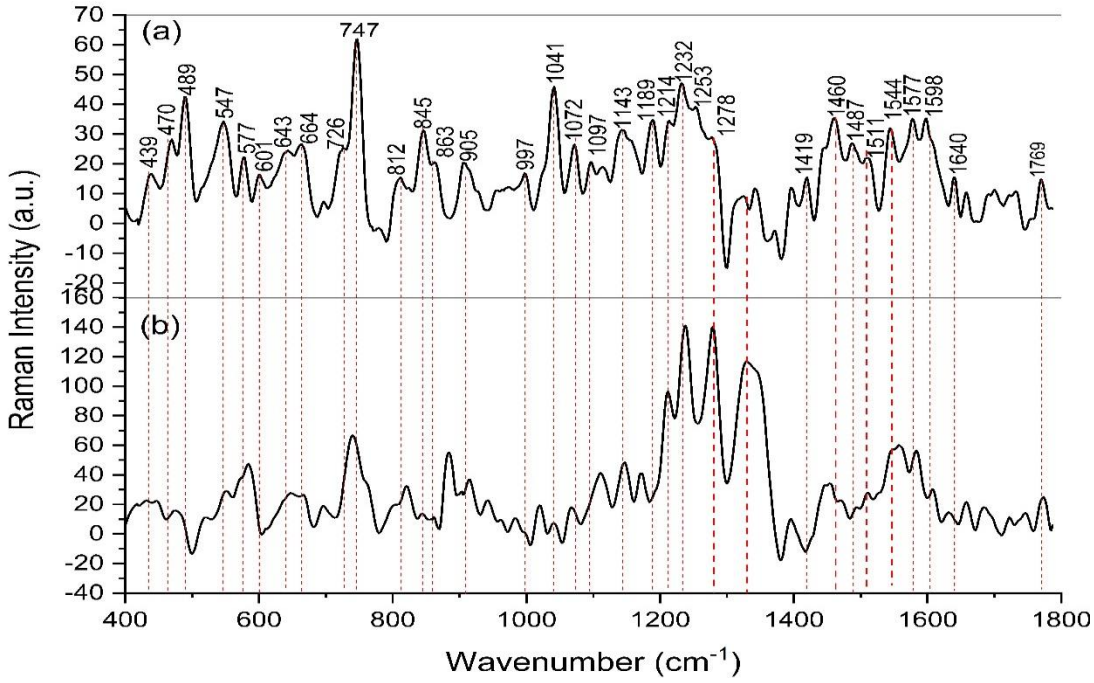

Figure 4.4: Mean Raman spectra of (a) Retanned crusts (b) Dyed crusts

All the peaks corresponding to amide I band were of negligible intensity to be detected in dyed crust spectrum. The carboxylic group usually participate in the hydrogen bonding which weakens the carbonyl group and hence pronounced decrease in their intensity. The dye components may have reacted with the carbonyl and nitrogen in the collagen hence reducing the number of groups of the amine group that take part in the C-N-H bending (Yao *et al*., 2008; Jastrzebska *et al*., 2003). Alternatively, low intensity may be due to a change of the bonding in the C=O group from covalent to partly ionic due to dyeing agents (Minceva-Sukarova *et al*, 2012). The amide II bands moved from 1543, 1577 and 1598 cm^{-1} to 1548 and 1583 cm^{-1}. The bonds at 1577 cm^{-1} may be attributed to the tyrosine modes in the collagen and to the double bonds of naphthalene moiety present in the dye (Aguayo *et al.*, 2013). The first two peaks shifted to a higher frequency after

dyeing process. Since amide II band involves carbonyl frequencies, therefore an increase in the frequency gives a possibility of hydrogen bonding such as OH and NH in the bonding mechanism (Mayo *et al.*, 2003). Hydroxyl group vibrations are most sensitive to the environment and exhibit pronounced shifts in the frequency of the spectrum of the hydrogen bonded species (Gorshkova *et al*., 2016). Presence of an OH group ortho to azo provides an extra potential hydrogen bonding site in similar compounds (Gorshkova *et al*., 2016). The Amide III bands in dyed crust spectrum occurred at 1238 and 1279 cm^{-1}. The increased intensity after dyeing process may possibly be due to the extra CH in-plane bending vibration of naphthalene (1) and (2) ring at 1238 cm^{-1} and 1279 cm^{-1} and the C-N=N-C chromophore group in the dye (Gorshkova *et al*., 2016). The shift in these bands therefore implies that structural order of the collagen in the dyed crust is affected by dyeing process (Rabotyagova *et al*., 2008; Janko *et al*., 2010). The effect of dyeing process may be related to the hydrophobicity of dyed crusts which in effect mimics dehydration and hence shift in frequency (Gonzales and Wess, 2008; Riaz *et al*., 2018). The two peaks of the band imply that dyed crust contains both random coil and ordered triple-helical secondary structures (Dehring *et al*., 2006). The intermediate state is evidenced by the drop in the intermediate peak implying that more helices were randomized or disordered in the process. The intensity of the peak increased greatly after dyeing process. The increase in intensity of the peak corresponding to the random coil structures at 1279 cm^{-1} corroborates the conclusion that dyeing reverses the crosslinking action (Jastrzebska *et al*., 2003). This conclusion was supported by the decrease in physical properties after dyeing process in section 4.1.

PCA was usd to segregate between the Raman spectral pattern of retanned and dyed crusts. From the score plot, the separation of the constituent was done using the first two PCs (figure 4.5).

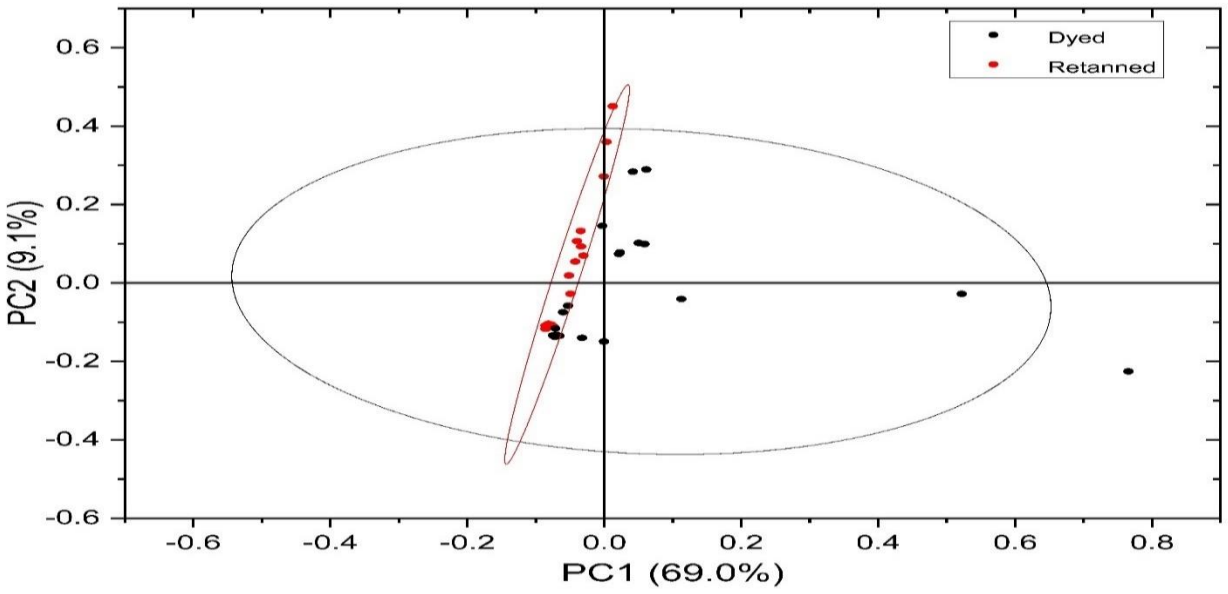

Figure 4.5: Score plot of the PC 1 and PC 2 for retanned and dyed crusts spectra

From the score plot, majority of the retanned crust spectra showed negative scores along the PC 1. Hence PC 1 can be used to distinguish between the dyed and retanned crusts. The loadings corresponding to the differences in the two spectra were plotted against the wavenumbers as shown in figure 4.6.

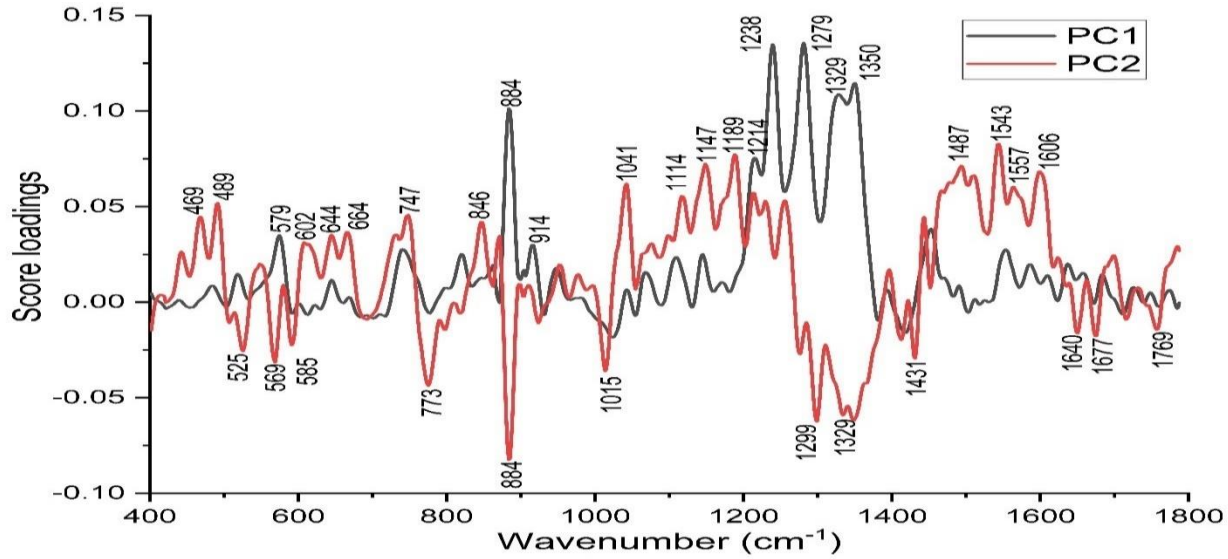

Figure 4.6: PC loadings of the Raman spectra differences in retanned and dyed crusts

The most significant variations due to dyeing process as highlighted by loadings in PC 1, are dominated by the Raman signals of the dyes observed in other studies (Aguayo *et al*., 2013; Cesaratto *et al*., 2017). Some other spectral changes allowed us to infer about the interactions of the dye with the crust.

The strong loadings at 1147 and 1189 cm^{-1} are due to upshift and downshift of the frequency, respectively, assigned to C-N and C-N azo symmetrical bend in the dyes, respectively (Gorshkova *et al*., 2016; Cesaratto *et al*., 2017). The shifts in the frequency can be related to the stronger absorptions and chemisorption of the dye molecules. It also shows that after dyeing process, C-N bonds in both collagen and collagen take part or interact chemically. Bands associated with the sulphur-containing molecules in the dye were also observed. The case for the v(-SO_2O-) stretching vibrations of the colourants were observed at 1214 cm^{-1} (Aguayo *et al*., 2013). Loading at 1238 cm^{-1} is likely to be due to the slight shift in frequency and increase in the intensity after dyeing process. This may be explained by phenyl-OH modes at this frequency present in the dye (Cesaratto *et al*., 2017). At 1279 cm^{-1}, a new peak emerged after dyeing process ascribed to phenyl-N vibrations (Cesaratto *et al*., 2017). The aromatic ring vibrations were observed at 1299, 1329 and 1350 cm^{-1}. The stretching vibration of aromatic nitro and N-phenyl molecules in dye were observed at 1329 and 1350 cm^{-1}, respectively (Cesaratto *et al*., 2006; Gorshkova *et al*., 2016). The band at 1350 cm^{-1} can also be attributed to the –SO_2-group. Studies have shown that dyes interact with other textile materials via these sulphone and sulphonate groups due to decrease in their intensity after interaction (Abbot *et al*., 2010; Aguayo *et al*., 2013). The intense loading at 1431 cm^{-1} is due to an emergence of a new peak after dyeing which can be ascribed to the dye chromophoric group, viz. –C-N=N-C. This group contains two bonds; C-N and N=N. The N=N stretching vibration, which due to its symmetry, has a very characteristic and intensive band in the Raman and they are difficult to observe in the infared spectrum. But the change of N=N bond length in the molecule which has two unequivalent C-N parts causes a change of dipole moment. Thus the N=N stretching mode is IR active and is predicted to be medium strength. Therefore the band occurring at 1431 cm^{-1} corresponds to the N=N stretch of an azo compound (Gorshkova *et al*., 2016; Cesaratto *et al*., 2017). The naphthalene ring stretch in the dye was also observed by its vibrations at 1543 and 1557 cm^{-1} (Cesaratto *et al*., 2017). The band at 1015 cm^{-1} could be ascribed to a breathing mode of the benzene rings (Aguayo *et al*., 2013).

At 1334 cm^{-1}, the shift occurred after dyeing which was assigned to the wagging vibrations of proline side chains (Badar *et al*., 2017). Peak at 1457 cm^{-1} are a result of deformation vibration of methyl (CH_3) and methylene (CH_2) molecules in proteins and other carbonate groups (Janko *et al*., 2010; Manfredi *et al*., 2015). The shifting of 820 cm^{-1} due to collagen C-C backbone to lower wavenumber indicates deformation (Wang *et al*., 2000b). After dyeing process, the band at 546 cm^{-1} shifted to 549 cm^{-1} and the intensity depreciated. The latter may be attributed to the decreased content of sulphur at dyeing. The disaaperance of the peaks at 842, 858, 919 and 940 cm^{-1} which correspond to the skeletal vibrations of C-C stretch of the protein backbone such as tyrosine amino acid chain modes in dyed crust imply that dyeing process alters the typical α-helical conformation (Pappas *et al*., 2000; Wang *et al*., 2000b; Jastrzebska *et al*., 2003; Rabotyagova *et al*., 2006; Gasior-Glogowska *et al*., 2010; Kavkler and Demsar, 2012; Olsztynska-Janus *et al*., 2012; Rygula *et al*., 2013). The bonds at 1400 cm^{-1} attributed to the C-C from the calcium carbonate were also not detected. This implies that retanning and dyeing process had completely displaced and expelled the calcium carbonate from the crust. The C-O-C deformation vibration and C-O-C symmetric stretching vibration at 487 and 1089 cm^{-1} were also missing in the crust spectrum (Jastrzebska *et al*., 2003).

4.4.3 Effect of fatliquoring process on the molecular structure of leather

The average Raman spectra of dyed and fatliquored crusts are as shown in figure 4.7.

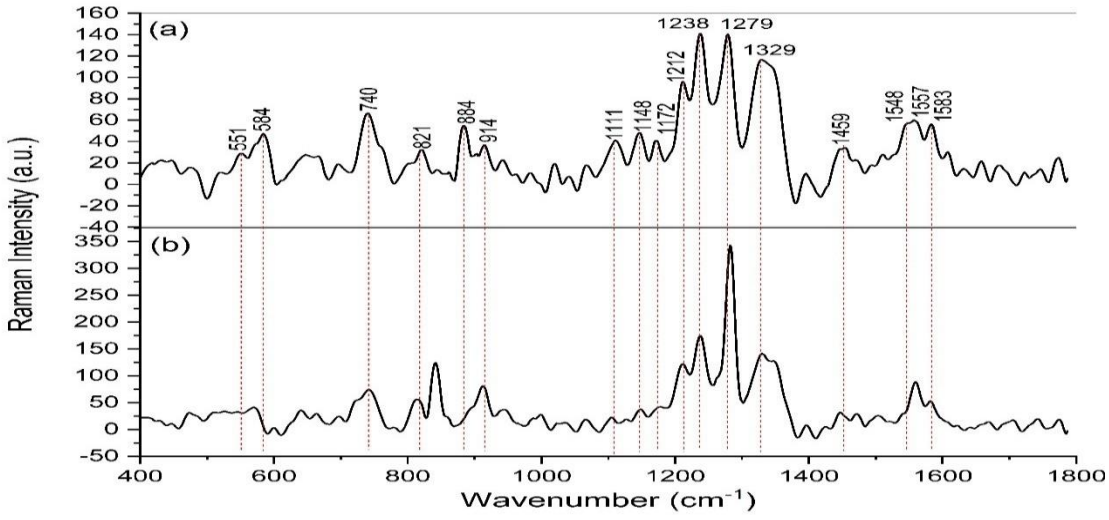

Figure 4.7: Mean Raman spectra of (a) Dyed crusts (b) Fatliquored crusts

Amide I band was expected to be strong in the fatliquored crust spectra due the stretching vibrations of the carbonyl (C=O) and olefinic bonds (C=C) in the glyceryl esters and fatty acids hydrocarbon chains in the fats.

PCA was able to distinguish between the fatliquored crust spectra from dyed crust spectra. The first two PCs of the dyed and fatliquored crusts spectra, explaining 93.3% of the data matrix variance are shown in figure 4.8.

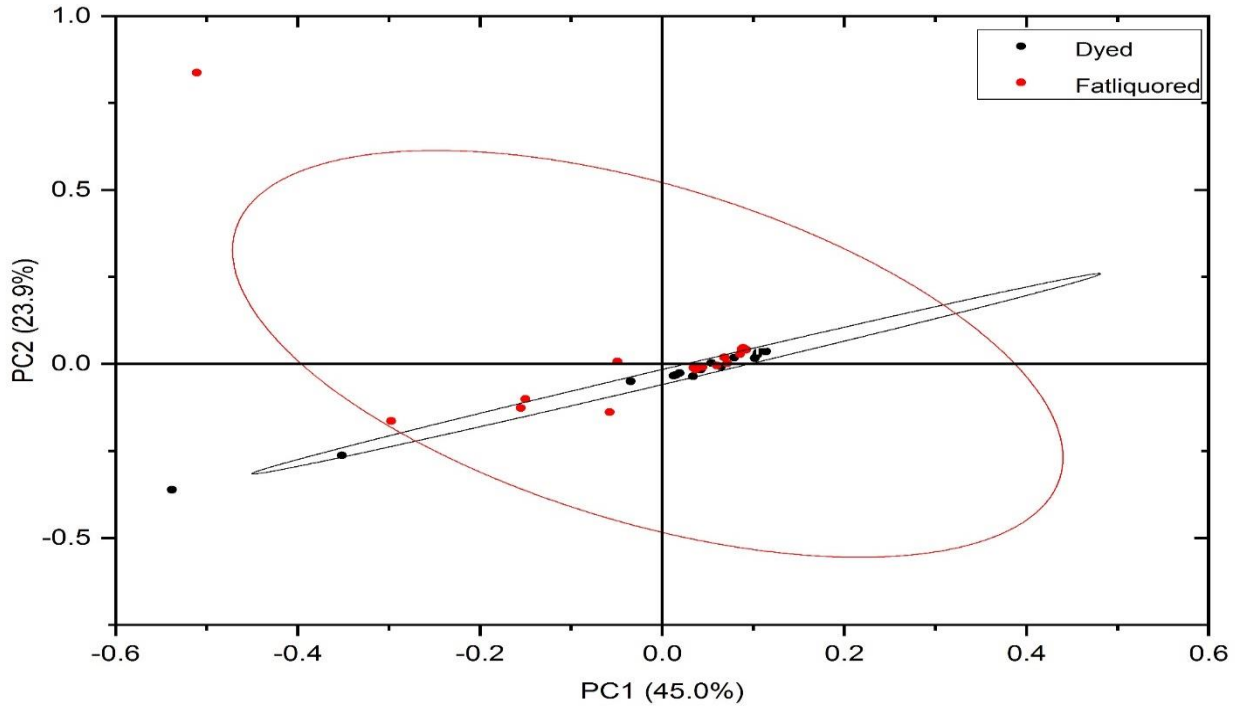

Figure 4.8: Score plot of the PC 1 and PC 2 for dyed and fatliquored crusts spectra

Separation among the dyed and fatliquored crusts can be observed along the PC 1 axis which explains the 45.0% of the total variance in the dataset. From figure 4.8, it can be shown that dyed crusts have positive scores while fatliquored samples exhibited negative scores along the PC 1 axis. The PC 2 seems to classify the samples into 2 groups: fatliquored samples were characterized by positive PC 2 values while dyed crusts by negative PC 2 value. The importance of the contribution into PC 1 of the spectrum at 1234 cm^{-1} were evident from the corresponding loading plot in figure 4.9. The PCA hence showed very good discrimination between dyed and fatliquored crusts spectra.

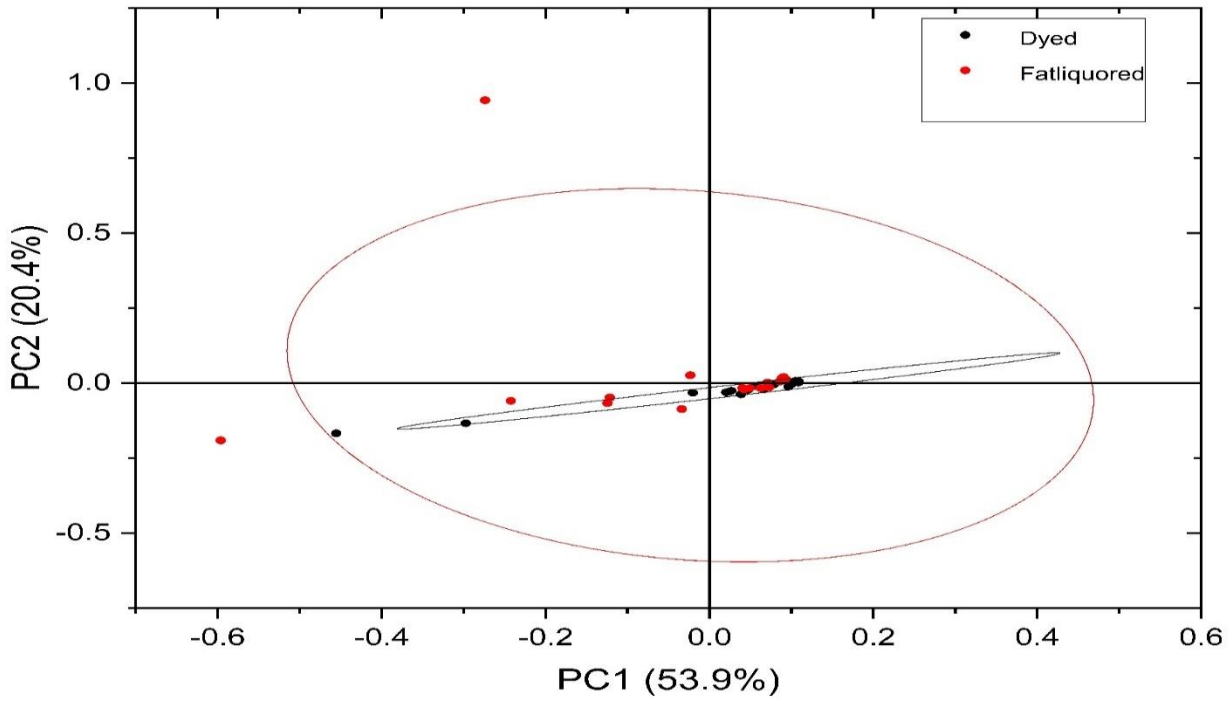

Figure 4.9: PC loadings of the Raman spectra differences in dyed and fatliquored crusts spectra.

The bands at 885 and 1451 cm^{-1} correspond to the carbonate groups in the crust (Manfredi et al, 2015). Disappearance or decrease of the band intensity at 548 cm^{-1} which is assigned to the S-S bonds may be due to the reduced amounts of sulphur bonds in the crust (Edwards *et al*., 2001). The bands at 1548 and 1583 cm^{-1} were assigned to amide II. The disappearance of these bands implies that fatliquoring either expels the corresponding groups or reacts with the groups decreasing the participating elements in the crust. Although the band position at 740, 912, 1212, 1238, 1279, 1330 and 1557 cm^{-1} remained unchanged after retanning process, the intensities of these peaks increased greatly. The intensity increase at 1330 cm^{-1} is probably due to the CH/CH_2 bending and CH_3 wagging of the fatliquors and decreased crosslinking level in fatliquored crust compared to dyed crust especially at 1330 cm^{-1} (Jastrzebska *et al*., 2003; Rabotyagova *et al*., 2006; Badar *et al*., 2017). After fatliquoring process, the band at 547 cm^{-1} corresponding to S-S vibrations disappeared. The intensive loading at 1279 cm^{-1} is due to increase in the intensity after fatliquoring attributed to the symmetric rock in cis double bond δ(=C-H)) of the lipids in fatliquors (Muik *et al*., 2005). A strong loading at 855 cm^{-1} is assigned to the –(CH_2)n molecule of the v(C-C) group in the fatliquors (Baeten *et al*., 1998).

4.4.4 Intensity ratio and full width at half maximum (FWHM) for leather

Simple and effective diagnostic algorithms have been proposed based on the Raman spectra in terms of peak intensity or peak intensity ratio measurements. Intensity ratio; the intensity of the peak height at amide III and of the peak at 1450 cm^{-1} was determined (Dehring *et al*., 2006; Liu *et al*., 2015b; Riaz *et al*., 2018). This ratio was used to confirm the triple helical structure of the crusts. The calculated ratio of tanned crust was 0.842. This ratio shows that the triple helical structure in tanned crust is significantly disrupted. After retanning process, the ratio increased to 0.974, confirming that the retanned crust is more orderly as compared to tanned crust. Dyeing process further reduced the ratio to 0.824 hence reduced triple helicity of leather. After fatliquoring, the ratio reduced further to 0.801. Fatliquoring process reduces further the orderliness of collagen. The full width at half maximum of the amide III band was determined in order to support results of the intensity ratio to confirm the orderliness of the collagen in the post tanned crust since increase in the FWHM is indicative of decrease in orderliness of protein structure (Wang *et al*., 2000b). The FWHM for tanned crust was 39 cm^{-1}. After retanning process, the FWHM decreased to 26 cm^{-1} implying that retanning process restores the orderliness in the collagen structure. The FWHM increased further after dyeing to 32 cm^{-1}. Increase in FWHM is an indication that bending of the molecular kinks is taking place and hence increased disorderliness of the protein structure (Wang *et al*., 2000b). The FWHM again decreased slightly to 31 cm^{-1}. This results agrees well with the measured intensity ratio and PCA results of the spectra.

4.5 Effect of *Aloe barbadensis* Miller and carrageenan on the molecular structure of leather

The mean Raman spectra from different spots of the crusts for tanned, retanned, dyed and fatliquored and their corresponding treated crusts with ABM and carrageenan are shown in figures 4.10-4.13.

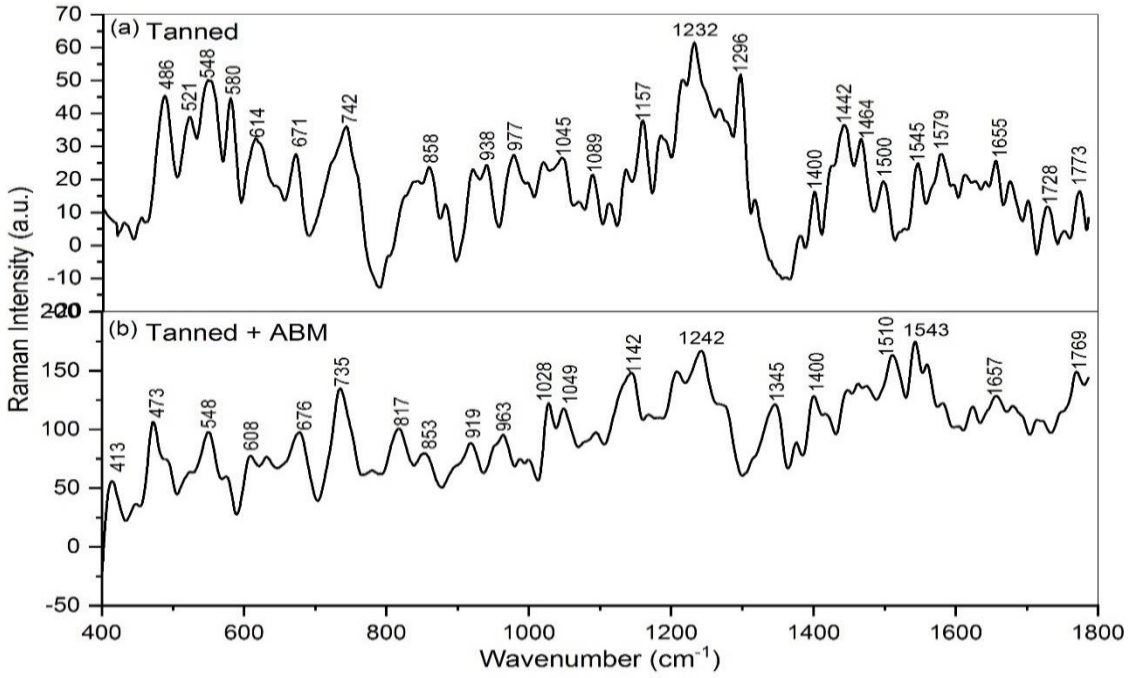

Figure 4.10: Mean Raman spectra of (a) tanned crusts (b) treated tanned crusts

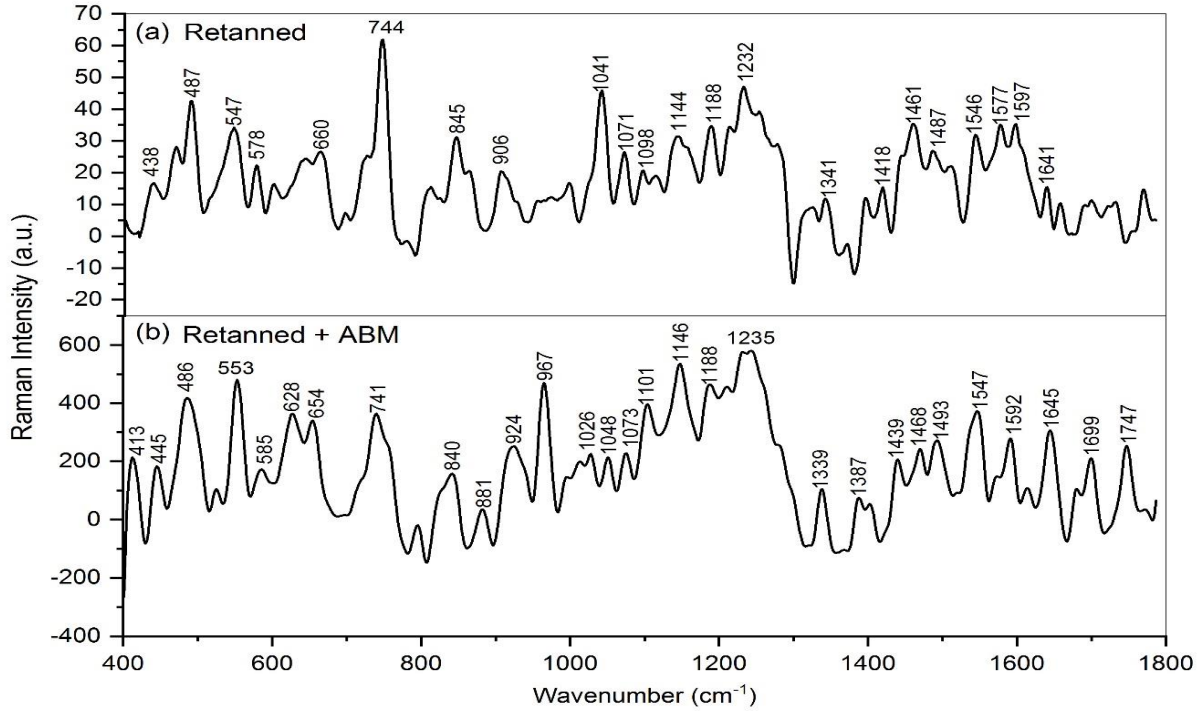

Figure 4.11: Mean Raman spectra of (a) Retanned crusts (b) treated retanned crusts

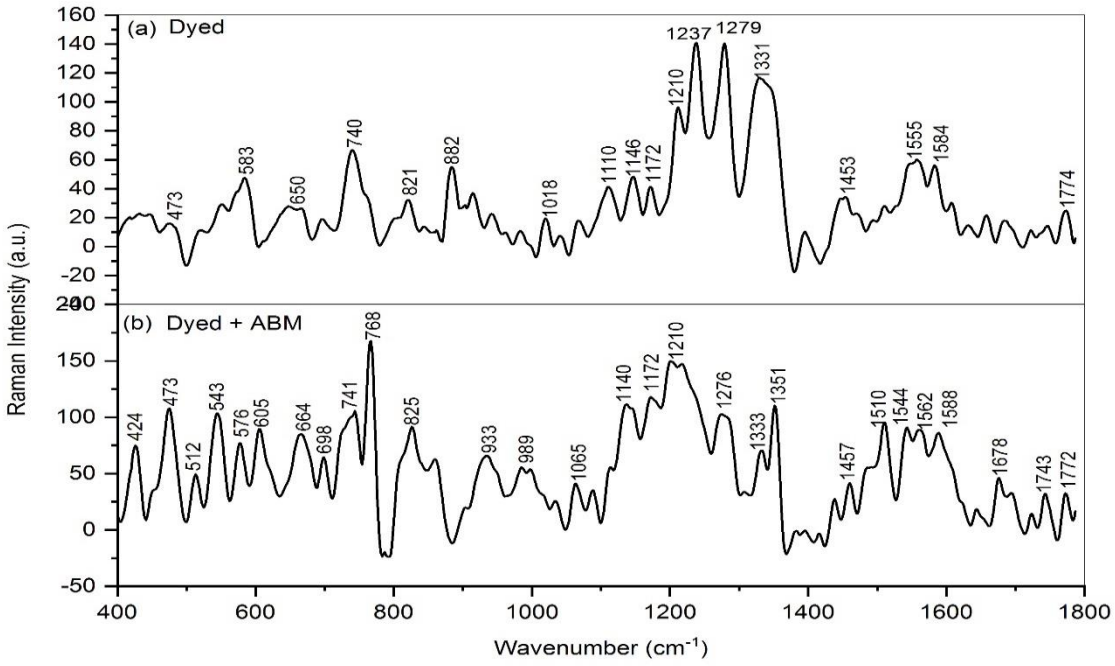

Figure 4.12: Mean Raman spectra of (a) dyed crusts (b) treated dyed crusts

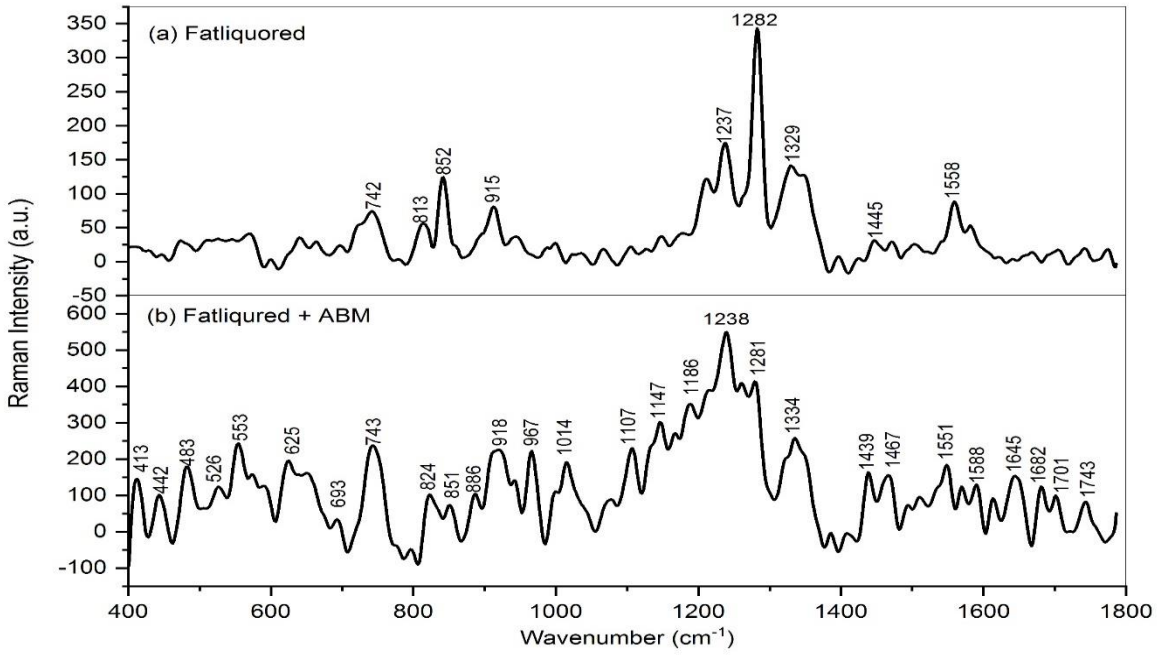

Figure 4.13: Mean Raman spectra of (a) fatliquored crusts (b) treated fatliquored crusts

From figures 4.10-4.13, the crust spectra are consistent with the treated crusts spectra except in their intensities and minor shift in wave numbers. The intensity in all the treated crust spectra was

higher than the intensity in the control spectra. It therefore implies that the carrageenan and ABM additives introduce extra absorbing molecules that increase the intensity (Kavkler and Demsar, 2012). Similarly, the functional groups in the leather are similar to those in ABM and carrageenan. As anticipated, the spectrum of the treated crusts contained all the bands that belong to collagen, ABM and carrageenan (Ibrahim *et al*., 2015).

Applying PCA, it was possible to define the trend in the data between crusted samples spectra from treated crusted samples spectra by using two PCs (figures 4.14-4.17).

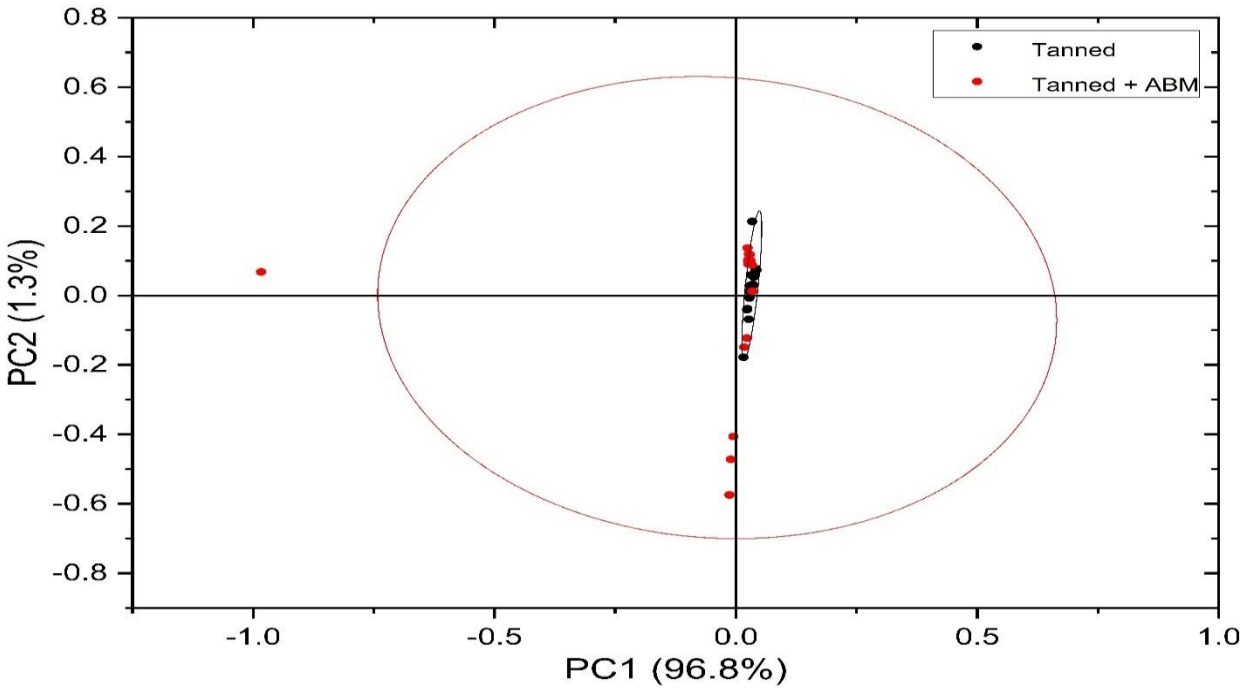

Figure 4.14: Score plot of the PC1 and PC 2 for tanned crusts and treated tanned crusts spectra

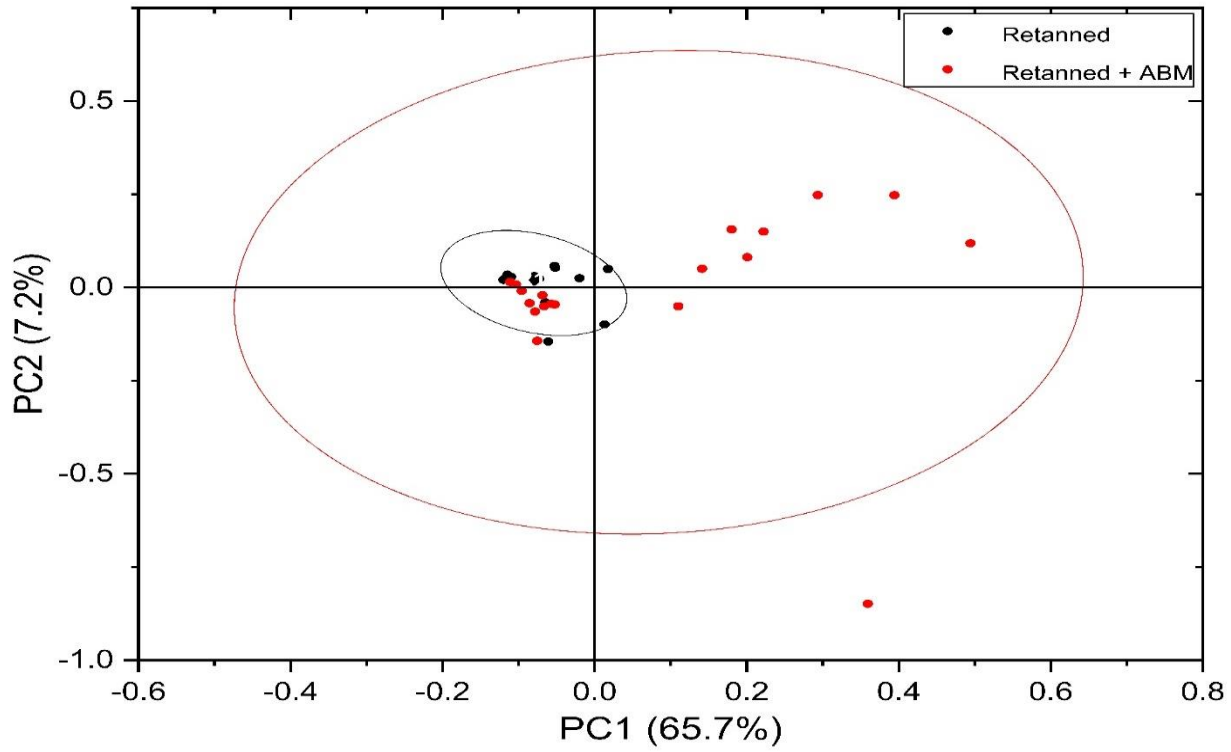

Figure 4.15: Score plot of the PC 1 and PC 2 for retanned crusts and treated retanned crusts spectra

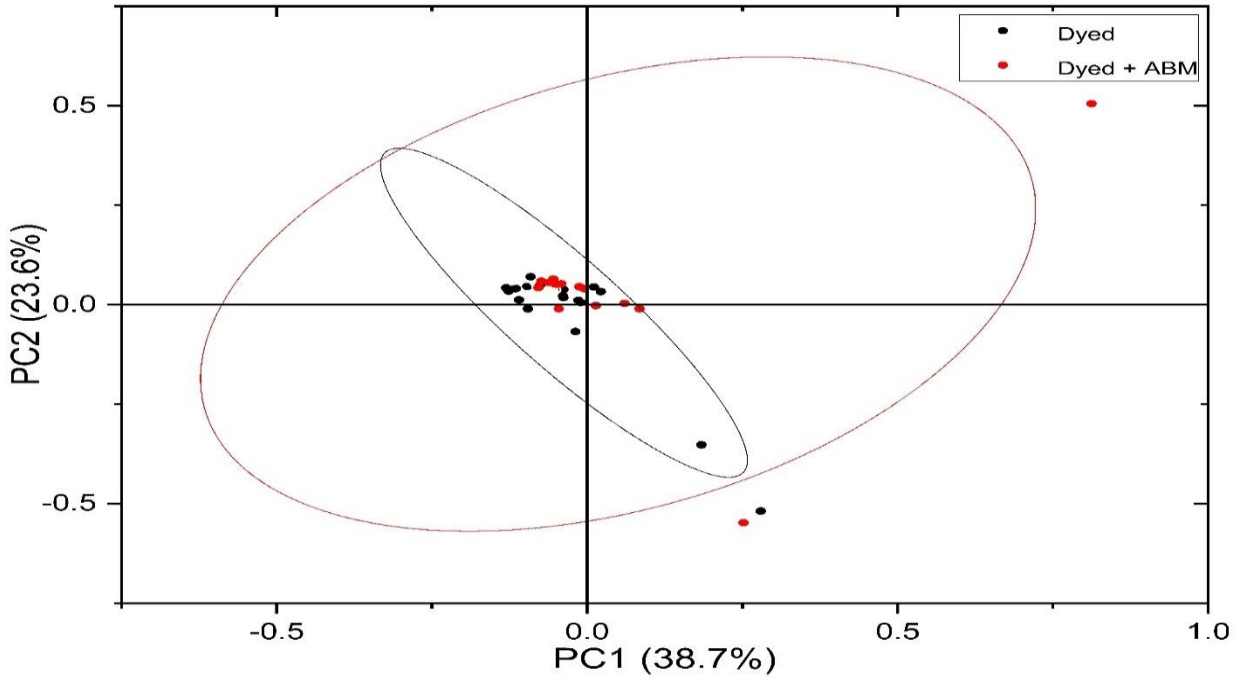

Figure 4.16: Score plot of the PC 1 and PC 2 for dyed crusts and treated dyed crusts

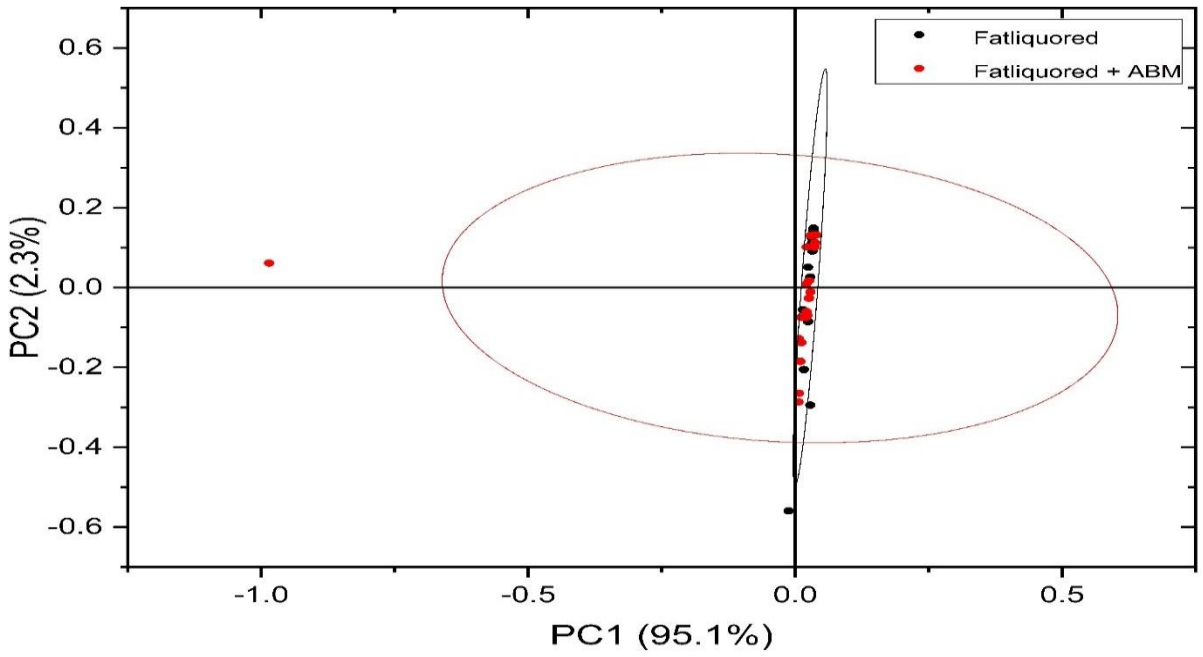

Figure 4.17: Score plot of the PC 1 and PC 2 fatliquored crusts and treated fatliquored crusts spectra

The score plots of PC 1 and PC 2 for tanned crust in figure 4.14 show that treated samples have both positive and negative scores while control samples have only positive scores along PC 1 which accounts for 96.8% of the total variance. Hence PC 1 can be used to distinguish control samples from treated tanned samples. The score plots for retanned crusts in figure 4.15 showed that majority of control retanned samples have negative scores while treated samples have both higher positive and negative scores aligned along PC 1 that accounts for 65.7% of the entire variance. In this case, PC 1 distinguishes between treated retanned crust spectra and control retanned crust spectra. PCA did not play much role in distinguishing the control dyed samples from treated dyed samples due to equally distributed scores in both principal components as shown in figure 4.16. However, dyed samples showed higher negative scores along the PC 1 as compared to treated dyed samples. The score plot for fatliquored crusts did not offer much aid in distinguishing the fatliquored crust from treated fatliquored crust spectra since the scores for both were equally distributed along the two principal components (figure 4.17).

The loadings for corresponding scores spectra were plotted against the wavenumbers in order to show the differences that separate the treated crusts from the control crusts (figures 4.18-4.21).

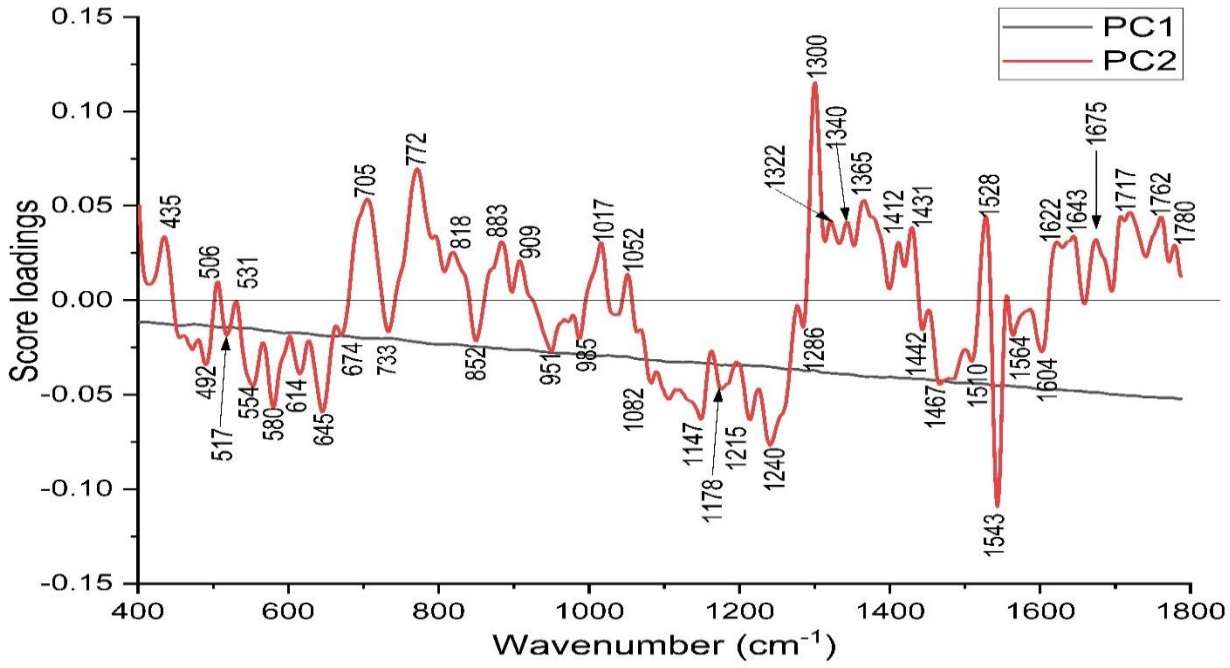

Figure 4.18: PC loadings of the Raman spectra differences in tanned and treated tanned crusts

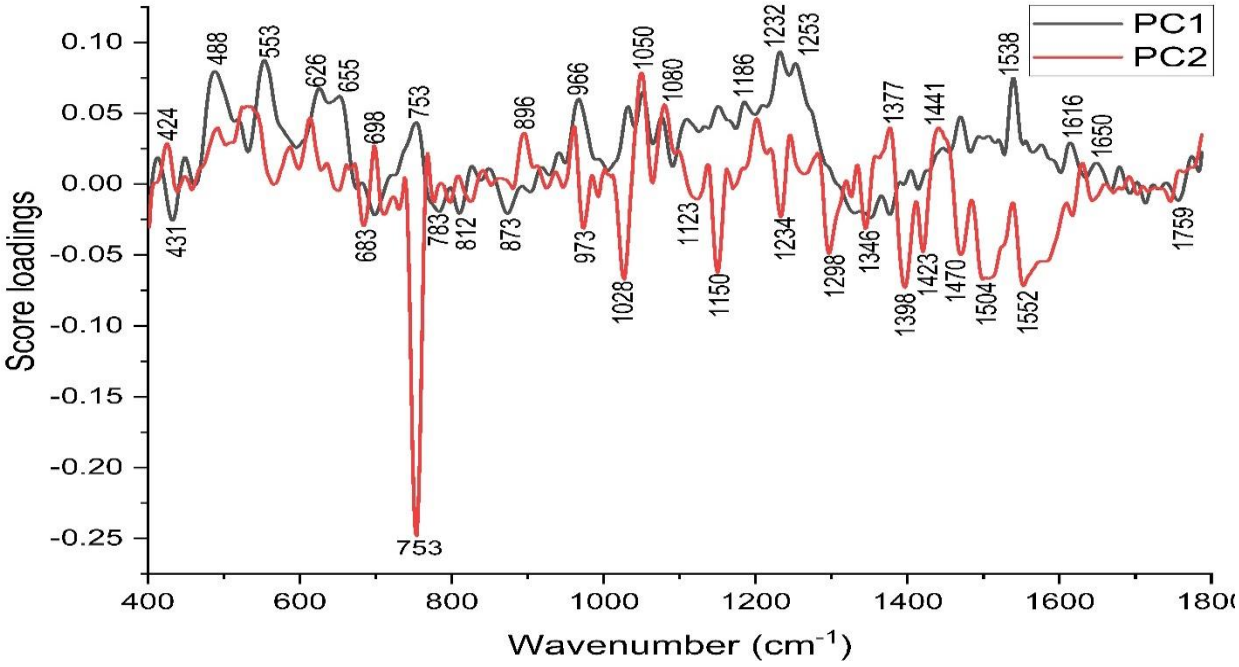

Figure 4.19: PC loadings of the Raman spetra differences in retanned crusts and treated retanned crusts.

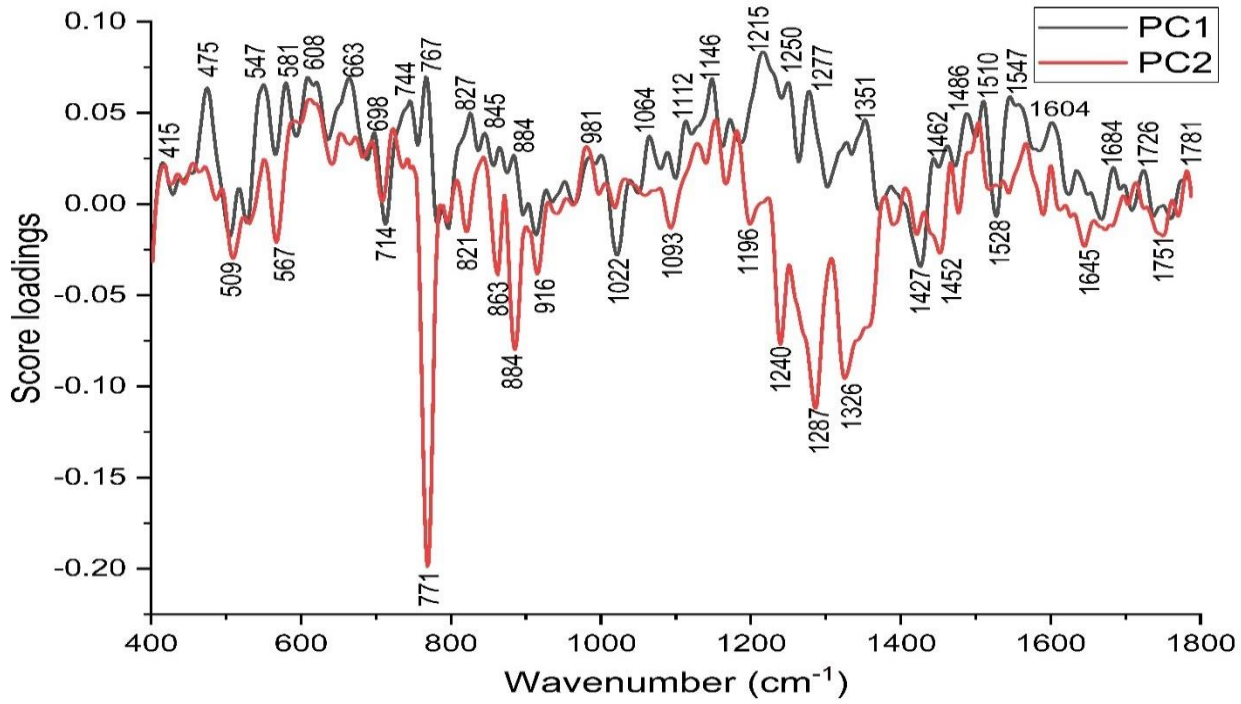

Figure 4.20: PC loadings of the Raman spectra differences in dyed crusts and treated dyed crusts.

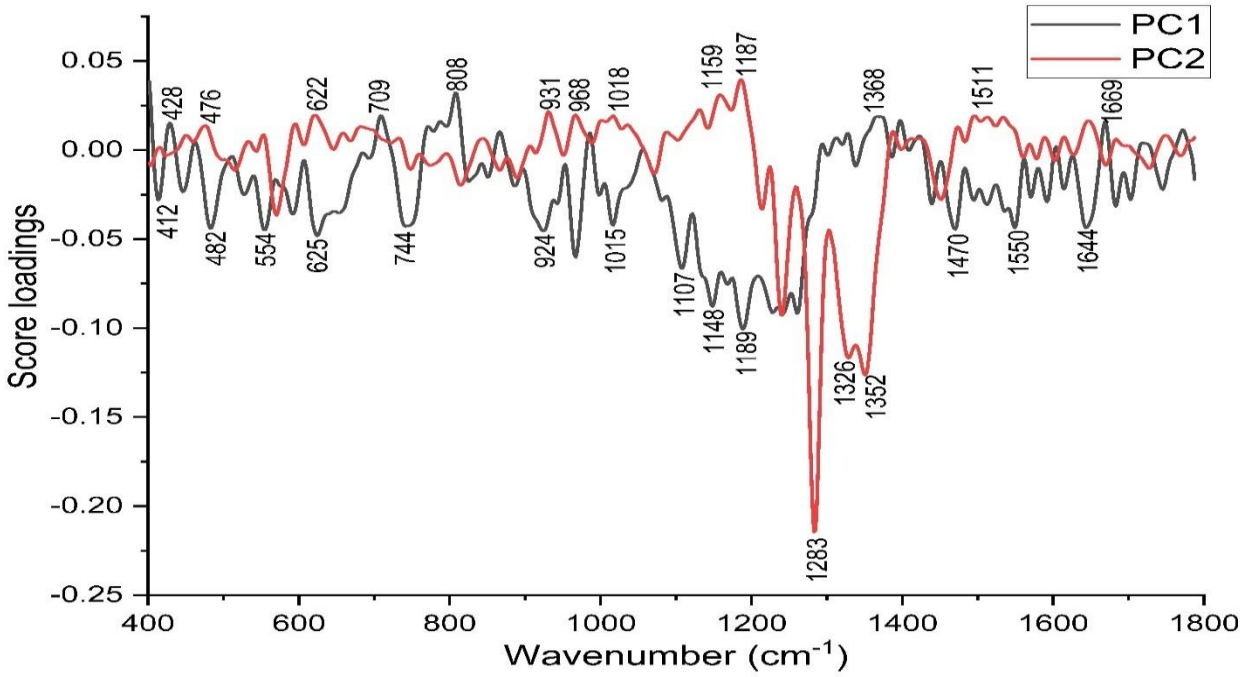

Figure 4.21: PC loadings of the Raman spectra differences in fatliquored crusts and treated fatliquored crusts.

From the loadings plots, majority of the strong loadings are in the range 1200-1700 cm^{-1}, the region that contain specific information, arising from amides bands. Since the amide are predominant bands in this region, therefore these results indicate that the discrimination between crusts and treated crust samples is greatly influenced by protein structure and a range of other bonds (Mobili *et al*., 2010). The loading plots also show that the stage of processing at which incorporation of the ABM and carrageenan is done plays a major role in determining the molecular structure.

Combining the mean spectra of crusts and loading plots, it's evident that most of the loadings are as a result of frequency shifts and change in intensity. The amide moiety plays vital role in crosslinking and bonding, and this makes it good indicator of protein conformation (Bandekar, 1992). The vibrational modes of collagen sensitive to secondary structures are amino acids because collagen consist of amino acids linked by peptide bonds (Jastrbezska *et al*., 2003). Similarly, amide bands are sensitive to the electron density change of the collagen backbone which are induced by the formation/disruption of hydrogen bonds with water molecules (Masic *et al*., 2015). For instance, amide I band is due to C=O stretching vibration of the peptide groups with some C-N stretching and N-H bending and therefore very sensitive to changes in the protein structure. The amide I band peak position can be used to indicate and determine formation and rupture of crosslinks (Jastrbezeka *et al*., 2003). The wavenumber of amide modes reflects the structure of the main polypeptide chain irrespective of side groups. For this reasons, the amide bands were analyzed to determine the structural alteration by the incorporation of the ABM and carrageenan.

Amide I band comprises of stretching vibrations of N-H of the amino groups and olefinic unsaturation (C=C) of the carbonyl components and stretching vibration of C=O that occurs in the range of 1600-1700 cm^{-1} (Frushour and Koenig, 1975; Jithendra *et al*., 2013; Kassam *et al*., 2015; Riaz *et al*., 2018). This band is highly sensitive to small changes in molecular geometry and hydrogen bonding of peptide groups (Talari *et al*., 1998). The band involves triple helical and random (elastin or fibrous) proteins and functional groups of ABM (Frushour and Koenig, 1975; Kassam *et al*., 2015; Riaz *et al*., 2018). The peaks at 1643, 1650, 1645 and 1644 cm^{-1} and 1675, 1685 and 1669 cm^{-1}, were assigned to amide I band of tanned, retanned, dyed and fatliquored crusts, respectively (Frushour and Koenig, 1975; Riaz *et al*., 2018). The loadings in the same

region are as a result of increase in both intensity and upshift of frequency due to the ABM and carrageenan (Gasior-Glogowska *et al*., 2010). The amines (N-H), aromatic nitro (NO_2), glycosidic bonds, in ABM have vibrational stretching in the same range of frequencies (Kassam *et al*., 2015; Agato, 2016; Ibrahim *et al*., 2015). Additionally, carrageenan has carotenoids whose C-C vibrates at 1658 cm^{-1} (Maice *et al*., 2015). Therefore, these molecules contribute to the intensity as a result of higher contributing molecules that vibrate at these frequencies (Edwards *et al*., 2001). Upshift in frequency after treatment is related to the transition from triple helical structure towards beta-pleated structure (Church *et al*., 1998). This reorganization and conformation is attributed to the changes in the hydrogen-bonded network arising from the ABM and carrageenan molecules (Edwards *et al*., 2001; Gasior-Glogowska *et al*., 2010). The FWHM of treated crust spectra was higher than non-treated crust spectra, showing that bending of molecular kinks has increased, an indication of induced disorderliness, lower crystallinity and decomposed skeletal structures (Wang *et al*., 2008; Jastrbezska *et al*., 2003; Kavkler and Demsar, 2012).

Generally, the peaks in the range 1500-1600 cm^{-1} are assigned to the aromatic ring stretch modes v(CCH) of the amino acids proline/hydroxyproline and tyrosine/ phenylalanine (Edwards *et al*., 1997). Bands in the spectral region 1538-1550 cm^{-1} were ascribed to the amide II band. These bands, arising from the NH deformation vibrations coupled with some carboxylic acids (COO-), are usually very weak in Raman spectra (Jastrbezska *et al*., 2003; Andreyeva and Maistrenko, 2014; Badar *et al*., 2017). The observed increase in band intensity at 1538-1550 cm^{-1} for treated crusts can support the partial reaction between the carotenoids of ABM and carrageenan and NH groups of peptide bonds together with functional carboxyl groups (aspartic and glutamic acid residues) in collagen (Maice *et al*., 2015; Badar *et al*., 2017; Riaz *et al*., 2018). The loadings in this region correspond to the variations in the wave numbers and intensity after the incorporation of ABM and carrageenan. The shoulders in the region 1583 to 1604 cm^{-1} were assigned to the aromatic ring stretch modes v(CCH) of the amino acids tyrosine/phenylalanine (Frushour and Koenig, 1975). After the incorporation, the wave numbers shifted to the higher wavenumber as indicated by the loadings at 1583 and 1604 cm^{-1}.

The amide III band comprise of stretching and deformation vibrations of C-O, C-N, N-H, O=CN and C-O-C modes with peaks at approximately 1240-1286 cm^{-1} (Frushour and Koenig, 1975;

Kassam *et al*., 2015; Badar *et al*., 2017). The incorporation elevated the concentrations of these bonds and upshift of frequency change as evidenced by strong loadings at these frequency range (Pereira *et al*., 2009; Jithendra *et al*., 2013; Andreva and Maistrenko, 2014; Kassam *et al*., 2015). Stretching vibration of C-O groups of esters and phenols in carrageenan and ABM occurs in the same frequency range (Jithendra *et al*., 2013). Similarly, C-N stretch of the aliphatic amines and C-O-C bridges of the esters and phenols in ABM also occur within the frequency range (Tarantilis *et al*., 1998; Pereira *et al*., 2009; Jithendra *et al*., 2013; Andreyeva and Maistrenko, 2014; Kassam *et al*., 2015). The upshift in frequency may be explained by the humectant nature of ABM (Milikan, 2001). ABM has molecules with one or more hydrophilic groups attached to them such as amines, amino acids, gycerine and sorbitol (Millikan, 2001). Additionally, ABM contains chemical compounds and phenolic OH group in the anthraquinones, which increases the number of hydrogen bonds and hence upward shift of frequency (Kavkler and Demsar, 2012; Ibrahim *et al*., 2015). This is consistent with increased crosslinking degree between and within triple helices by the ABM in form of hydrogen bonding stretching (Kavkler and Demsar, 2012; Badar *et al*., 2017). Indeed, hydrated collagen have their amide frequency shifted upwards (Gonzalez and Wess, 2008). A study by Masic *et al*., (2015) reported that dehydration of collagen shifts the band position which confirms that the triple helix backbone undergoes extensive conformational changes. A study by Jastrzbka *et al*., (2003) showed that when a peptide bond C=O is involved in hydrogen bonding, it increases the amide III band frequency. A positive shift in the amide region also implies that partial disruption of triple helicity of collagen occurs due to incorporation of the ABM and carrageenan (Gonzalez and Wess, 2008). This can also be corroborated further by the disappearance of the peak related to the ordered structure of collagen after the incorporation (Edwards *et al*., 2001; Janko *et al*., 2010). The loadings at 924, 933 and 938 cm^{-1} assigned to the skeletal backbone C-C stretching vibration of the triple helicity of collagen means that structural variation occurred during the process that affects this bond (Gasior-Glogowska *et al*., 2010). The variations may have been affected by v(C-O) of uronic acid residues due to the 3,6-anhydro-D-galactose in the carrageenan that vibrate at the same range of frequency (Huang *et al*., 2003; Pereira and Mesquita, 2004; Pereira *et al*., 2009). Presence of 3,6 anhydrogalactose can be supported by strong loadings at 852 cm^{-1} and 806 cm^{-1} which are attributed to the C_4 and C_2, respectively, of 3,6 anydrogalactose (Diharmi *et al*., 2017). A study by Janko *et al*., (2010) observed that change in intensity of the amide III testifies reorientation of collagen fibres. Hence, treating the leather with ABM and carrageenan

affects both the primary and secondary structure of collagen, transforming the triple-helical structure towards a randomly coiled structure (Gasior-Glogowska *et al*., 2010). Studies have shown that when chitosan are incorporated into collagen, the band intensity increases as its content is increased (Sionkowska *et al*., 2004; Riaz *et al*., 2018). Increased content ensures more available molecules for vibrations. However, when chitosan or glutaraldehyde, and collagen interacted and reacted to form crosslinkages, the bands intensity of the blend decreased (Jastrzebska *et al*., 2003; Sionkowska *et al*., 2004; Wang *et al*., 2008; Riaz *et al*., 2018). This is because the functional groups of the additives react to form crosslinks with collagen NH groups of the peptide bonds, the NH_2 groups change to N-H groups. The decrease in intensity is because all the molecules have taken part in the crosslinking reaction. Therefore, the study suggest that interaction of ABM and carrageenan with leather at crusting operations is majorly physical with minor interactions involving hydrogen bonding and sulphur. In this case, the particles squeeze themselves between the collagen fibrils. Due to the oily nature of ABM, the physical interaction is justified by the improvement of the organoleptic properties such as softness, the enhanced sliding of the fibril against each other (Litke and Widdemer, 2003; Bitlisli *et al*., 2010).

The deformation vibration of OCH of the polysaccharides and pectin in carrageenan and ABM were observed at loadings at 1017, 1028, 1022 and 1018 cm^{-1} (Dukor, 2002; Maice *et al*., 2015). The C=N vibration stretching are present in leather crusts due to lipids as shown by strong peaks at 1017, 1028, 1022, 1015 cm^{-1} and 1469 cm^{-1} (Shapiro *et al*., 2011). After incorporation, the frequency change and higher intensity as evidenced by strong loadings due to the aliphatic esters of ABM and carotenoids of carrageenan (Kassama *et al*., 2015; Maice *et al*., 2015). The C=N stretching vibration was observed at 1467 cm^{-1} assigned to the lipids present in collagen, ABM and carrageenan (Dukor, 2002; Shapiro *et al*., 2011). The other stretching vibration of C=N attributed to the aliphatic amines of the ABM and carotenoids of carrageenan occurred at 1152-1159 cm^{-1} **(**Puppels *et al*., 1993; Kassam *et al*., 2015). The concentration of the molecules exhibiting this vibration was high in the treated crust as compared to the untreated as evidenced by the intensity hence the high loadings. The C-O and C=O bonds are present in collagen due to carboxylate salts, carbohydrate residues and ether-type bonds in crust leather (Safandowska and Pietrucha, 2013; Badar *et al*., 2017). After treatment, the presence of loadings at 1080-1082, 1050-1052 cm^{-1} correspond to CH and C-O stretching vibrations of carbohydrates residues assigned to

the carboxylate salts and ester bonds present in both collagen and ABM/ carrageenan, respectively and flavanones or terpenoids (Safandowska and Pietrucha, 2013; Logaranjan *et al*., 2016; Badar *et al*., 2017).

The vibration stretching of C=O in native leather occurs at 1717 and 1726 cm^{-1} attributed to ketonic group valence (Puica *et al*., 2006; Gonzalez and Wess, 2008). Calcium calcite bond resulting from liming process vibrates at 1743-1747 cm^{-1} (Maice *et al*., 2015). This peak occurred in all the crusts. After treatment, the intensity and shifts of the frequency yielded a loading in the same frequency range due to presence of stretching vibration of C-O and C=O of the aliphatic esters in ABM and carrageenan (Muik *et al*., 2005; Kassama *et al*., 2015; Agato, 2016). The peaks at 1678-1701 cm^{-1} were only present in the treated samples. Therefore, the loadings at these frequencies were attributed to the groups from asparagine and glutamine acid residues of collagen and carboxylate groups in ABM and carrageenan that are able to bind Ca ions from the solution of $Ca(OH)_2$ (Badar *et al*., 2017). The loadings at 1146-1150 cm^{-1} are assigned to the v(C-C) and conjugated C=C of the glycogen and beta-carotene accumulation in the ABM (Huang *et al*., 2003). The loadings at 873, 884 and 1442 cm^{-1} assigned to v(C-C) associated with tanning system used (Ibrahim *et al*., 2015; Manfredi *et al*., 2015). After treatment, a reemergence of a carbonate bonds was observed evidenced by strong loading at 966 (967) cm^{-1} (Dehring *et al*., 2006). This implies that this bond originates from the ABM or carrageenan since the intensity of these peaks increased after the incorporation which gives additional C-C vibration stretching (Ibrahim *et al*., 2015).

The sulphur containing residues in the different physical states were observed at different loadings. C-S stretching with H at the trans position of the S atom: the loading at 645-674 cm^{-1} and C-S stretching with C at the trans position of the S atom; the loading 733-783 cm^{-1} (Edwards *et al*., 2001; OlszTynska-Janus *et al*., 2012; Rygula *et al*., 2013). The S-S stretching of glycine and other polysaccharides in collagen and carrageenan and disulphide crosslinking during tanning process (between 506-509 cm^{-1}) and cysteine (between 547-554 cm^{-1}) (Rygula *et al*., 2013; Edwards *et al*., 2001). The C-S stretching mode of cytosine at 1669 cm^{-1} (Stone *et al*., 2004). The loadings show that intensities of treated crusts are higher meaning that sulphur is more abundant in treated samples (Edwards *et al*., 2001). The loadings at 867 cm^{-1} is assigned to C-O-S linkages on C_6 of galactose, a marker conformation of carrageenan (Pereira *et al*., 2009; Krol *et al*., 2016). The

intensity of this peak in treated retanned crust spectrum was higher implying greater sulphur content, due to the ABM and carrageenan. The evidence for this sulphur can be observed at strong loadings at 825-830 cm^{-1} due to stretching vibration of C-O-SO_3 on C_6 of galactose from carrageenan (Perreira *et al*., 2003; Pereira *et al*., 2009). The –S=O of sulphate esters and phenols in ABM can further be evidenced by the loadings between 1210 cm^{-1} and 1260 cm^{-1} (Perreira and Mesquita, 2004; Pereira *et al*., 2009; Jithendra *et al*., 2013). The bands at 1065 and 1044 cm^{-1} are absorptions associated with combinations of S=O and C-O (uronic acid residues) modes of the aliphatic ether which are sensitive to hydrogen bonds (Krol *et al*., 2016).

According to literature, most prominent peaks from 1300 to 1400 cm^{-1} are bands arising from vibrational modes of methylene and methyls (Jastrzebka *et al*., 2003; Maice *et al*., 2015). Within this region, the crusts showed peaks at 1329, 1331, 1340 cm^{-1} that correspond to the twisting, wagging and deformation modes of CH_2 of methylene, respectively, of the proline side chains of collagen (Frushour and Koenig, 1975; Jastrzebka *et al*., 2003; Huang *et al*., 2003). After incorporation, other peaks emerged, peaks shifted and intensity increased as observed by the strong loadings within this region of frequency. The loadings at 1300, 1326, 1340, 1351, 1365 and 1377 cm^{-1} correspond to deformation, wagging and twisting vibrations of CH_2, stretching and deformation vibration of CH_3, respectively (Lakshmi *et al*., 2002; Gussen *et al*., 2005; Liu *et al*., 2008; Maice *et al*., 2015). Higher intensity can be attributed to the presence of tetradecanoic acid, methyl ester and squalene, the antimicrobials of the ABM (Lakshmi *et al*., 2002; Lakshmi *et al*., 2011). The other contributing factor are amino acid side chain of collagen (proline and tryptophan), phospholipids of carrageenan, aromatic rings, tannins and carboxylic acid of terpenes in ABM (Gussen *et al*., 2005; Puica *et al*., 2006; Liu *et al*., 2008; Rygula *et al*., 2013; Kassam *et al*., 2015; Maice *et al*., 2015; Badar *et al*., 2017**)**. The strong loading at 1442 cm^{-1} is the deformation vibration of methyl d(CH_3) and methylene d(CH_2) molecules that are present in proteins (Gniadecka *et al*., 1998; Jastrzebska *et al*., 2005). Scissoring mode of methylene d(CH_2) from the starch of the ABM and carrageenan and CH bending groups in the fatty acids and lipids in ABM explains the increase in intensity (Jastrzebska *et al*., 2003; Maice *et al*., 2015; Muik *et al*., 2015).

The peaks at 1462, 1467 and 1470 cm^{-1} were assigned to deformation vibration of methyl (CH_3) and methylene (CH_2) of the aliphatic side chains of amino acid residuals (Janko *et al*., 2010). The

intensity of these peaks increased significantly after incorporation as also evidenced by the loadings at these wavenumbers. This may be attributed to the additional deformation vibration, δ[CH]+ δ[CH_2]+ δ[C-O-H], from the amylose and amylopectin of the carrageenan and ABM whose vibrations occur at the same wavenumber (Liu *et al*., 2015c). Presence of the functional groups of ABM, C≡C-H:C-H (alkynes) were observed at loadings 547 and 554 cm^{-1} and also 1052 and 1050 cm^{-1} (Puica *et al*., 2006; Kassam *et al*., 2015). These loadings result from upshift in frequency and increase in intensity after treatment. The loadings at 475-492 cm^{-1} and 772 cm^{-1} were assigned to δ(C-C-C)+τ(C-O) attributed to amylose and amylopectin in carrageenan and ABM (Vandenabeele *et al*., 2000; Gussen *et al*., 2005; Liu *et al*., 2015c). These bonds are characteristic backbone vibration band of starch **(**Mahdad-Benzerdjeb *et al*., 2007; Liu *et al*., 2015c). Hence the intensity change in this range can be attributed to vibrations of the amylose and amylopectin in ABM and carrageenan (Kizil *et al*., 2002). The spectral differences contribute to large increase in the components, which are consistent with the changes associated with presence of carrageenan and ABM. The treatment induces modification in the 1717 and 1726 cm^{-1} loading that matches one of tannic acid band (attributable to C=O and COO groups) due to carbonyl groups in ABM (Bicchieri *et al*., 2011; Jithendra *et al*., 2013; Ibrahim *et al*., 2015). The loadings at 852 and 845 cm^{-1} were formed due to the shifting in the peaks to lower wave numbers assigned to the C-O-C bridges, skeletal mode of D-galactose-4-sulphate (G4S), present in carrageenan and amino acid sidechain modes of tyrosine, hydroxyproline and proline (Perreira *et al*., 2003; Pereira and Mesquita, 2004; Pereira *et al*., 2009; Rygula *et al*., 2013). The peaks at 1080-1093 cm^{-1} assigned to v(C-C) and v(C-O) attributed to the lipids, calcium carbonate (calcite) from the liming process and carbohydrate residues of collagen (Dukor, 2002; Maice *et al*., 2015). The variations in this frequency range are due to the v(C-O) +V(C-C) + δ(C-O-H) of the sugar groups of the glycosyl esters and pyranose ring of ABM and v(C-C) of the linoleic acid in carrageenan (Maice *et al*., 2015; Liu *et al*., 2015c; Badar *et al*., 2017). The loadings may also be assigned to the stretching vibration of aliphatic C-O-C bridges typical for polysaccharides of ABM and C-O of 3,6 anhydrogalactose of carrageenan (Pereira *et al*., 2009; Agato, 2016; Krol *et al*., 2016).

The symmetric stretching of Cr-O-Cr was witnessed at 547 and 554 cm^{-1} in crusts spectra (Vascova and Kolomaznik, 2016). The peaks at 852-858 cm^{-1} show the symmetric stretching of CrO_4^{2-} present in all the crusts spectra (Perez-Rodriguez *et al*., 2013). After the incorporation, the

loadings at these wavenumbers result from increase in intensity and slight downshift in frequency due to presence of o-galactose-4-sulphate and D-galactose-4-sulpahte in the carrageenan **(**Pereira *et al*., 2003; Perira and Mesquita, 2004; Pereira *et al*., 2009; Pereira *et al*., 2013).

4.6 Effect of post tanning operations on the elemental compositions and concentrations of leather

The typical spectral intensities of elements in tanned, retanned, dyed and fatliquored crusts for the five excitation conditions (secondary targets) are shown in figures 4.22-4.25.

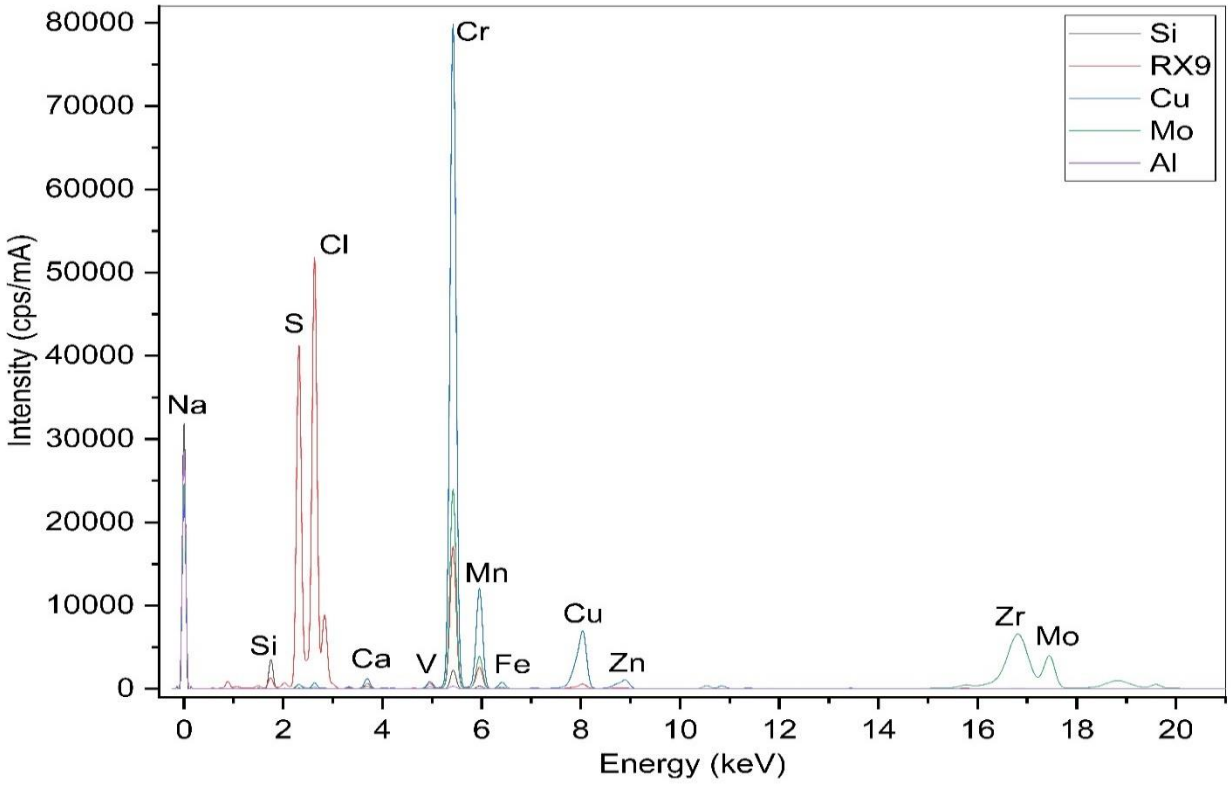

Figure 4.22: EDXRF spectra of elements in tanned crust by five secondary targets

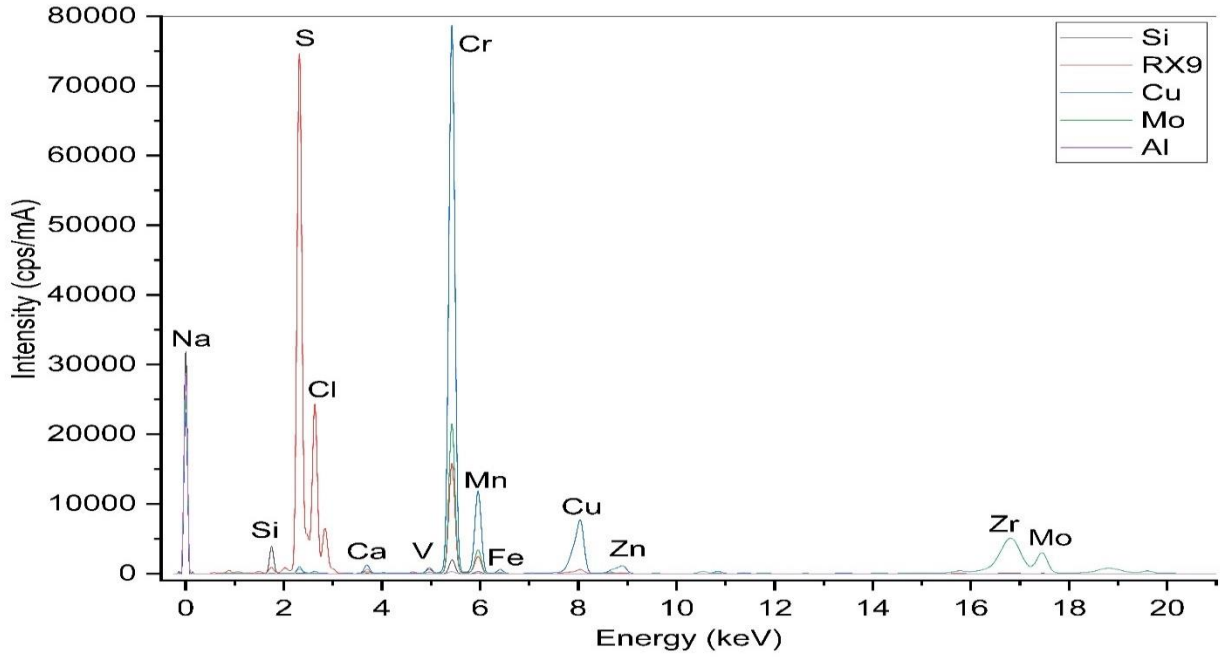

Figure 4.23: EDXRF spectra of elements in retanned crust by five secondary targets

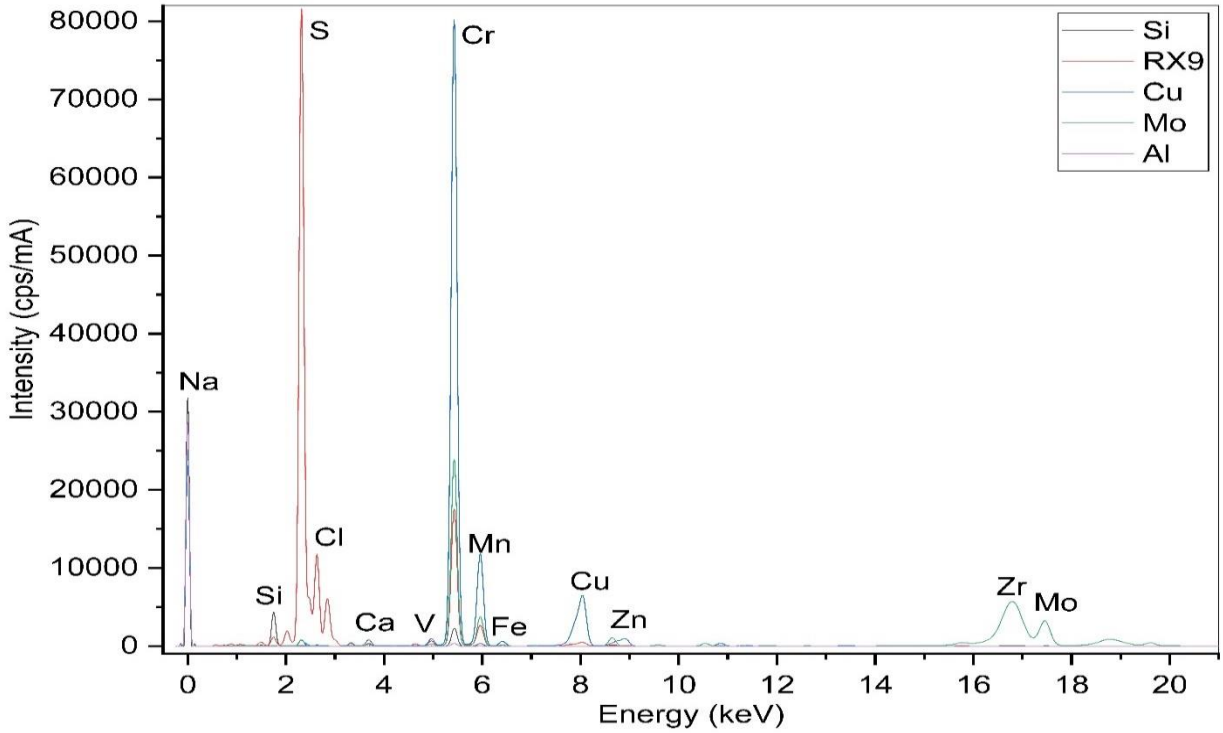

Figure 4.24: EDXRF spectra of elements in dyed crust by five secondary targets

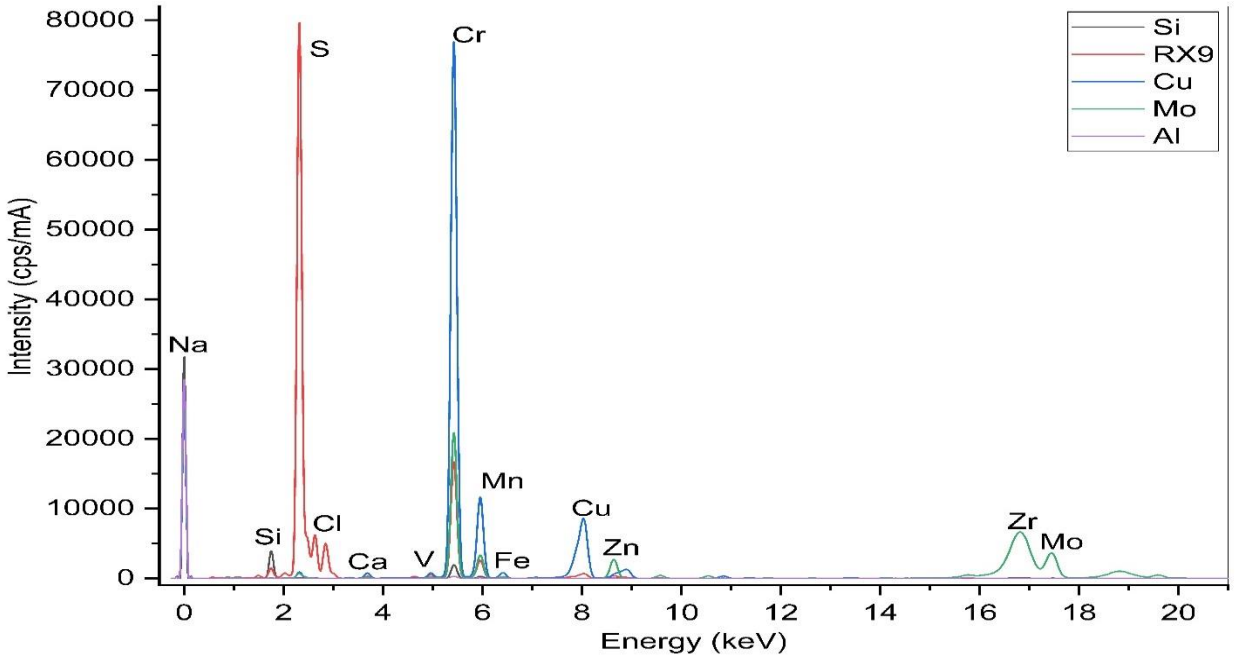

Figure 4.25: EDXRF spectra of elements in fatliquored crust by five secondary targets

In all the spectra shown, the predominance of Cr, S, Na, and Cl dwarfed the intensities of the other minor elements in leather crusts. The Cu secondary target showed excellent excitation efficiency for most of the elements detected such as K, Ca, V, Cr, Mn, Cu, and Zn. The RX9 secondary target exhibited excellent excitation efficiency for S, Na, and Cl whereas Mo target only showed efficiency to detect Zr and Mo. The Al and Si secondary targets detected Al and Si, respectively. Although a combination of the five secondary targets gives a wider spectrum of detection of different elements, a combination of RX9 and Cu is sufficient to efficiently detect key elements in post tanned crusts.

The elemental concentrations in tanned, retanned, dyed and fatliquored leather are summarized in table 4.8.

Table 4.8: Elemental Concentrations in tanned, retanned, dyed and fatliquored crust leathers

	Elemental concentration by means ± statistical error (mg/kg)			
Element	**Tanned**	**Retanned**	**Dyed**	**Fatliquored**
Cr	69200±129.7	80100±136.67	75167±151.3	63967±118.7
Hg	3.53±1.12	4.33±1.21	<3.28*	3.36±1.1
Pb	12.6±1.4	14.4±1.52	13.1±1.51	17.5±1.6
As	101±2.04	94.1±2.13	95.6±2.16	82.2±1.88
V	1046±16.4	1417±17.47	1048±20.4	832.3±14.34
Mn	163±45.7	<156.3*	<149*	<133*
Fe	439.3±12.4	386.7±12.07	364.7±12.1	390.7±11.23
Ni	7.49±1.55	9.67±1.8	9.19±1.71	8.94±1.7
Cu	15.5±1.66	17.3±1.91	19.5±1.9	16.4±1.75
Zn	19.43±1.46	760.7±2.76	81.53±8.63	1370±10.8
P	319±10.82	1633±12.6	397±21.47	292±9.8
K	661.3±34.1	2717±35.57	561.7±66.3	414.3±29
Ca	3257±65.03	1717±67.07	2907±60.67	981±48.2
S	23967±53.2	49967±78.97	48167±79	42500±65.97
Na	23967±3783.3	15633±4070	27567±2943.3	11667±2980
Ti	44.3±6.57	57.83±6.74	41.03±6.9	45.9±6.01
Zr	598±17.87	623±19.77	646±19.4	604±17.87
Ga	5.78±0.86	9.41±0.91	5.93±1.1	9.34±1.05
Al	3257±106	4123±117	3533±118.7	2550±88.37
Si	3490±52.77	2633±52.53	3097±46.73	2837±44.13
Cl	17267±32.8	4267±26.47	9347±18.17	1667±10.04
Br	6.38±0.56	2.92±0.51	3.73±0.55	<1.2*

Note *< Below Detection Level of the equipment

Abundance of the elements in all the post tanned leather crusts was in the order Cr > S > Na > Cl > Al > Si> Ca > V > K > P > Zr > Zn >Fe > Mn >As > Ti > Cu > Pb > Ni > Ga > Br > Hg. The concentrations of Cr ranged from 63967 to 80100 ppm, sulphur 23967 to 49967 ppm, sodium

23967 to 27567 ppm while chlorides from 1667 to 9347 ppm. These concentrations are slightly higher than the values reported in other related studies due to differences arising from the processing recipes and the techniques of measurement. The concentrations for Cr as determined by Aslan, (2009) using ICP-OES, ranged between 28000 and 44000 ppm. The results reported in this study for Br, Zn, Ni and Fe agree with results reported by Kapel and Speak (1979), Carneiro *et al*., (2003) and Okoh et al (2013), although the concentrations for Arsenic (As) was slightly higher. These studies used ICP-OES, INAA and AAS techniques to determine the concentrations, which have different limits of determination and quantification. The higher concentrations of chromium, sulphur, sodium and chlorine, can be attributed to their excessive use during preservation (industrial salt), dehairing (sodium sulphide), deliming (sodium metabisulphite), pickling (sodium chloride and sulphuric acid), tanning and retanning processes (chromium sulphate), basification and neutralization using sodium formate and sodium bicarbonate (Rastogi *et al*., 2008; Mikoczy and Hagmar, 2005).

Principal component analysis (PCA) was employed to identify the pattern in the elemental composition and concentrations during crusting operations in order to determine the effects of crusting operations on the elemental compositions of the resulting leather. Figure 4.26 shows the score plot for post tanned crusts.

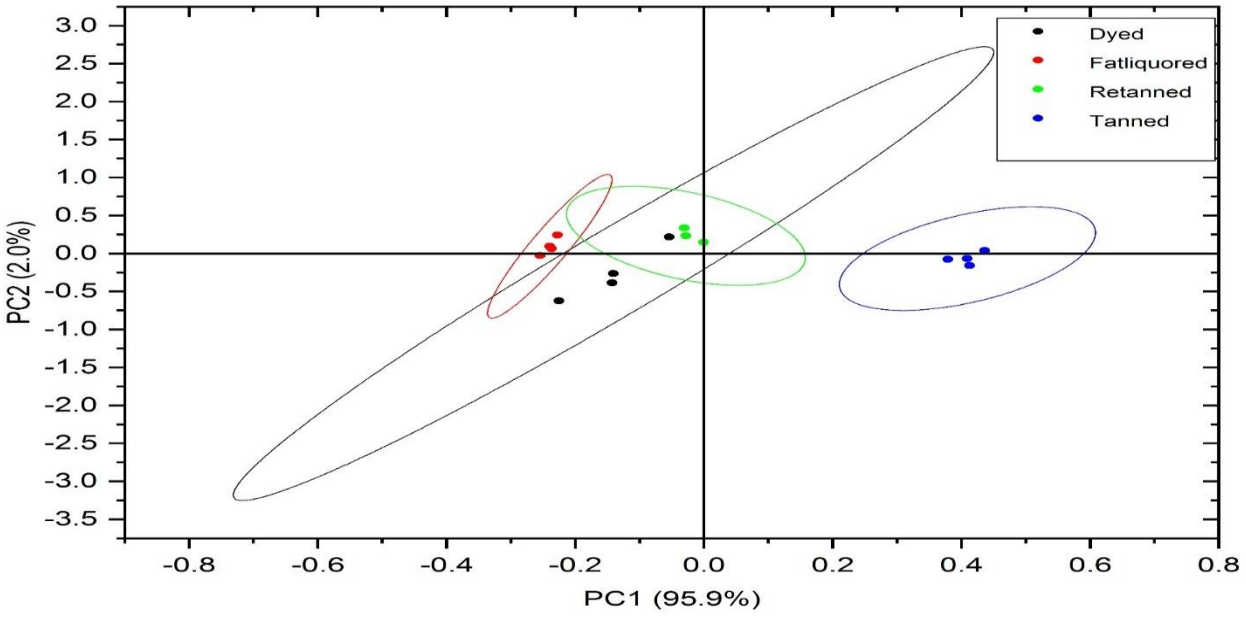

Figure 4.26: Score plots for all post tanned leather crusts

The first two PCs explained 97.9% of the variance in the entire dataset. The remaining 2.1% variation could be attributed to presence of outliers. From the plot, all the four processes have an effect on both the elemental composition and concentration as evidenced by classification of scores for each process. The first component (PC 1), which accounts for 95.9% of the variation in data, separates fatliquored and tanned crusts composition while PC 2, which accounts for 2.0% of the variations, separates the dyed from the retanned crusts. The tanned crusts show high positive scores while fatliquored samples show high negative scores along PC 1. Similarly, retanned crusts showed positive scores while dyed crusts showed negative scores. To determine the elements that account for these differences, examination of variable loadings was done on the two PCs as shown figure 4.27.

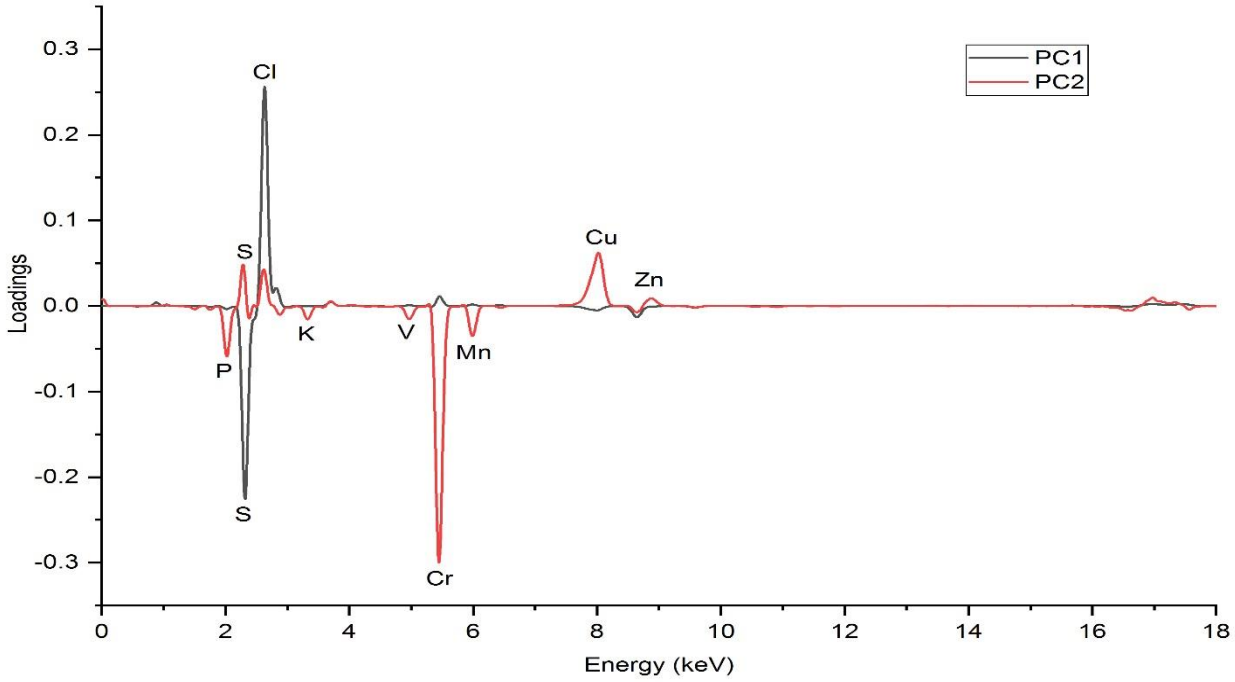

Figure 4.27: PCA loadings plot showing the trace elements responsible for the PCA clusters

The valuable tracers for the classification over various stages of processing are Cr, S, Cl, P, V, K, Mn and Zn. To determine the possible provenance and hence their pathway during crusting processes, comparisons were made between one stage and the subsequent stage. Comparison of the score plots of two successive processes was done. Figure 4.28 shows the score plot of tanned and retanned crusts.

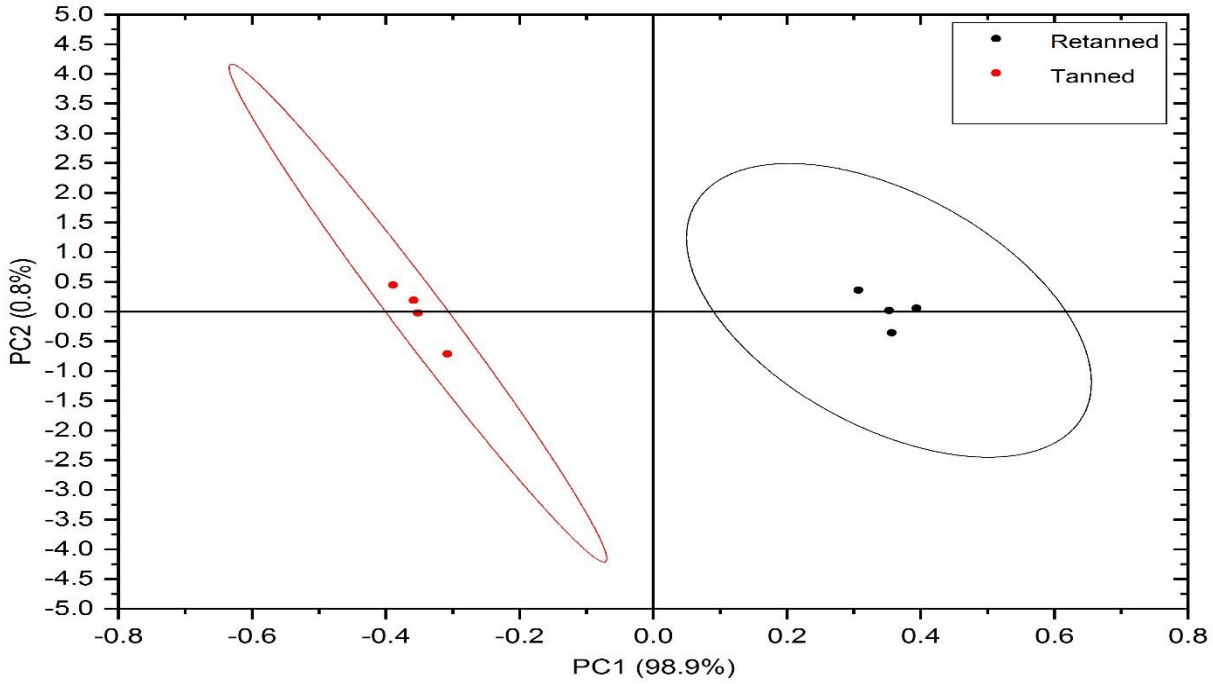

Figure 4.28: Score plot of the PC 1 and PC 2 for tanned and retanned crusts spectra

PC 1 can clearly be used to distinguish the elements of tanned crusts from retanned crusts since they are anti-correlated to each other. The elements that distinguish chemical elements of tanned from retanned crusts are S, Cu, and Cl as shown in figure 4.29.

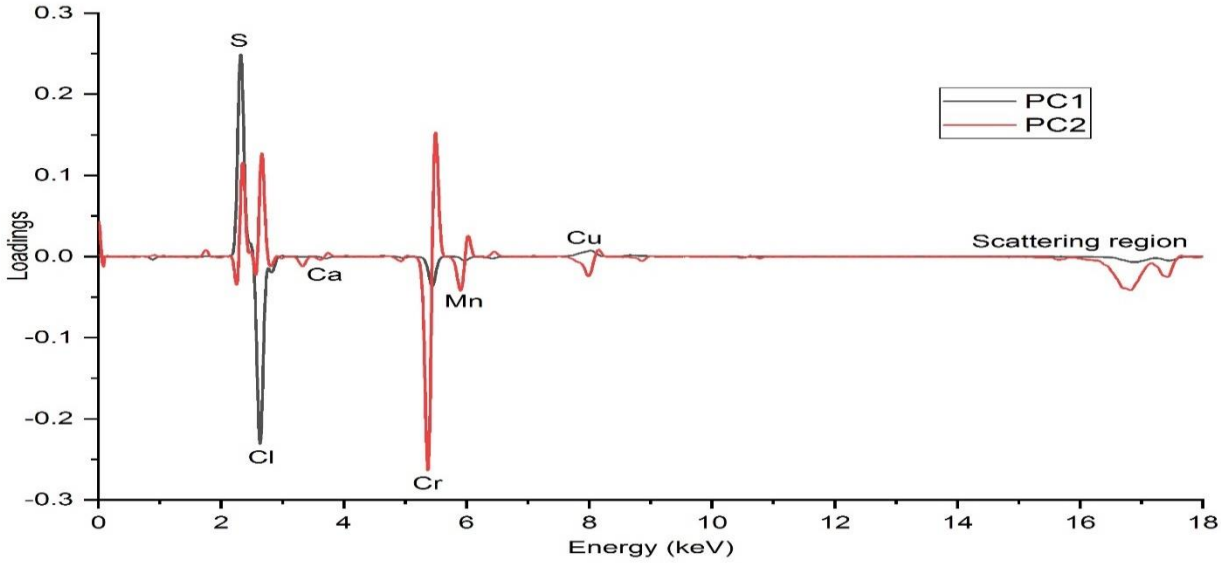

Figure 4.29: PC loadings of the EDXRF spectra differences in tanned and retanned crusts

Retanning process introduces more sulphur and copper into the leather fibres. This is attributed to the sulphate salts used in retanning (second chrome tanning) process. However, the levels of chloride salts decrease as retanning progresses. The main source of Cl is the salt used during preservation and pickling process. These salts are meant to inhibit any bacterial growth but their chemical reaction with the collagen is minimal and hence majority of the salts are physically suspended in the fibres and get displaced easily as retanning progresses (Fuck *et al*., 2011). This explains why Cl is lower at retanning stage than at tanning. Figures 4.30 and 4.31 show the score plot and loading plots, respectively, of retanned and dyed crusts.

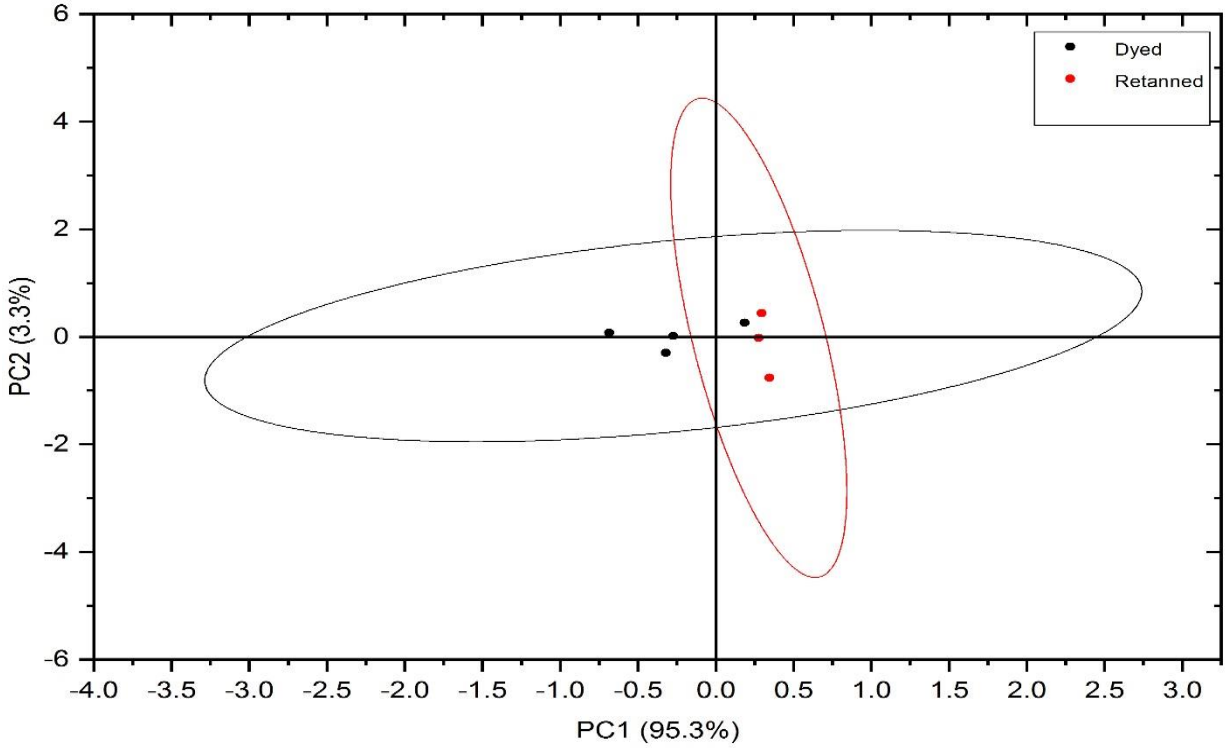

Figure 4.30: Score plot of the PC 1 and PC 2 for retanned and dyed crusts spectra

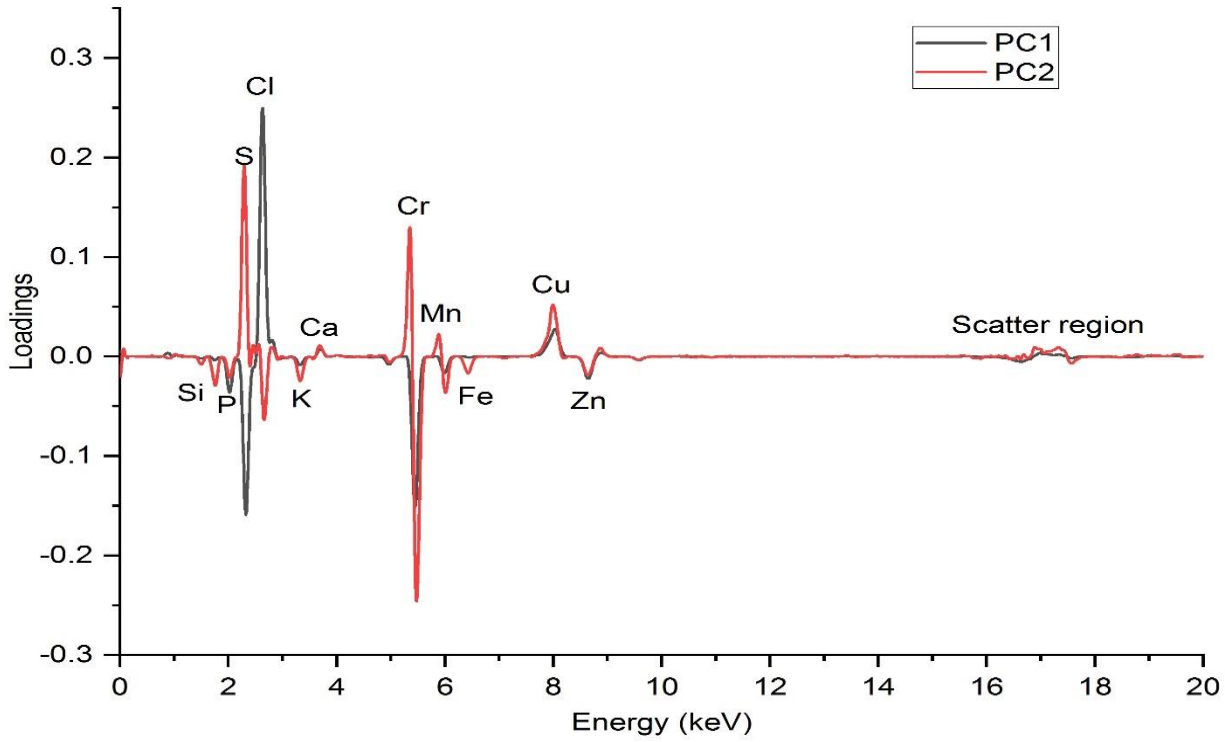

Figure 4.31: PC loadings of the EDXRF spectra differences in retanned and dyed crusts

The first two components accounted for 98.6% of the variations in the chemical elements of the two crusts. Therefore, the two components are sufficient to explain the variations and it can be seen that most of the scores for dyed crust are negative while for retanned crusts are positive. The elements responsible for the loadings in PC 1 are Cl, P, K, S, Cr and Cu. Dyeing process raises the levels of P, S, K, Mn, and Zn and lowers the levels of Cl and Cu. Dolgin *et al*., (2006) have attributed the presence of Mn in parchment to calcites. Similarly, Cl and Cu get displaced as processing progresses. The source of P, S, K, Zn and Mn may be present in dyes used (Pervaiz *et al*., 2017; Puntener, 1998; Thanikaivelan *et al*., 2003). Figures 4.32 and 4.33 show the score plot and loading plot, respectively, of dyed and fatliquored crusts.

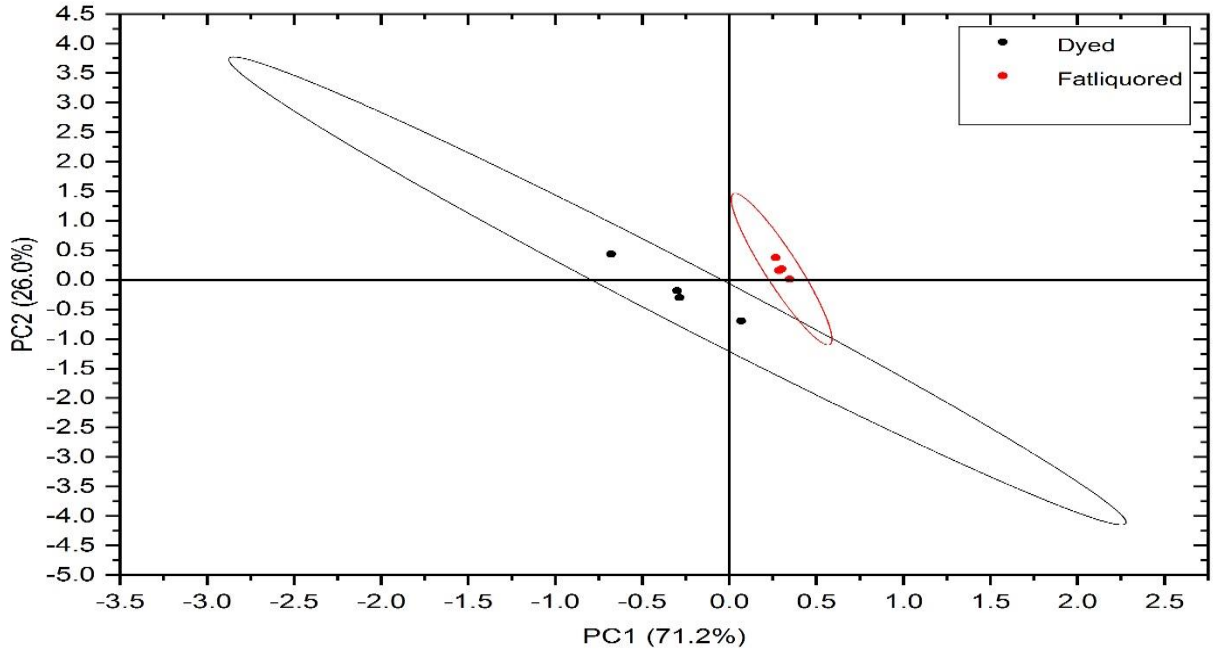

Figure 4.32: Score plot of the PC 1 and PC 2 for dyed and fatliquored crusts spectra

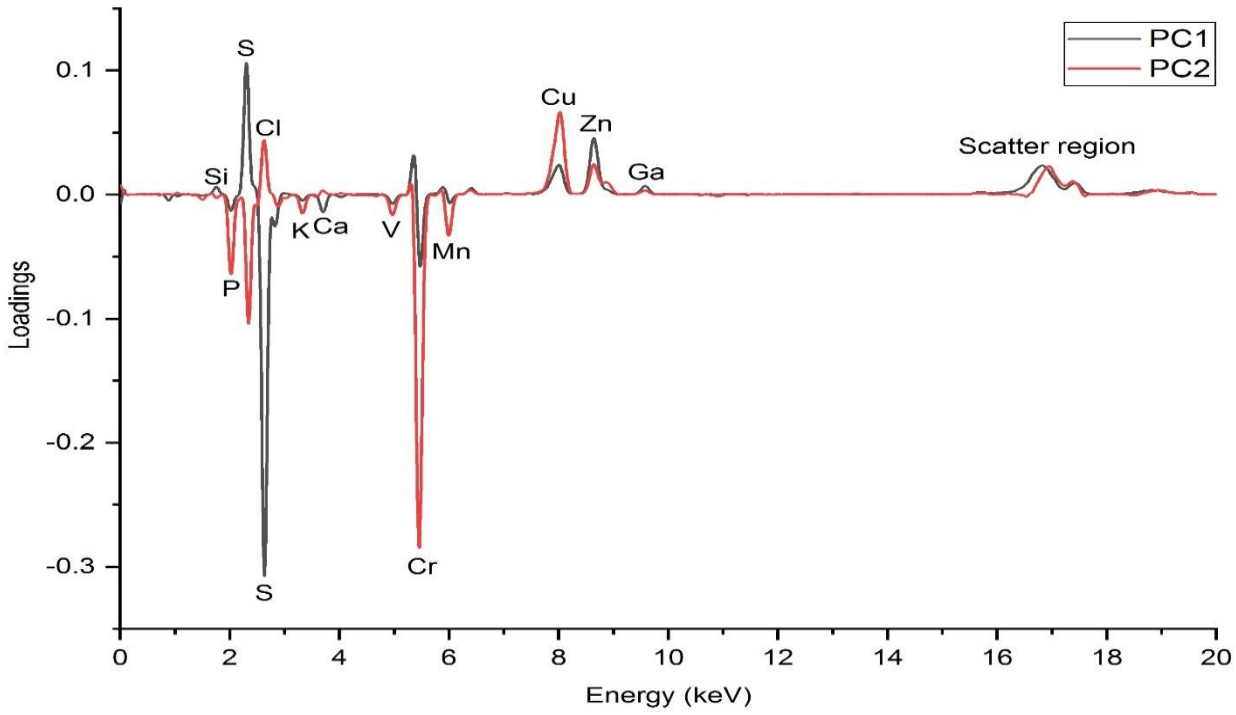

Figure 4.33: PC loadings of the EDXRF spectra differences in dyed and fatliquored crusts

PC 1 and PC 2 explain 97.2% of the variation in the chemical elements in the dyed and fatliquored crusts. The elements responsible for the variations are P, S, Ca, V, Cu, Zn and Ga (figure 4.33). Fatliquoring process increases the concentration levels of S, Si, Ga, Cu and Zn. The fatliquors used in this study were sulphited and hence this explains the increase in sulphur elements.

4.7 Effect of *Aloe barbadensis* Miller and carrageenan on the elemental composition and concentrations of leather

Effect ABM and carrageenan on the elemental composition of crusts was done by comparing the chemical components of leather crusts with the corresponding leather crusts treated with ABM and carrageenan. Principal component analysis helped to determine the effect of treatment at different stages of crusting operations. Figures 4.34-4.37 show the score plots of tanned, retanned, dyed and fatliquored crusts spectra and their corresponding crusts treated with ABM and carrageenan, respectively.

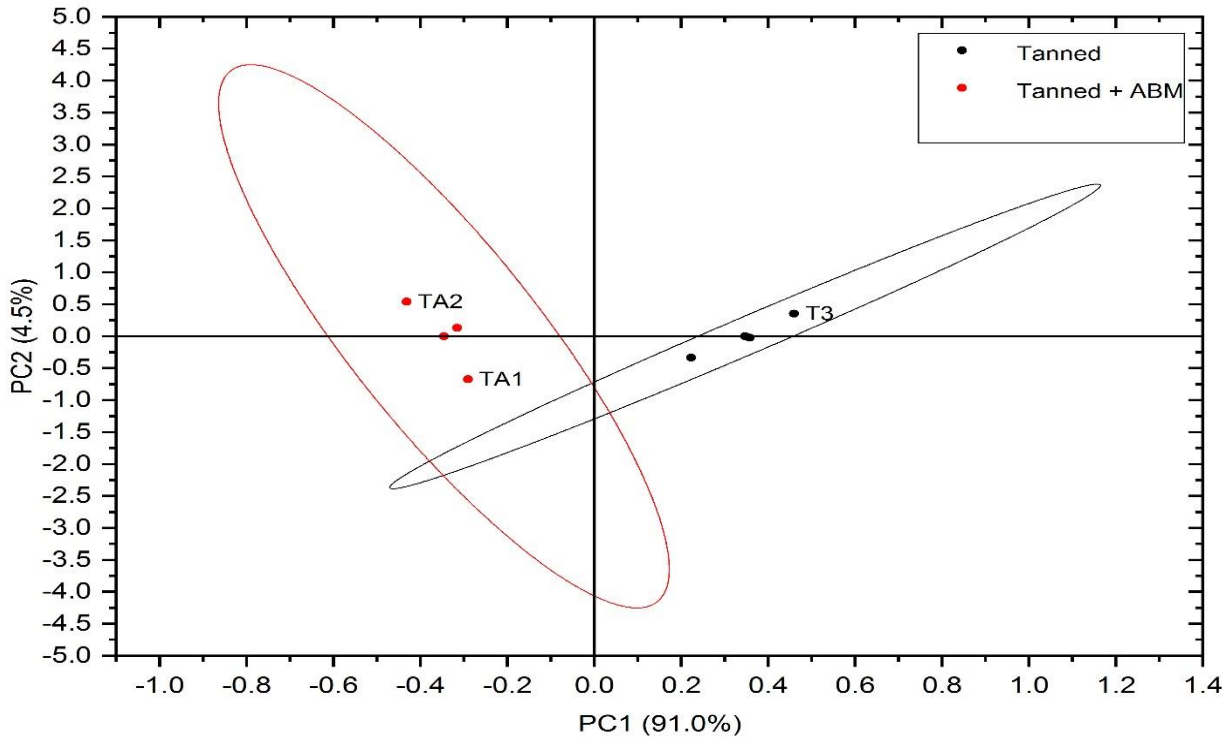

Figure 4.34: Score plot of PC 1 and PC 2 for tanned and treated tanned crusts spectra

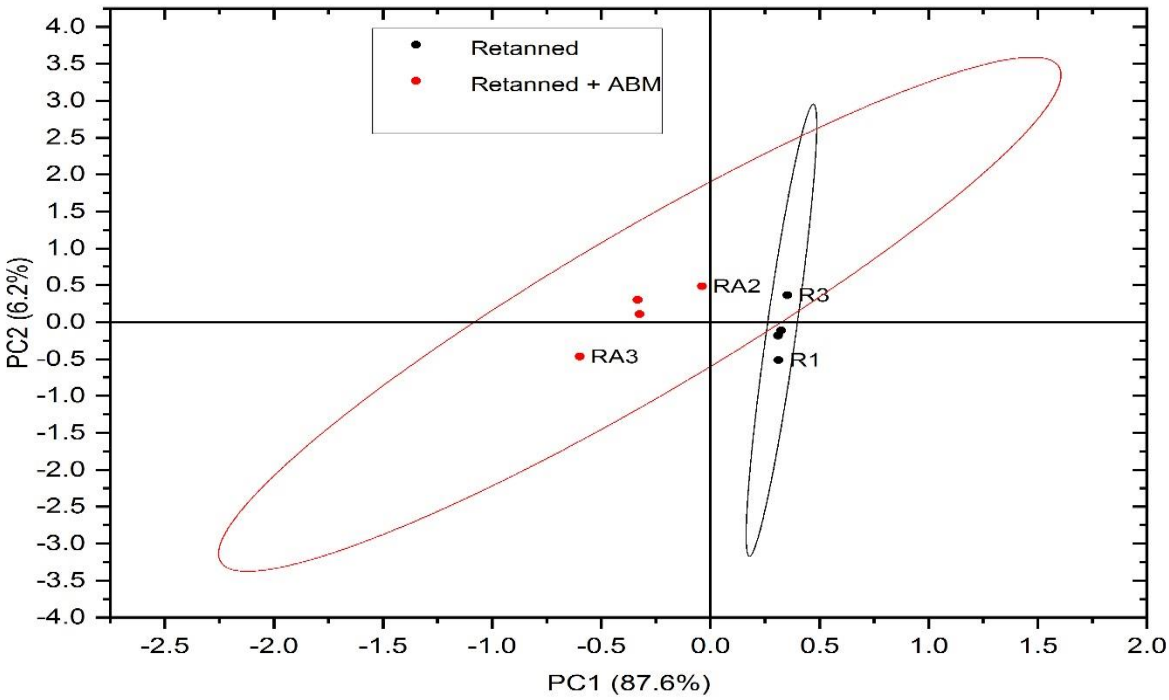

Figure 4.35: Score plot of PC 1 and PC 2 for retanned and treated retanned crusts spectra

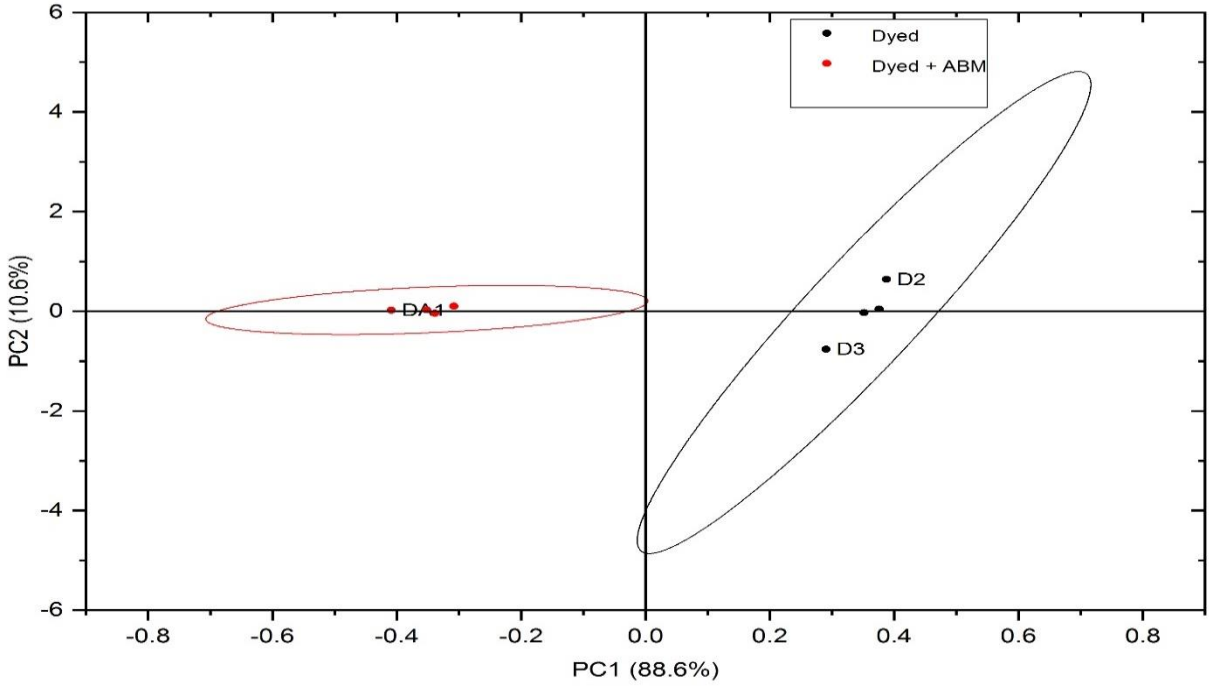

Figure 4.36: Score plot of the PC 1 and PC 2 for dyed and treated dyed crusts spectra

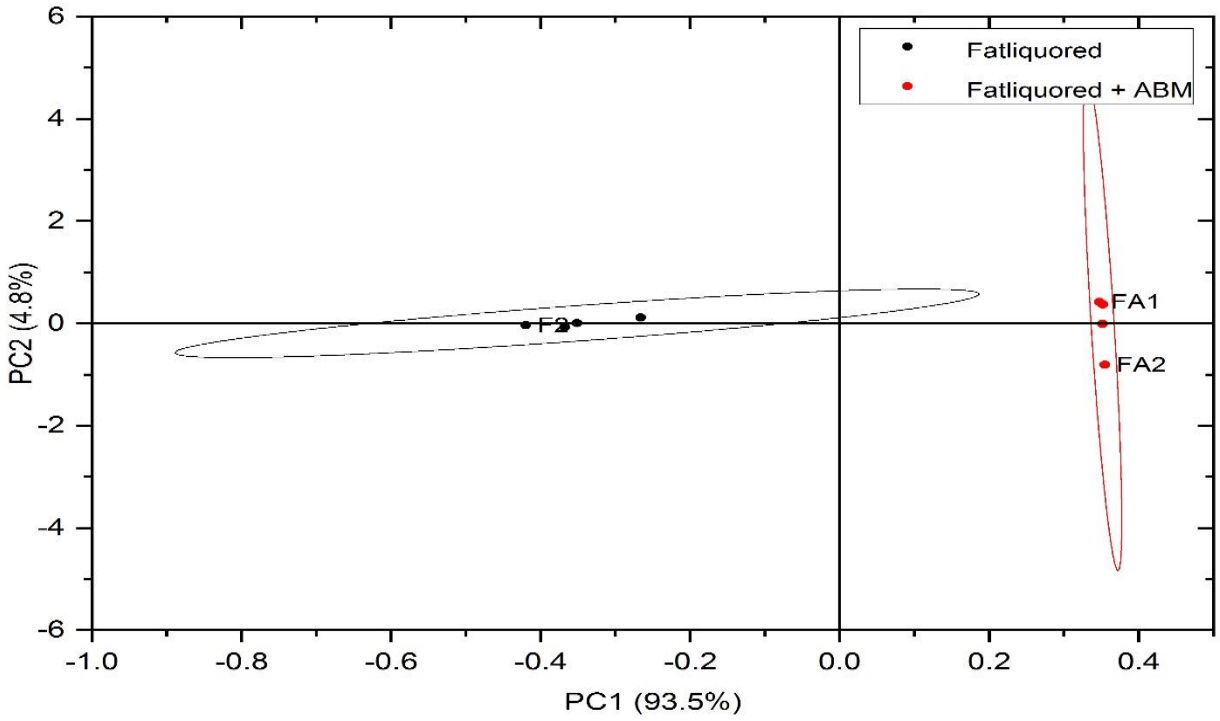

Figure 4.37: Score plot of the PC 1 and PC 2 for fatliquored and treated fatliquored crusts spectra

From the score plots, it's clear that elemental concentrations of crusts are significantly different from crusts treated with ABM and carrageenan as evidenced by clear separate scores from each other plots. The first two principal components explained more than 95% of the variations in the data, implying PC 1 and PC 2 are sufficient to explain the effect of incorporation of ABM and carrageenan. Similarly, PC 1 has shown to distinguish the crusts treated from those which are not treated. In tanned, retanned and dyed crust, PC 1 showed positive loadings while the corresponding crusts treated with ABM and carrageenan showed negative scores aligned along PC 1. For fatliquored crust, the scores were negative while fatliquored crust treated with ABM and carrageenan showed positive scores along the PC 1.

The score loadings for the scores of each crusts and their corresponding treated crusts were plotted to determine the exact elements of differentiation. Figures 4.38-4.41 show the loading plots for tanned, retanned, dyed and fatliquored crusts, respectively.

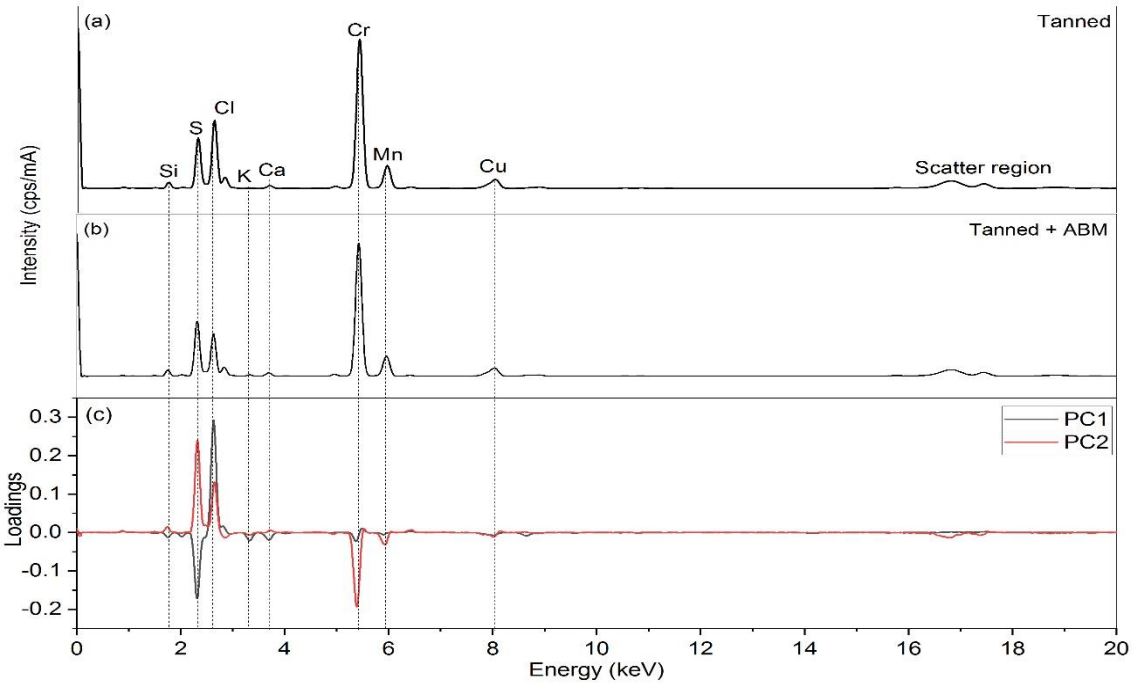

Figure 4.38: a) Average spectrum of tanned crusts b) average spectrum of tanned crust treated with ABM and carrageenan c) loadings of tanned crusts and tanned crusts with ABM and carrageenan

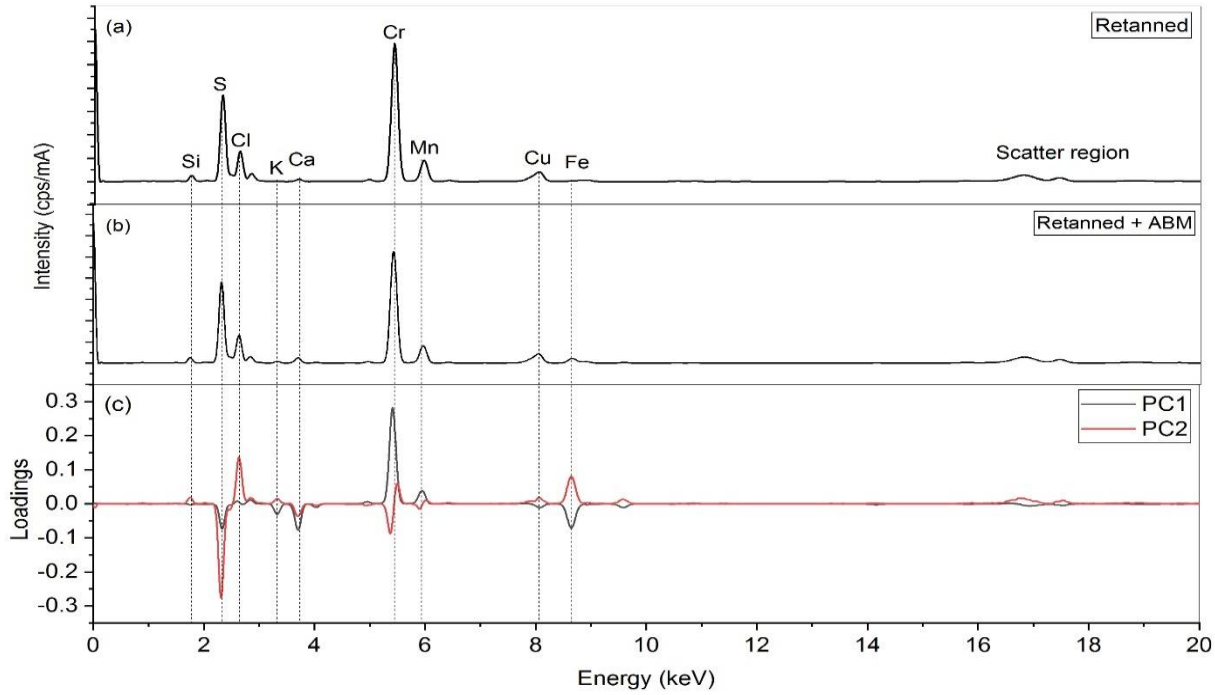

Figure 4.39: a) Average spectrum of retanned crusts b) average spectrum of retanned crusts c) Loadings of retanned crusts and retanned crusts treated with ABM and carrageenan.

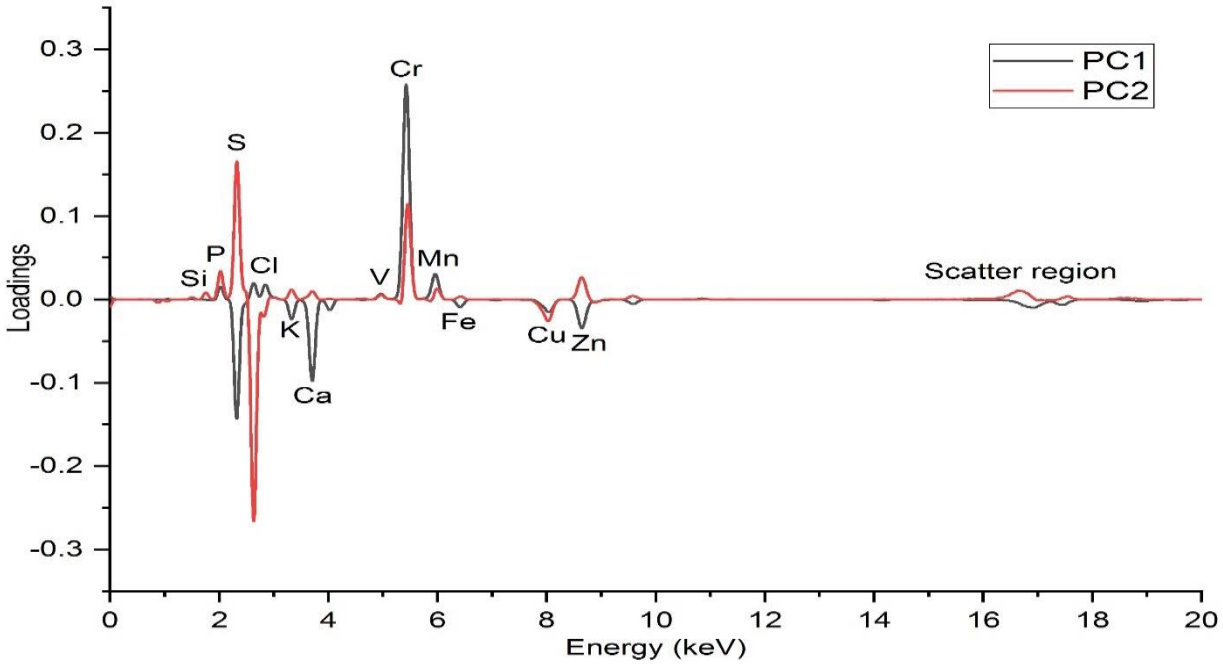

Figure 4.40: PC loadings of the EDXRF spectra differences in dyed crusts and treated dyed crusts

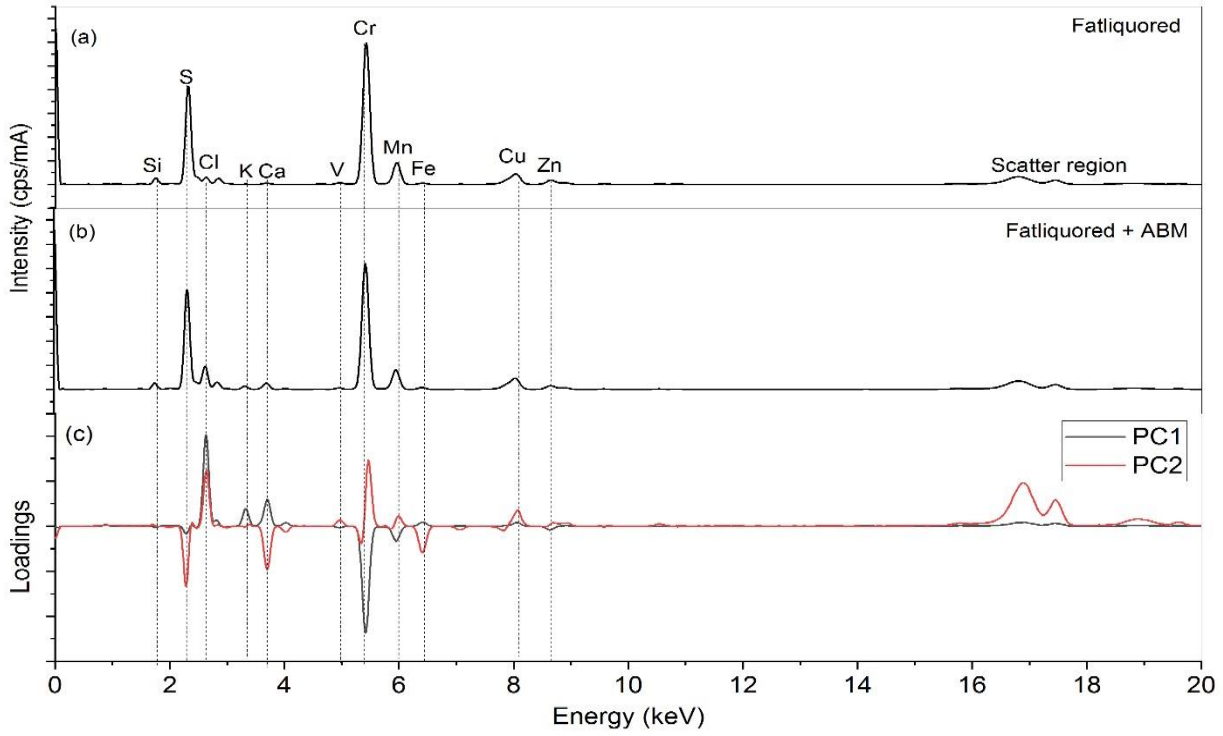

Figure 4.41: a) Average spectrum of fatliquored crusts b) average spectrum of fatliquored crusts treated with ABM and carrageenan c) PC loadings of fatliquored crusts and fatliquored crusts treated with ABM.

The main elements of discriminations are Si, S, Cl, Ca, Mn, Cr, Cu, K, Fe, Zn and V as evidenced by strong loadings in the loading plot. Tanned crust showed greater concentrations of Cl as compared to the treated tanned crusts. Treated tanned crusts showed higher concentrations of S, K, Ca, Mn, Cu, Cr, Si, Cr, Fe, Zn and V. The presence of Si and Cu may be attributed to the secondary targets used in the excitation. The possible sources of sulphur in leather are sulphuric acid used in pickling, sulphate in chromium and the wetting back sulphates (Hedberg *et al*., 2014). The greater concentrations of Ca, S, Cr, K, Mn, Fe, Zn and V in the crusts treated with the ABM and carrageenan may be traced to the trace elements in ABM (Sanghi, 2015; Agato, 2016). The carrageenan also contributes some sulphur, Ca and K into the crust (Pereira *et al*., 2003; Pereira *et al*., 2013). For retanned, dyed and fatliquored crusts, the concentrations of Cr were higher than in corresponding treated crusts. This may be explained by the residual or weakly fixed or unfixed/unreacted Cr used in retanning process (Palop *et al.*, 2008). Some Cr taken up by the dermal collagen during tanning and retanning process do not take part in the crosslinking action but only remain suspended in the leather fibres or fibrils (Miu *et al*., 2008; Fuck *et al*., 2011). These Cr are easily displaced or washed away by the ABM gels and carrageenan during treatment. Miu *et al* (2008) noted that chrome retannage increases drastically the amounts of extractable/unbound Cr. They also found out washing parchment with complex active surfactants reduces the amount of unbound Cr (III). This implies the amount of displaced Cr is higher than the trace Cr present in ABM used.

4.8 Effect of post tanning operations on the formation of Cr (VI) in leather

The absorbance of different concentrations of Cr (VI) is tabulated in table 4.9.

Table 4.9: Standard calibration data

Conc. of standard solution (µg/ml)	blank	1	3	6	9	12	15
Absorbance	0.000	0.016	0.046	0.090	0.134	0.179	0.225

Using the data in table 4.9, calibration curve was plotted as shown in figure 4.42.

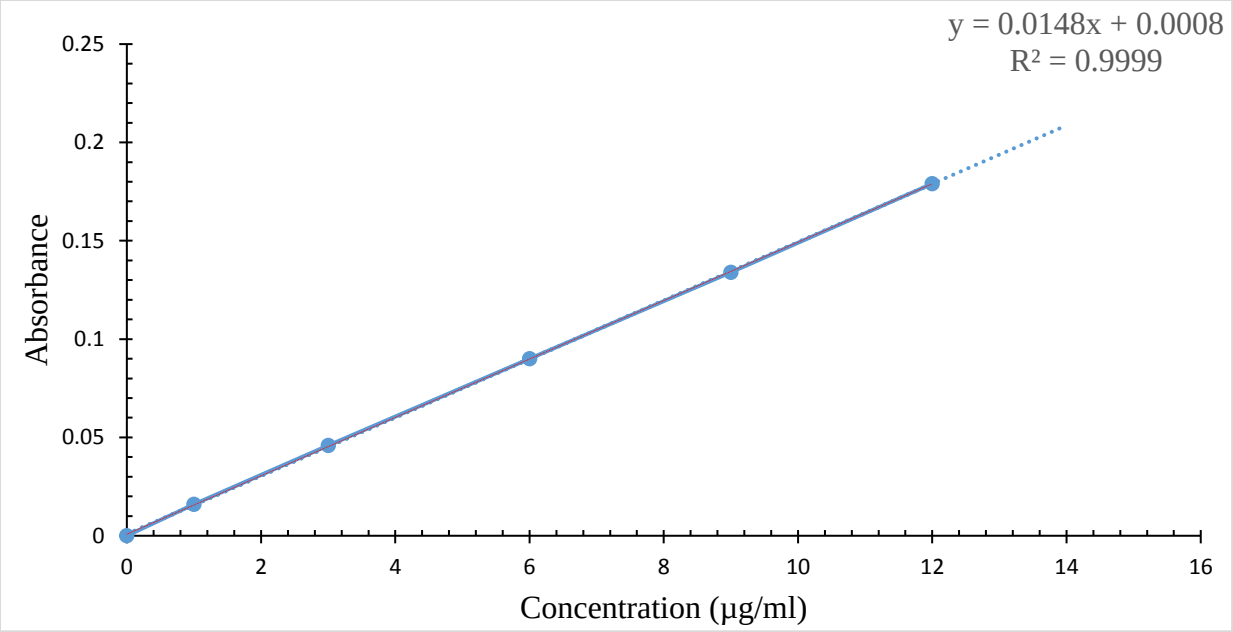

Figure 4.42: Calibration curve of Cr (VI) concentrations

The calibration curve is linear ($R^2 = 0.9999$). This evidently shows that the graph agrees with the Beer-Lambert's law of absorbance versus concentration very closely. Using equations 3.5 and 3.6 and the slope from figure 4.43, the limits of detection and quantification were determined to be 0.2872487 and 0.0948 mg/kg, respectively. The absorbance of the tanned, retanned, dyed and fatliquored crusts and their corresponding artificially aged samples were significantly different ($p<0.05$).

Table 4.10: Absorbance of post tanned crusts (132 hours UV+ 24 hours at 80 ºC)

Absorbance	**Crust**	**Tanned**	**Retanned**	**Dyed**	**Fatliquored**	**Recovery rate**
Control samples (Non-aged)	With DPC (A_1)	0.046	0.033	0.058	0.036	98.6%
	Without DPC (A_2)	0.046	0.023	0.058	0.036	
Aged samples	With DPC (A_1)	0.033	0.048	0.078	0.022	98.72%
	Without DPC (A_2)	0.017	0.047	0.067	0.017	

From the determined value of recovery rate of 98.2%, it indicates that the influence of matrix on the results was negligible and hence the procedure worked effectively according to ISO 17075.

Table 4.11: Calculated values of Cr (VI) in both control and artificially aged post tanned crusts

	Tanned	**Retanned**	**Dyed**	**Fatliquored**
Unaged samples	n.d.	152	n.d.	n.d.
Aged samples	15	241.6	76	167.23

*n. d: not detected

From table 4.11, the levels of Cr (VI) in both control and aged samples tested were influenced by the crusting operations. Among the control crusts, only the retanned crust tested positive for Cr (VI) with concentrations of 152 mg/kg. Girardi *et al*., (2013) also noted that ageing is necessary for the formation of Cr (VI), otherwise the concentration of Cr (VI) formed was below the detection limit. Although autoxidation occurs in all the samples to form reactive oxygen species (radicals) of hydro peroxides, the complex bonds of Cr (III) with collagen are too strong to be dismantled by autoxidation (Miu *et al*., 2008; Fuck *et al*., 2011). Hence only the unbound Cr (III) are culpable to react with the reactive species to form Cr (VI) (Candar *et al*., 2001; Miu *et al*., 2008). Retanning process in this case using chromium increases the free, soluble (unbound), extractible and total chromium concentration that correlates with the high Cr (VI) level observed (Candar *et al*., 2001; Miu *et al*., 2008; palop *et al*., 2008; Fuck *et al*., 2011; Mathiason *et al*., 2015; Cannot *et al*., 2016).

After ageing, significant levels of Cr (VI) were detected in all the post tanned crusts. An average level of 15 mg/kg Cr (VI) was detected in tanned crusts. These results are comparable to results published by Bayramoglu *et al* (2012); 9.39-24.02 mg/kg on chrome tanned leather crusts exposed to 80ºC and UV radiations for 72 hours. Font *et al* (1998) reported Cr (VI) concentrations of 40 mg/kg after exposing un-retanned leathers to UV light for 325 hours. The presence of the Cr (VI) in the aged tanned crust is due to thermal and photo ageing that induce the formation of Cr (VI) (Font *et al*., 1999). The average Cr (VI) concentration in aged retanned crust was 241.6 mg/kg. The pronounced increase in the concentration of Cr (VI) attributed to the more Cr (III) to be oxidized, the excess Cr (III) that are not chemically linked to the carboxylic group of collagen and hence oxidizable Cr (Fuck *et al*., 2011). A study by Hauber and Buljan (2000) explains that that due to less leachable Cr (III), there is no sufficient Cr (III) and hence no reaction to yield Cr (VI).

Similarly, the neutralization and basification or wetting back processes prior to retanning process play key role in the conversion of Cr (III) to Cr (VI). The use of sodium bicarbonate and ammonium bicarbonate in these processes provide mild oxidation agents especially at high pH that necessitate the formation of Cr (VI) in the crust (Hauber and Buljan, 1999). The results are agreeable to those reported by Colak *et al* (2014) of 136.3 mg/kg for chrome-retanned leathers exposed to 80 ºC heat and radiations for 170 hours. Font *et al* (1999) reported 65 mg/kg of Cr (VI) when naphthalene sulfonic acid retanned leather was exposed to UV light for 8 days.

The concentrations of Cr (VI) decreased in dyed crusts to an average of 76 mg/kg. Majority of the unbound and unfixed Cr from the retanning process have been washed away from the collagen fibres. This means that dyeing processes minimizes the free soluble and total chromium that are likely to be converted to Cr (VI) during ageing. This may be attributed to the neutralization and washing processes that removes significant amount of unfixed/unbound Cr present in the crust (Miu *et al*., 2008). This level was higher than those recorded in tanned crusts. The concentrations of Cr (VI) increased to an average of 167.23 mg/kg in fatliquored crusts. This means that the presence of fatliquors in leather enhances the conversion of Cr (III) to Cr (VI). The high concentrations of Cr (VI) can be explained by the unsaturated carbon-carbon bonds in the fatty acids both free and esterified. The free radicals released by the unsaturated lipids in the presence of UV light can significantly cause the formation of Cr (VI). In the presence of UV radiations and high temperatures, the unsaturated lipids and fatliquors decompose to form systems of conjugated double bonds (C-C) which initiate reactions that generate reactive oxygen species (Babu *et al*., 2005; Batema *et al*., 2015). These reactive oxygen species oxidize the Cr (III) to form Cr (VI) (Palop *et al*., 2008; Fuck *et al*., 2011; Tegtmeyer and Kleban, 2013).

4.9 Effect of Aloe *barbadensis* Miller and carrageenan on the formation of Cr (VI) in leather

Table 4.12: Standard calibration data

Conc. of standard solution (µg/ml)	blank	1	3	6	9	12	15
Absorbance	0.000	0.011	0.038	0.074	0.111	0.147	0.184

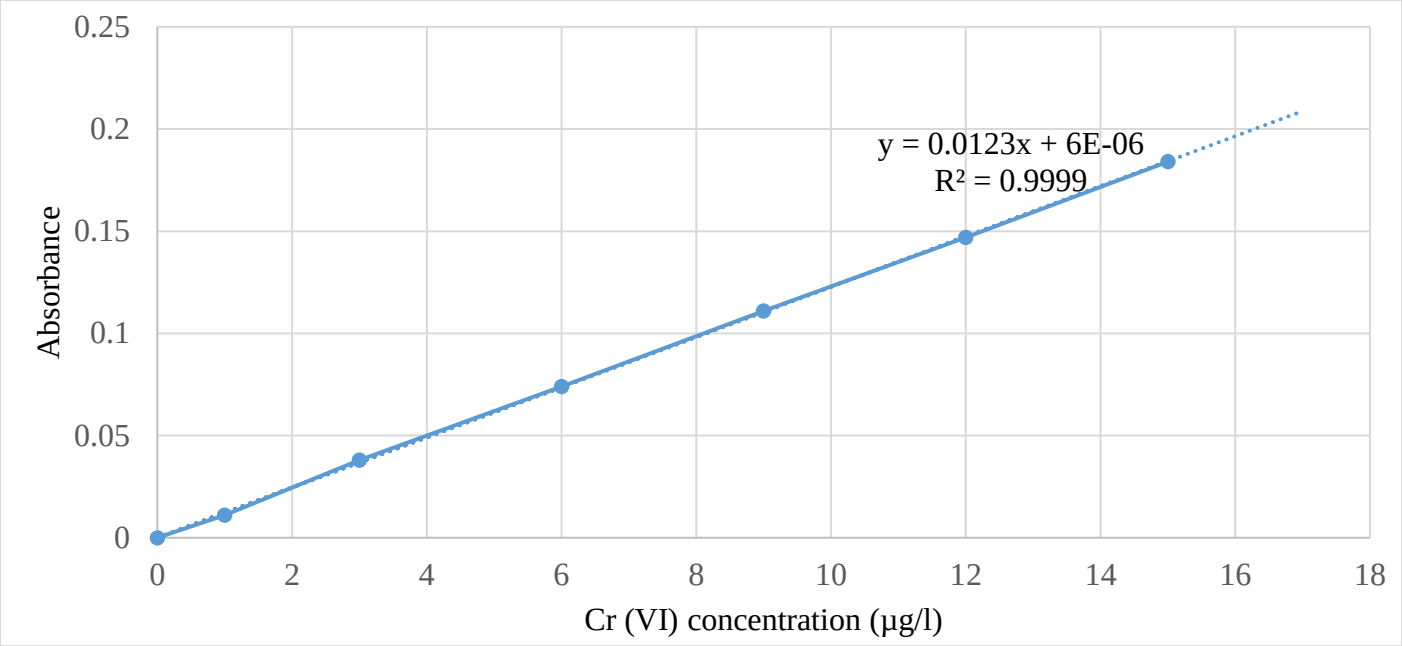

Figure 4.43: Calibration curve for Cr (VI) UV-VIS determination

The R^2 being 0.999, it's evident that the graph follows the Beer-Lambert law very closely. From figure 4.44, the limits of detection and quantification were determined to be 0.2872487 and 0.0948 mg/kg, respectively.

Table 4.13: Absorbance of post tanned crusts (132 hrs. UV+24 hours at 80 ºC)

		Without ABM & carrageenan		**With ABM & carrageenan**	
		Control	**Aged**	**Control**	**Aged**
Tanned	With DPC (A_1)	0.046	0.048	0.039	0.023
	Without DPC (A_2)	0.046	0.047	0.039	0.023
Retanned	With DPC (A_1)	0.033	0.033	0.072	0.071
	Without DPC (A_2)	0.023	0.017	0.072	0.071
Dyed	With DPC (A_1)	0.058	0.022	0.047	0.058
	Without DPC (A_2)	0.058	0.017	0.047	0.058
Fatliquored	With DPC (A_1)	0.036	0.078	0.022	0.035
	Without DPC (A_2)	0.036	0.067	0.022	0.035

Table 4.14: Calculated values of Cr (VI) (mg/kg)

Sample	Without ABM and carrageenan		With ABM and carrageenan	
	Control	**Aged**	**Control**	**Aged**
Tanned	0.00	18.3	0.00	0.00
Retanned	183	292.7	0.00	0.00
Dyed	0.00	91.46	0.00	0.00
Fatliquored	0.00	201.2	0.00	0.00

For the control (non-aged) post tanned crusts, only retanned crust recorded a detectable Cr (VI) concentration of 183 mg/kg. This observation highlights a considerable effect of retanning process using chrome tanning on the levels of Cr (VI) due to autoxidation. Autoxidation is not sufficiently strong enough to break the complex bonds of Cr (III) with the carboxylic groups of collagen (Miu *et al*., 2008). However, the unbound Cr (III) in the fibres that have not chemically crosslinked with collagen fibres take part in the autoxidation (Palop *et al.*, 2008). This study employed chromium Sulphate for retanning, a case of second tanning, absorption rate is not as strong as during the first tanning process. Hence many Cr (III) salts are expected to remain suspended in the fibres without exactly crosslinking and these salts undergo autoxidation more readily to form Cr (VI) (Fuck *et al*., 2011).

After ageing the samples for 24 hours at 80 °C and 132 hours UV radiations, Cr (VI) concentrations were detected in all the samples. The amount detected was highest in retanned crust followed by fatliquored crust. In tanned crust, the Cr (VI) was only 18.3 mg/kg while in dyed crust; it was 91.46 mg/kg. The results agree with those reported by other related investigations (Font *et al*., 1998; Font *et al*., 1999; Bayramoglu *et al*., 2012). Ageing increases the free radicals that convert the Cr (III) to Cr (VI) through oxidation. It's noteworthy that retanned crust has more unreacted Cr (III) salts which offers more oxidation and hence more Cr (VI) observed. The high pH involved in the previous stage before retanning may also contribute to high levels of Cr (VI) observed. Similarly, the presence of fatliquors which have unsaturated double bonds of carbon that increases the oxidation rate (Babu *et al*., 2005). This explains why the Cr (VI) levels were high in retanned and fatliquored crusts after ageing.

However, the Cr (VI) levels in the leather crusts processed with *Aloe barbadensis* Miller and carrageenan both aged and non-aged were below detection level. Therefore, the levels of Cr (VI) in these samples were below 0.087 mg/kg (detection limit determined form calibration curve). For all the ageing conditions conducted in this study, the effectiveness of the *Aloe barbadensis* Miller and carrageenan was demonstrated to be 100%. Using tannic acid, Colak *et al*., (2014) demonstrated that inhibitory effect improved with increase in the concentration of the acid and the levels of Cr (VI) were in the range of 1.5 to 5.3 mg/kg at concentration of 3%. Bayramoglu *et al*., (2012) used walnut leaves, hazelnut shells, olive shoots and thyme and the Cr (VI) formation rate was reduced by 45, 51, 80, and 80%, respectively on samples aged for 24 hours at 80 ºC and UV irradiation for 72 hours. Consequently, the inhibition rate of *Aloe barbadensis* Miller and carrageenan against formation of Cr (VI) as observed in this study has proven superior. The superior performance can be attributed to the high antioxidant activity due to high content of antioxidative components in the *Aloe barbad*ensis Miller such as polyphenols, indoles, alkaloids, tetradecanoic acid, methyl ester, squalene, ascorbic acid, tocopherol, campesterol and coumaric, limonene, carvone and pigments (Lakshmi *et al*., 2002; Botes *et al*., 2008; Patras *et al*., 2009; Coopoosamy, 2010; Pengseng *et al*., 2010; Lakshmi *et al*., 2011; Nejatzadeh-Barandozi, 2013; Pizzi *et al*., 2014). The catechins in the *Aloe barbadensis* Miller have the ability to reduce covalent modification of collagens induced by the reactive oxygen species (Vinson *et al*., 2001). The antioxidant activity of ABM has been determined by DPPH assay (%) to be in the range of 87.65 to 88.31 % and 65.65% of α-tocopherol (Anilakumar *et al*., 2010; Narsih *et al*., 2013; Agato, 2016). In this study, we hypothesize that the superior performance of the inhibition may have been related to the synergistic action of the compounds in both *Aloe barbadensis* Miller and carrageenan rather than a single fraction or extracts (Dagne *et al*., 2000).

This study suggests several mechanisms behind inhibiting action against the formation of Cr (VI) in leather crusts by the antioxidants in ABM and carrageenan.

a) The antioxidant components affect formation of Cr (VI) by delaying or preventing oxidation of substrate by stabilizing, deforming free radicals, or delay or prevent the oxidation of the substrate by chelating metals (Antolovich *et al*., 2002).

b) The presence of antioxidants hinders the absorption of UV radiations by the aromatic residues of collagen such as phenylalanine and tyrosine and thereby minimizing the collagen's sensitivity to UV (Metrevelli *et al*., 2010; Colak *et al*., 2014).

c) The antioxidants prevent or interfere with oxidative reactions in collagens by scavenging the free radicals and donating electrons (Gulcin *et al*., 2005; Tegtmeyer and Kleban, 2013). Scavenging free radicals and donating free electrons hinder the formation of reactive oxygen species and reverses the oxidation process (Batema *et al*., 2015). Phenolic structures in both ABM and carrageenan have hydrophobic benzoid rings and in this case, a hydrogen bond is formed between the groups N-H of collagen and C=O of antioxidants (Pereira *et al*., 2009; Metrevelli *et al*., 2010). The phenolic hydroxyl groups are good hydrogen donours which react with oxygen and reactive nitrogen species in a termination reaction, thereby breaking the cycle of generating the new radicals (Pereira *et al*., 2009). This way, the phenols inhibit the radical-mediated oxidation process and interfere with the covalent modification of the collagens already induced by the reactive oxygen species (Vinson *et al*., 2001).

The excellent antioxidant activity observed may be attributed to the varied antioxidant components in the ABM and carrageenan. All the components involve majority or all the above mechanism for superior performance.

CHAPTER FIVE
CONCLUSIONS AND RECCOMMENDATIONS

5.1 Conclusions

5.1.1 Effect of post tanning operations on the physical properties of leather

All the samples tested showed enough strength properties according to the recommended minimum tear strength, tensile strength, percentage elongation, distension at crack and burst and flexing for garment leathers, linings, and shoe upper leathers. Retanning process improves tear and tensile strengths, distensions at crack and burst, and shrinkage temperature. It also improves the organoleptic properties such as fullness and tightness. However, the uniformity coefficient and percentage elongation decreased after retanning process. Dyeing process increased the elongation at break, distensions at crack and burst, shrinkage temperature and uniformity coefficient whereas both tensile and tear strengths decreased after dyeing process. Similarly, fatliquoring increases elongation at break values, and distension values while it decreases tensile and tear strengths, shrinkage temperature and uniformity coefficient. All the samples tested at all stages of processing indicated no damage at 50,000 flexes. Among the other beneficial effects of fatliquoring, inducing tearing type of break instead of the undesirable snapping makes it a necessary process, since this type of break is desirable for quality leather that enthuses consumers.

5.1.2 Effect of *Aloe barbadensis* Miller and carrageenan on the physical properties of leather

The physical properties of control samples were not significantly different from the samples treated with *Aloe barbadensis* Miller and carrageenan. The potential to employ the two natural products to improve the organoleptic properties (sensorial characteristics) of chrome tanned leathers exists. All the properties of the samples treated with *Aloe barbadensis* Miller and carrageenan met the minimum required standards. Since both *Aloe barbadensis* Miller gel and carrageenan are biodegradables to some extent, the innovative application of these two components can be adopted by the leather industry due to their benefits to human health. Other studies can consider to work on ideal volume fraction, and particle sizes of carrageenan and *Aloe barbadensis* Miller. The *Aloe*

barbadensis Miller and carrageenan can be activated by sulphuric acids for better wetting to lower contact before being used to increase adhesion.

5.1.3 Investigating physical properties of leather treated with *Aloe barbadensis* Miller and carrageenan using existing theoretical models

The existing empirical models and semi-empirical equations appropriately predicted the strength properties of leather composites since they showed reasonable agreement with experimental data. Critical evaluation of the available theoretical and phenomenological models can be used to investigate the strengthening and weakening mechanism of fillers in leather. All models used in this study clearly indicated that adhesion strongly influenced strength properties of the resulting composites. Adhesion between *Aloe barbadensis* Miller-carrageenan and leather is poor at tanning, retanning and dyeing stage of leather manufacturing. Chemicals used at fatliquoring stage are probably the coupling agents which improve the wetting of the leather and improve the adhesion. The quantity of both *Aloe barbadensis* Miller and carrageenan to at most 3.784 % by weight of crust using Nielsen model of elongation. Fatliquoring stage is the most appropriate stage at which fillers are added into leather matrix. Effect of chromium on the filler distribution/ dispersion can also be investigated further. Parameters concerning the leather matrix irregularities and particle size are not accounted for in this study. The results also indicate that the interaction between leather matrix and *Aloe barbadensis* Miller and carrageenan is only physical. This study recommends processes such as sulphiting that can increase the surface free energy of the fillers to facilitate the work of adhesion at the interface. The study suggests use of smaller particles of *Aloe barbadensis* Miller and carrageenan in order to enhance disperibility for improved reinforcement and to avoid cracking. However, more studies are recommended to investigate the effect of particle sizes of *Aloe barbadensis* Miller and carrageenan on the adhesion and stress concentration in leather crusts.

5.1.4 Effect of post tanning operations on the molecular structure of leather

Principal component analysis showed to be useful in identifying the small structural differences among post tanned crusts. The observed differences in the spectra of post tanned crusts indicates structural alterations in the crusts, implying the establishment of new supramolecular arrangements within the matrix. The observed shifts in amide band positions indicate that triple helical structure

of collagen participated in the crusting operations. Post tanned crusts are carboxylate and amide compounds. Tanned crust has both intact triple helical contents and disrupted random coil chains but exhibited more content of alpha-helix structure as compared to the random coil structures. During retanning process, all the random coils chains and some triple helical structures took part in the crosslinking action. Retanning process dehydrates the crusts that alter the bonds and hence frequency of vibration. Retanning also aligns the helices or the molecules. Retanning causes structural and conformational alterations involving collagen reorientation or fibre ordering and rearrangement into stretching. The rearrangement of the helical structure tends to reverse the disruption caused by the previous processes due to increased crosslinking within or between triple helices. The dye components reacted with the carbonyl and nitrogen in the collagen hence reducing the number of groups of the amine group that take part in the C-N-H bending. The hydrophobicity effect of dyeing process mimics dehydration of the crust. Similarly, dyeing process reverses the crosslinking action. Dyeing process introduces new bonds as seen by emergence of new bands and peaks. The effect of dyes on the crusts structure is greatly related to the stronger absorptions and chemisorption of the dye molecules such as phenyl-OH modes. The intensity ratio increased retanning process and thereafter it decreased and dyeing and fatliquoring processes. The FWHM of the crust decreased after retanning process and thereafter increased after dyeing and finally decreased slightly after fatliquoring process.

5.1.5 Effect of *Aloe barbadensis* Miller and carrageenan on the molecular structure of leather

Treatment of the crust with ABM and carrageenan elevated the concentrations of most bonds and also slightly shifted the position of the frequency implying minor structural alterations. The triple helical structure was partially transformed into random coil structures. This was supported by higher full width at half maximum showing bending of molecular kinks indicating induced disorderliness, lower crystallinity and decomposed skeletal structures. It was also found that the incorporation affects both the primary and secondary structures. The intensity in all the treated crust spectra was higher than the intensity in the control spectra intensity implying that the carrageenan and ABM additives introduce extra absorbing molecules that increase the intensity due to the change in the supramolecular structure. Similarly, the functional groups in the leather are similar to those in ABM and carrageenan. As antipated, the spectrum of the treated crusts

contained all the bands that belong to collagen, ABM and carrageenan. Discrimination of the treated crust from the non-treated crust is influenced by protein structure and a range of other bonds. The stage of processing at which incorporation of the ABM and carrageenan is done plays a major role in determining the molecular structure. The results suggest that interaction of ABM and carrageenan with leather at post tanning operations is majorly physical with minor interaction involving hydrogen bonding and sulphur. In this case, the particles squeeze themselves between the collagen fibrils. Due to the oily nature of ABM, the physical interaction is justified by the improvement of the organoleptic properties such as softness, the enhanced sliding of the fibril against each other. The incorporation increases the sulphur content originating from ABM and carrageenan. Raman spectroscopy can successfully distinguish treated samples from the untreated samples. For the ABM and carrageenan molecules to completely react with collagen, the incorporation can be done before tanning in order for the molecules to fully interact with the collagen since the complexes formed by the tanning agents are usually very strong and leave the crust stable both mechanically and chemically. ABM being humectant, its effect on the molecular structure of crusts may be attributed to the hydrogen bonding. The hydration of the crust leads to unfolding of the kinks that cause frequency change. The study concludes that the interaction of ABM and carrageenan with the crust is majorly physical in nature as evidenced by increased intensity of the peaks. The minor chemical interaction result from crosslinking action with the OH bonding.

5.1.6 Effect of post tanning operations on the elemental compositions and concentrations of leather

The abundance of the elements in all the leather crusts was in the order Cr > S > Na > Cl > Al > Si> Ca > V > K > P > Zr > Zn >Fe > Mn >As > Ti > Cu > Pb > Ni > Ga > Br > Hg. The concentration levels for majority of the elements in all the crusts were higher than the recommended minimum for many applications. Combination of EDXRF and multivariate statistical analysis have shown to be vital in the leather industry to monitor chemical concentration. A combination of Cu and RX9 secondary targets exhibited sufficient and excellent excitation efficiency for majority of the elements detected in leather crusts. The valuable tracers for classification in the post tanning operations are Cr, S, Cl, P, V, K, Mn and Zn. Retanning increases

sulphur and copper elements in the crusts while decreasing the levels of Cl. Dyeing and fatliquoring processes raise the concentrations of sulphur in leather crusts while decreasing Cl.

5.1.7 Effect of *Aloe barbadensis* Miller and carrageenan on the elemental compositions and concentrations of leather

The PCA has shown to be handy in studying elemental composition of leather. Samples treated with the mixture possesses higher concentrations of S, K, Ca, V, Fe and Zn. The ABM and carrageenan displace the unreacted Cr suspended in the leather fibres especially at retanning and subsequent processes where the unreacted Cr are high.

5.1.8 Effect of post tanning operations on the formation of Cr (VI) in leather

The levels Cr (VI) in retanned crusts are detectably high. For tanned, dyed and fatliquored crusts, the Cr (VI) were below detection level. After artificial ageing treatment, the Cr (VI) tests were positive in all the samples. The levels were highest in retanned crusts followed by fatliquored crusts. Although the levels of Cr (VI) in dyed crusts were lowest, all the aged post tanned samples tested in this study exceeded the permissible value of extracted 3 mg/kg leather material. The study recommends a lower percentage of chromium Sulphate during chrome retanning process in order to minimize the unfixed Cr (III) and hence prevent spontaneous oxidation and minimize accelerated oxidation.

5.1.9 Effect of *Aloe barbadensis* Miller and carrageenan on the formation of Cr (VI) in leather

Autoxidation is sufficient to initiate formation of Cr (VI) in retanned crust to detectable levels due to high content of unbound Cr (III) salts. Ageing the samples for 24 hours at 80 °C and 132 hours UV radiations increased the levels of Cr (VI) in all crusts to detectable levels, the highest level recorded in retanned crusts. The levels of Cr (VI) in all the post tanned crusts were far higher than the permissible levels. Chrome tanning and fatliquors have profound influence on the concentrations of Cr (VI). The levels of Cr (VI) in leather crusts processed with *Aloe barbadensis* Miller and carrageenan, aged and unaged, were below detection level. The formation of Cr (VI) in leather should not be considered as a definitive barrier to chrome tanning technology. The study

has demonstrated that using *Aloe barbadensis* Miller mixed with carrageenan completely inhibits the conversion of Cr (III) to Cr (VI) under the ageing conditions referred to in this study.

5.2 Recommendations

The study recommends fatliquoring process since it induces a desirable tearing type of break instead the snapping type. Use of *Aloe barbadensis* Miller and carrageenan by leather industry is recommended to improve the sensorial characteristics of leather and other functional performance. Further studies are required to determine the ideal particle sizes of the ABM and carrageenan in order to improve the penetrability and distribution within the leather matrix. Smaller particles can be more appropriate to enhance reinforcement. Concerning the distribution, the study recommends activation of the ABM and carrageenan by sulphiting for improved wetting in order to lower the contact angle and increase adhesion. Other appropriate coupling agents need to be determined for adhesion and wetting back.

More studies are needful to model equations and simulations that specifically appropriate for collagen and their composites. The study suggests fatliquoring stage as the most appropriate stage of incorporation among the crusting processes. The quantity of both *Aloe barbadensis* Miller and carrageenan to at most 3.784 % by weight of crust. Other studies should consider to investigate further the influence of chromium, leather matrix irregularities and particle sizes, on the filler distribution/ dispersion.

More studies are required to determine the interaction level of *Aloe barbadensis* Miller and carrageenan with leather collagens at different stages of leather processes especially pretanning operations. The study suggests lower loading fraction of the *Aloe barbadensis* Miller and carrageenan to minimize randomizing structural alteration and weakening the physical strength of the leather. The study suggests lower amount of Cr (III) used at retanning process to minimize the amount of unbound Cr (III) in retanned crust and the subsequent crusts that easily get converted to Cr (VI) through autoxidation. Additional studies are required to investigate the existence of the synergistic action between ABM and carrageenan and among the whole components of ABM.

REFERENCES

Abba, H., Musa, H. and Ado, A. (2013). Comparative Properties of Pure and Sulphonated Dyes Extracted from Henna (*Lawsonia inermis* (Linnaeus) and Kolanut (*Cola nitida* (Vert.) Schott & Endl.) plants. *Ife journal of Science*, **15** (3), 429-434.

Abbas, M., Rahman, M.A. and Safdar, A. (2012). Detection of Heavy Metals Concentration Due to Leather Tanning Industry and Prevalent Disease Pattern in Kasur. *Pakistan, Environment and Urbanization ASIA*, **3**(2) 375–384.

Abbott, L.C., Batchelor, S.N., Lindsay, S.J.R. and Moore, J.N. (2010). Resonance Raman and UV-visible spectroscopy on textiles, *Forensic Sci*. Int. **202**, 54-63.

Adzu, B., Abbah, J., Vongtau, H. and Gamaniel, K. (2003). Studies on the use of *Cassia singueana* in malaria ethnopharmacy. *Journal of Ethnopharmacology*, **88** (2-3), 261–267.

Affiang, S.D., Ggamde, G., Okolo, V.N., Olabode, V., Jekada, J.Z. (2018). Synthesis of Sulphated-Fatliquor from Neem (Azadirachta Indica) Seed Oil for Leather Tannage. *American Journal of Engineering Research (AJER)*, **7**(4), 215-221.

Afzal, M., Al-Hussan, J.M. and Mohammed, N. (1980). Flavone glycosides from Lawsonia inermis. *Heterocycle*, **14**, 1973-1976.

Agarry, O.O., Olaleye, M.T. and Bello-Michael, C.O. (2005). Comparative antimicrobial activities of Aloe vera gel and leaf. *African Journal of Biotechnology*, **4**, 1413-1414.

Agato, N. (2016). Evalauation of bioactive compounds of aloe vera extract using sub-critical water method. *Biotechnology*, **12**(3), 113-120.

Aguayo, T., Garrido, C., Clavijo, R.E., Gomez-Jeria, J.C., Monasterio, C.A., Icaza, M., Moraga, F.E. and Vallette, M.M.C. (2013). Raman and surface enhanced Raman scattering of a black dyed silk. *Journal of Raman Spectroscopy*, **44**, 1238–1245.

Akinci, G., Dikmelik, Y. and Kaman, Y.N. (2013). *Composting and Beneficial Use of Tannery Wastewater Treatment Sludges*. Conference: XXXII. Congress of UILTCS, Istanbul, Turkey, 1-8.

Akkus, O., Addar, F. and Schaffler, M.B. (). Age-related changes in physiochemical properties of mineral crystals are related to impaired mechanical function of cortical bone. *Bone*, **34**, 443-2004453.

Ali, A.E.H., Gasmelseed, G.A., and Ahmed, A.H. (2016). Utilization of Improved Indigenous Tannins of Grain Powder (*Acacia Nilotica*) in Eco Friendly Tannage. *International Journal of Multidisciplinary and Current research*, **4**, 14-20.

Ali, S.B., Haroun, H.E. and Musa, A.E. (2013). Haraz Bark Powder Extract for manufacture of Nappa upper leather as alternative retanning agent. *Journal for production and Industry*, **2**(5), 25-29.

Aloy, M., Folachier, A. and Vulliermet, B. (1976). *Tannery and pollution*. Centre Technique D Cuir, Lyon, France, 230-260.

Amir, M., Mujeejb, M., Khan, A. (2012). Phytochemical analysis and in vitro antioxidant activity of Uncaria gambier. *International Journal of green pharmacy*, **6**, 67-72.

Anderyeva, O. and Maistrenko, L. (2014). The investigation of new polymeric compounds for leather treatments. *Acta Technica corviniensis Bulletin of Engineering, VII Fascicule*, **2**, 23-26.

Anilakumar, K.R., Sudarshanakrishna, K.R., Chandramohan, G., Ilaiyaraja, N., Khanum, F. and Bawa, A.S. (2010). Effect of Aloe vera (L.) gel extract on antioxidant enzymes and azoxymethane-induced oxidative stress in rat. *Indian Journal of Experimental Biology*, **48**, 837-842.

Anitha, T. (2012). Medicinal plants used in skin protection. *Asian Journal of Pharmaceut Clinical Research*, **5** (3), 35-38.

Antolovich, M., Prenzler, P.D., Patsalides, E., McDonald, S., Robards, K. (2002). Methods for testing antioxidant activity. *The Analyst,* **127**, 183-198.

Aquilar-Gavez, A., Noratto, G., and Chambi, F. (2014). Potential of tara (Caesalpinia spinosa) gallotannins and hydrolysates as natural antibacterial compounds. *Food Chemistry*, **156**, 301-304.

Aravindhan, R., Madhan, B. and Rao, R.J. (2015). Studies on Tara-Phosphonium Combination Tannage: Approach towards a Metal Free Eco-Benign Tanning System. *Journal of American Leather and Technologists Association*, **110**, 80-88.

Ashebre, A.M. (2014). Performance of Leather Uppers of Local Footwear products and the Determinants. *International Journal of Advancements in Research & Technology*, **3**(3), 26- 30.

Aslan, A. (2009). Determination of Heavy Metal Toxicity of Finished Leather Solid Waste. *Bulletin of Environmental Contamination and Toxicology*, **82**, 633–638 DOI 10.1007/s00128-009-9656-1.

Attenburrow, G.E. (1993). The rheology of leather-A review. *Journal of Society of Leather Technologists and Chemists*, 77, 107.

Babu, N.K.C., Asma, K., Raghupathi, A., Venba, R., Ramesh, R. and Sadulla, S. (2005). Screening of Leather Auxiliaries for their Role in Toxic Hexavalent Chromium Formation in Leather Posing Potential Health Hazard to the Users. *Journal of Cleaner Production*, **13**(12), 1189-1195.

Bacardit, A., Burgh, S., Armengol, J. and Olle, L. (2014). Evaluation of a new environment friendly tanning process. *Journal of Cleaner Production*, **65**, 568-573.

Badar, Z., Khan, S., Ahmed, S. and Choudhary, M.I. (2017). Enhanced production of aloe mannan using plant technology. *International journal of Biotech and Bioengineering*, **3**(9), 307-325.

Baeten, V., Hourant, P., Morales, M.T. and Aparicio, R. (1998). Oil and Fat Classification by FT-Raman Spectroscopy. *Journal of Agricultural Food and Chemistry,* **46**, 2638-2646.

Bajza, Z. and Vrcek, I.V. (2001). Fatliquoring agent and drying temperature effects on leather properties. *Journal of materials science*, **36**, 5265-5270.

Balasubramanian, S. and Pugalenthi, V. (1999). Determination of total chromium in waste watter by inductive coupled plasma-atomic emission spectrometry, flame atomic absorption spectrometry and Uv-visble spectrophotometric methods. *Talanta,* **50**, 457.

Bandekar, J. (1992). Amide modes and protein conformation. *Biochimica Biophysica Acta*, **1120**, 123–143.

Baranska, H., Labudzinska, A., Terpinski, J. (1987). *Laser Raman Spectrometry: Analytical Applications*. Ellis Horwood: Chichester, U.K.

Basil-Jones, M.M., Edmonds, R.L., Cooper, S.M., Kirby, N., Hawley, A. and Haverkamp, R.G. (2013). Collagen Fibril orientation and tear strength across ovine skins. *Journal of Agricultural food and Chemistry*, **61**(50), 1227-1233.

Basil-Jones, M.M., Edmonds, R.L., Norris. G.E., Haverkamp, R.G. (2012). Collagen fibril alignment and deformation during tensile strain of leather: A small-angle X-Ray scattering study. *Journal of Agricultural Food and Chemistry*, **60** (5), 1201-1208.

Batema, G., Behr, D.V., and Driesten, S.V. (2015). Oxidation stability of fatliquors; preventing the formation of Cr VI on leather, XXXIII IULTCS Congress, Nov 24-27, Novo Hamburgo/Brazil, 143-149.

Bayramoglu, E.E. (2007). Unique biocide for the leather industry; essential oil of Oregano. *Journal of American Leather and Chemical Association*, 102 (11), 347-352.

Bayramoglu, E.E., Gulumser, G. and Karaboz, I. (2006). Ecological and Innovative Fungicide for Leather Industry: Essential Oil of *Origanum minutiflorum. Journal of American Leather and Chemists Association*, 101 (3) 96-104.

Bayramoglu, E.E., Korgan, A., Kalender, D., Gulumser, G., Okcu, B. and Kilic, E. (2008). Elimination of free formaldehyde in leather by *Vinca rosea* and *Camellia sinensis* extracts. *Journal of American Leather and Chemists Association,* **103** (3), 119-123.

Bayramoglu, E.E., Onem, E. and Yorgancioglu, A. (2012). Reduction of Hexavalent Chromium Formation in Leather with Various Natural Products (*Coridothymus capitatus, Olea europaea, Corylus avellana,* and *Juglans regia*). *Ekoloji*, **21** (84), 114-120.

Bechoff, B., Kanngierfer, B., Weddel, R., Wolf, H. and Langoff, N. (2006). *Practical X-Ray Flourescent Analysis*, springer, Berlin.

Beghetto, V., Zancanaro, A., Scrivanti, A., Matteoli, U. and Pozza, G. (2013). The Leather Industry: A Chemistry Insight Part I: An Overview of the Industrial Process. *Sciences at ca' foscari,* **DOI: 10.7361/SciCF-448.**

Bella, J., Brodsky, D.B. and H.M. (1995). Berman, Hydration structure of a collagen peptide. *Structure,* 3, 893-906.

Berhanu, T. and Ratnapandian, S. (2017). Extraction and optimization of natural dye from Hambo Hambo (Cassia singueana) plant for coloration of tanned leather materials. A*dvances in materials science and engineering,* 2017, Article ID 75164095 pages.

Bicchieri, M., Monti, M., Piantanida, G., Pinzari, F. and Sodo, A. (2011). Non-destructive spectroscopic characterization of parchment documents. *Vibrational Spectroscopy,* **55**, 267–272.

Bielak, E. and Sygula-Cholewinska, J. (2017). Antimicrobial effect of lining leather fatliquored with the addition of essential oils. *Biotechnology and Food Science,* **81** (2), 149-157.

Bigg, D.M. (1987). Mechanical properties of particulate filled polymers. *Polymer Composite*, **8**, 115–22.

Bitlisli, B.O., Basaran, B., Sari, O, Aslan, A. and Zengin, G. (2004). Some physical and chemical properties of ostrich skins and leathers. *Indian Journal of chemical Tecnology*, 11, 654-658

Bitlisli, B.O., Yasa, I., Aslan, A., Cadırcı, B.H. and Basaran, B. (2010). Physical and antimicrobial characteristics of *Aloe vera* treated split suede leather. *Journal of American Leather and Chemistry Association*, **105**, 34–40.

Bordingnon, S., Gutterres, M., Velho, S.K., Fuck, W.F., Schor, A.V., Cooper, M. and Bresolin, L. (2012). Novel Natural Dyes for Eco-Friendly Leather Articles. *Journal aqeic*, 63, 93-100.

Botes, L., van der Westhuizen, F.H. and Loots, D.T. (2008). Phytochemical contents and antioxidant capacities of two Aloe greatheadii var. davyana extracts. *Molecules*,13, 2169-2180.

Bozec, L. and Horton, M. (2005). Topography and mechanical properties of single molecules of type I collagen using atomic force microscopy. *Biophysical Journal*, 88, 4223-4231.

Brereton, R.G. (2003). *Chemometrics: Data analysis for the laboratory and chemical plant*. John Wiley & Sons, Bristol.

Brinckmann, J, (2005). Collagens at a glance. *Top. Curr. Chem*, **247**, 1-6.

Brown, E.M. (2013). Development and utilization of a bovine type I collagen microfibril model. *International journal of Biological macromolecules*, **53**, 20-25.

Bryant, F.B. and Yarnold, P.R. (2010). *Principal-components analysis and exploratory and confirmatory factor analysis.* Washington, DC: American Psychological Association. 99-136.

Budrugeac, P., Trandafir, V. and Albu, M.G. (2003). The Effect of the Hydration Degree on the Hydrothermal and Thermo-Oxidative Stability of Some Collagenous Matrices. *Journal of Thermal Analysis and Calorimetry*, **72**, 581–585.

Buggy, M., Bradley, G. and Sullivan, A. (2005). Polymer–filler interactions in kaolin/nylon 6, 6 composites containing a silane coupling agent. *Composite Part A*, **36**, 437–42.

Candar, V, Eryasa, Y. and Reetz, I. (2008). Cr (VI) formation and prevention in leather Processing-Proposals for more convenient leather production. *Journal of Leather Science*, **4**, 2-9.

Cannot, J.C., Blanc, N., Fontaine, M. and Demesmay, C. (2016). *Study of the variation of chromium VI content inside the leather used in footwear.* International technical footwear congress, February 03-05, 2016, Chennai, India.

Carneiro, S., Almieda, M.F. and Ferreira, M.J. (2003). Factors influencing Chromium recovering from Chromium Sulphate tanned leather scrap. *Journal of the society of leather techologists and chemists*, **87**, 1-10.

Cassano, A., Drioli, E., and Molinari, R. (2001). Recovery and reuse of chemicals in unhairing, degreasing and chromium tanning processes by membranes. *Desalination*, **113**, 251.

Cattell, R.B. (1966). The scree test for the number of factors. *Multivariate Behavior Research,* **1**(2), 245-276.

Cesaratto, A., Centeno, S.A., Lombardi, JR, Shibayama N and Leona M (2017). A complete Raman study of common acid red dyes: application to the identification of artistic materials in polychrome prints, J. Raman Spectrosc, 48, 601–609

Chahine, C. (2000). Changes in hydrothermal stability of leather and parchment with deterioration: a DSC study. *Thermochimica Acta*, **365**, 101-110.

Chen, S.C. and Chung, K.T. (2000). Mutagenicity and antimutagenicity studies of tannic acid and its related compounds. *Food and Chemical Toxicology*, **38**, 1–5.

Chhabra, S., Mahunnah, R.L.A., Mushiu, E.N. (1987). Plants used in traditional medicine in eastern Tanzania. I. Pteridophyles and Angiosperms (Acanthaceae to Canellaceae). *Journal of Ethnopharmacology*, **21**, 253– 277.

Church, J.S., Corino, G.L., Woodheada, L. (1998). The effects of stretching on wool fibres asmonitored by FT-Raman spectroscopy. *Journal of Molecular Structure,* **440**, 15–23.

Colak, S.M. (2006). Soaking with Tannins: The Biocidal Activity of Vegetable Tannins Used in the Soaking Float. *Journal- Society of Leather Technologists and Chemists*, **90**, 193-196.

Colak, S.M., Dandar, U., Kilic, E. (2014). Antioxidant Effect of Tannic Acid on Formation of Formaldehyde and Hexavalent Chromium Compounds in Leather. *Tekstil ve Konfeksiyon,* **24** (1), 105-110.

Colak, S.M., Yapici, B.M. and Yapici, A.N. (2010). Determination of antimicrobial activity of tannic acid in pickling process. *Romanian Biotechnological Letters,* **15**(3), 5325-5330.

Congzheng, Y., Pengjie, L., Genxing, S. and Liming, D. and Huijun, R. (2005). The influence of relative humidity on the level of Cr (VI) in chrome-tanned leather. *Journal of the Society of Leather Technologists and Chemists*, **89**, 194-198.

Contini, M., Baccelloni, S., Massantini, R. and Anelli, G. (2008). Extraction of natural antioxidants from hazelnut (Corylus avellana L.) shell and skin wastes by long maceration at room temperature. *Food Chemistry*, **110** (3), 659-669.

Cook, N.C. and Samman, S. (1996). Flavonoids—Chemistry, metabolism, cardioprotective effects, and dietary sources. *The Journal of Nutritional Biochemistry*, **7**(2), 66–76. DOI:10.1016/0955-2863(95)00168-9.

Coopoosamy, R.M. (2010). Isolation of volatile compounds of Aloe excelsa (Berger). *African Journal of Biotechnology*, **9** (43), 7289-7294.

Covington AD (2009). *Tanning Chemistry-The Science of Leather*. The Royal Society of Chemistry, Cambridge.

Covington AD (2011). *Tanning chemistry*. RSC Publishing, Cambridge.

Covington, A.D. (1997). Modem tanning chemistry. *Chemical Society Reviews,* **26** (2), 111-126.

Covington, A.D. and Alexander, K.T.W. (1993). The Production of Soft Leather Part 1. The Mechanism of Chemical Softening by Lubrication. *Journal of American Leather Chemists Association*, **88**, 241-53.

Dagne, E., Bisrat, D., Viljoen, A. and Van, W.B.E. (2000). Chemistry of *Aloe* species. *Curr. Org. Chem*, **4**, 1055-1078.

Dan'Azumi, S. and Bichi, M.H. (2010). Industrial pollution and heavy metals profile of Challawa River in Kano, Nigeria. *Journal of Applied Sciences in Environmental Sanitation*, **5**(1), 23-29.

Danusso, F. and Tieghi, G. (1986) Strength versus composition of rigid matrix particulate composites. *Polymer*, **27**, 1385–90.

Das, D., Maulik, S.R., Bhattacharya, S.C. (2007). Dyeing of wool and silk with Bixa orellana. *Indian Journal of Fibre Text and Research,* **32**, 366–372.

Das, P.K., DesLauriers, P.J., Fahey, R., Wood, F.K. and Coruforth, F.J. (1994). Photo stabilization of poly (p-phenylene sulfide). *Polymer Degradation and Stability*, **48**, 1 – 10.

de Volder, N., Hallmanns, M. and Levy, J. (2007). *Annoying energy. II. Solar heating of dark leather*, in "Proceedings of the XXIX International Union of Leather Technologists and Chemists Societies Congress", Washington.

Dehring, K.A., Smukler, A.R., Roessler, B.J. and Morris, M.D. (2006). Correlating Changes in Collagen Secondary Structure with Aging and Defective Type II Collagen by Raman Spectroscopy. *Applied Spectroscopy,* **60**(4), 2006.

Derrick, M. (1991). *Evaluation of the state of degradation of Dead Sea scroll samples using FT-IR spectroscopy.* The Book and Paper specialty group session, AIC 19th Annual Meeting, Albuquerque, New Mexico.

Devikavathi, G., Suresh, S, Rose, C. and Muralidharan, C. (2014). Prevention of carcinogenic Cr (VI) formation in leather- a three pronged approach for leather products. *Indian Journal of Chemical Technology*, **21**, 7-13.

Diebschlag, W. (1975). Measurements of the elasticity of different shoe upper materials as well as their maximum pressure on the foot during walking. *Leder*, 26, 7-18.

Diharmi, A., Fardiaz, D., Andarwulan, N. and Heruwati, E.S. (2017). Chemical and physical characteristics of carrageenan extracted from Eucheuma spinosum harvested from three different Indonesian coastal sea regions. *Hycological Research*, **65**, *256–261*.

Ding, K., Taylor, M.M. and Brown, E.M. (2008). Tanning effects of aluminum- Genipin or vegetable tannin combinations. *Journal of American Leather and chemists Association*, **103**, 377-382.

Dixit, S., Yadav, A., Dwivedi, P.D. and Das, M. (2015). Toxic Hazards of Leather Industry and Technologies to Combat Threat: A Review. *Journal of Cleaner Production*, **87**, 39-49.

Dolgin, B., Bulatov, V. and Schechter, I. (2007). Non-destructive assessment of parchment deterioration by optical methods. *Analytical and Bioanalytical Chem*, **DOI 10.1007/s00216-007-1410-0**

Dolgin, B., Chen, Y., Bulatov, V. and Schechter, I. (2006). Use of LIBS for rapid characterization of parchment. *Analytical and Bioanalytical Chemistry*, **386**, 1535–1541.

Dukor, R.K. (2002). Vibrational spectroscopy in the detection of cancer. *Biomedical Applications*, **5**, 3335–3359.

Dutta, S.S. (2008). *An introduction to the principles of leather manufacturing*. 4th Ed Indian Leather Technologists Association, 506-557.

Edwards, H.G., Farwell, D.W., Holder, J.M. and Lawson, E.E. (1997). Fourier-transform Raman spectra of ivory. III. Identification of mammalian specimens. *Spectrochimica Acta A Molecular and Biomolecular Spectroscopy* 53A, 2403–2409, Doi: 10.1016/S13861425(97)00180-7

Edwards, H.G.M., Farwell, D.W., Newton, E.M., Perez, F.R., Villar, S.J. (2001). Application of FT-Raman spectroscopy to the characterization of parchment and vellum, I: novel information for paleographic and historiated manuscript studies. *Spectrochimica acta part A*, **57**, 1223-1234.

Einstein, A. (1956). Investigation on Theory of Brownian motion. Dover, New York, USA.

Emsley, J., Knight, C.G., Farndale, R.W., Barnes, M.J., Liddington, R.C. (2000). Structural basis of collagen recognition by integrin $\alpha_2\beta_1$. *Cell*, **101**, 47–-56.

Engel, T., Reid, P. and Hehre, W. (2013). *Physical Chemistry*. Boston: Pearson Education.

Ervina, J., Mariatti, M., Hamdan, S. (2016). Effect of Filler Loading on the Tensile Properties of Multi-walled Carbon Nanotube and Graphene Nano powder filled Epoxy Composites. *Procedia Chemistry*, **19**, 897–905.

ESA (Ethiopian Standards Agency) (2012). The quality standards for leather and leather products, Addis Ababa, Ethiopia.

EU (2002). Directive 2002/61/EC of the European Parliament & of the Council of 19 July 2002 Amending for the Nineteenth Time Council Directive 76/769/EEC Relating to Restrictions on the Marketing & Use of Certain Dangerous Substances & Preparations (Azo Colourants).

Falcao, L., Araujo, M.E.M. (2018). Vegetable tannins used in the manufacture of historic leathers. *Molecules*, **23**, 1081.

Fathima, N.N., Aravindhan, R., Rao, J.R. and Nair, B.U. (2006). Tannic Acid-Phosphonium Combination: A Versatile Chrome-Free Organic Tanning. *Journal of American Leather and Chemists Association*, **101**, 161-168.

Fathima, N.N., Chandrabose, M., Aravindhan, R., Rao, J.R. and Nair, B.U. (2005). Iron phosphonium combination tanning: towards a win-win approach. *Journal of American Leather and Chemists Association*, **100**, 273–281.

Fathima, N.N., Rao, J.R. and Nair, B.U. (2010). Cost effective fixing process for post tanning operations. *Journal of American Leather and Chemists Association*, **105**, 100-106.

Fathima, N.N., Saravanabhavan, S., Rao, R.J. and Nair, B.U. (2004). An Eco-Benign Tanning System Using Aluminium, Tannic Acid, and Silica Combination. *Journal of American Leather and Chemists Association*, **99**, 73-781.

Flory, P.J. (1953). *Principles of Polymer Chemistry*. Cornell University Press. Ithaca, NY, Chapter 11.

FMC BioPolymer (2010). Carrageenan.

Fonseca, Y., Catini, C., Vicentini, F., Cardoso, J., Cavalcanti, D, Albuquerque, R.J. and Fonseca, V.M. (2011). Efficacy of marigold extract-loaded formulations against UV induced oxidative stress, *Journal of Pharmaceutical Science*, **100** (6), 2182–2193.

Font, J., Cuadros, R.M., Lalueza, J., Orus, C., Reyes, M.R., Costa-Lopez, J. and Marsal, A. (1998). Presence of Chromium (VI) in Sheepskins: Influence of Tannery Processes. *Journal of the Society of Leather Technologists and Chemists*, **82**(49), 91-95.

Font, J., Cuadros, R.M., Reyes, M.R., Costa-Lopez, J. and Marsal, A. (1999). Influence of various factors on chromium (VI) formation by photo-ageing. *Journal of the Society of Leather Technologists and Chemists***, 83** (6), 300-306.

Fratzl, P., Misof, K., Zizak, I., Rapp, G., Amenitsch, H. and Bemstorff, S. (1998). Fibrillar structure and mechanical properties of collagen. *Journal of Structural Biology*, **122**, 119-122.

Freeman, J.J., Wopenka, B., Silva, M.J. and Pasteris, J.D. (2001). Raman spectroscopic detection of changes in bioapatite in mouse femora as a function of age and in vitro fluoride treatment. *Calcif Tissue International*, **68**, 156-162.

Frushour, B.G. and Koenig, J.L. (1975). Raman scattering of collagen, gelatin, and elastin. *Biopolymers*, **14**, 379-391. **Doi:10.1002/bip.1975.360140211**

Fu, S.Y., Feng, X.Q., Lauke, B. and Mai, Y.W. (2008). Eff ects of particle size, particle/matrix interface adhesion and particle loading on mechanical properties of particulate-polymer composites. *Composites B*, **39** (6), 933–961.

Fuck, W.F., Gutteres, M., Marcilio, N.R. and Bordingnon, S. (2011). The influence of chromium supplied by tanning and wet finishing processes on the formation of Cr VI in leather. *Brazilian Journal of Chemical Engineering*, **28** (2), 221-228.

Garp, T., Nielsen, K., Boghosian, S. (2002) In: Larsen R (ed) *Microanalysis of parchment*. Archetype, London.

Gąsior-Głogowska, M., Komorowska, M., Hanuza, J., Ptak, M. and Kobielarz, M. (2010). Structural Alteration of Collagen Fibres– Spectroscopic and Mechanical Studies. *Acta of Bioengineering and Biomechanics, **12** (4), 55-62.*

Gauglhofer, J. (1986). Environmental aspects of tanning with chromium. *Journal of the society of Leather technologists' and chemists*, **70**, 11.

Gautieri, A., Vesentini, S., Redaelli, A., Buehler, M.J. (2012). Viscoelastic properties of model segments of collagen molecules. *Matrix Biology,* **31**, 141–149.

Gelse, K., Poschl, E. and Aigner, T. (2003). Collagens-structure, function and biosynthesis. *Advanced Drug Delivery Reviews*, **55**, 1531-1546.

Girardi, V., Calanese, G., Naviglio, B. and Zollo, F. (2013). Study on the Cr VI formation in leather after ageing.

Giurginca, M., Badea, N., Miu, L. and Meghea, A. (2007). Spectral techniques for identifying tanning agents in the heritage leather items. Reviwes chimica, **58**(9), 923-926.

Gniadecka, M., Nielsen, O.F., Christensen, D.H. and Wulf, H.C. (1998). Structure of water, proteins, and lipids in intact human skin, hair, and nail. *Journal of Investigative Dermatology*, **110**, 393–398.

Gonzalez, L. and Wess, T. (2008). Use of Attenuated Total Reflectance Fourier Transform Infrared spectroscopy to measure collagen degradation in historical parchements. *Applied spectroscopy*, **62** (10), 1108-1114.

Goodier, J.N. (1933). Concentration of Stress around Spherical and Cylindrical Inclusions and Flaws. *Journal of Applied Mechanics,* **55**, A39.

Gorshkova, K.O., Tumkin, I.I., Myund, L.A., Tverjanovich, A.S., Mereshchenko, A.S., Panov, M.S. and Kochemirovsky, V.A. (2016). The investigation of dye aging dynamics in writing inks using Raman spectroscopy. *Dyes and Pigments*, **131**, 239-245.

Granger, R.A. and Hank, Y. (2016). *Instrumental Analysis*. Kettering: Oxford UP USA.

Grasseli, J.G. and Bulkin, B.J. (1991). *Analytical Raman Spectroscopy*. Wiley: New York, 1991.

Gulcin, I., Alici, H.A. and Cesur, M., (2005). Determination of in- vitro antioxidant and radical scavenging activities of propofol. *Pharmacology Bulletin,* **53**, 281-285.

Gulcin, I., Huyut, Z., Elmastas, M., Aboul-Enein, H.Y. (2010). Radical scavenging and antioxidant activity of tannic acid. *Arabian journal of chemistry*, **3**, 43-53.

Gulrajani, M.L., Gupta, G. and Gupta, P. (2002). Application of natural dyes on bleached in wool dyeing. *Journal of Textile Association,* **63**, 119–124.

Gumel, S.M. and Dambatta, B.B. (2013). Application and evaluation of the performance of polyvinyl alcohol and it's bled with nitrocellulose in leather top coating. *International Journal of Chemical Engineering and Applications*, **4**, 4-8.

Guptha, A.K. and Purwar, S.N. (1984). Melt rheological properties of polypropylene/SEBS (styrene–ethylene butylene–styrene block copolymer) blends. *Journal Applied Polymer Sciennce,* 29, 3513.

Gussen, K.D., Vandenabeele, P., Verbeken, A. and Moens, L. (2005). Raman spectroscopic study of Lactarius spores (Russulales, fungi). *Spectrochim Acta*, **61**, 2898-2908.

Gustauson, K.H. (1956). *The structure of skin and the chemistry of collagen, in Chemistry and Reactivity of Collagen*. Academic Press: New York. 30-52.

Guth, E. (1945) Theory of filler reinforcement. *Journal of Applied Physics*, **16**, 20–25.

Gutters, M. and Santos, L.M.D. (2009). Study of Fatliquoring Parameters Using Experimental Design. *Journal of the Society of Leather Technologists and Chemists*, **93**, 171-175.

Habib, A.B., Noor, I.A. and Musa, A.E. (2015). Effect of some Skin Defects on Physical Properties of the Leather. *Journal of Applied and Industrial Sciences*, **3** (3), 112-119.

Haines, B.M. (1999). *Parchment, the physical and chemical characteristics of parchment and the materials used in its conservation*. Northampton: The Leather Conservation Centre. 1-32.

Hamman, J.H. (2008). Composition and Applications of Aloe vera Leaf Gel. *Molecules*, **13**, 1599-1616.

Haroun, M., Palmina, K., Gurshi, A. and Covington, D. (2009). Potential of Vegetable Tanning Materials and Basic Aluminum Sulphate in Sudanese Leather Industry. *Journal of Engineering Science and Technology,* **4**(1), 20 - 31.

Hassan, E.A., Ibrahim, M.T. and Sally, K.A. (2014). Optimization of Chrome Retanning Process to the Garad (Acacia nilotica) Tanned Leather. *Journal of Agricultural and Veterinary Sciences*, **15**(1), 87-94.

Hauber, C. and Buljan, J. (1999). Sources, detection and avoidance of hexavalent chromium in leather and leather products, Technical Report of UNIDO under regional programme for pollution control in the Tanning industry in South Asia.

Hauber, C. and Buljan, J. (2000). Formation, prevention and determination of Cr (VI) in leather: Regional Programme for Pollution Control in the Tanning Industry in South -East Asia by UNIDO, US/RAS/92/120, 1-7.

He, F., and Espen, P.J.V. (1991). General Approach for Quantitative Energy Dispersive X-Ray Fluorescence Analysis Based on Fundamental Parameters. Analytical Chemistry, **63** (20), 2237–2244.

He, Y., Tang, L., Wu, X., Hou, X., Lee, Y.I. (2007). Spectroscopy: The Best Way Toward Green Analytical Chemistry? Applied Spectroscopy Reviews, **42** (2), 119–138.

Hedberg, Y.S., Lidén, C., Wallinder, I.O. (2014). Correlation between bulk- and surface chemistry of Cr-tanned leather and the release of Cr (III) and Cr (VI). *Journal of Hazardous Materials*, **280**, 654–661.

Hedberg, Y.S., Lidén, C., Wallinder, I.O. (2015). Chromium released from leather – I: exposure conditions that govern the release of chromium (III) and chromium (VI). *Contact Dermatitis*, **72**, 206–215.

Heidemann, E. (1993). *Fundamentals of Leather Manufacturing*, Eduard Roether KG, Darmstadt, London.

Hoshino, A., Fujioka, K., Oku, T., Nakamura, S., Suga, M., Yamaguchi, Y., Suzuki, K. and Yasuhara, M. (2004). Quantum dots targeted to be the assigned to the organelle in living cells. *microbiology and immunology*, **48**, 985-994.

Hu, Y., Jang, I., Sinnott, S.B. (2003). Modification of carbon nanotube-polystyrene matrix composites through polyatomic-ion beam deposition: predictions from molecular dynamics simulations. *Composites Science and Technology*, **63**, 1663 -1669.

Huang, Y.F. and Meek, K.M. (1999). Swelling studies on the cornea and sclera: the effects of pH and ionic strength. *Biophysics journal*, **77**, 1655-1665.

Huang, Z.W., McWilliams, A., Lui, H., McLean, D.I., Lam, S. and Zeng, H.S. (2003). Near infrared Raman spectroscopy for optical diagnosis of lung cancer. *International Journal Cancer*, **107** (6), 1047–1052.

Hui, C., Jun, G. and Zhi-Hua, S. (2010). A Cleaner Chrome-Free Tanning Regime: Sulfonated Urea-Phenol Formaldehyde Condensed Polymer and Ferrous Sulfate Tanning. *Journal American Leather and Chemists Association*, **105**, 18-24.

Hulmes, D.J.S. (2002). Building Collagen Molecules, Fibrils, and Suprafibrillar Structures. *Journal of Structural Biology*, **137**, 2-10.

Hussein, S.A. (2017). Utilization of Tannins Extract of Acacia seyal Bark (Taleh) in Tannages of Leather (2017). *Journal of Chemical Engineering & Process Technology*, **8**, 334, DOI: 10.4172/2157-7048.1000334.

Ibrahim, A.A., Youssef, M.S.A., Nashy, E.-S.H.A. and Eissa, M.M. (2013). Using of Hyperbranched Poly (amidoamine) as Pretanning Agent for Leather. *International Journal of Polymer Science*, **2013**, 1-8.

Ibrahim, I., Sekak, K.A. and Hesbullah, N. (2015). Preparation and characterization of chitosan/ aloe vera composite nanofiber generated by electrostatic spinning, AIP conference proceedings 1674, 020024; doi:10.1063/1.4928842.

Inanc, L. and Gulumser, G., (2015). Determination of the Effects of Splitting and Shaving Operations before Tanning at Shoe Upper Leathers on the Quality of Leather. *Tekstil ve Konfeksiyon,* **25**(4), 365-370.

INESCOP (Center for Technology and Innovation), (2013). http://www.manual for Oxazolidine Tanned Leather: Environmentally Friendly Oxazolidine-Tanned Leather (LIFE08 ENV/E/000140).com. Accessed on June 21, 2013.

Islam, S., Masoodi, R., Rostami, H. (2013). The Effect of Nanoparticles Percentage on Mechanical Behavior of Silica-Epoxy Nanocomposites. *Journal of Nanoscience,* **2013**, 1-10.

ISO 17075: 2007. Method for determining Cr (VI) in solutions leached from leather under defined conditions. The method described is suitable to quantify the Cr (VI) content in leathers down to 3 mg/kg.

ISO 2418:2002. Leather-Sampling for Physico-mechanical and Fastness Tests-sampling Location, Geneva, Switzerland Test.

ISO 2419: 2002. Leather – Conditioning of Test pieces for Physical Tests.

ISO 2589:2002. Determination of leather thickness-IULTCS

ISO 3376:2002. Leather Physical and Mechanical Tests. Determination of Tensile Strength and Percentage Extension.

ISO 3380:2005. Physical and mechanical tests. Determination of shrinkage temperature up to 100 °C.

ISO 3696: Water for analytical laboratory use- Specification and test methods

ISO 4044: Leather- Chemical tests- Preparation of chemical test samples

Iyer VG and Mastorakis NE (2006). Assessment of pollution load from unsafe leather tanneries in India. *WSEAS Transactions on Environment and Development*, **2**, 207-215.

Jacinto, M.A.C., Sobrinho, D.S.A.G. and Costa, R.G. (2004). Anatomic and structural characteristics of wool and non-wool sheep (*Ovis aries* L.) in regard to the physico-mechanical aspects of the leather. *Brazilian Journal of Animal Science*, **33** (4), 1001–1008.

Jadhao, N.U. and Rathod, S.P. (2013). The extraction process and antioxidant properties of patuletin dye from wasted temple French marigoldflower. *Asian Journal of Plant Science and Research*, **3**(2), 127-132.

Jagetia, G.C., Lalhmangaihi, C. (2018). Phytochemical profiling and antioxidant activity of Lajwanti mimosa pudica Linn. In vitro. *International journal of plant studies*, **1**, 1-13.

Jankauskaite, V., Jiyembetova, I., Gulbiniene, A., Sirvaityte, J., Beleska, K., Urbelis, V. (2012). Comparable Evaluation of Leather Waterproofing Behaviour upon Hide Quality. I. Influence of Retanning and Fatliqouring Agents on Leather Structure and Properties. *Materials Science (Medziagotyra)*, **18** (2), 150-158.

Janko, M., Davydovskaya, P., Bauer, M., Zink, A., Stark, R.W. (2010). Anisotropic Raman scattering in collagen bundles. *Optics Letters*, **35**, 2765–2767.

Jastrzebska, M., Wrzalik, R., Kocot, A., ZalewskaRejdak, J. and Cwalina, B. (2003). Raman spectroscopic study of glutaraldehyde-stabilized collagen and pericardium tissue. Journal of Biomaterials Science. *Polymer Edition*, **14(**2), 185-197, DOI: 10.1163/156856203321142605.

Jian, Z., Shuxiang, H., Yanan, W., Qiang, H., Xueping, L., Wenhua, Z., Bi, S. (2012). Release of Chrome in Chrome Tanning and Post Tanning Processes. *Journal of Society of Leather Technologists and Chemists*, **109**, 1-7.

Jithendra, P., Rajam, A.M., Kalaivani, T., Mandal, A.B., and Rose, C. (2013). Preparation and Characterization of Aloe Vera Blended Collagen Chitosan Composite Scaffold for Tissue Engineering Applications. *Applied Materials and interfaces*, **5**, 7291-7298.

Joseph, B. and Raj, S.J. (2010). Pharmacognostic and Phytochemical Properties of Aloe Vera Linn–an Overview. *International Journal of Pharmaceutical Sciences Review and Research*, **4**(2), 106-110.

Joseph, K. and Nithya, N. (2009). Material flows in the life cycle of leather. *Journal of Cleaner Production,* **17**, 676–682.

Jun, M., Zonghui, L. and Deqing, W. (1998). The rheological study on the structure and property of leather. *China Leather*, **27**(11), 1-3.

Kadler, K.E., Holmes, D.F., Trotter, J.A. and Chapman, J.A. (1996). Collagen fibril formation. *Journal of Biochemistry*, **316**, 1-11.

Kalaprasad, G., Joseph, K., Thomas, S., and Pavithran, C. (1997). Theoretical Modelling of Tensile Properties of Short Sisal Fibre-Reinforced Low-Density Polyethylene Composites. *Journal of Materials Science,* **32**, 4261-4267.

Kanagaraj, J., Babu, N.K. and Mandal, A.B. (2008). Recovery and reuse of chromium from chrome tanning wastewater aiming towards zero discharge of pollution. *Journal of Cleaner Production,* **16**, 1807-1813.

Kanagaraj., J., Velappan, K.C., Babu, N.K.C. and Sadulla, S. (2006). Solid wastes generation in the leather industry and its utilization for cleaner environment-a review. *Journal of Scientific and Industrial Research*, **65**, 541-548.

Kaniu, M.I., Angeyo, K.H., Mangala, M.J., Mwala, A.K. and Bartilol, S.K. (2011). Feasibility for chemometric energy dispersive X-ray fluorescence and scattering (EDXRS) spectroscopy method for rapid soil quality assessment. *X-Ray spectrometry*, **40**, 432-440.

Kapel, M., and Speak, A. (1979). The rapid determination of Iron, Chromium, Zirconium and Aluminium in leather. *Journal of the society of leather technologist and chemists,* **63**, 89-92.

Kassama, L.S., Kuponiyi, A.J. and Kuthtareva, T. (2015). Comparative effects of aloe vera (*Aloe barbadensis*) water verus ethanol extracts on the physico-chemical properties and stability of silver nanoparticles synthesize. *American international journal of contemporary research,* **5** (2), 30-39.

Kataoka, Y. (1989). Standardless X-Ray Fluorescence Spectrometry (Fundamental Parameter Method using Sensitivity Library). *The Rigaku journal,* **6** (1), 33-39.

Kataoka, Y., Kawahara, N., Hara, S., Yamada, Y., Matsuo, T. and Mantler, M. (2005). *Advances in X-ray analysis*, **40**, 255-260.

Kavkler, K. and Demsar, A. (2012). Application of FTIR and Raman Spectroscopy to qualitative analysis of structural changes in cellulosic fibres. *Tekstilec*, **55**, 19-31.

Kennedy, C.J. and Wess, T.J. (2003). The structure of collagen within parchment-a review. *Restuarator-international journal of preservation of library and archival material*, **24**, 61-80.

Kesarwani, P., Jahan, S. and Kesarwani, K. (2015). A Review on Leather Processing. *International Journal of Applied Research*, **1**(9), 977-982.

Khan, A.A., Iqbal, N., Adeel, S., Azeem, M., Batool, F. and Bhatti, I.A. (2014). Extraction of natural dye from red calico leaves: Gamma ray assisted improvements in colour strength and fastness properties. *Dyes Pigments*, **103**, 50–54. DOI: 10.1016/j.dyepig.2013.11.024.

Khanbabaee, K. and van Ree, T. (2001). Tannins: classification and definition. *Natural Product Rep*, **18**, 641-649.

Khilfi, S., Hachimi, E., Khalil, A., Es-Safi, A., Belahyam, A., Tellal, A. and El Abbouyi, A (2006). In-vitro antioxidant properties of Salvia verbenaca. L. hydromethanolic extract, *Indian Journal Pharmacology*, **38**, 276-280.

Kikuchi, S., Kawauchi, K., Kurosawa, M., Honjho, H. and Yagishita, T. (2005). Non-destructive Rapid Analysis Discriminating between Cr (VI) and Cr (III) Oxides in Electrical and Electronic Equipment Using Raman Spectroscopy. *Analytical Sciences*, **21** (3), 197-198.

Kizil, R., Irudayaraj, J. and Seetharaman, K. (2002). Characterization of irradiated starches by using FT-Raman and FTIR spectroscopy. *Journal of Agricultural food and chemistry*, **50**, 3912-3918.

Kocurek, P., Vaskova, H., Kolomaznik, K., and Barinova, M. (2015). Hexavalent Chromium Determination in Waste from Leather Industry Using Spectrophotometric Methods. *WSEAS Transactions on Environment and Development*, **11**, 256-263.

Kolomaznik, K., Adamek, M., Andel, I. and Uhlirova, M. (2008). Leather Waste-Potential Threat to Human Health, and a New Technology of its Treatment. *Journal of Hazardous Materials*, **160,** (2-3), 514-520.

Kolomaznik, K., Barinova, M. and Vaskova, H. (2012). Chromium VI Issue in Leather Waste - A Technology for the Processing of Used Leather Goods and Potential of Raman Spectroscopy in Chromium Traces Detection. *International Journal of Mathemats and Computers in Simulation*, **6** (5), 447-455.

Kolomaznik, K., Barinova, M. and Vaskova, H. (2012). Chromium VI issue in leather waste-a technology for the processing of used leater goods and potential of Raman spectroscopy in chromium traces detection. *International journal of mathematics and computers in simulation*, **6**(5), 447-455.

Komanowsky, M. (1990). Moisture-solid relations accompanying drying of leather. *Journal of American Leather Chemists Association*, **85**, 6–18.

Kowaiska, M. and Zbikowska, A. (2014). pH as a parameter for the exponential stability of fat liquor emulsions. *Journal of the Society of Leather Technologists and Chemists*, **98**, 23-29.

Kozar, O., Mokrousova, O. and Wozniak, B. (2014). Deformation characteristics of leather for shoe upper, filled with natural minerals. *Journal of Chemical Engineering*, **8**, 47-53.

Kramer, R.Z., Bella, J., Mayville, P., Brodsky, B. and Berman, H.M. (1999). Sequence dependent conformational variations of collagen triple-helical structure. *National Structural Biology*, **6**, 454–457.

Kramer, R.Z., Venugopal, M.G., Bella, J., Mayville, P., Brodsky, B. and Berman, H.M. (2000). Staggered molecular packing in crystals of a collagen-like peptide with a single charged pair. *Journal of Molecular Biology*, **301**, 1191–1205.

Krishnamoorthy, G., Sadulla, S., Sehgal, P.K. and Mandal, A.B. (2013). Greener approach to leather tanning process: D-Lysine aldehyde as novel tanning agent for chrome-free tanning. *Journal of Cleaner Production*, **42**, 277-286.

Krol, Z., Malik, M., Marycz, K. and Jarmoluk, A. (2016). Characteristic of Gelatine, Carrageenan and Sodium Alginate Hydrosols Treated by Direct Electric Current. *Polymers*, **8**, 275. doi:10.3390/polym8080275.

Kronick, P.L. (1996). Destabilization of Collagen in Hide Leather by Anionic Surfactants. I Differential Scanning Calorimetry of Complexes with Sulfates. *Journal of American Leather Chemists Association*, **91**, 246–251.

Kronick, P.L. and Beuchler, P.R. (1986). Fiber orientation in calfskin by laser light scattering or X-ray diffraction and quantitative relation to mechanical properties. *Journal of American Leather Chemists Association*, **81**, 221.

Kucharz, E.J. (2011). *The collagens: Biochemisry and pathophysiology*, Springer, Berlin Heidelberg.

Kumar, M.P., Fathima, N.N., Aravindhan, R., Rao, J.R., Nair, B.U. (2009). An Organic Approach for Wet White Garment Leathers. *Journal of American Leather Chemists Association*, **104**, *112-119.*

Kuria, A., Ombui, J., Onyuka, A., Sasia, A., Kipyegon, C., Kaimenyi, P., Ngugi, A. (2015). Quality Evaluation of Leathers Produced by Selected Vegetable Tanning Materials from Laikipia County, Kenya. *IOSR Journal of Agriculture and Veterinary Science (IOSR-JAVS)*, **9** (4), 13-17.

Kurouski, D., Postiglione, T., Deckert-Gadig, T., Deckert, V. and Lednev, I.K. (2013). *Analyst*, **138**, 1665-1673.

Kusumawati, F., Riyadi, P.H., Rianingsih, L. (2016). Applications Indigo (*Indigofera tinctoria* L.) as Natural Dyeing in Milkfish [*Chanos chanos* (Forsskal, 1775)] Skin Tanning Process. *Aquatic Procedia*, **7**, 92 – 99.

Lakhsmi, P.T.V. and Rajalakshmi, P. (2011). Identifcation of phyto-components and its biological activities of Aloe vera (L.) through Gas Chromatography-Mass Spectrometry. *International Research Journal of Pharmacy*, **2** (5), 247-249.

Lakshmi, R.J., Kartha, V.B., Krishna, C.M., Solomon, J.G.R., Ullas, G., and Devi, P.U. (2002). Tissue Raman spectroscopy for the study of radiation damage: Brain irradiation of mice. *Radiation Reserach*, **157** (2), 175–182.

Landmann, W. (2003). *The Machines in the Tannery, a Review of Leather Producing Machinery and Equipment in Current Use*. West Yorkshire, UK: World Trades Publishing.

Larsen, R. (2000). Experiments and observations in the study of environmental impact on historical vegetable tanned leathers. *Thermochimica Acta*, **365**, 85.

Lawson, R. (2008). *Anatomy and physiology of Animals*. Wikibooks, Dunedin, New Zealand, 2-5.

Lee, C.H., Singla, A. and Lee, Y. (2001). Biomedical applications of collagen. *Internal Pharmarcy,* **221**, 1-22.

Leidner, J. and Woodhams, R.T. (1974). Strength of polymeric composites containing spherical fillers. *Journal of Applied Polymer Science,* **18**, 1639–54.

Levita, G., Marchetti, A., Lazzeri, B. (1989). A Fracture of ultrafine calcium carbonate/ polypropylene composites. *Polymer Composite*, **10**, 39–43.

Li, Z., Paudercerf, D. and Yang, J. (2009). Mechanical behavior of natural cow leather in tension. *Acta Mechanica Solida Sinica*, **22**, 234-239.

Liang, J.Z. and Li, R.K.Y. (1933). Prediction of tensile yield strength of rigid inorganic particulate filled thermoplastic composites. *Journal of Materials Processing and Technology,* **83**, 127–30.

Liao, L.L., Chen, W.Y., Shan, Z.H., Dan, W.H. (2005a). *Tanning chemistry and technology*. Beijing: Science Press.

Liao, M.-C. (2007). *Small and Large Strain Rheological and Fatigue Characterisation of Bitumen-Filler Mastics*, Thesis submitted to The University of Nottingham for the degree of Doctor of Philosophy.

Litke, K.S., Widdemer, J.D. (2003). *Aloe vera Processed Leather and Leather Gloves, Garments, Shoes and Sandals made from Aloe vera processed Leather and a process for making Aloe vera processed Leather*. Patent Application Publication (10) Pub. No.: US 2003/0217416A1.

Liu, C.K., Aldema- Ramos, M., Latona, N.P., Latona, R.J. (2009). Leather coated with mixture of humectant and antioxidants to improve ultraviolet and heat resistance. *Journal of the American Leather Chemists Association*, **104**, 161-168.

Liu, C.K., Latona, N., Dimaio, G.L. (2002). Physical Property Studies for Leather Lubricated with Various Types of Fatliquors. *Journal of American Leather Chemists Association*, **97**, 431-440.

Liu, C.K., Latona, N.P., Ashby, R., Ding, K. (2006). Environmental effects on chrome–free leather. *Journal American Leather Chemists Association*, **101**, 368–75.

Liu, C.K., Latona, N.P., Taylor, M., Eble, C., Aldema-RaMos, M.L. (2015a) Characterization of mechanical properties of leather with airborne Ultrasonics. *Journal of American Leather Chemists Association*, **110**, 88-93.

Liu, Y., Xu, Y., Yan, Y., Hu, D., Yang, L. and Shen, R. (2015b). Application of Raman spectroscopy in structure analysis and crystallinity calculation of corn starch. *Journal of starch*, **67**, 612-619.

Liu, Y., Xu, Y., Yan, Y., Hu, D., Yang, L. and Shen, R. (2015c). Application of Raman spectroscopy in structure analysis and crystallinity calculation of corn starch. *Starch/Stärke*, **67**, 612–619, DOI 10.1002/star.201400246.

Liu, Z., Davis, C., Cai, W., He, L., Chen, X. and Dai, H. (2008). Circulation and long-term fate of functionalized, biocompatible single-walled carbon nanotubes in mice probed by Raman spectroscopy. *Proceedings of National Academy of Science United States of American.* **105** (5), 1410–1415.

Logaranjan, K., Raiza, A.J., Gopinath, S.C.B., Chen, Y. and Pandian, K. (2016). Shape and size-controled synthesis of silver nanoparticles using alove vera plant extract and their antimicrobial activity. *Nanoscale research Letter*, **11**, 520-524.

Looney, M., Kyratzis, I., Truong, Y. and Wassenberg, J. (2002). Enhancing the Unique Properties of Kangaroo Leather, A report for the Rural Industries Research and Development Corporation (RIRDC), Publication No 02/105, RIRDC Project No CWT-1A

Lu, S., Liang, G., Ren, H., Wang, J. and Yang, Q. (2005). Synthesis and application of graft copolymer retannage of degraded starch and vinyl monomers. *Journal of the Society of Leather Technologies and Chemists*, **89** (2), 63-66.

Lv, S., Gong, R., Duan, J., Ma, Y. and Gao, R. (2011). Preparation and Properties of Graft Copolymer of Phenols and Starch with HRP Catalysis. *Advanced Materials Research*, **201/203**, 2825-2828.

Ma, J., Gao, J., Wang, H. (2017). Dissymmetry Gemini Sulfosuccinate Surfactant from Vegetable Oil: A Kind of Environmentally Friendly Fatliquoring Agent in the Leather Industry. *ACS Sustainable Chem Eng*, **5,** 10693–10701.

Ma, J., Gao, J., Wang, H., Lyu, B. and Gao, D. (2017). Dissymmetry Gemini Sulfosuccinate Surfactant from Vegetable Oil: A Kind of Environmentally Friendly Fatliquoring Agent in the Leather Industry. *CS Sustainable Chemical Engineering*, **5** (11), 10693–10701 **DOI:**10.1021/acssuschemeng.7b02662.

Mahdad-Benzerdjeb, A., Taleb-Mokhtari, I.N. and Sekkal-Rahal, M. (2007). Normal coordinates analysis of dissacharides constituted by D-glucose, D-galactoseand D-fructose units. *Spectrochimica Acta A*, **68**, 284-299.

Mahmoud, Z.F., Abdel, Salam, N.A. and Khafagy, S.M. (1980). Constituents of henna leaves-Lawsonia inermis L. growing in Egypt. *Fitoterapia*, **51**, 153-155.

Maice, L.F., Fernandes, R.F., Almeida, M.R., and Oliveira, L.F.C. (2015). Rapid assessment of chemical compound from phylogorgia dilatata using Raman spectroscopy. *Revista Brasileira de Farmacognosia*, **25**, 619-626.

Malek, A., Hachemi, M. and Didier, V. (2009). New approach of depollution of solid chromium leather waste by the use of organic chelates. Economical and environmental impacts. *Journal of hazardous materials*, **170**, 156-162.

Malone, J.P. and Veis, A. (2004). Heterotrimeric type I collagen C-telopeptide conformation as docked to its helix receptor. *Biochemistry*, **43** (49), 15359-15366.

Mandal, A.C., Santra, S., Mitra, D., Sarkar, M. and Bhattacharya, D. (2003). EDXRF as a Routine Tool for Numismatic Studies. *Currurrent Science*, **85**(2), 134–135.

Mandal, A.C., Sarkar, M. and Bhattacharya, D. (2002). A Simple EDXRF Technique to Analyse Alloys. *European Physical Journal of Applied Physics*, **17**(1), 81–84.

Manfredi, M., Bearman, G., France, F., Shor, P., Marengo, E. (2015). Quantitative multispectral imaging for the detection of parchment ageing caused by light: A comparison with ATR FTIR, GC-MS and TGA analyses. *International Journal of Conservation Science*, **6**(1), 3-14

Mannucci, E., Pastorelli, R., Zerbi, G., Bottani, C. and Facchini, A. (2000). Recovery of ancient parchment: characterization by vibrational spectroscopy. *Journal of Raman Spectroscopy*, **31** (12), 1089–1097.

Markowicz, A. (2011). An Overview of Quantification Methods in Energy-Dispersive X-Ray Fluorescence Analysis. *Pramana*, **76**(2), 321–329.

Martinetti, R. (1995). *Theory of chromium tanning, industry of leather review*, France, 5.

Masic, A., Bertinetti, L., Schuetz, R., Chang, S., Metzger, T.H., Buehler, M.J. and Fratzl, P. (2015). Osmotic pressure induced tensile forces in tendon collagen. *Nature Communications*, **6**, 5942, DOI: 10.1038/ncomms6942.

Masic, A., Bertinetti, L., Schuetz, R., Galvis, L., Timofeeva, N., Dunlop, J.W.C., Seto, J., Hartmann, M.A. and Fratzl, P. (2011). Observations of Multi-scale, Stress-Induced Changes of Collagen orientation in Tendon by Polarized Raman Spectroscopy. **DOI:** 10.1021/bm201008b

Mathiason, F., Liden, C. and Hedberg, S.Y. (2015). Chromium released from leather-II: the importance of environmental parameters. *Contact Dermatitis*, **72**, 275-285.

Maxwell, C.A., Wess, T.J. and Kennedy, C.J. (2006). X-ray Diffraction Study into the Effects of Liming on the Structure of Collagen. *Biomacromolecules*, **7**, 2321-2326.

Mayo, D.W., Miller, F.A. and Hannah, R.W. (2003). Course notes on the interpretation of infrared and Raman spectra, Wiley-Interscience, 1-583.

McHugh, D.J. (2003). Carrageenan. In A guide to the seaweed industry: FAO fisheries technical paper 441. Food and agriculture organization of the United Nations, Rome.

Metreveli, N., Namicheishvili, L., Jariashvili, K., Mrevlishvili, G., Sionkowska, A., 2006. Mechanisms of the Influence of UV Irradiation on Collagen and Collagen-Ascorbic Acid Solutions. *International Journal of Photoenergy*, **2006**, 1–4.

Metreveli, N.O., Jariashvili, K.K., Namicheishvili, L.O., Svintradze, D.V., Chikvaidze, E.N., Sionkowska, A. (2010) UV–vis and FT-IR spectra of ultraviolet irradiated collagen in the presence of antioxidant ascorbic acid. *Ecotoxicology and Environmental Safety*, **73**, 448–455. doi: 10.1016/j.ecoenv.2009.12.005.

Mikoczy, Z. and Hagmar, L. (2005). Cancer incidence in the Swedish leather tanning industry: updated findings 1958–99. *Occupational and environmental medicine*, **62**, 461–464.

Miles, C.A. and Ghelashvili, M. (1999). Polimer-in-a-Box Mechanism for the Thermal Stabilization of Collagen Molecules in Fibres. *Biophysical Journal*, **76**, 3243-3252.

Millikan, L.E. (2001). Cosmetology cosmetic cosmeceutical definitions and regulations. *Clinics in dermatology*, **19**(4), 371-374.

Minceva-Sukarova, B., Mangovska, B., Bogoeva-Gaceva, G., and Petrusevski, V.M. (2012). Micro-Raman and Micro-FT-IR Spectroscopic Investigation of Raw and Dyed Pan Fibers. *Croatian Chemical Acta,* **85** (1) 63–70.

Miri, S. (2018). Phytochemistry, antioxidant and lipid peroxidation inhibition of the oils of Lavandula officianalis L. in Iran. *International Journal of Food properties,* **21**, 2550-2556

Mishra, A.K., Sahu, N., Mishra, A. (2010). Phytochemical screening and antioxidant activity of essential oil of eucalyptus leaf. *Pharmacognosy journal*, **2**, 25-28.

Miu, L., Giurginca, M. and Meghea, A. (2008). Study on the Roamnian historical parchment by molecular spectroscopy techniques. *UPB Science Bulletin series B*, **70** (4), 51-56.

Mobili P., Londero, A., Antoni, G. and Gomez-Zavaglia, A. (2010). Multivariate analysis of Raman spectra applied to microbiology: discrimination of microorganisms at the species level. *Revista Mexicana De Fisica*, **56** (5), 378-385.

Mogilner, G.I., Ruderman, G., Grigera, R. (2002). Collagen hydration and native state. *Journal of Molecular Graphic and Modelling*, **21**, 209-213.

Moloney, A.C., Kausch, H.H., Kaiser, T., Beer, H.R. (1987). A review – parameters determining the strength and toughness of particulate filled epoxide resins. *Journal of Materials Science,* **22**, 381–93.

Monteiro, M.I.C., Fraga, I.C.S., Yallouz, A.V., de Oliveira, N.M.M. and Ribeiro, S.H. (2002). Determination of total chromium traces in tannery effluents by electrothermal atomic absorption spectrometry, flame atomic absorption spectrometry and UV-Visible spectrophotometric methods, *Talanta*, 58, 629.

Mori, H., Tone, Y., Shimizu, K., Zikihara, K., Tokutomi, S., Ida, T. (2013). Studies on fish scale collagen of Pacific saury (Cololabis saira). *Materials Science Engineering C,* **33**, 174–181. doi:10.1016/j. msec.2012.08.025.

Moriyama, T. (2013). Analysis of environmental samples using energy-dispersive X-ray fluorescence spectrometer NEX CG. *The Rigaku journal*, **29** (1), 27-31.

Mozir, A., Gonzalez, L., Cigic, I.K., Wess, T.J., Rabin, I., Hahn, O. and Strli, M. (2012). A Study of Degradation of Historic Parchment Using Small-Angle XRay Scattering, Synchrotron-IR, and Multivariate Data Analysis. *Analytical and Bioanalytical Chemistry*, **402**, 1559-1566.

Muik, B., Lendl, B., Molina-Dıaz, A., and Ayora-Canada, M.J. (2005). Direct monitoring of lipid oxidation in edible oils by Fourier transform Raman spectroscopy. *Chemistry and Physics of Lipids*, **134**, 173–182.

Mullertz, A., Perrie, Y. and Rades, T. (2016). *Analytical Techniques in the Pharmaceutical Sciences*. Springer.

Musa, A.E. and Gasmelseed, G.A. (2012). Characterization of Lawsoniainermis (Henna) as a vegetable tanning material. *Journal of Forest Products and Industries*, **1**, 35-40.

Musa, A.E. and Gasmelseed, G.A. (2013a). Development of Eco-friendly Combination Tanning System for the Manufacture of Upper Leathers. *International Journal of Advanced Industrial Engineering*, **1**(1), 9-15.

Musa, A.E. and Gasmelseed, G.A. (2013b). Eco-friendly Vegetable Combination Tanning System for Production of Hair-on Shoe Upper Leather. *Journal of Forest Products & Industries*, **2**, 5-12

Musa, A.E., Madhan, B., Kanth, S.V., Rao, J.R., Chandrasekaran, B., Gasmelseed, G.A. (2010). Cleaner tanning process for the manufacture of upper leathers. *Clean Technology and Environmental Policy*, **12**, 381–388 DOI 10.1007/s10098-009-0216-5

Musa, A.E., Madhan, B., Madhulatha, W., Sadulla, S., Gasmelseed, G.A. (2008). Henna extract: Can it be an alternative retanning agent? *Journal of American Leather Chemists Association*, **103**, 188-193.

Musa, A.E., Madhan, W., Rao, J.R., Gasmelseed, G.A. and Sadulla, S. (2009). Colouring of leather using henna-natural alternative material for dyeing. *Journal of American Leather Chemists Association*, **104**, 183-190.

Mutlu, M.M., Ork, N., Yegin, O., Bas, S. (2014). A Study on using 3D Visualization and Simulation program (Optitex 3d) on Leather apparel. *Annals of University of Oradea*, **51**, 157-162.

Naher, U.H.B., Hasan, M. and Ali, F.M., (2017). Pollution Level Caused by the Effluents of Leather Industry and their Abatement. *Journal of Environmental Analytical Chemistry*, **4**, 3 DOI: 10.4172/2380-2391.1000209.

Naidansuren, E., Dondog, A., Erdenesaikhan, B. and Byambanyam, E. (2017). Heavy Metal Pollution near a tannery in Ulaanbaatar, Mongolia. *Journal of Health & Pollution*, **7** (16),1-10.

Nalyanya, K.M., Rop, R.K., Onyuka, A. and Kamau, J. (2015). Tensile properties of Kenyan Indigenous Boran bovine Pickled and Tanned hide. *International Journal of Science & Research*, **4** (3), 2149-2154.

Nalyanya, K.M., Rop, R.K., Onyuka, A., Migunde, P.O. and Ngumbu, R.G. (2016b). Thermal and mechanical analysis of pickled and tanned cowhide: Effect of solar radiations. *Journal of Applied Polymer Science*, 133, **DOI: 10.1002/app.43208.**

Nalyanya, K.M., Rop, R.K., Onyuka, A., Migunde, P.O., Ngumbu, R.G. (2016a). Influence of UV Irradiation on the Viscoelastic Properties and Dynamic Viscosity of Bovine hide using Dynamic Mechanical Analysis. *Journal of Thermal Analysis* & *Calorimetry*, **123**(1), 363-370.

Narsih, K., Kumalaingsih, S., Wijana, S. and Wignyanto, L. (2013). Microencapsulation of natural antioxidant powder from Aloe vera (L.) skin using foam mat drying method. *International Food Research Journal*, **20**(1), 285-289.

Nashy, E.H.A., Hussein, A., Essa, M.M. (2011). Novel retanning agents for chrome tanned leather based on emulsion - nano particles of styrene / butyl acrylate. *Journal of American Leather Chemists Association*, **106** (9), 241- 248.

Nasr, A.I., Abdelsalam, M.M., and Azzam, A.H. (2013). Effect of tanning method and region on physical and chemical properties of Barki sheep leather. *Egyptian journal of sheep and goat sciences*, **8**, 123-130.

Nayak, C.A., Chethana, S., Rastogi, N.K. (2006). Enhanced mass transfer during solid –liquid extraction of gamma irradiated red beetroot. *Radiat phys chem*, **75**, 173-1778.

Nayak, C.A., Chethana, S., Rastogi, N.K., Raghavarao, K.S.M.S. (2006). Enhanced mass transfer during solid –liquid extraction of gamma irradiated red beetroot. *Journal of radiation physics and chemistry*, **75**(1), 173-1778.

Nedkova, M., Pavlov, P. and Pishev, D. (2005). The influnec of acid dyes some structural and physio-mechanical indices of polyamide fibres. *Autex Research journal*, **5** (3), 162-175.

Negi, B.S. and Dave, B.P. (2010). In vitro antimicrobial activity of Acacia catechu and its phytochemical analysis. *Indian Journal of microbial*, **50**, 369-374.

Negussie, F., Urge, M., Mekasha, Y. and Animut, G. (2015). Effects of different feeding regimes on leather quality of finished blackhead Ogaden Sheep. *Science and Technology Arts Research Journal*, **4**(2), 222-227.

Nejatzadeh-Barandozi, F. (2013). Antibacterial activities and antioxidant capacity of *Aloe vera*. *Organic and Medicinal Chemistry Letters*, **3** (3), 1-8.

Nicolais, N.L. and Narkis, N.M. (1971). Stress-strain behavior of styrene-acrylonitrile/glass bead composites in the glassy region. *Polymer Engineering and Science*, **11**, 194–199.

Nielsen, L.E. (1966). Simple theory of stress–strain properties of filled polymers. *Journal of Applied Polymer Science*, **10**, 97–103.

Nurbalia, E. (2016). Characteristics Identification Gambier *(Uncaria Gambier Roxb)* As Leather Tanning Agent. *International Conference on Technology, Innovation, and Society*, **2016**, 62-67. DOI 10.21063/ICTIS.2016.1011

Okoh, S., Adeyemo, D.J., Onoja, R.A. and Arabi, S.A. (2013). Determination of Some trace elements in Leather. *International journal of applied science and technology*, **3** (1), 101-105.

Olsztynska-Janus, S., Gąsior-Głogowska, M., Szymborska-Małek, K., Komorowska, M., Witkiewicz, W., Pezowicz, C., Szotek, S., Kobielarz, M. (2012). Spectroscopic techniques in the study of human tissues and their components. Part II: Raman spectroscopy. *Acta of Bioengineering and Biomechanics*, **14**(4), 1122-1128.

Omur, S. and Mutlu, M.M. (2016). Modification of Mimosa and quebracho tannins and the lightfastness properties of the processed leathers. *Tekstil ve Konfeksiyon*, **26**(2), 230-235.

Onal, A., Sari, A. and Soylak, M. (2005). Ellagic acid from gallnut (Quercus infectoria): Extraction and determination of its dyeing conditions for natural fibres. *Journal of scientific and industrial research*, **64**, 491-495.

Ork, N., Ozgunay, H., Mutlu, M.M., Ondogan, Z. (2014). Comparative Determination of Physical and Fastness Properties of Garment Leathers Tanned with Various Tanning Materials for Leather Skirt Production. *Tekstil ve Konfeksiyon*, **24**(4), 413-418.

Owlad, M., Aroua, M.K., Daud, W.A.W., Baroutian, S. (2009). Removal of hexavalent chromium-contaminated water and waste water: A review. *Water Air Soil Pollut*, **200**, 59-77.

Ozgunay, H., Afsar, A., Colak, S., Zengin, G., Yilmaz, O., Dandar, U., Simion, D., Gaidau, C. (2012). Investigations On Determination of Antioxidant Properties of Certain Plant Products

and their Effects on the Prevention of Cr (VI) And Formaldehyde Formation in Leather, ICAMS 2012 – 4th International Conference on Advanced Materials and Systems

Ozgunay, H., Colak, S., Mutlu, M.M., Akyuz, F. (2007). Characterization of Leather Industry Wastes. *Polish Journal of Environmental Studies*, **16** (6), 867-873.

Ozkan, C.K. and Ozgunay, H. (2016). Usage of Starch in Leather Making, proceedings of the 6th conference on International Conference on Advanced Materials and Systems (ICAMS).

Ozkan, C.K., Ozgunay, H. and Kalender, D. (2017). A novel way to avoid Cr (VI) formation in leather: Copper mordanting. *Journal of Society of Leather Technologists and Chemists*, **101**, 94-95.

Ozkan, C.K., Zengin, A.C.A., Dandar, U., Zengin, G., Kilic, E. (2015). A new vegetable tanning material for leather industry: Acacia nilotica L. XXXIII IULTCS Congress November, 24th – 27th, 2015 Novo Hamburgo/Brazil, 169-174.

Padhi, B.S. (2012). Pollution due to synthetic dyes toxicity and carcinogenicity studies and remediation. *International Journal of Environmental Sciences*, **3**(3), 940.

Palop, R., Parareda, J., Ballus, O. and Marsala, A. (2008). Leather ageing and hexavalent chromium formation as a function of the fatliquoring agent. Part II: chrome retanned leathers. *Journal of the society of leather technologist and chemists*, **92** (6), 233-237.

Pappas, D., Smith, B.W. and Winefordner, J.D. (2000). Raman spectroscopy in bioanalysis. *Talanta*, **51**, 131– 144.

Park, H.M., Moon, E., Lee, S., Kim, S.Y., Do, S.G., Kim, J., Liu, K.H. and Lee, C.H. (2015). Topical application of baby- and adult-aloe on ultraviolet B irradiated mouse skin with metabolite profiling. *Metabolomics*. **DOI: 10.1007/s11306-015-0783-x.**

Paschalis, E.P., Verdelis, K., Doty, S.B., Boskey, A.L., Mendelsohn, R., Yamauchi, M. (2001). Spectroscopic characterization of collagen cross-links in bone. *Journal of Bone and Minerals Research*, **16**, 1821-1828.

Patras, A., Brunton, N.P., Pieve, S.D. and Butler, F. (2009). Impact of high pressure processing on total antioxidant activity, phenolic, ascorbic acid, anthocyanin content and colour of strawberry and blackberry purées. *Innovative Food Science and Emerging Technologies*, **10**, 308–313.

Paul, G.R. and Bailey, A.J. (2003). Chemical Stabilisation of Collagen as a Biomimetic. *The Scientific World journal*, **3**, 138–155

Payne, K. and Veis, A. (1988). Fourier transform IR spectroscopy of collagen and gelatin solutions: deconvolution of the amide I band for conformational studies. *Biopolymers*, **27**, 1749–1760.

Pellerano, R.G., Unates, M.A., Cantarelli, M.A., Camina, J.M. and Marchevsky, E.J. (2012). Analysis of trace elements in multifloral Argentine honeys and their classification according to provenance. *Food Chemistry*, **134**(1), 578–582.

Pengseng, N., Siripongvutikorn, S., Usawakesmanee, W. and Wattanachant, S. (2010). Effect of thermal processing and protein nutrients on antioxidant activity of Tom-kha paste extract. *Asian Journal of Food Agro-Industry*, **3** (4), 389-399.

Pereira, J.A., Oliveira, I., Sousa, A., Valentao, P., Andrade, P.B., Ferreira, I.C.F.R., Ferreres, F., Bento, A., Seabra, R., Estevinho, L., (2007). Walnut (*Juglans regia* L.) leaves: Phenolic compounds, antibacterial activity and antioxidant potential of different cultivars. *Food and Chemical Toxicology*, **45** (11), 2287-2295.

Pereira, L. and Mesquita, J.F. (2004). Population studies and carrageenan properties chondracanthus teedei var. lusitanicus (Gigartinaceae, Rhodophyta). *Journal of Applied phycology*, **16**, 369-383.

Pereira, L., Amado, A.M., Critchley, A.T., Velde, F.V., Ribeiro-Claro, P.J.A. (2009). Identification of selected seaweed polysaccharides (phycocolloids) by vibrational spectroscopy (FTIR-ATR and FT-Raman). *Journal of food and hydrocolloids*, DOI: 10.1016/j.foodhyd.2008.11.014.

Pereira, L., Gheda, S.G., and Ribeiro-Claro, P.J.A. (2013). Analysis by vibrational spectroscopy of seaweed polysaccharides with potential use in food, pharmaceautical and cosmetic industries. *International journal of carbohydrate chemistry*, **2**, 1-7.

Pereira, L., Souza, A., Coelho, H., Amado, A.M., Ribeiro-Claro, P.J.A. (2003). Use of FTIR, FT-Raman and C-NMR spectroscopy for identification of some seaweed phycocolloids. *Biomolecular Engineering*, **20**, 223-228.

Perez-Rodriquez, J.L., Robador, M.D., Haro, M.C.J., Blanes, J.M.M., Garefano, I., Odriozola, C. and Duran, A. (2013). Non-invasive analystical techniques applied to characterize the components of ancient golden medallions. *Heritage Science*, **4** (4), 1-14.

Pervaiz, S., Mughal, T.A., Khan, F.Z. (2016a). Green Fashion Colours: A Potential Value for Punjab Leather Industry to Promote Sustainable Development. *Pakistan Journal of Contemporary Sciences*, **1**(1), 28-36.

Pervaiz, S., Mughal, T.A., Khan, F.Z., Hayat, S., Aslam, A., Shah, S.F. (2017). Environmental friendly leather dyeing using Tagetes erecta L. (Marigold) waste flowers, **10** (1), 382-390.

Pervaiz, S., Mughal, T.A., Najeebullah, M., and Khan, F.Z. (2016b). Extraction of natural dye from Rosa damascena Miller. -a cost effective approach for leather industry. *International Journal of Biosciences*, **8** (6), 83-92.

Piggott, M.R. and Leidner, J. (1974). Misconceptions about filled polymers. *Journal of Applied Polymer Science*, **18**, 1619–1623.

Pinto, P.C.R., Sousa, G., Crispim, F., Silvestre, A.J.D. and Neto, C.P. (2013). Eucalyptus globulus Bark as Source of Tannin Extracts for Application in Leather industry. *ACS Sustainable Chemistry and Engineering*, **1**, 950-955.

Pizzi, A., Simon, C., George, B., Perrin, D. and Triboulot, M.C. (2004). Tannin Antioxidant Characteristics in Leather versus Leather Light Stability: Models. *Journal of Applied Polymer Science*, **91**, 1030-1040.

Plavan, V., koliada, M. and Valeika, V. (2017). Ecobenign semi-metal tanning system-cleaner leather production. *Journal of society of leather tecnologists and chemists*, **101** (5), 260-265.

Potts, J. and Webb, P.C. (1992). X-ray fluorescence spectroscopy. *Journal of Geochemical exploration*, **44**, 251-296.

Puica, N.M., Pui, A. and Florescu, M. (2006). FTIR Spectroscopy for the Analysis of Vegetable Tanned Ancient Leather. *European Journal of Science and Theology*, **2**(4), 49-53.

Puntener, A.G. (1998). Risk assessment of leather stuff. *Journal of the society of leather technologists and chemists*, **83**, 142-147.

Puppels, G.J., Garritsen, H.S.P., Kummer, J.A. and Greve, J. (1993). Carotenoids located in human lymphocyte subpopulations and natural-killer-cells by Raman microspectroscopy. *Cytometry*, **14**, 251–256.

Purkanszky, B. (1990). Influence of interface interaction on the ultimate tensile properties of polymer composites. *Composites*, **21**, 255–262.

Purkanszky, B., Turcsanyi, B. and Tudos, F. (1988). Eff ect of interfacial interaction on the tensile yield stress of polymer composites. In Interfaces in Polymer, Ceramic and Metal Matrix Composites, H. Ishida, Eds.: Elsevier, Amsterdam Netherlands, 467–477.

Purslow, P.P., Wess, T.J. and Hukins, D.W.L. (1998). Collagen orientation and molecular spacing during creep and stress-relaxation in soft connective tissues. *The journal of Experimental Biology*, **201**, 135-142.

Quadery, A.H., Uddin, M.T., Azad, M.A.K., Chowdhury, M.J., Deb, A., Hassan, M.N. (2015). Fatliquor preparation from Karanja seed oil (Pongamia pinnata L.) and its application for leather processing. *IOSR Journal of Applied Chemistry*, **8**(1), 54-58.

Rabotyagova, O.S., Cebe, P. and Kaplan, D.L. (2008). Collagen structural hiercarhy and susceptibility to degradation by ultraviolet radiation. *Journal of material science engineering C Materials Biology Applications*, **28**(8), 1420-1429. DOI: 10.1016/j.msec.2008.03.012.

Rai, H.S., Bhattacharyya, M.S., Singh, J., Bansal, T.K., Vats, P. and Banerjee, U.C. (2005). Removal of dyes from the effluent of textile and dyestuff manufacturing industry: a review of emerging techniques with reference to biological treatment. *Critical Reviews Environmental Science and Technology*, **35** (3), 219–238. DOI: 10.1080/10643380590917932.

Raman, C. and Krishnan, K. (1928) A new type of secondary radiation. *Nature*, **121**, 501-502.

Ramasami, T. (1999). From ore to brick: travel of chromium through the cross roads of Indian leather sector, workshop on building ceramics from industrial waste (international Centre for science and Technology and UNIDO, Trivandum), 132-149.

Ramshaw, J.A.M., Shah, N.K., Brodsky, B. (1998). Gly-X-Y tripeptide frequencies in collagen: a context for hostguest triple-helical peptides. *Journal of Structural Biology*, **122**, 86–91.

Rastogi, S.K., Pandey, A. and Tripathi, S. (2008). Occupational health risks among the workers employed in leather tanneries at Kanpur. *Indian journal of occupational and environmental medicine*, **12**, 132.

Ray, A., Gupta, S.D., Ghosh, S. (2013). Isolation and characterization of potent bioactive fraction with antioxidant and UV absorbing activity from *Aloe barbadensis* Miller gel. *Journal of Plant Biochemistry and Biotechnology*, **22**(4), 483–487.

Redgrove, H.S., Gilbert, A.F. and Bari-Woollss, J. (1939). Hair-dyes and Hair Dyeing: Chemistry and Technique. London.

Rezic, I. and Zeiner, M. (2008). Determination of extractable chromium from leather. *Monatsh Chem*, **DOI** 10.1007/s00706-008-0026-1.

Riaz, T., Zeeshan, R., Zarif, F., Ilyas, K., Muhammad. N., Safi, S.Z., Rahim, A., Rizvi, S.A.A. and Rehman, I.U. (2018). FTIR analysis of natural and synthetic collagen. *Applied Spectroscopy Reviews*, DOI:10.1080/05704928.2018.1426595.

Rich, A. and Crick, F.H.C. (1961). The Molecular Structure of Collagen. *Journal of Molecular Biology*, **3**, 483–506.

Robinson, J.W., Skelly, F.E.M. and Frame, G.M. (2014). Undergraduate Instrumental Analysis. Boca Raton, Fla: CRC.

Roig, M., Segarra, V., Bertazzo, M., Martínez, M.A., Ferrer, J., Raspi, C. (2012). Chrome-free leather, tanned with oxazolidine. *Journal of aqeic*, **63**(4), 101-111.

Rydin, S. (2002). Investigation of the content of Cr (VI) and Cr (III) in leather products on the Danish market. Survey of Chemical Substances in Consumer Products No 3. Danish Environmental Protection Agency, Copenhagen.

Rygula, A., Majzner, K., Marzec, K.M., Kaczor, A., Pilarczyk, M. and Baranska, M. (2013). Raman spectroscopy of proteins: a review. *Journal of Raman Spectroscopy*, **44**, 1061–1076.

Safandowska, M. and Pietrucha, K. (2013). Effect of fish collagen modification on its thermal and rheological properties. *International Journal of Biology Macromolecular*, **53**, 32–37. Doi: 10.1016/j.ijbiomac.2012.10.026.

Sahu, B., Rathinam, A., Javid, M.A., Gupta, S. (2017). Preparation of fatliquor having antifungal activity using the oil of Citrullus colocynthis for application in leather applications. *Journal of Industrial crops and products*, **10**, 553-557.

Salehi, M., Lavvaf, A. and Farahvash, T. (2013). Skin Quality and Physical Properties of Leather Based on Sex, Age and Body Parts of Goats Reared on Sub-Humid Hill Country. *Iranian Journal of Applied Animal Science*, **3** (4), 853-857.

Sanghi, S.B. (2015). Aloe vera: A medicinal herb. *International Journal of research*, **3**(11), 32-34.

Sanz, M., Cadahia, E., Esteruelas, E. (2010). Phenolic Compounds in Chestnut (Castanea sativa Mill.) Heartwood: Effect of Toasting at Cooperage. *Journal of Agricultural Food Chemistry*, **58**, 9631–9640.

Saravanabhavan, S., Fathima, N.N., Rao, J.R. and Nair, B.U. (2004). Combination of White Minerals with Natural Tannins Chrome-Free Tannage for Garment Leathers. *Journal of the Society of Leather Technologists and Chemists*, **88**, 76-81.

Saravanabhavan, S., Rao, J.R. and Nair, B.U. (2005). Integration of chrome tanning and wet finishing process for making garment leathers. *Journal of American Leather Chemistry Association*, **100**, 225-232.

Saravanan, P., Chandramohan, G., Mariajancyrani, J. and Kiruthikajothi, K. (2014). Eco-friendly dyeing of cotton fabric with natural dye extracted from flowers of Lantana camara Linn. *International Journal of Bioassays*, **3**(01), 1653-1656.

Sarkar, K.T. (1991). *Preparation of hides and skins for tanning*. Theory and practice of leather manufacture. India: Sarkar KT, 99.

SATRA (2011). Testing Equipment Catalogue.

Schafer, R. and Schmidt, P.C. (2012). *Methods in physical chemistry*. John Wiley & Sons.

Schutz, R., Bertinetti, L., Rabin, I., Fratzl, P. and Masic, A. (2013). Quantifying degradation of collagen in ancient manuscripts: the case of the Dead Sea Temple Scroll. *Analyst*, **138**, 5594–5599.

Seabra, I.J., Chim, R.B., Salgueiro, P., Braga, M.E.M. and Sousa, H.C. (2017). Influence of solvent additives on the aqueous extraction of tannins from pine bark: potential extracts for leather tanning. *Journal of Chemical Technology and Biotechnology*, 94, 1169-1182, **DOI** 10.1002/jctb.5478.

Seggiani, M., Puccini, M., Vitolo, S., Chiappe, C., Pomelli, C.S. and Castiello, D. (2014). Eco-friendly titanium tanning for the manufacture of bovine leathers: Pilot scale studies. *Clean Technology Environmental Policy*, **16**, 1795-1803.

Selvi, A.T., Aravindhan, R., Madhan, B. and Rao, R.J. (2013). Studies on the application of natural dye extract from Bixa orellana seeds for dyeing and finishing of leather. *Industrial Crops and Products*, **43**, 84–86.

Shackley, M.S. (2011). *An Introduction to X-Ray Fluorescence (XRF) Analysis in Archaeology*. In: M.S. Shackley (ed.) X-ray Fluorescence Spectrometry (XRF) in Geoarchaeology. New York, NY: Springer, Chap. 2, 7–14.

Shahid, M., and Mohammad, F. (2013). Recent advancements in natural dye applications: a review. *Journal of Cleaner Production*, **53**, 310-331.

Shapiro, A., Gofrit, O.N., Pizov, G., Cohen, J.K. and Maier, J. (2011). Raman molecular imaging: A novel spectroscopic technique for diagnosis of bladder cancer in urine specimens. *European Urology*, **59** (1), 106–112.

Sharphouse, J.H. (1983). Leather technicians' handbook. Northampton (UK): leather producer's association, 64.

Singh, P., Rani, B., Maheshwari R. and Chauhan, A.K. (2011). Diverse Therapeutic Applications of *Aloe vera*. *Journal of Advanced Scientific Research*, **2**(4), 4-11.

Sionkowska, A., Wisniewski, M., Skopinska, J. and Mantovani, D. (2006). Effects of solar radiation on collagen-based biomaterials. *International Journal Photoenergy*, **2006**. doi:10.1155/IJP/2006/29196.

Sionkowska, A., Wisniewski, M., Skopinska, J., Kennedy, C.J. and Wess, T.J. (2004). Molecular interactions in collagen and chitosan blends. *Biomaterials*, **25**, 795–801.doi:10.1016/S0142-9612(03)00595-7.

Sirvaityte, J., Siugzdaite, J., Valeika, V. (2011). Application of Commercial Essential Oils of Eucalyptus and Lavender as Natural Preservative for Leather Tanning Industry. *Reviews Chimica (Bucharest)*, **62**, (9), 884-893.

Sirvaityte, J., Siugzdaite, J., Valeika, V. and Dambrauskiene, E. (2012). Application of essential oils of thyme as a natural preservative in leather tanning. *Proceedings of the Estonian Academy of Sciences*, **61**, 3, 220–227.

Sivakumar, V., Mohan, R., Rangasamy, T. and Muralidharan, C. (2016). Antimicrobial activity of Terminalia chebula Retz. (Myrobalan). *Indian Journal of Natural Products and Resources*, **7** (1), 65-68.

Sivakumar, V., Prakash, P.R., Rao, P.G., Ramabrahmam, B.V., Swaminathan, G. (2008). Power ultrasound in fatliquor preparation based on vegetable oil for leather application. *Journal of Cleaner Production*, **16**, 549-553.

Sizeland, K.H., Wells, H.C., Norris, G.E., Edmonds, R.L., Kirby, N., Hawley, A., Mudie, S. and Haverkamp, R.G. (2015). Collagen D-spacing and the effect of fat liquor addition. *Journal of American Leather Chemists Association*, **110** (3), 66−71.

Smith, E. and Dent, G. (2013). Modern Raman spectroscopy: a practical approach. John Wiley & Sons.

Song, Y.S., Youn, J.R. (2005). Influence of dispersion states of carbon nanotubes on physical properties of epoxy nanocomposites. *Carbon*, **43**, 1378–1385.

Stone, N., Kendall, C., Smith, J., Crow, P. and Barr, H. (2004). Raman spectroscopy for identification of epithelial cancers. *Faraday Discuss*, **126**, 141–157.

Sumita, M., Shizuma, T., Miyasaka, K., and Ishikawa, K. (1983). Effect of reducible properties of temperature, rate of strain, and filler content on the tensile yield stress of nylon 6 composites filled with ultrafine particles. *Journal of Macromolecular Science. B*, **22**, 601–18.

Summerour, R. (2012). The examination and conservation of a snake skin suit jacket, Buffalo State College, Anagpic, 2-65.

Sundari, N. (2015). Extraction and optimization of Mucura pruriens for dyeing of leather. *Polish journal of chemical Technology*, **17** (2), 57-63. DOI: 10.1515/pjct-2015-0030.

Surjushe, A., Vasani, R. and Saple, D.G. (2008). Aloe Vera: A Short Review. *Indian Journal of Dermatology*, **53**(4), 163–166. Doi: 10.4103/0019-5154.44785

Svab, I., Musil, V. and Leskovac, M. (2005). The adhesion phenomena in polypropylene / wollastonite Composites. *Acta Chimica Slovania*, **52**, 264–271.

Talari, A.C.S., Movasaghi, Z., Rehman, S. and Rehman, I.U. (2014). Raman spectroscopy of Biological tissues. *Applied spectroscopy Reviews*, **50**, (1), 46-111. DOI: 10.1080/ 05704928. 2014.923902.

Tarantilis, P.A., Beljebbar, A., Manfait, M. and Polissiou, M. (1998). FTIR, FT-Raman spectroscopic study of carotenoids from saffron (Crocus sativus L.) and some derivatives. *Spectrochimica Acta part A*, **54**, 651-657.

Tariq, L., Reyaz, A.l. (2012). Phytochemical analysis of Camellia sinensis leaves. *International Journal of drug development and research*, **4**, 311-316.

Tawfik, H.M., Gasmelseed, G.A. and Mohammed, F.E.F. (2017). Using Characterization and Synthesis of Fatliquor from Sudanese Castor Oil. *International Journal of Engineering Sciences & Research Technology*, **6**(2), 11-16 DOI: 10.5281/zenodo.266664

Tegtmeyer, D. and Kleban, M. (2013). Chromium and Leather research: A balanced view of scientific facts and figures, IULTCS IUR-1, 1-10.

Thanikaivelan, P., Rao, J.R., Nair, B.U. and Ramasami, T. (2003). Progress and trecent trends in biotechnological methods for leather processing. *Trends in biotechnology*, **22** (4), 181-188.

Thiyagarajan, S., Balakrishnan, K., Tamilarasi, S. (2015). A Study of extraction and dyeing hehavior of natural dye obtained from cotton a study. *IOSR Journal of Applied Chemistry*, **8** (5), 85-89.

Thomson, R. (2002). Conserving historical leathers: Saving our past for the future. *Journal of American Leather Chemists Association*, **97**, 307.

Tian, B. and Hua, Y. (2005). Concentration-dependence of prooxidant and antioxidant effects of aloin and aloe-emodin on DNA. *Food Chemistry*, **91**(3), 413–4182005.

Tillet, G., Boutevin, B. and Ameduri, B. (2011). Chemical reactions of polymer crosslinking and post-crosslinking at room and medium temperature. *Progress in Polymer Science*, **36**, 191.

Treloar, L.R.G. (1956). The Physics of Rubber Elasticity. Clarendon Press, Oxford.

Tshuma, J., Zvavamwe, C., Mkandhla, C.K., Mpofu, C., Gwaze, I., Bgwoni, F., Mudenge, T. and Sibutha, M. (2016). Yellow dye extraction from Eucalyptus Grandis Bark. *American Journal of Engineering Research (AJER)*, **5**(10), 10-18.

Tsuboi, Y., Kimoto, N., Kabeshita, M. and Itaya, A. (2001). Pulsed laser deposition of collagen and keratin. *Journal of Photochemisyry and Photobiology A: Chemistry*, **145**(3), 209–214.

Turcsanyi, B., Pukanszky, B. and Tudos, F. (1988). Composition dependence of tensile yield stress in filled polymers. *Journal of Materials Science Letters*, **7**, 160–162.

Tyagi, P.K. (2017). A Comparative assessment of mechanical properties of skin, fatliquored with polymeric fat and vegetablef. *International Journal of Engineering Technology, Management and Applied Sciences*, **5**(7), 216-221.

Tylingo, R., Mania, S., Panek, A., Piatek, R. and Pawowicz, R. (2016). Isolation and characterization of acid soluble collagen from the skin of African Catfish (Clarias gariepinus), Salmon (Salmosalar) and baltic Cod (Gadus morhua). *Journal of Biotechnology and Biomaterials*, **6**, 2. doi:10.4172/2155-952X.1000234.

UNEP (1991). Tanneries and the Environment: a technical guide to reducing the environmental impact of tannery operations. United Nations Environment Programme, Industry and Environment, Programme Activity Centre (UNIDO, IE/PAC), Paris

UNIDO (1996). Acceptable quality standards in the leather and foot wear industries.

Upadhyay, A., Agrahari, P., Singh, D.K. (2014). A review on the pharmacological aspects of Terminalia chebula. *International Journal of pharmacology*, **10**, 289-298.

Urbanija, V. and Gersak, J. (2004). Impact of the mechanical properties of nappa clothing leather on the characteristics of its use. *Journal of the Society of Leather Technologists and Chemists*, **88**, 181-190.

Valeika, V., Kestutisbeleska, J. and Valeikiene, V. (2012). Essential Oils as Antioxidants for Fatliquoring Emulsion. ICAMS 2012 –4th International Conference on Advanced Materials and Systems.

Valeika, V., Sirvaityte, J., Beleska, K. (2010). Estimation of Chrome-free Tanning Method Suitability in Conformity with Physical and Chemical Properties of Leather. *Materials Science (Medziagotyra)*, **16**(4), 330-336.

Vandenabeele, P., Wehling, B., Moens, L. and Edwards, H. (2000). Analysis with micro-Raman spectroscopy of natural organic binding media and varnishes used in Art. *Analytica Chimica Acta*, **407**, 261-274.

Varmuza, K. and Filzmoser, P. (2009). *Introduction to multivariate statistical analysis in chemometrics*. Boca Raton, CRC Press.

Vaskova, H., and Kolomaznik, K. (2016). Spectroscopic measurement of trivalent and hexavalent chromium, 2016 17th international Carpathian Control Cnference (ICCC), 775-778.

Veit, G., Kobbe, B., Keene, D.R., Paulsson, M., Koch, M., Wagener, R. (2006). Collagen XXVIII, a novel von Willebrand factor a domain-containing protein with many imperfections in the collagenous domain. *Journal of Biology and Chemistry*, **281**, 3494–3504.

Vinson, J.A., Su, X., Zubik, L., Bose, P. (2001). Phenol antioxidant quantity and quality in foods: fruits. *Journal of Agricultural food and Chemistry*, **49**, (11), 5315-5321.

Vollenberg, P.H.T. and Heikens, D. (1989). Particle size dependence of the Young's modulus of filled polymers: 1. Preliminary experiments. *Polymer*, **30**, 1656–1662.

Vornicu, N., Deselnicu, V., Bibire, C., Ivanov, D., and Doroftei, F. (2015). Analytical Techniques Used for the Characterization and authentication of Six Ancient Religious Manuscripts (XVIII–XIX Centuries). *Microscopy Research and Technique*, **78**, 70–84.

Walsh, A.R., and Halloran, J. (1996). Chromium speciation in tannery effluent – 1: An assessment of techniques and role of organic Cr (III) complexes. *Water Resources,* **30**, 2393–2400.

Wang, F., Chen, G., and Fang, Z.Q. (2009b). Study on synergistic effect of surface sizing starch and synthesized agent. *Paper science and technology*, **128** (6), 56-60.

Wang, X.H., Li, D.P., Wang, W.J., Feng, Q.L., Cui, F.Z., Xu, X.Y., Seog, X.H. and Werf, M. (2008). Crosslinked collagen/chitosan matrix for artificial livers. *Biomaterials*, **24,** 3213-3220.

Wang, X.S., Li, Z.Z. and Tao, S.R. (2009a). Removal of chromium (VI) from aqueous solution using walnut hull. *Journal of Environmental Management*, **90**, 721-729.

Wang, Y.N., Galiotis, C. and Bader, D.L. (2000b). Determination of molecular changes in soft tissues under strain using laser Raman microscopy. *Journal of Biomechanics*, **33**, 483–486.

Wang, Y.N., Galiotis, C., Bader, D.L. (2000). Determination of molecular changes in soft tissues under strain using laser Raman microscopy. *Journal of Biomechanics*, **33**(4), 483-486.

Wegrzynek, D., Bamford, S.A. and Chinea-Cano, E. (2004). Advanced X-Ray Fluorescence Techniques. In: Analytical Applications of Nuclear Techniques. Vienna, Austria: International Atomic Energy Agency, 37–40.

Wells, H.C., Edmonds, R.L., Kirby, N., Hawley, A., Mudie, S.T., Haverkamp, R.G. (2013). Collagen fibril diameter and leather strength. *Journal of Agricultural Food and Chemistry*, **61**(47), 11524−11531.

Wells, H.C., Sizeland, K.H., Kelly, S.J.R., Kerby, N., Hawley, A., Mudie, S. and Haverkamp, R.G. (2017). Collagen fibril intermolecular spacing changes with 2-propanol: A mechanism for tissue stiffness, ACS Biomaterials science and Engineering, DOI: 10.102/acs.biomaterials.7b00418

Wess, T.J. and Orgel, J.P. (2000). Changes in collagen structure: drying, dehydrothermal treatment and relation to long term deterioration. *Thermochimica Acta*, **365** (1-2), 119–128.

Wobrauscheck P and Christina S (2010). *Energy dispersive flourescenec analysis, X-Ray spectrometry*. John Wiley & sons Ltd, 1-7.

Wolf, G. (2002). Formaldehyde in leather: causes and avoidance, World leather February/March, 46, 2002.

Wu, B., Mu, C., Zhang, G. and Lin, W. (2009). Effects of Cr 3+ on the structure of collagen fibre. *Langmuir*, **25** (19), 11905-11910.

Xiaosheng, D., Hui, C., Rui, D. and Zhihua, S. (2012). Preparation and Application of Denatured Starches. *Journal of the Society of Leather Technologies and Chemists*, **96**(5), 189-194.

Yaon, J., Liu, Y., Yang, S. and Liu, J. (2008). Characterization of secondary structure transformation of stretched and slenderized wool fibres with FTIR spectra. *Journal of engineered fibres and fabrics*, **3**, 34-39.

Yi, I., Liu, Z., Wang, K., Chen, M., Peng, S., Zhao, W., He, J., Zhao, G. (2015). A New Background Subtraction Method for Energy Dispersive X-Ray Fluorescence Spectra Using a Cubic Spline Interpolation. *Nuclear Instrumentation Methods Physics Research Section A*, **775**, 12–14.

Yildrim, A., Oktay, M. and Bilaloglu, V. (2001). The antioxidant activity of leaves of Cydonia vulgaris. *Turkish Journal of Medical Science*, **31**, 23-27.

Yu, C.Z., Wang, R., Ma, X.Y., Yang, M.Y. (2010). Antioxidant effects of phenolic compounds on unsaturated lipids preventing the oxidation of chrome (III). *Journal of the Society of Leather Technologists and Chemists*, **94** (1), 33-38.

Zapletal, P., Szarek, J., Weglarz, A., Gardzina, E. (1996). Histological studies of hides and crossbreeds by Italian beef breed bulls and the physical properties of the leather. *Journal of the Society of Leather Technologists and Chemists*, **80**, 118.

Zengin, A.C.A., Colak, S.M., Zengin, G. and Kilic, E. (2014). Eco-Friendly Soaking Process Using Tannic Acid as an Alternative Bactericide. *Arch Environ Protec*, **40** (1), 3–12.

Zengin, A.C.A., Crudu, M., Maier, S.S., Deselnicu, V., Albu, L., Gulumser, G., Bitlisli, B.O., Basaran, B., Mutlu, M.M. (2012). Eco-leather: Chromium-free leather production using Titanium, Oligomeric Melamine, Formaldehyde Resin and Resorcinol Tanning Agents and the Properties of the Resulting Leathers. *Ekoloji*, **21** (82), 17-25.

Zhang, X., Young, M.A., Lyandres, O., Van Duyne, R.P. (2005). Rapid Detection of Anthrax Biomarkerker by Surface Enhanced Raman Spectroscopy. *Journal of American Chemical Society*, **127** (12), 4484-4489.

Zhengjun, L., Wuhou, F., Qinhuan, Y. and Ye, T. (2015). A Comparison of Low Temperature Softness of Leather Lubricated with Various Types of Fatliquor. *Journal of Society of Leather Technologists and Chemists*, **98**, 167-171.

APPENDICES

Appendix 1:

First Publication

EFFECT OF CRUSTING OPERATIONS ON THE PHYSICAL PROPERTIES OF LEATHER

Kallen Mulilo NALYANYA[1], Ronald K. ROP[1], Arthur ONYUKA[2], Zephania BIRECH[3], Alvin SASIA[2]

[1]Department of Physics, Faculty of Science, Egerton University, Nakuru, Kenya, kallenmulilo@ymail.com

[2]Kenya Industrial Research and Development Institute, Nairobi, Kenya

[3]Department of Physics, School of Biological and Physical Sciences, University of Nairobi, Kenya

Received: 19.07.2018 Accepted: 13.10.2018 https://doi.org/10.24264/lfj.18.4.4

EFFECT OF CRUSTING OPERATIONS ON THE MECHANICAL PROPERTIES OF LEATHER

ABSTRACT. Physical properties of leather form vital quality parameters that determine the performance characteristics in their areas of applications. However, the transformational processing of hide to leather involves a series of both chemical and physical/mechanical changes that affect these mechanical properties. Many researches have been published regarding the effect of processing on the mechanical properties of leather. However, the effect of entire crusting operations (post tanning) on the mechanical properties is not documented. This study reports the findings of the effect of crusting operations (retanning, dyeing and fatliquoring) on the mechanical properties of the final leather. Results have shown that retanning process improves tear and tensile strengths, distensions at crack and burst, and shrinkage temperature. An improvement in the organoleptic properties such as fullness was recorded in retanned crust leather. However, the uniformity coefficient and percentage elongation significantly decreased after retanning. Dyeing raises the elongation at break, distensions at crack and burst, shrinkage temperature and uniformity coefficient whereas both tensile and tear strengths decreased after dyeing. Similarly, fatliquored samples recorded higher elongation at break values, and distension values. Conversely, tensile and tear strengths, shrinkage temperature and uniformity coefficient decreased as a result of fatliquoring process. All the samples tested at tanning, retanning, dyeing and fatliquoring processes indicated no damage at 50,000 flexes. The study discussed these effects using transmission of fracture and damage mechanics in leather, structural implication of the resulting leather and existing models of materials.
KEYWORDS: physical properties, crusting operations, leather anisotropy and uniformity, fracture and damage mechanics, micromechanical deformation, stress concentration

EFECTUL OPERAŢIUNILOR DE FINISARE UMEDĂ ASUPRA PROPRIETĂŢILOR MECANICE ALE PIELII

REZUMAT. Proprietăţile fizice ale pielii constituie parametri de calitate importanţi care determină caracteristicile de performanţă ale pielii în domeniile în care vor fi utilizate. Cu toate acestea, transformarea pieii crude în piele finită implică o serie de modificări chimice şi fizico-mecanice care afectează proprietăţile mecanice ale pielii. Au fost publicate multe cercetări privind efectul prelucrării asupra proprietăţilor mecanice ale pielii. Cu toate acestea, efectul ansamblului de operaţiuni de finisare umedă (post-tăbăcire) asupra rezistenţei mecanice nu este documentat. Acest studiu prezintă constatările privind efectul operaţiunilor de finisare umedă (retăbăcire, vopsire şi ungere) asupra proprietăţilor mecanice ale pieii finite. Rezultatele au arătat că procesul de retăbăcire îmbunătăţeşte rezistenţa la rupere şi la sfâşiere, alungirea la crăpare şi rupere şi temperatura de contracţie. S-a înregistrat o îmbunătăţire a proprietăţilor organoleptice, cum ar fi plinătatea, la pielea retăbăcită şi finisată umed. Cu toate acestea, coeficientul de uniformitate şi alungirea procentuală au scăzut semnificativ după retăbăcire. Vopsirea creşte alungirea la rupere, alungirea la crăpare şi rupere, temperatura de contracţie şi coeficientul de uniformitate, în timp ce rezistenţa la rupere şi la sfâşiere scad după vopsire. În mod similar, eşantioanele unse au înregistrat valori mai mari ale alungirii la rupere şi ale alungirii la crăpare şi rupere. Dimpotrivă, rezistenţa la rupere şi la sfâşiere, temperatura de contracţie şi coeficientul de uniformitate au scăzut ca rezultat al procesului de ungere. Nicio probă testată după tăbăcire, retăbăcire, vopsire şi ungere nu a prezentat deteriorare la 50.000 de flexiuni. Studiul a prezentat aceste efecte prin propagarea fracturii şi deteriorările mecanice ale pielii, proprietăţile structurale ale pielii rezultate şi modelele de materiale existente.
CUVINTE CHEIE: proprietăţi fizice, operaţiuni de finisare umedă, anizotropia şi uniformitatea pielii, fracturi şi deteriorări mecanice, deformare micromecanică, concentraţie de stres

L'EFFET DES OPÉRATIONS DE FINITION HUMIDE SUR LES PROPRIÉTÉS MÉCANIQUES DU CUIR

RÉSUMÉ. Les propriétés physiques du cuir forment des paramètres de qualité vitaux qui déterminent les caractéristiques de performance dans leurs domaines d'application. Cependant, le traitement de la peau en cuir implique une série de modifications tant chimiques que physiques/mécaniques qui affectent les propriétés mécaniques du cuir. De nombreuses recherches ont été publiées concernant l'effet du traitement sur les propriétés mécaniques du cuir. Cependant, l'effet de l'ensemble des opérations de finition humide (après tannage) sur la résistance mécanique n'est pas documenté. Cette étude présente les résultats de l'effet des opérations de finition humide (retannage, teinture et nourriture) sur les propriétés mécaniques du cuir final. Les résultats ont montré que le processus de retannage améliore les résistances à la déchirure et à la traction, l'extension à la gerçure et à l'éclatement, la température de rétraction. Une amélioration des propriétés organoleptiques telles que la plénitude a été enregistrée dans le cuir retanné et fini humide. Cependant, le coefficient d'uniformité et le pourcentage d'allongement ont significativement diminué après retannage. La teinture augmente l'allongement à la rupture, l'extension à la gerçure et à l'éclatement, la température de rétraction et le coefficient d'uniformité, tandis que les résistances à la traction et à la déchirure diminuent après la teinture. De manière similaire, les échantillons nourris ont enregistré des valeurs plus élevées d'allongement à la rupture et d'extension. Inversement, les résistances à la traction et à la déchirure, la température de rétraction et le coefficient d'uniformité ont diminué à la suite du processus de nourriture. Aucun des échantillons testés lors des processus de tannage, de retannage, de teinture et de nourriture n'indiquent aucun dommage après 50 000 flexions. L'étude a examiné ces effets en utilisant la transmission de la rupture et les dommages mécaniques dans le cuir, les propriétés structurelles du cuir résultant et les modèles de matériaux existants.
MOTS CLÉS : propriétés physiques, opérations de finition humide, anisotropie et uniformité du cuir, rupture et dommages mécaniques, déformation micromécanique, concentration de stress

** Correspondence to: Kallen Mulilo NALYANYA, Department of Physics, Faculty of Science, Egerton University, Nakuru, Kenya, P.O. Box 536, Egerton-20115, Phone: +254712627620, Fax: 254 51 22178257, email: kallenmulilo@ymail.com*

Second publication

Polymer Bulletin
https://doi.org/10.1007/s00289-019-02706-1

ORIGINAL PAPER

Investigating mechanical properties of leather treated with *Aloe barbadensis* Miller and Carrageenan using existing theoretical models

Kallen Mulilo Nalyanya[1] · Ronald K. Rop[1] · Arthur Onyuka[2] · Zephaniah Birech[3] · Alvin Sasia[2]

Received: 20 July 2018 / Revised: 10 October 2018 / Accepted: 7 February 2019

Abstract
Several studies have alluded to the possibility and importance of utilizing *Aloe barbadensis* Miller and Carrageenan to increase leather functionalities without impacting on the environment negatively and retaining the mechanical performance of the final leather. In order to understand the actual effect of *A. barbadensis* Miller and Carrageenan on the mechanical effect, there is need to understand the mechanism of reinforcement or weakening. This will enhance the scientific understanding of the processes of deformation and mechanical failure of the leather materials, and the connections between the structure, processing and their underlying mechanisms. This study presents the results of using the existing empirical models and semi-empirical equations to both predict the strength properties of leather treated with *A. barbadensis* Miller mixed with Carrageenan and determine their mechanism of strengthening/weakening in the leather matrix. Prediction using the existing empirical models and equations shows reasonable agreement with experimental data and can be used to explain the strengthening/weakening mechanism. Results clearly indicate that adhesion is strong in fatliquored leather, and it significantly influences the strength properties. Fatliquoring agents act as coupling agents that improve wetting and hence adhesion. The study recommends at most 3.784% of the *A. barbadensis* Miller and Carrageenan by weight of crust and incorporation be done after fatliquoring process. Although parameters concerning leather matrix irregularities and particle sizes were not accounted for, the study suggests any processes that can increase surface free energy of the fillers to increase the work of adhesion at the interface such as filler sulphiting and surfactants.

Keywords Crust leather · Adhesion · Mechanical properties · Theoretical models and relations · *Aloe barbadensis* Miller and Carrageenan · Reinforcement theory

✉ Kallen Mulilo Nalyanya
kallenmulilo@ymail.com

Extended author information available on the last page of the article

Published online: 12 February 2019

Appendix 2: Outputs of Key Data Analyses

ANOVA for Effect of sampling orientation on Tensile Strength

ANOVAOneWay (5/30/2019 19:10:2

Input Data

	Data	Range
Tensile strength	[Book1]Sheet1!A"Tensile strength"	[6:16]
Tensile strength	[Book1]Sheet1!B"Tensile strength"	[1:16]

Descriptive Statistics

	N Analysis	N Missing	Mean	Standard Deviation	SE of Mean
Tensile strength	11	0	20.24	4.01712	1.21121
	16	0	21.68937	3.84228	0.96057

One Way ANOVA

Overall ANOVA

	DF	Sum of Squares	Mean Square	F Value	Prob>F
Model	1	13.69337	13.69337	0.89425	0.35338
Error	25	382.81869	15.31275		
Total	26	396.51207			

Null Hypothesis: The means of all levels are equal.
Alternative Hypothesis: The means of one or more levels are different.
At the 0.05 level, the population means are not significantly different.

Fit Statistics

	R-Square	Coeff Var	Root MSE	Data Mean
	0.03453	0.18547	3.91315	21.09889

ANOVA for Effect of sampling orientation on Tear Strength

ANOVAOneWay (5/30/2019 18:56:5

Input Data

	Data	Range
Tear strength	[Book1]Sheet1!A"Tear strength"	[1:16]
	[Book1]Sheet1!B"Tear strength"	[1:16]

Descriptive Statistics

	N Analysis	N Missing	Mean	Standard Deviation	SE of Mean
Tear strength	16	0	173.62313	43.79128	10.94782
	16	0	169.39063	40.51577	10.12894

One Way ANOVA

Overall ANOVA

	DF	Sum of Squares	Mean Square	F Value	Prob>F
Model	1	143.31245	143.31245	0.08053	0.77853
Error	30	53388.05744	1779.60191		
Total	31	53531.36989			

Null Hypothesis: The means of all levels are equal.
Alternative Hypothesis: The means of one or more levels are different.
At the 0.05 level, the population means are not significantly different.

Fit Statistics

	R-Square	Coeff Var	Root MSE	Data Mean
	0.00268	0.24597	42.18533	171.50688

Means Comparisons

Tukey Test

	MeanDiff	SEM	q Value	Prob	Alpha	Sig	LCL	UCL
Tear strength Tear strength	-4.2325	14.91477	0.40132	0.77853	0.05	0	-34.69261	26.22761

Sig equals 1 indicates that the difference of the means is significant at the 0.05 level.
Sig equals 0 indicates that the difference of the means is not significant at the 0.05 level.

ANOVA for Effect of sampling orientation on Percentage Elongation

ANOVAOneWay (5/30/2019 19:20:2

Input Data

	Data	Range
Percentage elongation	[Book1]Sheet1!A"Percentage elongation"	[1:16]
Percentage elongation	[Book1]Sheet1!B"Percentage elongation"	[1:16]

Descriptive Statistics

	N Analysis	N Missing	Mean	Standard Deviation	SE of Mean
Percentage elongation	16	0	23.72125	4.83537	1.20884
	16	0	21.3	4.66296	1.16574

One Way ANOVA

Overall ANOVA

	DF	Sum of Squares	Mean Square	F Value	Prob>F
Model	1	46.89961	46.89961	2.0787	0.15973
Error	30	676.86037	22.56201		
Total	31	723.75999			

Null Hypothesis: The means of all levels are equal.
Alternative Hypothesis: The means of one or more levels are different.
At the 0.05 level, the population means are not significantly different.

Fit Statistics

	R-Square	Coeff Var	Root MSE	Data Mean
	0.0648	0.21101	4.74995	22.51063